



universität
wien

DISSERTATION / DOCTORAL THESIS

Titel der Dissertation /Title of the Doctoral Thesis

„Estrogen Metabolism in Gynecological Cancer Cells:
Impacts of Dietary Supplements and Drug Resistance“

verfasst von / submitted by

Mag.pharm. Stefan Poschner

angestrebter akademischer Grad / in partial fulfilment of the requirements for the degree of

Doktor der Naturwissenschaften (Dr.rer.nat.)

Wien, 2020 / Vienna, 2020

Studienkennzahl lt. Studienblatt /
degree programme code as it appears on the student
record sheet:

UA 796 610 449

Dissertationsgebiet lt. Studienblatt /
field of study as it appears on the student record sheet:

Pharmazie

Betreut von / Supervisor:

ao. Univ.-Prof. Mag. Dr. Walter Jäger

ACKNOWLEDGEMENTS

First of all, I would like to express my deepest gratitude to my supervisor ao. Univ.-Prof. Mag. Dr. Walter Jäger for giving me the great opportunity to conduct this doctoral thesis in his working group “Clinical Pharmacy and Diagnostics” at the Department of Pharmaceutical Chemistry, Faculty of Life Sciences, University of Vienna (Vienna, Austria). His constant encouraging advice, his patience during many valuable discussions and his numerous critical suggestions made this thesis possible.

In addition, I greatly thank my fantastic colleagues at the Department of Pharmaceutical Chemistry for supporting me with brilliant tips and tricks concerning the practical work for this thesis, assisting me with the experiments and, last but not least, for the enjoyable social atmosphere and friendship.

Finally, I wish to offer special thanks to my parents, my wife, my daughter, my son and my friends for their patience during the whole working episode of this thesis and for supporting me throughout my life.

TABLE OF CONTENTS

ABSTRACT.....	1
CHAPTER I	3
Introduction	
References	
CHAPTER II	37
Aims of the Thesis	
CHAPTER III	41
Simultaneous Quantification of Estrogens, their Precursors and Conjugated Metabolites in Human Breast Cancer Cells by LC-HRMS without Derivatization	
CHAPTER IV	49
The Impacts of Genistein and Daidzein on Estrogen Conjugations in Human Breast Cancer Cells: A Targeted Metabolomics Approach	
CHAPTER V	61
Resveratrol Inhibits Key Steps of Steroid Metabolism in a Human Estrogen-Receptor Positive Breast Cancer Model: Impact on Cellular Proliferation	

CHAPTER VI..... 79

Actaea Racemosa L. Extract Inhibits Steroid Sulfation in Human Breast
Cancer Cells: Effects on Androgen Formation

CHAPTER VII 111

Metabolism of Estrogens: Turnover Differs between Platinum-Sensitive
and -Resistant High-Grade Serous Ovarian Cancer Cells

CHAPTER VIII..... 133

Conclusions and Outlook

APPENDIX 137

Abbreviations

Zusammenfassung

List of Scientific Publications

ABSTRACT

Estrogens play a pivotal role in human physiology; however, little is known regarding the interaction of dietary supplements or different disease states with their endogenous metabolism. Altered metabolism may affect the levels of active hormone concentrations and consequently drive the development or progression of various diseases, particularly hormone-sensitive gynecological cancers. To the best of my knowledge, the present thesis therefore investigated for the first time the interactions of selected natural dietary supplements used for the treatment of menopausal disorders with the endogenous metabolism of estrogens in human estrogen receptor α -negative (ER α -) and -positive (ER α +) breast cancer cells, using a newly established and validated liquid chromatography high-resolution mass spectrometry method. Due to the high sensitivity and selectivity of this assay, even small changes in the metabolism of the ten major human estrogen precursors, active estrogens and their respective conjugated biotransformation products could be detected simultaneously. Incubation of cells with the soy isoflavones genistein and daidzein or resveratrol, a polyphenol found in grapes, revealed a strong inhibition of steroid glucuronidation and sulfation at low micromolar or even sub-micromolar concentrations, with a concomitant increase in the levels of unconjugated steroid hormones, especially the most potent estrogen 17 β -estradiol (E2). This increase of E2 levels caused a stimulation of ER α + breast cancer cell proliferation *in vitro*, highlighting the need for further human investigations to assess the safety of botanical applications in patients with breast cancer.

By contrast, treatment of the same breast cancer cells with black cohosh extract and its major constituent actein, another plant-derived supplement for menopausal disorders, revealed no changes in the conjugation of estrogens, which is in line with the observed lack of additional cancer cell proliferation. Indeed, a minor inhibition of ER α - and ER α + breast cancer cell growth was found, thereby suggesting that the use of black cohosh supplements by women diagnosed with breast cancer appears to be safe. However, a selective inhibition of

dehydroepiandrosterone sulfation via the sulfotransferase 2A1 was identified, which led to a strongly induced formation of the unconjugated androgens 4-androstene-3,17-dione and testosterone, possibly explaining the clinically proven effect of black cohosh against climacteric vasomotor symptoms, especially hot flashes.

The last part of this thesis further demonstrated that targeted estrogen metabolomics can also be used as a marker to determine cancer resistance against platinum-based drugs, which is a major obstacle in the treatment of ovarian cancer. Using two carboplatin-sensitive and four carboplatin-resistant high-grade serous ovarian cancer cell lines, a significant inhibition of steroid metabolism was observed in carboplatin-resistant cells, which was reversible by treatment with the monoclonal anti-interleukin-6-receptor antibody tocilizumab.

Future studies monitoring the levels of conjugated and unconjugated steroids in the absence and presence of dietary supplements or in different disease states are highly warranted to further prove the importance of steroid metabolomics in patients.

CHAPTER I

INTRODUCTION

Estrogens

Estrogens represent the major female sex steroid hormones, although they are also present at lower concentrations in men. Their main sites of endogenous production are the female ovaries, but they can also be formed in adipose tissue (especially in the breast), adrenal glands, bones, brain cells and the male testicles (Simpson, 2003; Hess and Cooke, 2018). Estrone (E1), 17 β -estradiol (E2) and estriol (16 α -hydroxy-17 β -estradiol; E3) are the major endogenous human estrogens (**Figure 1**). While E2 is the most potent human estrogen, the relative receptor binding affinities of E1 and E3 are much lower, resulting in much weaker estrogenic activities that amount to only around 10 and 1%, respectively (Labhart, 2012).

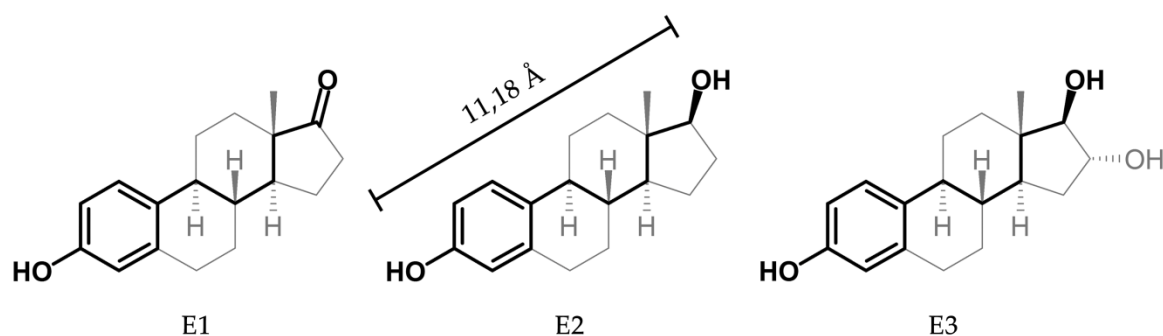


Figure 1: Chemical structures of E1, E2 and E3. Structural parts necessary for estrogen receptor interaction are highlighted in bold. Distance according to Nikov *et al.*, 2001. E1, estrone; E2, 17 β -estradiol; E3, estriol.

All three steroids share their common estrane scaffold with an aromatized A-ring, and differences can only be found in the number of hydroxyl groups in the molecule, which is also represented in the respective abbreviation. This specific structure is essential for their binding affinity to the estrogen receptors (ERs), which requires a phenolic group (or at least phenol bio-isostere) as a hydrogen bond donor and another oxygen atom in a 11 to 12 Å distance, connected via a rather lipophilic linker (Paterni *et al.*, 2014; Lee and Barron, 2017).

Estrogen Receptors

Up to date, two classes of ERs have been identified: The nuclear ERs α (ER α) and β (ER β ; **Figure 2**), which regulate cellular functions slowly by altering gene expression, and the group of membrane-associated ERs (mERs) that are located on the cellular surface and regulate cellular activity rapidly through altered signal transduction cascades. The most investigated mER is the G protein-coupled ER 1 (GPER), also known as G protein-coupled receptor 30 (GPR30), besides the two membrane-associated ERs α (mER α) and β (mER β); however, there is evidence that several other receptors such as ER-X, ERx and the G_q-coupled membrane ER (G_q-mER) may also play an important role in human physiology, especially neuronal signaling. All receptors share the common agonist E2, while all other known estrogens only individually activate selected ERs (Toran-Allerand *et al.*, 2002; Kampa *et al.*, 2012; Soltysik and Czekaj, 2013; Laredo *et al.*, 2014; Arnal *et al.*, 2017).

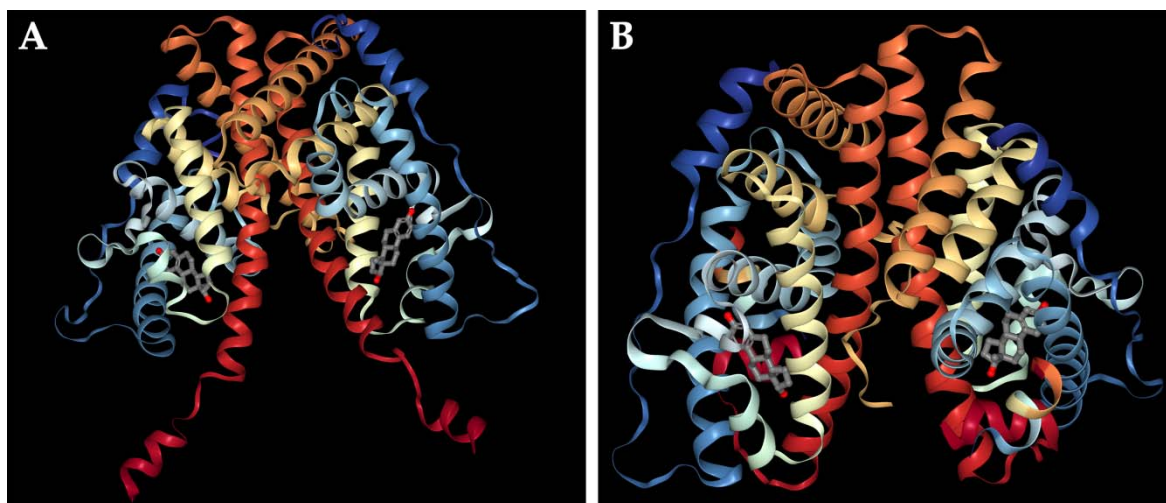


Figure 2: X-ray crystallography of the nuclear ERs. The ligand binding domains of (A) ER α and (B) ER β , both complexed to 17 β -estradiol, were generated using the RCSB Protein Data Bank based on experimental data from Tanenbaum *et al.* (1998) and Moecklinghoff *et al.* (2010). ER, estrogen receptor.

These receptors are essential for the function of numerous organ systems and therefore distributed over a variety of tissues. Nuclear ER α is mainly expressed in reproductive tissues, such as the ovaries, uterus, breast tissue and male testicles,

but also found in the bones, liver, kidney, cardiovascular system, brain and adipose tissue. In the uterus and ovaries, ER α -mediated effects are essential for organ maturation and function, regulation of the menstrual cycle and induction of cell proliferation and ovulation, consequently enabling female fertility. Correspondingly, in men, ER α regulates the development and function of the testicles, as well as spermatogenesis (Kuhl, 2005; Lee *et al.*, 2012; Bondesson *et al.*, 2015). Furthermore, ER α is the main receptor responsible for an estrogen-driven cell proliferation in the mammary gland, thereby mediating pubertal breast growth and development; however, in some cases, it may also induce carcinogenesis in the breast (Scaling *et al.*, 2014). Besides the stimulation of the reproductive system, ER α induces the formation of growth factors in the bones, regulating bone maintenance and preventing osteoporosis. In the brain, ER α signaling allows negative feedback on the hypothalamic-pituitary-gonadal (HPG) axis by reducing the release of both gonadotropins [follicle-stimulating hormone (FSH) and luteinizing hormone (LH)] and consequently controls the stimulation of the ovaries/testicles, but also protects against neurodegenerative disorders and stimulates synaptic remodeling (Hewitt *et al.*, 2000; Lee *et al.*, 2012).

Similar to ER α , ER β is localized in the ovaries, breast, bones, heart, adipose tissue, different endothelial cells (e.g. in the blood vessels, lungs, prostate or the intestine) and several parts of the brain (Babiker, 2002; Koehler *et al.*, 2005). However, ER β mediates anti-proliferative effects on the reproductive tissues, thereby opposing an ER α -induced cellular growth in the uterus and ovaries (Weihua *et al.*, 2000). In the breast, ER β is only involved in the maintenance of breast cell differentiation and function, but shows no stimulatory effect on mammary proliferation. It is therefore assumed that ER β acts as a tumor suppressor for several cancer entities (Kyriakidis and Papaioannidou, 2016; Thomas and Gustafsson, 2018). Moreover, ER β signaling protects against cardiovascular disease and acts as a neuroprotective agent, especially reducing the risk of Alzheimer's (Li *et al.*, 2014; Luo and Kim, 2016).

Also GPER is, similar to the nuclear ERs, expressed in the ovaries and testicles, where its stimulation modulates organ development and contributes to fertility. In the breast, however, GPER only controls the function of the gland, but does not mediate cell proliferation and is, like ER β , tumor suppressive (Hazell *et al.*, 2009; Chimento *et al.*, 2014; Scaling *et al.*, 2014). High expression of GPER can also be found in the blood vessel endothelium and kidneys, where it regulates key enzymes of the renin-angiotensin-aldosterone system, namely renin and the angiotensin-converting enzyme (ACE), thereby causing vasodilation, reducing blood pressure and protecting the cardiovascular system (Han *et al.*, 2013). GPER has also been reported as a tumor suppressor for various cancer entities (similar to ER β) through the stimulation of the mitogen-activated protein kinase (MAPK) pathway and modulation of epidermal growth factor receptors (Prossnitz and Arterburn, 2015). Of note, this has been reported for both estrogen-independent cancer types, including colorectal, non-small cell lung and gastric cancer (Zhu *et al.*, 2016; Liu *et al.*, 2017; Tian *et al.*, 2019), as well as for hormone-sensitive gynecological cancers of the breast and ovaries (Ariazi *et al.*, 2010; Ignatov *et al.*, 2013).

Estrogens in Gynecological Cancers

The importance of estrogens for the development and progression of hormone-sensitive cancers is undoubted, as several *in vitro* and *in vivo* studies have reported an induction of cellular proliferation upon exposure of reproductive tissues to steroid hormones. Most importantly, ER α has been proven responsible for this stimulation of cellular growth via mitogenic, intracellular changes, while ER β and GPER may counteract this activity and induce apoptosis. The expression status of ER α is therefore an important factor for the characterization of gynecological cancers and provides the molecular basis for the application of endocrine disruptive therapies (Thomas and Gustafsson, 2011; Awolaran, 2015).

Breast Cancer

Breast cancer is the most prevalent gynecological malignancy worldwide and, after lung cancer, the second leading cause of cancer mortality in women. Recent predictions have further estimated an increase in its incidence by up to 2.6% per year until 2030, especially in moderately to highly developed countries (Bray *et al.*, 2012). Nearly 80% of all breast tumors express ER α ; therefore, the presence of estrogens plays a pivotal role for carcinogenesis and disease progression (Toss and Cristofanilli, 2015). When breast epithelium is exposed to high levels of estrogens, mutations causing malignant transformation of the cells may occur (Scimeca *et al.*, 2019). An ~50% increased risk of breast cancer due to elevated total estrogen levels was found in a clinical study analyzing serum and urine samples from 2,822 postmenopausal women (Sampson *et al.*, 2017). In premenopausal women diagnosed with breast cancer before the age of 50 years old, a strong correlation between cancer risk and the follicular plasma concentrations of androgens and estrogens was observed, especially for total and free E2 levels (Eliassen *et al.*, 2006; Endogenous Hormones and Breast Cancer Collaborative Group, 2013). Moreover, estrogens drive the progression of breast cancer and contribute to migration and invasion. Data from 92 postmenopausal patients revealed a strong inverse association of disease-free interval duration with plasma estrogen levels. High circulating steroid hormone concentrations further stimulated the growth of micrometastases (Lønning *et al.*, 1996). Interestingly, this induction of breast cancer cell metastasis by estrogens may not be limited to ER α -expressing tumors, as some studies reported a possible pro-metastatic interaction of estrogens with other signaling targets, such as GPER (Jiang *et al.*, 2013).

The inhibition of estrogenic signaling is consequently a successful strategy to prevent breast cancer growth and progression. Several clinical studies revealed lower rates of metastasis and a significantly longer disease-free interval following treatment with anti-estrogens, thereby reducing mortality by up to 57%. Consequently, these therapies have been established as the gold standard in the treatment of breast cancer, at least for those expressing ER α (EBCTCG, 2005).

Ovarian Cancer

As compared with breast cancer, the global prevalence of epithelial ovarian cancer (EOC) is much lower, amounting for only 300,000 new cases in 2018 worldwide. However, its case fatality rate is markedly higher than that of breast cancer, causing nearly 200,000 deaths in the same year. EOC is thereby the fourth leading cause of cancer mortality among women, and the most fatal type of gynecological malignancy (Longuespée *et al.*, 2012; Bray *et al.*, 2018). Almost 75% of all EOC cases are classified as high-grade serous ovarian cancer (HGSOC), the most aggressive and lethal subtype, with a 5-year survival rate of <30% (Rainczuk *et al.*, 2014, Kroeger and Drapkin, 2017).

These poor numbers are most likely a result of the combination of a usually too late diagnosis and the lack of efficient treatment options for HGSOC. While most patients show a good response to standard therapy (surgery followed by chemotherapy with platinum-based drugs) in the beginning, up to 90% of all cases relapse already after one year and become resistant to chemotherapeutics (Mungenast and Thalhammer, 2014; Bowtell *et al.*, 2015). The presence of estrogens may be a key factor in the development and progression of HGSOC, as *in vitro* studies reported that a stimulation of ER α induces ovarian tumorigenesis and promotes morphological changes in cancer cells, thereby facilitating metastasis (Park *et al.*, 2008). Therefore, opposing estrogenic activity could be a novel approach for the treatment of recurrent and platinum-resistant HGSOC.

There are two major options to achieve a reduction of estrogenic activity in gynecological cancers: The first one includes direct ER inhibition with ER antagonists such as fulvestrant, or selective estrogen receptor modulators (SERMs), including tamoxifen. The second strategy aims at decreasing the tumor tissue concentration of active estrogens via the modulation of estrogen forming and metabolizing enzymes, such as the aromatase inhibitors anastrozole and letrozole (Riggins *et al.*, 2005).

Estrogen Biotransformation Pathways

In premenopausal women, estrogens are mainly produced in the ovaries via the “aromatase pathway” upon stimulation by FSH and LH from the precursor steroid dehydroepiandrosterone (DHEA) and its 3-*O*-sulfate (DHEA-S), which are initially formed from cholesterol (Rutkowski *et al.*, 2014; Rižner, 2016). First, DHEA is metabolized to the androgen 4-androstene-3,17-dione (AD) by two 3 β -hydroxysteroid dehydrogenases, namely hydroxysteroid dehydrogenase (HSD)3B1 and HSD3B2. AD is then further transformed via the aldo-keto reductase AKR1C3, also known as the 17 β -hydroxysteroid dehydrogenase type 5 (HSD17B5), to testosterone (T), a major androgen in women. Of note, while the dehydrogenation of DHEA to AD is irreversible, AD and T can be reversibly interconverted in both directions, using HSD17B2 or HSD17B3 for the backward reaction (Samavat and Kurzer, 2015; Rižner *et al.*, 2017).

Subsequently, the name-giving key-enzyme of this pathway, aromatase [cytochrome P450 (CYP)19A1], converts these two androgens, AD and T, irreversibly through the aromatization of the A-ring to the estrogens E1 and E2, respectively. Similar to AD and T, several 17 β -HSDs (HSD17B1, HSD17B2, HSD17B4, HSD17B7 and HSD17B12) also mediate the reversible conversion of E1 to E2 and vice versa, thereby controlling the levels of E2, and consequently estrogenic activity (Escande *et al.*, 2006; Kuhl, 2005; Hilborn *et al.*, 2017). The activity of E2 is further regulated by either the irreversible hydroxylation of E2 to E3, a much weaker estrogen, via CYP3A4, or the conjugation to completely inactive metabolites, as steroid conjugates cannot bind to the ERs and can therefore not exert estrogenic effects (Mueller *et al.*, 2015). The major conjugation reactions in women include the sulfotransferases (SULT)1A1 and 1E1-mediated sulfation of E1 and E2 to their respective 3-*O*-sulfates (E1-S and E2-S), as well as – to a lesser extent – the 3-*O*- β -D-glucuronidation of E2 to E2-G, which is catalyzed by the uridine 5'-diphospho-glucuronosyltransferase 1A1 (UGT1A1). Cellular efflux of these conjugates is subsequently achieved via the two ATP-binding cassette (ABC) transporters multidrug-resistant protein (MRP) 1 and 4. While

glucuronidation of estrogens mainly results in renal excretion of the metabolites, the sulfates remain in the bloodstream as an “inactive circulating pool” of estrogens (Purohit *et al.*, 2002; Mueller *et al.*, 2015; Samavat and Kurzer, 2015).

This is particularly important for the regulation of estrogen activity during and after menopause, when the ovarian estrogen production is almost quantitatively reduced and the formation of DHEA and AD is limited to the adrenal cortex. Aromatase expressed in several extragonadal tissues, especially adipose cells, undertakes then their conversion to estrogens, which are subsequently sulfated and released into the circulation (Labrie, 2015; Barakat *et al.*, 2016; Poschner *et al.*, 2019). After their uptake into target tissues through several organic-anion-transporting polypeptides (OATPs), including OATP1C1, OATP2B1, OATP3A1 and OATP4C1, these inactive sulfates can be reactivated by the action of the steroid sulfatase (STS) and again promote estrogenic activity via ER interaction. This mechanism is commonly known as the “sulfatase pathway” of estrogen formation (**Figure 3**) (Mueller *et al.*, 2015; Rižner, 2016; Rižner *et al.*, 2017).

Besides sulfation and glucuronidation, another possible, yet in humans minor, pathway of estrogen biotransformation is the hydroxylation of estrogens in position 2 (via CYP1A1, CYP1A2 or CYP3A4) or position 4 (via CYP1B1), which forms catechol estrogens that can be further oxidized to their respective semiquinones and quinones by enzymes such as CYPs or peroxidases. The latter highly reactive compounds might bind to DNA strands, thereby causing carcinogenesis of the affected tissues. Detoxification of these compounds is consequently essential for preserving cellular functions and integrity. Possible mechanisms are either the conjugation of the catechol estrogens to sulfates, glucuronides or O-methylates before they could be oxidized to their respective quinones, or the inactivation of these quinones via their conjugation with glutathione, or quinone reductase activity (Cavalieri and Rogan, 2016; Poschner *et al.*, 2019).

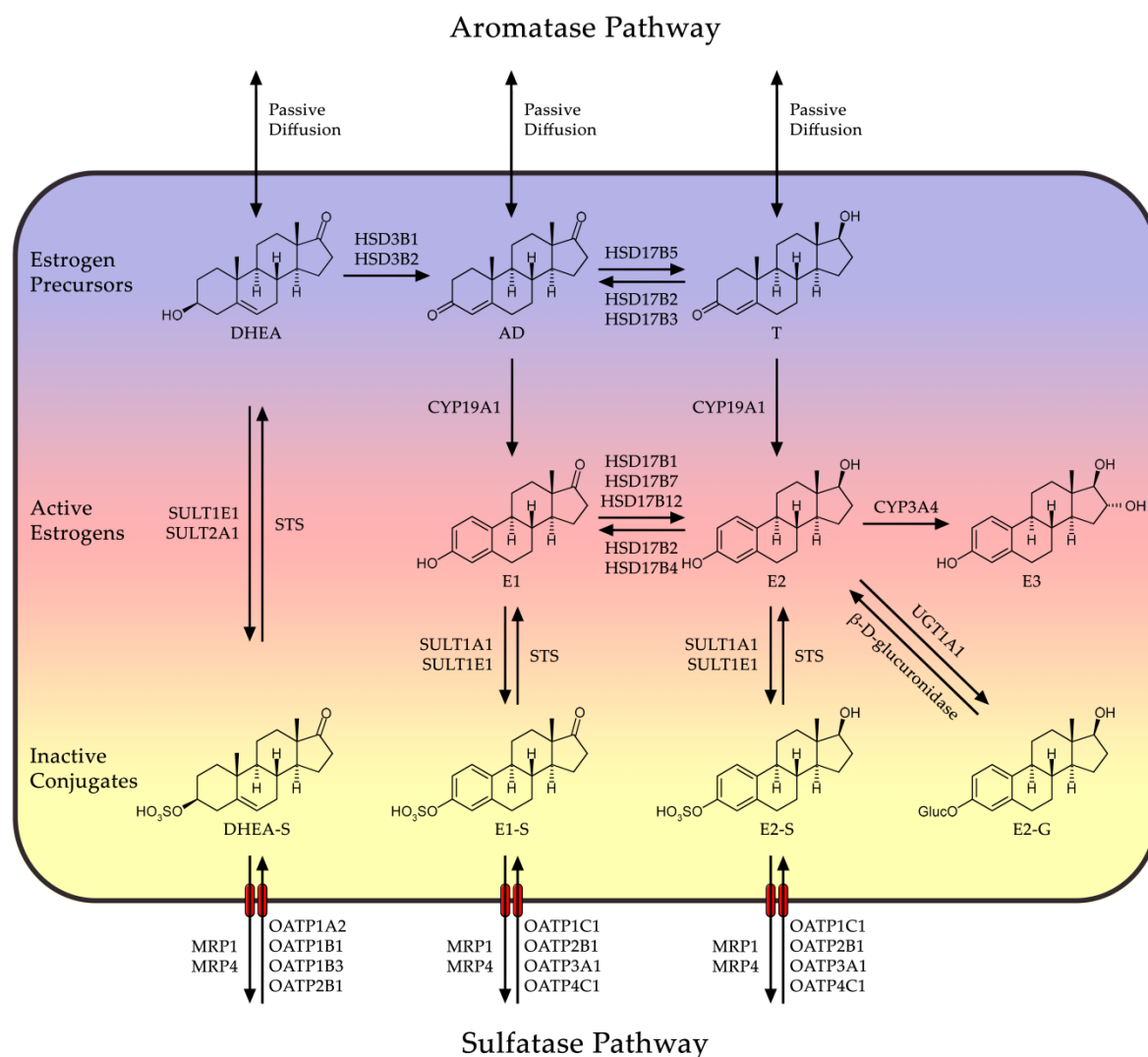


Figure 3: Estrogen formation and metabolism pathways. In the “aromatase pathway”, the estrogen precursor DHEA is converted into the active estrogens E1, E2 and E3 via the androgen intermediates AD and T. Subsequently, the reversible inactivation of the active hormones is mediated via SULTs or UGTs. These conjugates are then excreted via MRPs and can be re-uptaken via OATPs in the “sulfatase pathway” of estrogen formation. It should be noted that unconjugated steroids can diffuse unrestrictedly through cell membranes due to their lipophilicity. Data obtained from Mueller *et al.*, 2015 and figure modified from Poschner *et al.*, 2019. AD, 4-androstene-3,17-dione; CYP, cytochrome P450 isoenzyme; DHEA, dehydroepiandrosterone; DHEA-S, DHEA-3-O-sulfate; E1, estrone; E1-S, estrone-3-O-sulfate; E2, 17β-estradiol; E2-G, 17β-estradiol-3-O-(β-D-glucuronide); E2-S, 17β-estradiol-3-O-sulfate; E3, estriol; HSD, hydroxysteroid dehydrogenase; MRPs, multidrug resistance proteins; OATPs, organic-anion-transporting polypeptides; STS, steroid sulfatase; SULTs, sulfotransferases; T, testosterone; UGTs, uridine 5'-diphospho-glucuronosyltransferases.

Estrogens in Therapy

Due to their effects on estrogen responsive tissues, naturally occurring estrogens and their respective chemical derivatives can be used as hormonal contraception or for the treatment of several hormone-related medical conditions, including polycystic ovary syndrome, hypogonadism, infertility, androgen-dependent prostate cancer, and especially to compensate menopausal disorders (Oh, 2002; Christin-Maitre, 2017; Pinheiro *et al.*, 2017).

For the classical oral hormonal birth control, an estrogen, mostly the synthetic E2-analog ethinylestradiol or its prodrug mestranol, is applied in combination with a progestin (such as dienogest, levonorgestrel or norgestimate) to suppress FSH and LH release in the pituitary gland, which subsequently suppresses ovulation and prevents pregnancy (Evans and Sutton, 2015). Ethinylestradiol has been reported to be superior to E2, as it is less susceptible to first-pass metabolism in the intestine and liver and shows therefore a higher oral bioavailability (45 vs. 5%) (Stanczyk *et al.*, 2013; De Leo *et al.*, 2016). Ethinylestradiol is also used for transdermal contraceptive patches and intravaginal rings, while injectable contraceptives mostly require the application of depot estrogens, such as lipophilic E2 esters (**Figure 4**) (Düsterberg and Nishino, 1982). The same mechanism of action can also be employed for the treatment of androgen-dependent prostate cancer: While estrogens cannot stimulate the proliferation of prostate cancer cells, their presence suppresses the HPG axis, which causes a decrease in androgen plasma concentrations to castrate levels. Consequently, the resulting lack of androgens in the circulation inhibits further cancer growth (Oh, 2002; Ockrim *et al.*, 2006).

The major use of estrogens as medication, however, is still for hormone replacement therapy (HRT) in order to ameliorate menopausal disorders, such as hot flashes, vaginal atrophy, sexual dysfunction, sleep disturbance, depression, bone loss and osteoporosis, which are caused by the decrease of serum estrogen levels during and after menopause (Stuenkel *et al.*, 2015; Stute *et al.*, 2020). For this purpose, estrogens are regularly administered orally, via transdermal therapeutic

systems, locally as vaginal gels or injected into the muscular/subcutaneous tissue. The use of native E2, its esters or conjugated estrogens as HRT has been proven superior to any other synthetic treatment option, and the transdermal administration route is not only safer than oral application, but also most likely more effective (Bennink, 2004; Beck *et al.*, 2017).

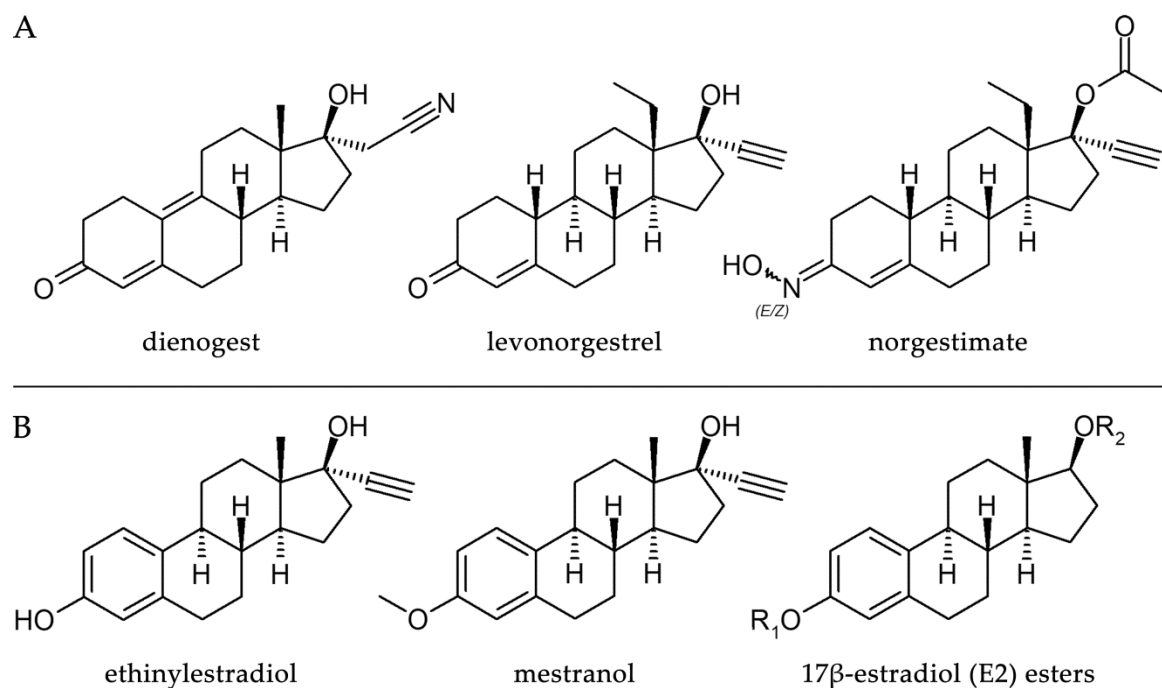


Figure 4: Chemical structures of synthetic (A) progestins and (B) E2 derivatives used in therapy. Typical E2 esters include benzoate, cypionate, dipropionate, enantate, undecylate and valerate. E2, 17β-estradiol.

Plant-Derived Alternatives to HRT

Considering the potential for severe adverse reactions upon the administration of classical HRT, many women seek natural, plant-derived estrogen alternatives to relieve their menopausal complaints. More than 300 plants have been reported to contain compounds with estrogenic activity, which are consequently increasingly marketed as dietary supplements or registered drugs against menopausal complaints worldwide, and especially in Western countries (Price and Fenwick, 1985; Patisaul and Jefferson, 2010). Several studies have been conducted that prove the efficacy of these products for the treatment of psychological and somatic-

vegetative symptoms (e.g. hot flashes), as well as against bone loss, dyslipidaemia or similar menopause-related health concerns in postmenopausal women. Their application is consequently highly recommended for women with moderate symptoms to increase quality of life during the climacteric period (Speroff, 2005; Beer and Neff, 2013; Rosic *et al.*, 2013).

Most of these products contain compounds that are generally classified as “phytoestrogens”, a large group of plant substances and metabolites that share the mutual ability to modulate endogenous estrogen levels or transduce estrogenic activity via ER interaction (Sunita and Pattanayak, 2011). Phytoestrogens are naturally occurring in soy beans and other legumes, clover and various fruits or berries. Several structural classes have been identified to date, including isoflavones, chalcones, coumestans, lignans and diphenolic compounds such as stilbenoids (Patisaul and Jefferson, 2010; Di Gioia and Petropoulos, 2019). Although these structures are widely inhomogeneous, all of these compounds possess the same core scaffold of two phenolic hydroxyl groups in the distance of 11 to 12 Å, which mimics the structure of estrogens (Lee and Barron, 2017).

Furthermore, several non-phytoestrogenic herbal treatment options have been described, whose main constituents do not contain an estrogen-like structure and therefore do not exert estrogenic effects. The best established and most investigated plant of this group is black cohosh (*Actaea racemosa* L.), but dong quai (*Angelica sinensis* (Oliv.) Diels), chasetree (*Vitex agnus-castus* L.), wild yam (*Dioscorea villosa* L.) and evening primrose (*Oenothera biennis* L.) have also been successfully used for the relief of somatic-vegetative climacteric symptoms, especially hot flashes. Extracts of these plants are often used in combination with ginkgo (*Ginkgo biloba* L.), ginseng (*Panax ginseng* C. A. Mey), kava (*Piper methysticum* G. Forst.), valerian (*Valeriana officinalis* L.), motherwort (*Leonorus cardiaca* L.) or St. John’s wort (*Hypericum perforatum* L.), which have been established as treatment options for concomitant psychological complaints, such as sleep disturbance, depression or mood swings. However, most of these herbal treatments have only been applied based on their “traditional use” for decades, or

even centuries, and the data on the mechanisms of action or clinical evidence of their efficacy and safety are scarce, and even conflicting (Geller and Studee, 2006). More recently, a pollen extract from various cereal grasses, including rye (*Secale cereale* L.), orchard grass (*Dactylis glomerata* L.) and corn (*Zea mays* L.), was sold as a “novel, non-estrogenic alternative” for menopausal treatment based on a single clinical study, even though no active constituents had been determined yet (Hellström and Muntzing, 2012).

Soy Isoflavones

The most studied phytoestrogens are the isoflavones genistein (4',5,7-trihydroxyisoflavone) and daidzein (4',7-dihydroxyisoflavone) from soy (*Glycine max* (L.) Merr.), which amount for ~47 and 44% of the total isoflavone content in soybeans (**Figure 5**). In native plant material, genistein and daidzein are predominantly present as their respective glycosylated conjugates, mostly malonyl- β -D-glucosides besides the β -D-glucosides genistin and daidzin, while only a very minor amount of free aglycones (1-2%) can be found. Subsequent heat-treatment and fungal fermentation of soy beans results in β -D-glucosidase-mediated hydrolysis of the sugar moieties; consequently, the aglycone content in processed soy products, such as tofu or tempeh, is strongly increased, amounting for 37 and 50% of the total isoflavone content, respectively (Murphy *et al.*, 2002; Wisemann *et al.*, 2002; Clarke *et al.*, 2008).

This amount of unconjugated genistein and daidzein is essential for the *in vivo* activity of soy products, as conjugated isoflavones cannot be directly absorbed through the intestinal wall following oral consumption. The cleavage of the sugar side-chain may also be mediated by gut microbiota in the intestine; however, a huge inter- and intraindividual variation depending on the composition of the intestinal microflora has been observed. Therefore, isoflavone supplementation for therapeutic purposes should be based on purified aglycones only, or needs application of bioavailability enhancers such as lipid-based formulations and complexation with cyclodextrins (Okabe *et al.*, 2011; Vitale *et al.*, 2013).

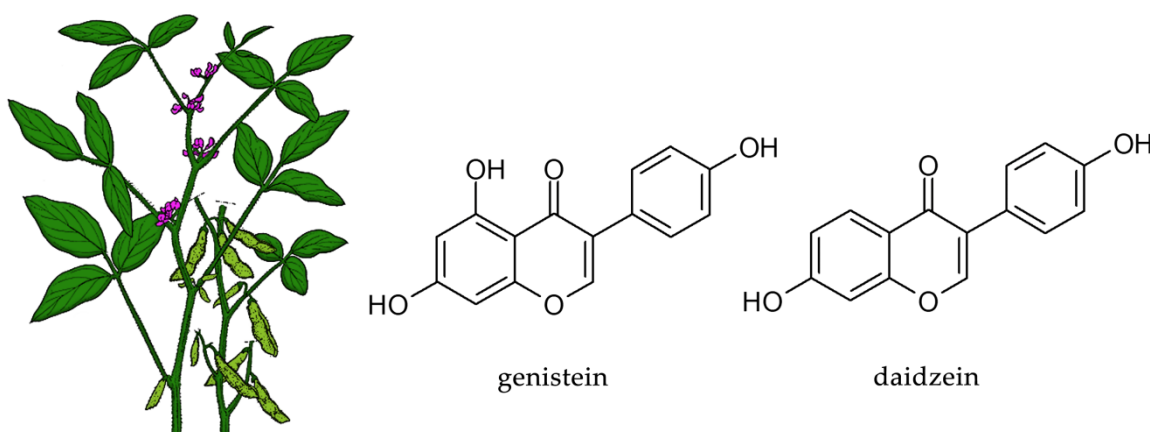


Figure 5: Botanical illustration of soy and the chemical structures of its major isoflavones genistein and daidzein. Illustration adapted and colorized from Wikimedia Commons (2020a).

Several clinical studies have confirmed the beneficial effects of soy isoflavones on climacteric complaints and menopause-related health concerns. Daily treatment of postmenopausal women with 54 mg genistein over 24 months revealed a significant increase (+13%) in bone mineral density, but also a decline in the placebo cohort (-7%), suggesting that genistein not only reduces osteoporosis, but even counteracts it (Arcoraci *et al.*, 2017). The same amount of isoflavones (54 mg) also reduced the severity and intensity of menopausal symptoms by up to 65% within 8 weeks (Husain *et al.*, 2015). Similar results were also found with regard to the reduction of somatic and urogenital menopausal symptoms besides improvement of the cardiovascular and bone system in a Taiwanese and a Spanish trial, using 35 mg/day soy extract for 6 months and 50 mg/day soy isoflavones for 12 weeks, respectively, consequently proving an increase in quality of life (Yang *et al.*, 2012; Tranche *et al.*, 2016). Moreover, the daily intake of 30 mg genistein by 84 postmenopausal women reduced the frequency, severity and duration of hot flashes by 51% within 12 weeks (Evans *et al.*, 2011). By contrast, a clinical study including 270 postmenopausal women found no significant reduction of menopausal symptoms following the consumption of soy flour (40 g/day) or purified daidzein (63 mg/day) (Liu *et al.*, 2014).

The same controversy also exists around the safety of soy products, due to

their estrogenic properties: While most clinical studies have reported no increase of adverse effects, especially concerning malignancies of the endometrium or the breast, upon soy supplementation (Palacios *et al.*, 2010; Quaas *et al.*, 2013), a metaanalysis of 174 clinical trials reported phytoestrogen-related side effects, including mainly gastrointestinal disorders, as well as headaches and sleepiness (Tempfer *et al.*, 2009). Following treatment with soy in 140 women, an overexpression of cell cycle regulating genes in favor of increased proliferation was observed when genistein plasma levels were increased, thereby possibly increasing the risk of breast cancer (Shike *et al.*, 2014). However, the appearance and severity of adverse reactions upon isoflavone intake is dependent on several factors, including the patient dietary and health status, age and composition of the gut microbiome, resulting in a huge variability, therefore rendering further studies confirming the safety of soy products, especially high-dose supplements (>100 mg), highly warranted (Kass-Annese, 2000; Fritz *et al.*, 2013).

Resveratrol

Another naturally occurring compound promoting estrogenic effects *in vivo* is resveratrol (*trans*-3,5,4'-trihydroxystilbene), a stilbenoid polyphenol that can be mainly found in the skin of grapes or other berries (**Figure 6**), nuts and products thereof, such as red wine or peanut butter (Aiyer *et al.*, 2012).

Based on its chemical structure, resveratrol cannot only interact with ERs, but is also an effective radical scavenger and anti-oxidative agent (Bors *et al.*, 1990). Furthermore, it affects cellular signaling via the inhibition of kinases, sirtuins, adenylyl cyclases or the transcription factors *TP53*, *NF-κB* and *Bcl-2*, and inhibits cyclooxygenase-2, thereby preventing the formation of inflammatory prostaglandins (Kim *et al.*, 2004; Pirola and Fröjdö, 2008; Csaki *et al.*, 2009).

For these reasons, resveratrol is widely marketed to reduce body weight and blood sugar levels, as an anti-aging agent or for neuro- and cardioprotection. It may even prevent or alleviate severe chronic conditions, such as the metabolic syndrome, which includes diabetes, obesity and hypertension, or Alzheimer's

disease, and has been proven to enhance bone health by increasing the two key bone biomarkers, serum- and bone alkaline phosphatase, consequently reducing the risk of osteoporosis (Kasiotis *et al.*, 2013; Kulashekar *et al.*, 2018; Asis *et al.*, 2019). Moreover, as many of the factors inhibited by resveratrol are crucial for cell proliferation, it has also been reported as a natural treatment option against carcinogenesis and tumor progression. Indeed, a study conducted by Levi *et al.* (2005) including 971 female patients revealed that the daily intake of 230 g grapes (corresponding to 126.4 μg resveratrol) cut the risk of breast cancer development almost in half (OR: 0.55).

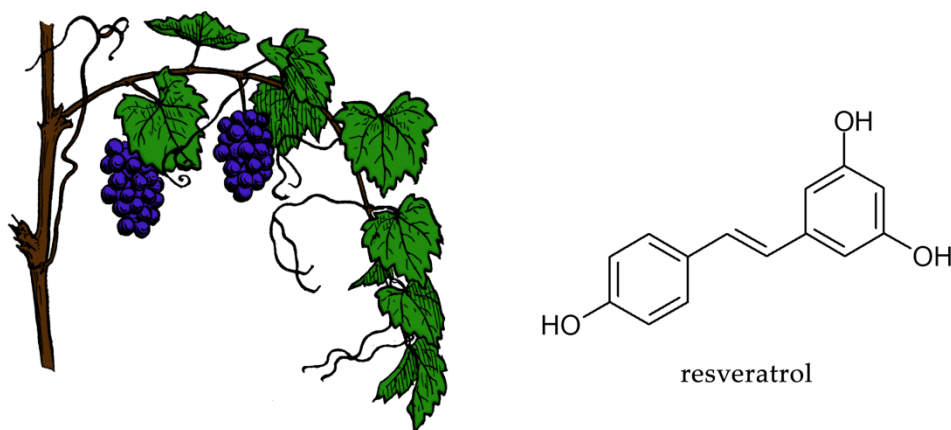


Figure 6: Resveratrol (*trans*-3,5,4'-trihydroxystilbene), a phytoestrogenic polyphenol, is mainly found in the skin of grapes. Botanical illustration of the common grape vine (*Vitis vinifera* L.), adapted and colorized from Wikimedia Commons (2020b).

Additionally, data from double-blinded, placebo-controlled clinical trials have suggested that resveratrol may be an effective treatment option for the relief of climacteric complaints during and following menopause. Psychological symptoms and cognitive function were improved in 80 postmenopausal women (aged 45-85) following twice daily administration of 75 mg resveratrol for 14 weeks (Evans *et al.*, 2017). The treatment of 50 menopausal women with resveratrol also significantly reduced the number and intensity of hot flashes by 57.1 and 78.6%, respectively (Leo *et al.*, 2015), strengthening its use against vasomotor disorders, which was further supported by another study proving the efficacy of a sublingual

resveratrol spray in 30 climacteric women (Milia, 2015). Of note, these effects of resveratrol against menopausal disorders can even be potentiated when administered in combination with other phytoestrogens, such as soy isoflavones (Davinelli *et al.*, 2017).

Black Cohosh

Black cohosh, scientifically termed *Actea racemosa* L. (or former *Cimicifuga racemosa* L.), is a North American herb from the buttercup family, whose roots and rhizomes have been used for centuries in Native American traditional medicine for the treatment of gynecological conditions, such as amenorrhea or menopause (McKenna *et al.*, 2001). In contemporary medicine, black cohosh extract is certainly the most studied non-phytoestrogenic plant and marketed in over 40 countries on all continents (Schaper & Brümmer GmbH, 2020). It contains several triterpene glycosides as active constituents, with actein as the main compound (**Figure 7**), in addition to tannins, various acids, starch and sugars.

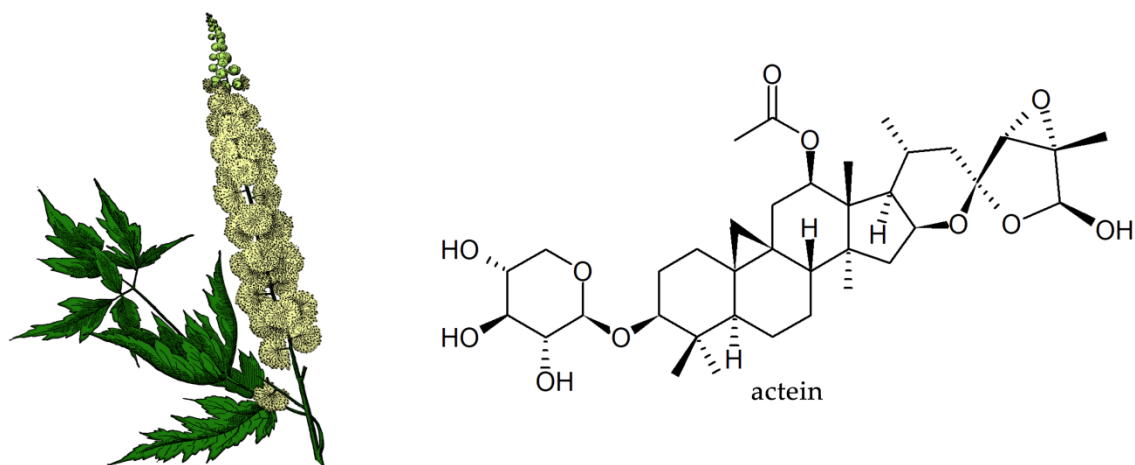


Figure 7: Black cohosh (*Actea racemosa* L.) and its major active constituent actein. Botanical illustration adapted and colorized from Wikimedia Commons (2020c).

Earlier studies have also reported that black cohosh contains the isoflavone formononetin and therefore exhibits estrogenic properties; however, more recent analyses could not confirm the presence of this compound in any plant material or

extract (Jiang *et al.*, 2006; Avula *et al.*, 2009; Ross, 2012). Indeed, no phytoestrogenic effects were observed in two major clinical trials that included data from >10,000 and 35,000 postmenopausal women, respectively (Obi *et al.*, 2009; Brasky *et al.*, 2010).

Numerous other clinical studies have been conducted that prove the efficacy of black cohosh against menopause-related symptoms, such as sleep disturbance, sweating and especially hot flashes (Rostock *et al.*, 2011; Jiang *et al.*, 2015). A study in 244 women even found that daily supplementation with 5 mg black cohosh extract for 12 weeks is as effective as classical synthetic HRT with tibolone (2.5 mg p. o. daily) against vasomotor disorders (Bai *et al.*, 2007). However, the safety of black cohosh during long-term supplementation is approached with caution, as certain cases of severe liver damage (including hepatitis and liver failure) have been reported (Adnan *et al.*, 2014). By contrast, data from much larger cohorts could not verify this connection, as no changes in liver function tests were observed (Thomsen and Schmidt, 2003; Tanmahasamut *et al.*, 2015). Still, monitoring liver enzymes is therefore advised as a cautionary measure in women taking black cohosh extract as long-term treatment (Ross, 2012).

Mechanisms of Action of Phytoestrogens

While data concerning the detailed mechanisms of non-phytoestrogenic plants against menopausal complaints are scarce, the binding of classical phytoestrogens to the ERs due to their structural similarity with E2 has been thoroughly studied. In comparison to endogenous E2, which transactivates both nuclear ER subtypes equally, phytoestrogens preferably bind to ER β than ER α , thereby promoting ER β -related health benefits, whereas ER α -mediated stimulation of cell proliferation in reproductive tissues is much less pronounced. Genistein and daidzein, for example, exhibit 500- and 850-fold lower EC₅₀ concentrations for ER β than ER α (Kostelac *et al.*, 2003; Messina, 2016; Rietjens *et al.*, 2017).

Moreover, their potency in activating ER-related signal transduction is up to six orders of magnitude lower than that of E2, causing “endocrine disruption”, as

the presence of the weak phytoestrogens displaces receptor-binding of more potent endogenous estrogens, which results in an overall antagonistic effect and suppression of hormonal signaling (Shanle and Xu, 2011; van Duursen, 2017). On the other hand, the circulating levels of phytoestrogens following dietary intake or administration as therapeutic supplements are ~100,000-fold higher than the average E2 plasma concentrations in postmenopausal women, possibly leading to increased ER-mediated cell activity (van der Velpen *et al.*, 2014). Based on these bilateral properties, phytoestrogens are often classified as SERMs that can both induce and inhibit estrogen-related effects dependent on the hormonal status *in vivo* (Oseni *et al.*, 2008).

In addition to ER-interaction, phytoestrogens also act as radical scavengers, mediate serotonergic effects and affect several epigenetic mechanisms, including histone modification and DNA methylation. Furthermore, they regulate important factors for cell proliferation and apoptosis, such as DNA topoisomerases, tyrosine- and serin/threonine-kinases (e.g. MAPK) and transcription factors such as NF- κ B, which may contribute to the often proposed anti-cancer effects of phytoestrogens (Vina *et al.*, 2011; Hajirahimkhan *et al.*, 2013; Ming *et al.*, 2013; Rietjens *et al.*, 2013).

However, data concerning possible side-effects of phytoestrogens remain conflicting, especially with regard to the development and progression of hormone-sensitive malignancies, such as breast or ovarian cancer. While certain studies have concluded that high phytoestrogen levels may reduce the risk of cancer (Fritz *et al.*, 2013; Lee *et al.*, 2016), others have pointed out that more physiological doses could even promote tumor growth (Ju *et al.*, 2006; Mense *et al.*, 2008). A possible explanation for this discrepancy may be an impact of phytoestrogens on the endogenous metabolism of steroid hormones. Several *in vitro* and *in vivo* studies documented a pronounced inhibition of enzymes involved in estrogen biotransformation by phytoestrogens. The soy isoflavones genistein and daidzein, for example, have been proven to inhibit SULT1A1, SULT1A3 and SULT1E1, as well as UGT1A1, different 3 β - and 17 β -HSDs and various members of all CYP families at low- or even sub-micromolar concentrations. Similarly,

resveratrol, as well as the isoflavones quercetin and naringenin, affect the activity of estrogen-metabolizing enzymes, including CYPs, SULTs and STS, thereby influencing hormonal homeostasis in favor of increased active E2 levels (Harris *et al.*, 2004; Mohamed and Frye, 2011; van Duursen, 2017).

Estrogen Metabolism in Disease

In the last decades, altered metabolic activities of enzymes responsible for steroid biotransformation have been reported in various diseases, especially different types of cancers, but also in autoimmune disorders such as systemic lupus erythematosus, and gynecological diseases such as endometriosis (Lahita *et al.*, 1982; Huhtinen *et al.*, 2012; Asavasupreechar *et al.*, 2019).

The metabolism of estrogens is a key factor in the progression and metastasis of cancer, as increased estrogen formation with a concurrent loss of the cellular ability to deactivate these steroids fuels their intracellular activity. The analysis of 794 breast cancer specimens revealed that 17HSD5 and 17HSD1, both driving the formation of estrogens in the “aromatase pathway” by converting AD to T and E1 to E2, respectively, are often overexpressed in breast cancer; an overexpression that was found to be correlated with a poorer survival (Oduwale *et al.*, 2004). Similarly, Shibuya *et al.* (2008) observed up to 18-fold increases in the levels of 17 β -HSDs and 4-fold increases in the levels of aromatase in malignant tissues, as compared with non-malignant ones. Furthermore, the levels of STS were also found to be elevated 9.5-fold, suggesting that the formation of estrogens can not only be strongly increased via the “aromatase pathway”, but also via the “sulfatase pathway” in cancer. On the other hand, a decreased activity and expression of SULT1A1, SULT1E1 and SULT2A1, the major enzymes responsible for the inactivation of estrogens, has been observed in different tumor tissues (e.g. breast or liver), as compared to their respective surroundings, resulting in an accumulation of active steroid hormones in the cancer cells (McNamara *et al.*, 2013; Xie *et al.*, 2017). The same reduction of SULT1E1 expression concomitant with increased STS activity was also found in patients with endometriosis, further

driving disease severity and progression by providing an intracellular pile-up of active E2 (Piccinato *et al.*, 2016).

A possible explanation for these reported metabolic changes may be the increased inflammatory status of the affected cells. Indeed, inflammatory cytokines, such as TNF α , interleukin (IL)-6, IL-11 or prostaglandins, have been proven to stimulate the expression of aromatase in adipose tissues, thereby increasing the circulating levels of active E2 in obese patients (Zahid *et al.*, 2016). In diseases associated with chronic liver inflammation, such as steatosis and diabetic or alcoholic cirrhosis, a strong reduction in the activity of SULT1A1, SULT1E1 and SULT2A1 was observed, which further correlated with disease severity (Yalcin *et al.*, 2013). Similarly, in endometriosis, which is characterized by a chronic inflammation of the endometriotic lesions, IL-1 α and -1 β may inhibit the expression of SULTs and promote the “sulfatase pathway” via increased STS activity (Piccinato *et al.*, 2016).

Metabolomic analysis of active estrogens in relation to their respective precursors or metabolites may therefore also reflect the inflammatory status of cells in various diseases. Future research investigating this correlation of estrogens with the onset or progression of diseases, as well as developing rapid and comprehensive metabolomic assays, is consequently highly warranted.

Estrogen Analytics

Accurate quantification of steroid hormones has been a challenge in analytical chemistry for decades. Due to their low abundance in biological samples, mostly in the pg/ml range (**Table 1**), sensitivity of metabolomic assays needs to be extremely high to ensure detection and accurate quantification of all relevant metabolites (Wang *et al.*, 2015a).

Another major problem to overcome is selectivity, as many steroids are very similar to each other (e.g. AD and T, or E1 and E2) and consequently possess almost identical chemical properties. On the other hand, the polarity range of all metabolites in the estrogenic pathway is wide, ranging from highly hydrophilic

conjugates, such as E2-G, to apolar steroid aglycones, such as AD. Conventional enzyme-linked immunosorbent assays (ELISAs) often fail to discriminate between conjugated and unconjugated steroids, which results in inaccurate values for unconjugated hormones or only allows for an estimation of the total hormone concentrations. Furthermore, most commercially available ELISA kits lack adequate validation, causing unreliable results (Stanczyk *et al.*, 2003). The use of radiolabeled molecules for immunoassays (radioimmunoassays) certainly increases sensitivity and selectivity (Shirtcliff *et al.*, 2000); however, in addition to requiring special precautions due to the radioactivity of the “hot” antigens used, these methods still fail to sufficiently quantify estrogens and their metabolites in postmenopausal women (Wang *et al.*, 2005; Santen *et al.*, 2007).

Table 1. Median serum concentrations of selected steroids involved in the metabolic pathway of estrogens in healthy postmenopausal women.

Analyte	Conc.	Analyte	Conc.	Analyte	Conc.
AD	440 pg/ml	E1	14.6 pg/ml	E1-S	170 pg/ml
DHEA	1.9 ng/ml	E2	3.4 pg/ml	E2-G	2.5 pg/ml
DHEA-S	600 ng/ml	E3	13.5 pg/ml	T	140 pg/ml

Data obtained from Audet-Walsh *et al.*, 2011 and Fuhrman *et al.*, 2012. AD, 4-androstene-3,17-dione; DHEA, dehydroepiandrosterone; DHEA-S, DHEA-3-O-sulfate; E1, estrone; E1-S, estrone-3-O-sulfate; E2, 17 β -estradiol; E2-G, 17 β -estradiol-3-O-(β -D-glucuronide); E3, estriol; T, testosterone.

The current state of the art methods are therefore based on chromatographic separation of the analytes using gas chromatography (GC) or high-performance liquid chromatography (LC) to increase selectivity before mass spectrometry (MS)-based quantification (Wang *et al.*, 2015b; Hennig *et al.*, 2018; Moon *et al.*, 2018). Sensitivity can also be further improved via concentrating the samples during sample preparation, e.g. on solid phase extraction (SPE) cartridges (Qin *et al.*,

2008). However, these techniques require stable isotope internal standards to compensate for losses during sample extraction and preparation, matrix effects and variable ionization efficacy of the molecules (Wang *et al.*, 2015a). Ideally, ^{13}C -labeled steroid analogues are used for this purpose, as these show identical elution characteristics, as compared with the unlabeled analytes. By contrast, deuterated standards might slightly separate from the target compounds on column, potentially resulting in differential ion suppression and biased quantification results. Nevertheless, ^{13}C -labeled standards are far more expensive than deuterated ones and not commercially available for all analytes, especially estrogen conjugates (Bussy *et al.*, 2017).

To enhance ionization efficacy in the applied electrospray ionization (ESI) or atmospheric pressure chemical ionization (APCI) sources, many LC-MS methods rely on pre-column derivatization of the analytes using reagents like dansyl chloride or pentafluorobenzyl bromide (Lin *et al.*, 2007; Penning *et al.*, 2010; Wang *et al.*, 2015b). Similarly, all GC-MS assays need derivatization to allow vaporization of the analytes, usually by introducing trimethylsilyl-groups into the molecules (Moon *et al.*, 2018). However, these procedures cause hydrolysis of conjugated metabolites, so that conjugated and unconjugated estrogens cannot be discriminated anymore. Consequently, only total steroid levels can be quantified in a single analysis (Wang *et al.*, 2015a) or sophisticated methods are required to achieve separate quantification. Recently, assays using SPE fractionation of conjugated and unconjugated steroids have been described, where the first fraction containing the intact conjugates (showing adequate ionization in negative ESI mode) is quantified directly, while the unconjugated analytes in the second fraction are subsequently derivatized and analyzed separately in positive ionization mode (Zhao *et al.*, 2014; van der Berg, 2020). Other studies have developed LC-MS assays that can be conducted without prior derivatization of the analytes (Harwood *et al.*, 2009; Tournier *et al.*, 2015; Wooding *et al.*, 2015), allowing a simultaneous analysis of estrogens and their respective conjugated metabolites. However, these techniques are mostly restricted to few selected compounds of

interest instead of covering the whole metabolomic pathway, and their lower limits of quantification are usually only low for conjugated metabolites, while those for unconjugated steroids are much higher, as compared with assays using pre-column derivatization. Therefore, the development of rapid and sensitive analytical assays is essential before comprehensive targeted metabolomics of estrogens may be established as a routine in clinical practice.

References

- Adnan, M. M.; Khan, M.; Hashmi, S.; Hamza, M.; Abdulmujeeb, S.; Amer, S. Black Cohosh and Liver Toxicity: Is There a Relationship? *Case Reports in Gastrointestinal Medicine* **2014**, 2014, 1–3.
- Aiyer, H. S.; Warri, A. M.; Woode, D. R.; Hilakivi-Clarke, L.; Clarke, R. Influence of berry polyphenols on receptor signaling and cell-death pathways: implications for breast cancer prevention. *Journal of Agricultural and Food Chemistry* **2012**, 60, 5693–5708.
- Arcoraci, V.; Atteritano, M.; Squadrito, F.; D'Anna, R.; Marini, H.; Santoro, D.; Minutoli, L.; Messina, S.; Altavilla, D.; Bitto, A. Antiosteoporotic Activity of Genistein Aglycone in Postmenopausal Women: Evidence from a Post-Hoc Analysis of a Multicenter Randomized Controlled Trial. *Nutrients* **2017**, 9, pii: E179.
- Ariazi, E. A.; Brailoiu, E.; Yerrum, S.; Shupp, H. A.; Slifker, M. J.; Cunliffe, H. E.; Black, M. A.; Donato, A. L.; Arterburn, J. B.; Oprea, T. I.; Prossnitz, E. R.; Dun, N. J.; *et al.* The G protein-coupled receptor GPR30 inhibits proliferation of estrogen receptor-positive breast cancer cells. *Cancer Research* **2010**, 70, 1184–1194.
- Arnal, J.-F.; Lenfant, F.; Metivier, R.; Flouriot, G.; Henrion, D.; Adlanmerini, M.; Fontaine, C.; Gourdy, P.; Chambon, P.; Katzenellenbogen, B.; Katzenellenbogen, J. Membrane and Nuclear Estrogen Receptor Alpha Actions: From Tissue Specificity to Medical Implications. *Physiological Reviews* **2017**, 97, 1045–1087.
- Asavasupreechar, T.; Chan, M. S. M.; Saito, R.; Miki, Y.; Boonyaratanakornkit, V.; Sasano, H. Sex steroid metabolism and actions in non-small cell lung carcinoma. *The Journal of Steroid Biochemistry and Molecular Biology* **2019**, 193, 105440.
- Asis, M.; Hemmati, N.; Moradi, S.; Nagulapalli Venkata, K. C.; Mohammadi, E.; Farzaei, M. H.; Bishayee, A. Effects of resveratrol supplementation on bone biomarkers: a systematic review and meta-analysis. *Annals of the New York Academy of Sciences* **2019**, 1457, 92–103.
- Audet-Walsh, É.; Lépine, J.; Grégoire, J.; Plante, M.; Caron, P.; Têtu, B.; Ayotte, P.; Brisson, J.; Villeneuve, L.; Bélanger, A.; Guillemette, C. Profiling of Endogenous Estrogens, Their Precursors, and Metabolites in Endometrial Cancer Patients: Association with Risk and Relationship to Clinical Characteristics. *The Journal of Clinical Endocrinology & Metabolism* **2011**, 96, E330–E339.
- Avula, B.; Wang, Y. H.; Smillie, T. J.; Khan, I. A. Quantitative determination of triterpenoids and formononetin in rhizomes of black cohosh (*Actaea racemosa*) and dietary supplements by using UPLC-UV/ELS detection and identification by UPLC-MS. *Planta Medica* **2009**, 75, 381–386.
- Awolaran, O. T. Cellular Mechanisms of Oestrogen in Breast Cancer Development. *The Open Access Journal of Science and Technology* **2015**, 3, 1–7.
- Babiker, F. Estrogenic hormone action in the heart: regulatory network and function. *Cardiovascular Research* **2002**, 53, 709–719.

- Bai, W.; Henneicke-von Zepelin, H. H.; Wang, S.; Zheng, S.; Liu, J.; Zhang, Z.; Geng, L.; Hu, L.; Jiao, C.; Liske, E. Efficacy and tolerability of a medicinal product containing an isopropanolic black cohosh extract in Chinese women with menopausal symptoms: a randomized, double blind, parallel-controlled study versus tibolone. *Maturitas* **2007**, *58*, 31–41.
- Barakat, R.; Oakley, O.; Kim, H.; Jin, J.; Ko, C. J. Extra-gonadal sites of estrogen biosynthesis and function. *BMB Reports* **2016**, *49*, 488–496.
- Beck, K. L.; Anderson, M. C.; Kirk, J. K. Transdermal estrogens in the changing landscape of hormone replacement therapy. *Postgraduate Medicine* **2017**, *129*, 632–636.
- Beer, A. M.; Neff, A. Differentiated Evaluation of Extract-Specific Evidence on Cimicifuga racemosa's Efficacy and Safety for Climacteric Complaints. *Evidence-based Complementary and Alternative Medicine* **2013**, *2013*, 860602.
- Bennink, H. J. C. Are all estrogens the same? *Maturitas* **2004**, *47*, 269–275.
- Bondesson, M.; Hao, R.; Lin, C.-Y.; Williams, C.; Gustafsson, J.-Å. Estrogen receptor signaling during vertebrate development. *Biochimica et Biophysica Acta (BBA) - Gene Regulatory Mechanisms* **2015**, *1849*, 142–151.
- Bors, W.; Heller, W.; Michel, C.; Saran, M. Flavonoids as antioxidants: determination of radical-scavenging efficiencies. *Methods in Enzymology* **1990**, *186*, 343–355.
- Bowtell, D. D.; Böhm, S.; Ahmed, A. A.; Aspuria, P. J.; Bast, R. C.; Beral, V.; Berek, J. S.; Birrer, M. J.; Blagden, S.; Bookman, M. A.; Brenton, J. D.; Chiappinelli, K. B.; *et al.* Rethinking ovarian cancer II: reducing mortality from high-grade serous ovarian cancer. *Nature Reviews Cancer* **2015**, *15*, 668–679.
- Brasky, T. M.; Lampe, J. W.; Potter, J. D.; Patterson, R. E.; White, E. Specialty supplements and breast cancer risk in the VITamins And Lifestyle (VITAL) Cohort. *Cancer Epidemiology, Biomarkers & Prevention* **2010**, *19*, 1696–1708.
- Bray, F.; Jemal, A.; Grey, N.; Ferlay, J.; Forman, D. Global cancer transitions according to the Human Development Index (2008-2030): a population-based study. *Lancet Oncology* **2012**, *13*, 790–801.
- Bray, F.; Ferlay, J.; Soerjomataram, I.; Siegel, R. L.; Torre, L. A.; Jemal, A. Global cancer statistics 2018: GLOBOCAN estimates of incidence and mortality worldwide for 36 cancers in 185 countries. *CA - A Cancer Journal for Clinicians* **2018**, *68*, 394–424.
- Bussy, U.; Chung-Davidson, Y.-W.; Buchinger, T. J.; Li, K.; Li, W. High-sensitivity determination of estrogens in fish plasma using chemical derivatization upstream UHPLC–MSMS. *Steroids* **2017**, *123*, 13–19.
- Cavalieri, E. L.; Rogan, E. G. Depurinating estrogen-DNA adducts, generators of cancer initiation: their minimization leads to cancer prevention. *Clinical and Translational Medicine* **2016**, *5*, 12.
- Chimento, A.; Sirianni, R.; Casaburi, I.; Pezzi, V. Role of Estrogen Receptors and G Protein-Coupled Estrogen Receptor in Regulation of Hypothalamus–Pituitary–Testis Axis and Spermatogenesis. *Frontiers in Endocrinology* **2014**, *5*, 1.
- Christin-Maitre, S. Use of Hormone Replacement in Females with Endocrine Disorders. *Hormone Research in Paediatrics* **2017**, *87*, 215–223.
- Clarke, D. B.; Bailey, V.; Lloyd, A. S. Determination of phytoestrogens in dietary supplements by LC-MS/MS. *Food Additives & Contaminants: Part A: Chemistry, Analysis, Control, Exposure & Risk Assessment* **2008**, *25*, 534–547.
- Csaki, C.; Mobasher, A.; Shakibaei, M. Synergistic chondroprotective effects of curcumin and resveratrol in human articular chondrocytes: inhibition of IL-1 β -induced NF- κ B-mediated inflammation and apoptosis. *Arthritis Research & Therapy* **2009**, *11*, R165.
- Davinelli, S.; Scapagnini, G.; Marzatico, F.; Nobile, V.; Ferrara, N.; Corbi, G. Influence of equol and resveratrol supplementation on health-related quality of life in menopausal women: A randomized, placebo-controlled study. *Maturitas* **2017**, *96*, 77–83.

- De Leo, V.; Musacchio, M. C.; Cappelli, V.; Piomboni, P.; Morgante, G. Hormonal contraceptives: pharmacology tailored to women's health. *Human Reproduction Update* **2016**, *22*, 634–646.
- Di Gioia, F.; Petropoulos, S. A. Phytoestrogens, phytosteroids and saponins in vegetables: Biosynthesis, functions, health effects and practical applications. *Advances in Food and Nutrition Research* **2019**, *90*, 351–421.
- Düsterberg, B.; Nishino, Y. Pharmacokinetic and pharmacological features of oestradiol valerate. *Maturitas* **1982**, *4*, 315–324.
- Early Breast Cancer Trialists' Collaborative Group (EBCTCG). Effects of chemotherapy and hormonal therapy for early breast cancer on recurrence and 15-year survival: an overview of the randomised trials. *Lancet* **2005**, *365*, 1687–1717.
- Eliassen, A. H.; Missmer, S. A.; Tworoger, S. S.; Spiegelman, D.; Barbieri, R. L.; Dowsett, M.; Hankinson, S. E. Endogenous steroid hormone concentrations and risk of breast cancer among premenopausal women. *Journal of the National Cancer Institute* **2006**, *98*, 1406–1415.
- Endogenous Hormones and Breast Cancer Collaborative Group; Key, T. J.; Appleby, P. N.; Reeves, G. K.; Travis, R. C.; Alberg, A. J.; Barricarte, A.; Berrino, F.; Krogh, V.; Sieri, S.; Brinton, L. A.; Dorgan, J. F.; Dossus, L.; *et al.* Sex hormones and risk of breast cancer in premenopausal women: a collaborative reanalysis of individual participant data from seven prospective studies. *Lancet Oncology* **2013**, *14*, 1009–1019.
- Escande, A.; Pillon, A.; Servant, N.; Cravedi, J.-P.; Larrea, F.; Muhn, P.; Nicolas, J.-C.; Cavaillès, V.; Balaguer, P. Evaluation of ligand selectivity using reporter cell lines stably expressing estrogen receptor alpha or beta. *Biochemical Pharmacology* **2006**, *71*, 1459–1469.
- Evans, G.; Sutton, E. L. Oral Contraception. *Medical Clinics of North America* **2015**, *99*, 479–503.
- Evans, H. M.; Howe, P. R.; Wong, R. H. Effects of Resveratrol on Cognitive Performance, Mood and Cerebrovascular Function in Post-Menopausal Women; A 14-Week Randomised Placebo-Controlled Intervention Trial. *Nutrients* **2017**, *9*, pii: E27.
- Evans, M.; Elliott, J. G.; Sharma, P.; Berman, R.; Guthrie, N. The effect of synthetic genistein on menopause symptom management in healthy postmenopausal women: a multi-center, randomized, placebo-controlled study. *Maturitas* **2011**, *68*, 189–196.
- Fritz, H.; Seely, D.; Flower, G.; Skidmore, B.; Fernandes, R.; Vadeboncoeur, S.; Kennedy, D.; Cooley, K.; Wong, R.; Sagar, S.; Sabri, E.; Fergusson, D. Soy, red clover, and isoflavones and breast cancer: a systematic review. *PLoS One* **2013**, *8*, e81968.
- Fuhrman, B. J.; Schairer, C.; Gail, M. H.; Boyd-Morin, J.; Xu, X.; Sue, L. Y.; Buys, S. S.; Isaacs, C.; Keefer, L. K.; Veenstra, T. D.; Berg, C. D.; Hoover, R. N.; *et al.* Estrogen Metabolism and Risk of Breast Cancer in Postmenopausal Women. *JNCI: Journal of the National Cancer Institute* **2012**, *104*, 326–339.
- Geller, S. E.; Studee, L. Contemporary alternatives to plant estrogens for menopause. *Maturitas* **2006**, *55*, S3–13.
- Hajirahimkhan, A.; Dietz, B. M.; Bolton, J. L. Botanical modulation of menopausal symptoms: mechanisms of action? *Planta Medica* **2013**, *79*, 538–553.
- Han, G.; Li, F.; Yu, X.; White, R. E. GPER: A novel target for non-genomic estrogen action in the cardiovascular system. *Pharmacological Research* **2013**, *71*, 53–60.
- Harris, R. M.; Wood, D. M.; Bottomley, L.; Blagg, S.; Owen, K.; Hughes, P. J.; Waring, R. H.; Kirk, C. J. Phytoestrogens Are Potent Inhibitors of Estrogen Sulfation: Implications for Breast Cancer Risk and Treatment. *The Journal of Clinical Endocrinology & Metabolism* **2004**, *89*, 1779–1787.
- Harwood, D. T.; Handelsman, D. J. Development and validation of a sensitive liquid chromatography–tandem mass spectrometry assay to simultaneously measure androgens and estrogens in serum without derivatization. *Clinica Chimica Acta* **2009**, *409*, 78–84.
- Hazell, G. G. J.; Yao, S. T.; Roper, J. A.; Prossnitz, E. R.; Ocarroll, A.-M.; Lolait, S. J. Localisation of GPR30, a novel G protein-coupled oestrogen receptor, suggests multiple functions in rodent brain and peripheral tissues. *Journal of Endocrinology* **2009**, *202*, 223–236.

- Hellström, A. C.; Muntzing, J. The pollen extract Femal--a nonestrogenic alternative to hormone therapy in women with menopausal symptoms. *Menopause* **2012**, *19*, 825–829.
- Hennig, K.; Antignac, J. P.; Bichon, E.; Morvan, M.-L.; Miran, I.; Delalogue, S.; Feunteun, J.; Bizec, B. L. Steroid hormone profiling in human breast adipose tissue using semi-automated purification and highly sensitive determination of estrogens by GC-APCI-MS/MS. *Analytical and Bioanalytical Chemistry* **2017**, *410*, 259–275.
- Hess, R. A.; Cooke, P. S. Estrogen in the male: a historical perspective. *Biology of Reproduction* **2018**, *99*, 27–44.
- Hewitt, S. C.; Couse, J. F.; Korach, K. S. Estrogen receptor transcription and transactivation Estrogen receptor knockout mice: what their phenotypes reveal about mechanisms of estrogen action. *Breast Cancer Research* **2000**, *2*, 345.
- Hilborn, E.; Stål, O.; Jansson, A. Estrogen and androgen-converting enzymes 17 β -hydroxysteroid dehydrogenase and their involvement in cancer: with a special focus on 17 β -hydroxysteroid dehydrogenase type 1, 2, and breast cancer. *Oncotarget* **2017**, *8*, 30552–30562.
- Huhtinen, K.; Stähle, M.; Perheentupa, A.; Poutanen, M. Estrogen biosynthesis and signaling in endometriosis. *Molecular and Cellular Endocrinology* **2012**, *358*, 146–154.
- Husain, D.; Khanna, K.; Puri, S.; Haghighizadeh, M. Supplementation of soy isoflavones improved sex hormones, blood pressure, and postmenopausal symptoms. *Journal of the American College of Nutrition* **2015**, *34*, 42–48.
- Ignatov, T.; Modl, S.; Thulig, M.; Weißenborn, C.; Treeck, O.; Ortmann, O.; Zenclussen, A.; Costa, S. D.; Kalinski, T.; Ignatov, A. GPER-1 acts as a tumor suppressor in ovarian cancer. *Journal of Ovarian Research* **2013**, *6*, 51.
- Jiang, B.; Kronenberg, F.; Balick, M. J.; Kennelly, E. J. Analysis of formononetin from black cohosh (*Actaea racemosa*). *Phytotherapy* **2006**, *13*, 477–486.
- Jiang, K.; Jin, Y.; Huang, L.; Feng, S.; Hou, X.; Du, B.; Zheng, J.; Li, L. Black cohosh improves objective sleep in postmenopausal women with sleep disturbance. *Climacteric* **2015**, *18*, 559–567.
- Jiang, Q. F.; Wu, T. T.; Yang, J. Y.; Dong, C. R.; Wang, N.; Liu, X. H.; Liu, Z. M. 17 β -estradiol promotes the invasion and migration of nuclear estrogen receptor-negative breast cancer cells through cross-talk between GPER1 and CXCR1. *The Journal of Steroid Biochemistry and Molecular Biology* **2013**, *138*, 314–324.
- Ju, Y. H.; Doerge, D. R.; Woodling, K. A.; Hartman, J. A.; Kwak, J.; Helferich, W. G. Dietary genistein negates the inhibitory effect of letrozole on the growth of aromatase-expressing estrogen-dependent human breast cancer cells (MCF-7Ca) in vivo. *Carcinogenesis* **2008**, *29*, 2162–2168.
- Kampa, M.; Notas, G.; Pelekanou, V.; Troullinaki, M.; Andrianaki, M.; Azariadis, K.; Kampouri, E.; Lavrentaki, K.; Castanas, E. Early membrane initiated transcriptional effects of estrogens in breast cancer cells: First pharmacological evidence for a novel membrane estrogen receptor element (ERx). *Steroids* **2012**, *77*, 959–967.
- Kasiotis, K. M.; Pratsinis, H.; Kletsas, D.; Haroutounian, S. A. Resveratrol and related stilbenes: their anti-aging and anti-angiogenic properties. *Food and Chemical Toxicology* **2013**, *61*, 112–120.
- Kass-Annese, B. Alternative Therapies for Menopause. *Clinical Obstetrics and Gynecology* **2000**, *43*, 162–183.
- Kim, Y. A.; Choi, B. T.; Lee, Y. T.; Park, D. I.; Rhee, S. H.; Park, K. Y.; Choi, Y. H. Resveratrol inhibits cell proliferation and induces apoptosis of human breast carcinoma MCF-7 cells. *Oncology Reports* **2004**, *11*, 441–446.
- Koehler, K. F.; Helguero, L. A.; Haldosén Lars-Arne; Warner, M.; Gustafsson Jan-Åke Reflections on the Discovery and Significance of Estrogen Receptor β . *Endocrine Reviews* **2005**, *26*, 465–478.
- Kostelac, D.; Rechkemmer, G.; Briviba, K. Phytoestrogens modulate binding response of estrogen receptors alpha and beta to the estrogen response element. *Journal of Agricultural and Food Chemistry* **2003**, *51*, 7632–7635.

- Kroeger, P. T.; Drapkin, R. Pathogenesis and heterogeneity of ovarian cancer. *Current Opinion in Obstetrics and Gynecology* **2017**, *29*, 26–34.
- Kuhl, H. Pharmacology of estrogens and progestogens: influence of different routes of administration. *Climacteric* **2005**, *8*, 3–63.
- Kulashekar, M.; Stom, S. M.; Peuler, J. D. Resveratrol's Potential in the Adjunctive Management of Cardiovascular Disease, Obesity, Diabetes, Alzheimer Disease, and Cancer. *The Journal of the American Osteopathic Association* **2018**, *118*, 596–605.
- Kyriakidis, I.; Papaioannidou, P. Estrogen receptor beta and ovarian cancer: a key to pathogenesis and response to therapy. *Archives of Gynecology and Obstetrics* **2016**, *293*, 1161–1168.
- Labhart, A. *Clinical Endocrinology: Theory and Practice*. Springer Science & Business Media, Berlin / Heidelberg **2012**, p 548. ISBN 978-3-642-96158-8.
- Labrie, F. All sex steroids are made intracellularly in peripheral tissues by the mechanisms of intracrinology after menopause. *The Journal of Steroid Biochemistry and Molecular Biology* **2015**, *145*, 133–138.
- Lahita, R. G.; Bradlow, L.; Fishman, J.; Kunkel, H. G. Estrogen metabolism in systemic lupus erythematosus: patients and family members. *Arthritis & Rheumatology* **1982**, *25*, 843–846.
- Laredo, S. A.; Landeros, R. V.; Trainor, B. C. Rapid effects of estrogens on behavior: Environmental modulation and molecular mechanisms. *Frontiers in Neuroendocrinology* **2014**, *35*, 447–458.
- Lee, G. A.; Hwang, K. A.; Choi, K. C. Roles of Dietary Phytoestrogens on the Regulation of Epithelial-Mesenchymal Transition in Diverse Cancer Metastasis. *Toxins (Basel)* **2016**, *8*, pii: E162.
- Lee, H.-R.; Kim, T.-H.; Choi, K.-C. Functions and physiological roles of two types of estrogen receptors, ER α and ER β , identified by estrogen receptor knockout mouse. *Laboratory Animal Research* **2012**, *28*, 71.
- Lee, S.; Barron, M. G. Structure-Based Understanding of Binding Affinity and Mode of Estrogen Receptor α Agonists and Antagonists. *PLoS One* **2017**, *12*, e0169607.
- Leo, L.; Surico, D.; Deambrogio, F.; Scatuzzi, A.; Marzullo, P.; Tinelli, R.; Molinari, C.; Surico, N. [Preliminary data on the effectiveness of resveratrol in a new formulation in treatment of hot flushes]. *Minerva Ginecologica* **2015**, *67*, 475–483.
- Levi, F.; Pasche, C.; Lucchini, F.; Ghidoni, R.; Ferraroni, M.; La Vecchia, C. Resveratrol and breast cancer risk. *European Journal of Cancer Prevention* **2005**, *14*, 139–142.
- Li, R.; Cui, J.; Shen, Y. Brain sex matters: Estrogen in cognition and Alzheimer's disease. *Molecular and Cellular Endocrinology* **2014**, *389*, 13–21.
- Lin, Y.-H.; Chen, C.-Y.; Wang, G.-S. Analysis of steroid estrogens in water using liquid chromatography/tandem mass spectrometry with chemical derivatizations. *Rapid Communications in Mass Spectrometry* **2007**, *21*, 1973–1983.
- Liu, Q.; Chen, Z.; Jiang, G.; Zhou, Y.; Yang, X.; Huang, H.; Liu, H.; Du, J.; Wang, H. Epigenetic down regulation of G protein-coupled estrogen receptor (GPER) functions as a tumor suppressor in colorectal cancer. *Molecular Cancer* **2017**, *16*, 87.
- Liu, Z. M.; Ho, S. C.; Woo, J.; Chen, Y. M.; Wong, C. Randomized controlled trial of whole soy and isoflavone daidzein on menopausal symptoms in equol-producing Chinese postmenopausal women. *Menopause* **2014**, *21*, 653–660.
- Longuespée, R.; Boyon, C.; Desmons, A.; Vinatier, D.; Leblanc, E.; Farré, I.; Wisztorski, M.; Ly, K.; D'Anjou, F.; Day, R.; Fournier, I.; Salzet, M. Ovarian cancer molecular pathology. *Cancer and Metastasis Reviews* **2012**, *31*, 713–732.
- Lønning, P. E.; Helle, S. I.; Johannessen, D. C.; Ekse, D.; Adlercreutz, H. Influence of plasma estrogen levels on the length of the disease-free interval in postmenopausal women with breast cancer. *Breast Cancer Research and Treatment* **1996**, *39*, 335–341.
- Luo, T.; Kim, J. K. The Role of Estrogen and Estrogen Receptors on Cardiomyocytes: An Overview. *Canadian Journal of Cardiology* **2016**, *32*, 1017–1025.

- McKenna, D. J.; Jones, K.; Humphrey, S.; Hughes, K. Black cohosh: efficacy, safety, and use in clinical and preclinical applications. *Alternative Therapies in Health and Medicine* **2001**, *7*, 93–100.
- McNamara, K. M.; Nakamura, Y.; Miki, Y.; Sasano, H. Phase two steroid metabolism and its roles in breast and prostate cancer patients. *Frontiers in Endocrinology (Lausanne)* **2013**, *4*, 116.
- Mense, S. M.; Hei, T. K.; Ganju, R. K.; Bhat, H. K. Phytoestrogens and breast cancer prevention: possible mechanisms of action. *Environmental Health Perspectives* **2008**, *116*, 426–433.
- Messina, M. Soy and Health Update: Evaluation of the Clinical and Epidemiologic Literature. *Nutrients* **2016**, *8*, pii: E754.
- Milia, R. Improvement of climacteric symptoms with a novel sublingual product containing trans-resveratrol. *Progress in Nutrition* **2015**, *17*, 68–72.
- Ming, L. G.; Chen, K. M.; Xian, C. J. Functions and action mechanisms of flavonoids genistein and icariin in regulating bone remodeling. *Journal of Cellular Physiology* **2013**, *228*, 513–521.
- Moecklinghoff, S.; Rose, R.; Carraz, M.; Visser, A.; Ottmann, C.; Brunsveld, L. Crystal structure of estrogen receptor beta ligand binding domain. *RCSB Protein Data Bank* **2010**, 3OLS.
- Mohamed, M. E.; Frye, R. F. Effects of herbal supplements on drug glucuronidation. Review of clinical, animal, and in vitro studies. *Planta Medica* **2011**, *77*, 311–321.
- Moon, J.-Y.; Lee, H. S.; Kim, J. H.; Lee, J. H.; Choi, M. H. Supported liquid extraction coupled to gas chromatography-selective mass spectrometric scan modes for serum steroid profiling. *Analytica Chimica Acta* **2018**, *1037*, 281–292.
- Mueller, J. W.; Gilligan, L. C.; Idkowiak, J.; Arlt, W.; Foster, P. A. The Regulation of Steroid Action by Sulfation and Desulfation. *Endocrine Reviews* **2015**, *36*, 526–563.
- Mungenast, F.; Thalhammer, T. Estrogen biosynthesis and action in ovarian cancer. *Frontiers in Endocrinology (Lausanne)* **2014**, *5*, 192.
- Murphy, P. A.; Barua, K.; Hauck, C. C. Solvent extraction selection in the determination of isoflavones in soy foods. *Journal of Chromatography B: Analytical Technologies in the Biomedical and Life Sciences* **2002**, *777*, 129–138.
- Nikov, G.; Eshete, M.; Rajnarayanan, R.; Alworth, W. Interactions of synthetic estrogens with human estrogen receptors. *Journal of Endocrinology* **2001**, *170*, 137–145.
- Obi, N.; Chang-Claude, J.; Berger, J.; Braendle, W.; Slinger, T.; Schmidt, M.; Steindorf, K.; Ahrens, W.; Flesch-Janys, D. The use of herbal preparations to alleviate climacteric disorders and risk of postmenopausal breast cancer in a German case-control study. *Cancer Epidemiology, Biomarkers & Prevention* **2009**, *18*, 2207–2213.
- Ockrim, J.; Lalani, E.-N.; Abel, P. Therapy Insight: parenteral estrogen treatment for prostate cancer—a new dawn for an old therapy. *Nature Clinical Practice Oncology* **2006**, *3*, 552–563.
- Oduwole, O. O.; Li, Y.; Isomaa, V. V.; Mäntyniemi, A.; Pulkka, A. E.; Soini, Y.; Vihko, P. T. 17 β -hydroxysteroid dehydrogenase type 1 is an independent prognostic marker in breast cancer. *Cancer Research* **2004**, *64*, 7604–7609.
- Oh, W. K. The Evolving Role of Estrogen Therapy in Prostate Cancer. *Clinical Prostate Cancer* **2002**, *1*, 81–89.
- Okabe, Y.; Shimazu, T.; Tanimoto, H. Higher bioavailability of isoflavones after a single ingestion of aglycone-rich fermented soybeans compared with glucoside-rich non-fermented soybeans in Japanese postmenopausal women. *Journal of the Science of Food and Agriculture* **2011**, *91*, 658–663.
- Oseni, T.; Patel, R.; Pyle, J.; Jordan, V. C. Selective estrogen receptor modulators and phytoestrogens. *Planta Medica* **2008**, *74*, 1656–1665.
- Palacios, S.; Pornel, B.; Vázquez, F.; Aubert, L.; Chantre, P.; Marès, P. Long-term endometrial and breast safety of a specific, standardized soy extract. *Climacteric* **2010**, *13*, 368–375.
- Park, S. H.; Cheung, L. W.; Wong, A. S.; Leung, P. C. Estrogen regulates Snail and Slug in the down-regulation of E-cadherin and induces metastatic potential of ovarian cancer cells through estrogen receptor alpha. *Molecular Endocrinology* **2008**, *22*, 2085–2098.

- Paterni, I.; Granchi, C.; Katzenellenbogen, J. A.; Minutolo, F. Estrogen receptors alpha (ER α) and beta (ER β): Subtype-selective ligands and clinical potential. *Steroids* **2014**, *90*, 13–29.
- Patisaul, H. B.; Jefferson, W. The pros and cons of phytoestrogens. *Frontiers in Neuroendocrinology* **2010**, *31*, 400–419.
- Penning, T. M.; Lee, S.-H.; Jin, Y.; Gutierrez, A.; Blair, I. A. Liquid chromatography–mass spectrometry (LC–MS) of steroid hormone metabolites and its applications. *The Journal of Steroid Biochemistry and Molecular Biology* **2010**, *121*, 546–555.
- Piccinato, C. A.; Neme, R. M.; Torres, N.; Sanches, L. R.; Derogis, P. B. M. C.; Brudniewski, H. F.; Rosa e Silva, J. C.; Ferriani, R. A. Effects of steroid hormone on estrogen sulfotransferase and on steroid sulfatase expression in endometriosis tissue and stromal cells. *The Journal of Steroid Biochemistry and Molecular Biology* **2016**, *158*, 117–126.
- Pinheiro, L. M. A.; Cândido, P. D. S.; Moreto, T. C.; Almeida, W. G. D.; Castro, E. C. D. Estradiol use in the luteal phase and its effects on pregnancy rates in IVF cycles with GnRH antagonist: a systematic review. *JBRA Assisted Reproduction* **2017**, *21*, 247–250.
- Pirola, L.; Fröjdö, S. Resveratrol: one molecule, many targets. *IUBMB Life* **2008**, *60*, 323–332.
- Poschner, S.; Maier-Salamon, A.; Thalhammer, T.; Jäger, W. Resveratrol and other dietary polyphenols are inhibitors of estrogen metabolism in human breast cancer cells. *The Journal of Steroid Biochemistry and Molecular Biology* **2019**, *190*, 11–18.
- Price, K. R.; Fenwick, G. R. Naturally occurring oestrogens in foods--a review. *Food Additives and Contaminants* **1985**, *2*, 73–106.
- Prossnitz, E. R.; Arterburn, J. B. International Union of Basic and Clinical Pharmacology. XCVII. G Protein-Coupled Estrogen Receptor and Its Pharmacologic Modulators. *Pharmacological Reviews* **2015**, *67*, 505–540.
- Purohit, A.; Reed, M. J. Regulation of estrogen synthesis in postmenopausal women. *Steroids* **2002**, *67*, 979–983.
- Qin, F.; Zhao, Y.-Y.; Sawyer, M. B.; Li, X.-F. Hydrophilic Interaction Liquid Chromatography–Tandem Mass Spectrometry Determination of Estrogen Conjugates in Human Urine. *Analytical Chemistry* **2008**, *80*, 3404–3411.
- Quaas, A. M.; Kono, N.; Mack, W. J.; Hodis, H. N.; Felix, J. C.; Paulson, R. J.; Shoupe, D. Effect of isoflavone soy protein supplementation on endometrial thickness, hyperplasia, and endometrial cancer risk in postmenopausal women: a randomized controlled trial. *Menopause* **2013**, *20*, 840–844.
- Rainczuk, A.; Rao, J. R.; Gathercole, J. L.; Fairweather, N. J.; Chu, S.; Masadah, R.; Jobling, T. W.; Deb-Choudhury, S.; Dyer, J.; Stephens, A. N. Evidence for the antagonistic form of CXC-motif chemokine CXCL10 in serous epithelial ovarian tumours. *International Journal of Cancer* **2014**, *134*, 530–541.
- Rietjens, I. M. C. M.; Sotoca, A. M.; Vervoort, J.; Louisse, J. Mechanisms underlying the dualistic mode of action of major soy isoflavones in relation to cell proliferation and cancer risks. *Molecular Nutrition and Food Research* **2013**, *57*, 100–113.
- Rietjens, I. M. C. M.; Louisse, J.; Beekmann, K. The potential health effects of dietary phytoestrogens. *British Journal of Pharmacology* **2017**, *174*, 1263–1280.
- Riggins, R. B.; Bouton, A. H.; Liu, M. C.; Clarke, R. Antiestrogens, aromatase inhibitors, and apoptosis in breast cancer. *Vitamins & Hormones* **2005**, *71*, 201–37.
- Rižner, T. L. The Important Roles of Steroid Sulfatase and Sulfotransferases in Gynecological Diseases. *Frontiers in Pharmacology* **2016**, *7*, 30.
- Rižner, T. L.; Thalhammer, T.; Özvey-Laczka, C. The Importance of Steroid Uptake and Intracrine Action in Endometrial and Ovarian Cancers. *Frontiers in Pharmacology* **2017**, *8*, 346.
- Rosic, S.; Kendic, S.; Rosic, M. Phytoestrogens impact on menopausal symptomatology. *Materia Socio Medica* **2013**, *25*, 98–100.

- Ross, S. M. Menopause: a standardized isopropanolic black cohosh extract (remifemin) is found to be safe and effective for menopausal symptoms. *Holistic Nursing Practice* **2012**, *26*, 58–61.
- Rostock, M.; Fischer, J.; Mumm, A.; Stammwitz, U.; Saller, R.; Bartsch, H. H. Black cohosh (*Cimicifuga racemosa*) in tamoxifen-treated breast cancer patients with climacteric complaints - a prospective observational study. *Gynecological Endocrinology* **2011**, *27*, 844–848.
- Rutkowski, K.; Sowa, P.; Rutkowska-Talipska, J.; Kuryliszyn-Moskal, A.; Rutkowski, R. Dehydroepiandrosterone (DHEA): Hypes and Hopes. *Drugs* **2014**, *74*, 1195–1207.
- Samavat, H.; Kurzer, M. S. Estrogen metabolism and breast cancer. *Cancer Letters* **2015**, *356*, 231–243.
- Sampson, J. N.; Falk, R. T.; Schairer, C.; Moore, S. C.; Fuhrman, B. J.; Dallal, C. M.; Bauer, D. C.; Dorgan, J. F.; Shu, X. O.; Zheng, W.; Brinton, L. A.; Gail, M. H.; *et al.* Association of Estrogen Metabolism with Breast Cancer Risk in Different Cohorts of Postmenopausal Women. *Cancer Research* **2017**, *77*, 918–925.
- Santen, R. J.; Demers, L.; Ohorodnik, S.; Settlege, J.; Langecker, P.; Blanchett, D.; Goss, P. E.; Wang, S. Superiority of gas chromatography/tandem mass spectrometry assay (GC/MS/MS) for estradiol for monitoring of aromatase inhibitor therapy. *Steroids* **2007**, *72*, 666–671.
- Scaling, A. L.; Prossnitz, E. R.; Hathaway, H. J. GPER Mediates Estrogen-Induced Signaling and Proliferation in Human Breast Epithelial Cells and Normal and Malignant Breast. *Hormones and Cancer* **2014**, *5*, 146–160.
- Schaper & Brümmer GmbH. International. Available online: <https://www.schaper-bruemmer.com/company/international.html> (accessed on April 7th, 2020).
- Scimeca, M.; Urbano, N.; Bonfiglio, R.; Duggento, A.; Toschi, N.; Schillaci, O.; Bonanno, E. Novel insights into breast cancer progression and metastasis: A multidisciplinary opportunity to transition from biology to clinical oncology. *Biochimica et Biophysica Acta* **2019**, *1872*, 138–148.
- Shanle, E. K.; Xu, W. Endocrine disrupting chemicals targeting estrogen receptor signaling: identification and mechanisms of action. *Chemical Research in Toxicology* **2011**, *24*, 6–19.
- Shibuya, R.; Suzuki, T.; Miki, Y.; Yoshida, K.; Moriya, T.; Ono, K.; Akahira, J.; Ishida, T.; Hirakawa, H.; Evans, D. B.; Sasano, H. Intratumoral concentration of sex steroids and expression of sex steroid-producing enzymes in ductal carcinoma in situ of human breast. *Endocrine-Related Cancer* **2008**, *15*, 113–124.
- Shike, M.; Doane, A. S.; Russo, L.; Cabal, R.; Reis-Filho, J. S.; Gerald, W.; Cody, H.; Khanin, R.; Bromberg, J.; Norton, L. The effects of soy supplementation on gene expression in breast cancer: a randomized placebo-controlled study. *Journal of the National Cancer Institute* **2014**, *106*, pii: dju189.
- Shirtcliff, E. A.; Granger, D. A.; Schwartz, E. B.; Curran, M. J.; Booth, A.; Overman, W. H. Assessing Estradiol in Biobehavioral Studies Using Saliva and Blood Spots: Simple Radioimmunoassay Protocols, Reliability, and Comparative Validity. *Hormones and Behavior* **2000**, *38*, 137–147.
- Simpson, E. Sources of estrogen and their importance. *The Journal of Steroid Biochemistry and Molecular Biology* **2003**, *86*, 225–230.
- Soltysik, K.; Czekaj, P. Membrane estrogen receptors - is it an alternative way of estrogen action? *Journal of Physiology and Pharmacology* **2013**, *64*, 129–142.
- Speroff, L. Alternative therapies for postmenopausal women. *International journal of fertility and women's medicine* **2005**, *50*, 101–114.
- Stanczyk, F. Z.; Cho, M. M.; Endres, D. B.; Morrison, J. L.; Patel, S.; Paulson, R. J. Limitations of direct estradiol and testosterone immunoassay kits. *Steroids* **2003**, *68*, 1173–1178.
- Stanczyk, F. Z.; Archer, D. F.; Bhavnani, B. R. Ethinyl estradiol and 17 β -estradiol in combined oral contraceptives: pharmacokinetics, pharmacodynamics and risk assessment. *Contraception* **2013**, *87*, 706–727.
- Stuenkel, C. A.; Davis, S. R.; Gompel, A.; Lumsden, M. A.; Murad, M. H.; Pinkerton, J. V.; Santen, R. J. Treatment of Symptoms of the Menopause: An Endocrine Society Clinical Practice Guideline. *The Journal of Clinical Endocrinology & Metabolism* **2015**, *100*, 3975–4011.

- Stute, P.; Spyropoulou, A.; Karageorgiou, V.; Cano, A.; Bitzer, J.; Ceausu, I.; Chedraui, P.; Durmusoglu, F.; Erkkola, R.; Goulis, D. G.; Hirschberg, A. L.; Kiesel, L.; *et al.* Management of depressive symptoms in peri- and postmenopausal women: EMAS position statement. *Maturitas* **2020**, *131*, 91–101.
- Sunita, P.; Pattanayak, S. Phytoestrogens in postmenopausal indications: A theoretical perspective. *Pharmacognosy Reviews* **2011**, *5*, 41.
- Tanenbaum, D. M.; Wang, Y.; Sigler, P. B. Estrogen Receptor Aalpha Ligand-Binding Domain Complexed To Estradiol. *RCSB Protein Data Bank* **1998**, 1A52.
- Tanmahasamut, P.; Vichinsartvichai, P.; Rattanachaiyanont, M.; Techatraisak, K.; Dangrat, C.; Sardod, P. Cimicifuga racemosa extract for relieving menopausal symptoms: a randomized controlled trial. *Climacteric* **2015**, *18*, 79–85.
- Tempfer, C. B.; Froese, G.; Heinze, G.; Bentz, E.-K.; Hefler, L. A.; Huber, J. C. Side Effects of Phytoestrogens: A Meta-analysis of Randomized Trials. *The American Journal of Medicine* **2009**, *122*, 939–946.e9.
- Thomas, C.; Gustafsson, J. Å. The different roles of ER subtypes in cancer biology and therapy. *Nature Reviews Cancer* **2011**, *11*, 597–608.
- Thomas, C.; Gustafsson, J.-Å. Estrogen Receptor β and Breast Cancer. In: Zhang, X. (eds) *Estrogen Receptor and Breast Cancer. Cancer Drug Discovery and Development*. Humana Press, Cham **2018**, 309–342. ISBN: 978-3-319-99350-8.
- Thomsen, M.; Schmidt, M. Hepatotoxicity from Cimicifuga racemosa? Recent Australian case report not sufficiently substantiated. *Journal of Alternative and Complementary Medicine* **2003**, *9*, 337–340.
- Tian, S.; Zhan, N.; Li, R.; Dong, W. Downregulation of G Protein-Coupled Estrogen Receptor (GPER) is Associated with Reduced Prognosis in Patients with Gastric Cancer. *Medical Science Monitor* **2019**, *25*, 3115–3126.
- Toran-Allerand, C. D.; Guan, X.; Maclusky, N. J.; Horvath, T. L.; Diano, S.; Singh, M.; Connolly, E. S.; Nethrapalli, I. S.; Tinnikov, A. A. ER-X: A Novel, Plasma Membrane-Associated, Putative Estrogen Receptor That Is Regulated during Development and after Ischemic Brain Injury. *The Journal of Neuroscience* **2002**, *22*, 8391–8401.
- Toss, A.; Cristofanilli, M. Molecular characterization and targeted therapeutic approaches in breast cancer. *Breast Cancer Research* **2015**, *17*, 60.
- Tournier, M.; Pouech, C.; Quignot, N.; Lafay, F.; Wiest, L.; Lemazurier, E.; Cren-Olivé, C.; Vulliet, E. Determination of endocrine disruptors and endogenic androgens and estrogens in rat serum by high-performance liquid chromatography-tandem mass spectrometry. *Steroids* **2015**, *104*, 252–262.
- Tranche, S.; Brotons, C.; Pascual de la Pisa, B.; Macías, R.; Hevia, E.; Marzo-Castillejo, M. Impact of a soy drink on climacteric symptoms: an open-label, crossover, randomized clinical trial. *Gynecological Endocrinology* **2016**, *32*, 477–482.
- van der Berg, C.; Venter, G.; van der Westhuizen, F. H.; Erasmus, E. Development and validation of LC-ESI-MS/MS methods for quantification of 27 free and conjugated estrogen-related metabolites. *Analytical Biochemistry* **2020**, *590*, 113531.
- van der Velpen, V.; Hollman, P. C.; van Nielen, M.; Schouten, E. G.; Mensink, M.; Van't Veer, P.; Geelen, A. Large inter-individual variation in isoflavone plasma concentration limits use of isoflavone intake data for risk assessment. *European Journal of Clinical Nutrition* **2014**, *68*, 1141–1147.
- van Duursen, M. B. M. Modulation of estrogen synthesis and metabolism by phytoestrogens in vitro and the implications for womens health. *Toxicological Research* **2017**, *6*, 772–794.
- Vina, J.; Gambini, J.; Lopez-Grueso, R.; Abdelaziz, K. M.; Jove, M.; Borras, C. Females live longer than males: role of oxidative stress. *Current Pharmaceutical Design* **2011**, *17*, 3959–3965.

- Vitale, D. C.; Piazza, C.; Melilli, B.; Drago, F.; Salomone, S. Isoflavones: estrogenic activity, biological effect and bioavailability. *European Journal of Drug Metabolism and Pharmacokinetics* **2013**, 38, 15–25.
- Wang, Q.; Bottalico, L.; Mesaros, C.; Blair, I. A. Analysis of estrogens and androgens in postmenopausal serum and plasma by liquid chromatography–mass spectrometry. *Steroids* **2015**, 99, 76–83.
- Wang, Q.; Rangiah, K.; Mesaros, C.; Snyder, N. W.; Vachani, A.; Song, H.; Blair, I. A. Ultrasensitive quantification of serum estrogens in postmenopausal women and older men by liquid chromatography–tandem mass spectrometry. *Steroids* **2015**, 96, 140–152.
- Wang, S.; Paris, F.; Sultan, C. S.; Song, R. X.-D.; Demers, L. M.; Sundaram, B.; Settlege, J.; Ohorodnik, S.; Santen, R. J. Recombinant Cell Ultrasensitive Bioassay for Measurement of Estrogens in Postmenopausal Women. *The Journal of Clinical Endocrinology & Metabolism* **2005**, 90, 1407–1413.
- Weihua, Z.; Saji, S.; Makinen, S.; Cheng, G.; Jensen, E. V.; Warner, M.; Gustafsson, J. Å. Estrogen receptor (ER) beta, a modulator of ERalpha in the uterus. *Proceedings of the National Academy of Sciences* **2000**, 97, 5936–5941.
- Wikimedia Commons. File:Dessin Glycine max.gif. Available online: https://commons.wikimedia.org/wiki/File:Dessin_Glycine_max.gif (accessed on April 15th, 2020).
- Wikimedia Commons. File:Grapevine 964 (PSF).png. Available online: [https://commons.wikimedia.org/wiki/File:Grapevine_964_\(PSF\).png](https://commons.wikimedia.org/wiki/File:Grapevine_964_(PSF).png) (accessed on April 15th, 2020).
- Wikimedia Commons. File:Black Cohosh-Guide Wild Flowers-237-79.png. Available online: https://commons.wikimedia.org/wiki/File:Black_Cohosh-Guide_Wild_Flowers-237-79.png (accessed on April 15th, 2020).
- Wiseman, H.; Casey, K.; Clarke, D. B.; Barnes, K. A.; Bowey, E. Isoflavone aglycon and glucoside content of high- and low-soy U.K. foods used in nutritional studies. *Journal of Agricultural and Food Chemistry* **2002**, 50, 1404–1410.
- Wooding, K. M.; Hankin, J. A.; Johnson, C. A.; Chosich, J. D.; Baek, S. W.; Bradford, A. P.; Murphy, R. C.; Santoro, N. Measurement of estradiol, estrone, and testosterone in postmenopausal human serum by isotope dilution liquid chromatography tandem mass spectrometry without derivatization. *Steroids* **2015**, 96, 89–94.
- Xie, C.; Yan, T. M.; Chen, J. M.; Li, X. Y.; Zou, J.; Zhu, L. J.; Lu, L. L.; Wang, Y.; Zhou, F. Y.; Liu, Z. Q.; Hu, M. LC-MS/MS quantification of sulfotransferases is better than conventional immunogenic methods in determining human liver SULT activities: implication in precision medicine. *Scientific Reports* **2017**, 7, 3858.
- Yalcin, E. B.; More, V.; Neira, K. L.; Lu, Z. J.; Cherrington, N. J.; Slitt, A. L.; King, R. S. Downregulation of sulfotransferase expression and activity in diseased human livers. *Drug Metabolism & Disposition* **2013**, 41, 1642–1650.
- Yang, T. S.; Wang, S. Y.; Yang, Y. C.; Su, C. H.; Lee, F. K.; Chen, S. C.; Tseng, C. Y.; Jou, H. J.; Huang, J. P.; Huang, K. E. Effects of standardized phytoestrogen on Taiwanese menopausal women. *Taiwanese Journal of Obstetrics & Gynecology* **2012**, 51, 229–235.
- Zahid, H.; Simpson, E. R.; Brown, K. A. Inflammation, dysregulated metabolism and aromatase in obesity and breast cancer. *Current Opinion in Pharmacology* **2016**, 31, 90–96.
- Zhao, Y.; Boyd, J. M.; Sawyer, M. B.; Li, X.-F. Liquid chromatography tandem mass spectrometry determination of free and conjugated estrogens in breast cancer patients before and after exemestane treatment. *Analytica Chimica Acta* **2014**, 806, 172–179.
- Zhu, G.; Huang, Y.; Wu, C.; Wie, D.; Shi, Y. Activation of G-Protein-Coupled Estrogen Receptor Inhibits the Migration of Human Non-small Cell Lung Cancer Cells via IKK-β/NF-κB Signals. *DNA and Cell Biology* **2016**, 35, 434–442.

CHAPTER II

AIMS OF THE THESIS

Estrogens play a pivotal role in human physiology, but may also induce hormone-dependent carcinogenesis and drive cancer progression. There is evidence that natural dietary supplements might impair the endogenous estrogen metabolism in women, thereby contributing to their reported effects against menopausal disorders. However, changes in the delicate balance of activated and inactivated steroid hormones by natural remedies might also trigger the proliferation of breast cancer cells. Targeted estrogen metabolomics therefore hold promise for better understanding the underlying molecular mechanisms of the potential interactions between exogenous natural compounds and the endogenous steroid metabolism in breast cancer patients. Yet, in-depth data on this topic are scarce, most likely because the quantitative analysis of estrogens is still a major challenge in analytical chemistry, due to their low abundance in biological matrices. The first aim of this thesis was therefore to establish and validate a specific and sensitive LC-high resolution MS (LC-HRMS) assay (**Chapter III**) to simultaneously quantify the ten major unconjugated and conjugated steroids of the estrogenic metabolic pathway, namely DHEA, DHEA-S, AD, T, E1, E1-S, E2, E2-G, E2-S and E3, in the low pg/ml range.

This targeted metabolomics assay should then be used to monitor the levels of estrogens in established human ER α ⁺ and ER α ⁻ breast cancer models (based on commercially available cancer cell lines, authenticated via short tandem repeat profiling) to investigate for the first time the formation kinetics of estrogens and their respective metabolites in the presence and absence of natural compounds. These cell-based models are, despite their limitations, an ideal way of studying human metabolism without performing experiments on humans, with all applying terms and restrictions, allowing faster experiments and better reproducibility. Using the commonly used soy isoflavones genistein and daidzein (**Chapter IV**), resveratrol (**Chapter V**) and a standardized black cohosh extract in combination with its major active constituent actein (**Chapter VI**) as compounds of interest, these studies might provide a better assessment of the efficacy and safety of these natural dietary supplements in breast cancer patients.

The final aim of this thesis was to investigate whether targeted estrogen metabolomics may also act as diagnostic markers for cancer cell resistance, which remains a major challenge in the treatment of gynecological malignancies. This is particularly important for the treatment of HGSOC, the most lethal subtype of ovarian cancer, as it often becomes resistant to the standard treatment, which is based on platinum complexes. Therefore, formation kinetics of estrogens and their metabolites should be determined in four HGSOC cell lines that were recently established by the Translational Gynecology Group at the Medical University of Vienna in comparison to two commercially available HGSOC models. The obtained data from the LC-HRMS analyses should then be correlated with the respective inhibitory concentrations (IC_{50} values) of carboplatin in these six cell lines (**Chapter VII**). Such comprehensive analysis could potentially further the understanding of the mechanisms of platinum-resistance in HGSOC, and might lay the foundation for the establishment of targeted metabolomics as future resistance markers prior to or during chemotherapy in the clinic. **Chapters III-VII** present already published or recently submitted manuscripts.

CHAPTER III

SIMULTANEOUS QUANTIFICATION OF ESTROGENS, THEIR PRECURSORS AND CONJUGATED METABOLITES IN HUMAN BREAST CANCER CELLS BY LC-HRMS WITHOUT DERIVATIZATION

Authors:

Stefan Poschner, Martin Zehl, Alexandra Maier-Salamon and Walter Jäger

Published in:

Journal of Pharmaceutical and Biomedical Analysis **2017**, 138, 344–350

doi: 10.1016/j.jpba.2017.02.033



Contents lists available at ScienceDirect

Journal of Pharmaceutical and Biomedical Analysis

journal homepage: www.elsevier.com/locate/jpba

Simultaneous quantification of estrogens, their precursors and conjugated metabolites in human breast cancer cells by LC–HRMS without derivatization

Stefan Poschner^a, Martin Zehl^{a,b}, Alexandra Maier-Salamon^a, Walter Jäger^{a,*}^a Department of Pharmaceutical Chemistry, Division of Clinical Pharmacy and Diagnostics, University of Vienna, 1090 Vienna, Austria^b Department of Analytical Chemistry, Faculty of Chemistry, University of Vienna, 1090 Vienna, Austria

ARTICLE INFO

Article history:

Received 20 December 2016

Received in revised form 15 February 2017

Accepted 16 February 2017

Available online 22 February 2017

Keywords:

Liquid chromatography

Mass spectrometry

Estrogens

Metabolomics

Steroids

ABSTRACT

Liquid chromatography–mass spectrometry (LC–MS) is the state of the art technique for quantification of steroid hormones. Currently used methods are typically limited by the need of pre-column derivatization to increase ionization efficiency; however, this causes hydrolysis of conjugated metabolites. Our newly established LC–HRMS method is able to simultaneously quantify conjugated and unconjugated steroids without prior derivatization using deuterated internal standards and solid-phase extraction. This assay was validated according to ICH Q2(R1) guidelines for the analysis of the 10 main steroids of the estrogenic pathway, namely 4-androstene-3,17-dione, dehydroepiandrosterone (DHEA), DHEA-3-sulfate, estrone, 17 β -estradiol, estriol (16 α -OH-17 β -estradiol), estrone-3-sulfate, 17 β -estradiol-3-(β -D-glucuronide), 17 β -estradiol-3-sulfate and testosterone. Assay performance characteristics were excellent with results for accuracy (98.8–101.2%), precision (mean: 2.05%, all \leq 2.80%), stability over five freeze–thaw–cycles (95.7–100.4%) and SPE accuracy (96.9–102.0%), as well as suitable lower and upper limits of quantification for cell culture experiments (LLOQ 0.005–2 ng/ml, ULOQ 3–2000 ng/ml). Furthermore, we demonstrated the functionality of our method for the monitoring of steroid levels in the human breast cancer cell line MCF-7. This sensitive assay allows for the first time detailed investigations on estrogen metabolomics in breast cancer cells and may also apply to other estrogen-dependent tumor entities.

© 2017 Elsevier B.V. All rights reserved.

1. Introduction

Breast cancer is the leading cause of death among women, causing 522,000 deaths in 2012 worldwide [1]. Carcinogenesis of breast cancer is strongly dependent on systemic concentrations of active estrogens, as these steroids drive cellular proliferation [2].

In addition to endogenous differences in estrogen levels, epidemiological and experimental evidence indicates that natural dietary constituents as well as many pharmaceutical drugs significantly alter estrogen metabolism, leading to inhibition or promotion of mammary carcinogenesis [3]. However, understanding of this food- or drug induced alterations of estrogen biosynthesis is limited. A human cellular model combined with a specific and sensitive analytical assay to quantify formation of key estrogens, their precursors and metabolites would provide a deeper insight in biochemical mechanisms of breast cancer development and progression.

In pre-menopausal women, the three major estrogens, namely estrone (E1), 17 β -estradiol (E2) and estriol (16 α -hydroxy-17 β -estradiol, E3) are mainly formed via the aromatase pathway. The main estrogen precursors dehydroepiandrosterone (DHEA) and its sulfate (DHEA-S) are transformed to the androgens 4-androstene-3,17-dione (AD) and testosterone (T), with 3 β -hydroxysteroiddehydrogenase (3 β -HSD) and 17 β -hydroxysteroiddehydrogenase (17 β -HSD) as the responsible enzymes. A key step in this pathway is the aromatase (CYP19A1)-catalyzed conversion of AD and T to E1 and to the most potent

Abbreviations: 3 β -HSD, 3 β -hydroxysteroiddehydrogenase; 17 β -HSD, 17 β -hydroxysteroiddehydrogenase; AD, androstenedione; DHEA, dehydroepiandrosterone; DHEA-S, dehydroepiandrosterone-3-sulfate; DMEM, Dulbecco's Modified Eagle Medium F-12; DMSO, dimethylsulfoxide; DPBS, Dulbecco's phosphate buffered saline; E1, estrone; E1-S, estrone-3-sulfate; E2, 17 β -estradiol; E2-G, 17 β -estradiol-3-(β -D-glucuronide); E2-S, 17 β -estradiol-3-sulfate; E3, 16 α -hydroxy-17 β -estradiol; EIC, extracted ion chromatogram; HRMS, high resolution mass spectrometry; LLOQ, lower limit of quantification; RSD, relative standard deviation; STS, steroid sulfatase; SULT, sulfotransferase; T, testosterone; UGT, UDP-glucuronosyltransferase; ULOQ, upper limit of quantification.

* Corresponding author at: Department of Pharmaceutical Chemistry, Division of Clinical Pharmacy and Diagnostics, University of Vienna, Althanstrasse 14, 1090 Vienna, Austria.

E-mail address: walter.jaeger@univie.ac.at (W. Jäger).

<http://dx.doi.org/10.1016/j.jpba.2017.02.033>

0731-7085/© 2017 Elsevier B.V. All rights reserved.

estrogen E2, which can additionally be formed from E1 by 17 β -HSD. Consequently, E2 is further hydroxylated to the lesser active E3 by CYP3A4 activity [4–6].

The formation of estrogen conjugates, mainly 17 β -estradiol-3-(β -D-glucuronide) (E2-G) and 17 β -estradiol-3-sulfate (E2-S) by UDP-glucuronosyltransferases (UGTs) and sulfotransferases (SULTs) leads to inactivation of the estrogens. However, in tissues, lacking aromatase expression and especially in postmenopausal women, these conjugates can be reactivated by hydrolysis via steroid sulfatase (STS) and β -glucuronidase. This so-called “sulfatase pathway” is an important mechanism in the pre-receptor regulation of estrogen activity (Fig. 1) [6–8].

Specific and sensitive methods for the quantification of estrogens and their main metabolites are still a challenge in analytical chemistry. Such assay would not only allow a rapid screening of drug or dietary induced metabolic alterations *in vitro*, but also the monitoring of steroid levels in patients in order to better predict future risks of hormone responsive cancer development [9]. However, current assays are technically limited by the methodology used to quantitate steroids, particularly E2 [2], as none can quantify all relevant steroids and metabolites simultaneously [10–14]. These assays often rely on pre-analytical derivatization to increase ionization efficiency [15], which leads to hydrolysis of the conjugated metabolites. As a consequence, only total hormone concentrations can be determined [16] or multiple analytical procedures for quantification are needed [17,18].

The present work presents for the first time a reliable liquid chromatography–high resolution mass spectrometry (LC–HRMS) assay to quantify simultaneously the 10 main steroids of the estrogenic pathway without prior derivatization in a human breast cancer model.

2. Materials and methods

2.1. Materials

AD, E3, E2, E2-G, DHEA, dehydroepiandrosterone-2,2,3,4,4,6-d₆ (DHEA-d₆), DHEA-S, dehydroepiandrosterone-3-sulfate-2,2,3,4,4,6-d₆ sodium salt (DHEA-S-d₆), E1 and T, as well as acetic acid, acetonitrile, ammonium acetate and dimethylsulfoxide (DMSO) were purchased from Sigma Aldrich Chemical Co. (Munich, Germany). E2-S and E1-S were obtained from Steraloids Inc. (Newport, RI, USA). 4-Androstene-3,17-dione-2,2,4,6,6,16,16-d₇ (AD-d₇), 16 α -hydroxy-17 β -estradiol-2,4,17-d₃ (E3-d₃), 17 β -estradiol-2,4,16,16-d₄ (E2-d₄), 17 β -estradiol-16,16,17-d₃-3-(β -D-glucuronide) sodium salt (E2-G-d₃), 17 β -estradiol-2,4,16,16-d₄-3-sulfate sodium salt (E2-S-d₄), estrone-2,4,16,16-d₄ (E1-d₄), estrone-2,4,16,16-d₄-3-sulfate sodium salt (E1-S-d₄) and testosterone-2,2,4,6,6-d₅ (T-d₅) were purchased from C/D/N-Isotopes Inc. (Pointe-Claire, Quebec, Canada). Purified water was obtained using an arium[®] pro ultrapure water system (Sartorius AG, Göttingen, Germany). All standard compounds were separately dissolved in DMSO at a concentration of 1 mg/ml and stored at –80 °C until further usage. All deuterated standards were diluted with DMSO to their final concentration and mixed to obtain the final internal standard master mix composition, which was stored at –80 °C until further usage. MCF-7 cancer cells were purchased from the American Type Culture Collection (ATCC, Rockville, MD, USA). Dulbecco's Modified Eagle Medium F-12 (DMEM), Dulbecco's phosphate buffered saline (DPBS) and PenStrep[®]-solution were obtained from Invitrogen (Karlsruhe, Germany). HyClone[®] heat-inactivated charcoal-stripped fetal bovine serum (U.S. origin) was purchased from THP Medical Products (Vienna, Austria).

2.2. Cell culture

MCF-7 breast cancer cells were cultivated at 37 °C (95% humidity and 5% CO₂) in phenol red free DMEM containing 1% PenStrep[®]-solution and 10% heat-inactivated charcoal stripped fetal bovine serum in order to prevent any influence by external hormone sources. Cells were seeded in 6-well-plates containing 1 \times 10⁶ cells/well and allowed to attach overnight. After washing with DPBS, the cells were treated with 2.5 ml DMEM containing either 100 nM DHEA or 100 nM E1 (dissolved in DMSO, final concentration 0.05%). For each condition, four time-points (0 h, 24 h, 48 h and 72 h) were measured and three independent replicates were prepared per time-point. After the planned incubation time, all culture media were collected and stored at –80 °C until further analysis. Conjugated and unconjugated steroids were stable in these samples for at least 2 weeks.

2.3. Sample preparation

All plastic vials (Eppendorf AG, Hamburg, Germany) were rinsed with acetonitrile to get rid of any possible lipophilic contaminants and dried at room temperature. Oasis HLB 1 cc SPE cartridges (30 mg, Waters Corporation, Milford, MA, USA) were preconditioned with 2 \times 1.0 ml acetonitrile and 3 \times 1.0 ml ammonium acetate buffer (10 mM, pH=5.0). Frozen cell culture media (2.0 ml/sample) were thawed at room temperature, mixed with 20 μ l internal standard solution and 2.0 ml ammonium acetate buffer (10 mM, pH=5.0), vortexed gently and loaded onto the SPE cartridge. After washing with 1 \times 1.0 ml ammonium acetate buffer (10 mM, pH=5.0) and 2 \times 1.0 ml acetonitrile/ammonium acetate buffer (10 mM, pH 5.0) 10:90 (v/v), analytes were eluted into Eppendorf[®] vials using 2 \times 650 μ l acetonitrile/ammonium acetate buffer (10 mM, pH=5.0) 95:5 (v/v) and evaporated to dryness using firstly a Concentrator plus[®] vacuum centrifuge (Eppendorf, Hamburg, Germany) for 1.5 h and secondly a Telstar LyoQuest[®] freeze-dryer (VWR, Vienna, Austria) for another hour. The dried residues were reconstituted in 270 μ l acetonitrile/ammonium acetate buffer (10 mM, pH=5.0) 25:75 (v/v), centrifuged at 14,000 rpm for 5 min and the clear supernatant transferred into two separate HPLC vials. Both vials were stored at –80 °C until LC–HRMS analysis (one vial each for positive and negative ion mode measurement).

2.4. LC conditions

Liquid chromatography was performed using an UltiMate 3000 RSLC-series system (Dionex/Thermo Scientific, Germering, Germany) coupled to a maXis HD ESI-Qq-TOF mass spectrometer (Bruker Daltonics, Bremen, Germany). Solvent A was aqueous ammonium acetate buffer (10 mM, pH=5.0), solvent B acetonitrile. For all analyses, a Phenomenex Luna[®] 3 μ m C18(2) 100 Å LC column (250 \times 4.6 mm I.D., Phenomenex Inc., Torrance, CA, USA) with a Hypersil[®] BDS-C18 guard column (5 μ m, 10 \times 4.6 mm I.D., Thermo Scientific) was used, the column oven temperature was 43 °C and the flow rate was set to 1 ml/min. The injected volume was 100 μ l for each sample. The gradient used was as follows: 25% solvent B at 0 min, 56.3% solvent B at 19 min, a washing step at 90% solvent B from 19.5 to 24.0 min and column re-equilibration with 25% solvent B from 24.5 to 30.5 min. In order not to overload the ESI source, a T-piece splitter was positioned between the LC system and the mass spectrometer, passing only about 12.5% of the flow for further analysis.

prepared calibration standards (six to eight different concentrations, depending on the analyte, distributed over the entire concentration range) that were prepared and analyzed on three different days in triplicate each. The concentration ranges were defined different for each steroid as listed in Table 2. A linear least-squares regression curve excluding zero was fitted to these data with a weighting factor of $1/x^2$ according to Gu et al. [20] using GraphPad Prism 5 software (GraphPad Software Inc., La Jolla, CA, USA).

In addition, three different concentrations of quality control samples (QCs) were analyzed in biological triplicates on three different days. The concentrations were 6-fold, 100-fold and 600-fold of the respective LLOQ for each analyte. The assay accuracy was calculated by comparing the means of the measured steroid concentrations of the QC samples to their theoretical content and calculating the percent relative standard deviation (RSD) of this value for each steroid. Accuracy results were reported as the mean of all nine QC values for each analyte.

Intra-day precision was expressed as the mean RSD of the normalized data obtained for calibration standards of three different concentrations (distributed over the entire concentration range) and calculated for each of the three days separately. Inter-day precision was assessed by comparing the means and standard deviations of these three concentration levels for each day using an unpaired Student's *t*-test. Sample stability was verified for each steroid by freezing (-80°C) and thawing (room temperature) a set of three independently prepared samples for five times and comparing the remaining steroid concentration to three independent reference samples that were treated according to the standard protocol.

SPE-recovery was assessed by comparing quality control samples in cell media that underwent SPE as described in Section 2.3 with samples of the same concentration that were obtained only by dilution of the standard compounds into acetonitrile/ammonium acetate buffer (10 mM, pH = 5.0) 25:75 (v/v) as matrix. The SPE recovery was calculated based on the peak areas of the analytes, showing negligible to moderate loss of the different analytes, while the SPE accuracy was determined with the peak area ratios of the analytes and their respective deuterated internal standards, demonstrating identical recovery for the analyte/internal standard-pairs and thus precise analytical results.

3. Results and discussion

3.1. Method development

3.1.1. SPE protocol

Prior to LC–HRMS analysis, SPE clean-up of samples was performed using a previously published method [21] for the extraction of conjugated steroids which was further adopted for lipophilic compounds. The use of the ammonium acetate buffer for pre-conditioning of the SPE-cartridges and dilution of the samples before sample loading ensured stable pH-conditions. Preliminary experiments with different mixtures of acetonitrile and ammonium acetate buffer as washing solution revealed that a ratio of 10:90 (v/v) was sufficient to almost completely elute cell media components while steroids were still retained on the SPE column. For simultaneous elution of conjugated and unconjugated steroids, acetonitrile content in the mixture was raised to 95% giving highest yields when elution was carried out in two consecutive steps. After evaporation to dryness, samples were reconstituted with 270 μl LC mobile phase to ensure quantitative dissolution of all compounds.

3.1.2. LC method

The analyzed steroids show a wide range of polarity from very lipophilic unconjugated structures to rather hydrophilic conju-

gated metabolites. Furthermore, many of these compounds are structurally similar, requiring a sophisticated LC–MS assay. The most challenging part of the LC method development was the separation of E1, DHEA and AD, as these steroids show very similar elution characteristics. Among eight LC columns with different solid phase materials and dimensions only the Phenomenex Luna[®] C18(2) 100 Å LC column (3 μm , $250 \times 4.6 \text{ mm}$) achieved satisfying separation of all analytes in a reasonably short runtime at a flow rate of 1 ml/min. This column also allowed injections of larger sample volumes, thereby increasing sensitivity. The column was constantly kept at 43°C to allow baseline-separation of the three lipophilic compounds E1, DHEA and AD. During LC method development, several mobile phases consisting of a continuous gradient mixed from different polar and apolar solvents were tested to optimize separation characteristics of all analytes. Aqueous ammonium acetate buffer (10 mM, pH = 5.0) was chosen as the polar component, as this solvent is compatible with ESI-MS analysis and ensures stability of the conjugated metabolites. Acetonitrile as the apolar phase in the gradient resulted in significantly better peak symmetry in comparison to methanol.

3.1.3. MS method

One of the objectives in the method development was to avoid prior derivatization of the analytes, as this leads to hydrolysis of the conjugated compounds. To compensate the significantly poorer ionization efficiency of the unconjugated steroids [15], we developed very specific MS conditions (see Section 2.5). Quantification of the steroids was further performed using extracted ion chromatograms (EICs) from full scan spectra, as this strategy is based on very good specificity due to high mass resolution and accuracy. Preliminary experiments showed a mediocre fragment ion yield of the unconjugated compounds resulting in better sensitivity for the intact ion compared to the multiple reaction monitoring mode. For instance, signal-to-noise ratio was approximately two times and peak area five times higher for T using EICs from full scan spectra. The typical extracted ion chromatograms of a quality control sample containing all 10 steroids at a concentration of 600 times LLOQ are shown in Fig. 2.

3.2. Assay validation

3.2.1. Linearity, accuracy and precision

The method was validated for all 10 steroids according to ICH Q2(R1) guidelines [19]. For the assessment of linearity, precision and accuracy, calibration standards were analyzed on three different days with three independently prepared samples each. Determined detection and quantification limits are given in Table 2. While conjugated steroids showed very low LLODs and LLOQs due to high ionization efficiency, DHEA and E2 demonstrated significantly higher values. This lower ionization efficiency of the unconjugated analytes can be explained by not using any derivatization protocol. Nevertheless, sensitivity of this method was high enough to selectively quantify all 10 steroids in the breast cancer cell model.

Based on the respective LLOQ, concentration ranges for the calibration curves were chosen individually for each single compound. Linear response was observed with R^2 values ranging from 0.9978 to 0.9999 (Table 2). Intra-day precision complied with the ICH guidelines with a mean RSD of 2.05% and all values $\leq 2.8\%$. Inter-day precision was proven by statistical comparison of data obtained on three different days by using an unpaired Student's *t*-test with calculated *t*-values ranging from 0.042 to 1.929 (upper limit = 3.747, $df = 4$, $p = 0.99$). Accuracy was demonstrated for all three QC concentration levels, with recovery rates ranging from 98.8% to 101.2% (Table 3).

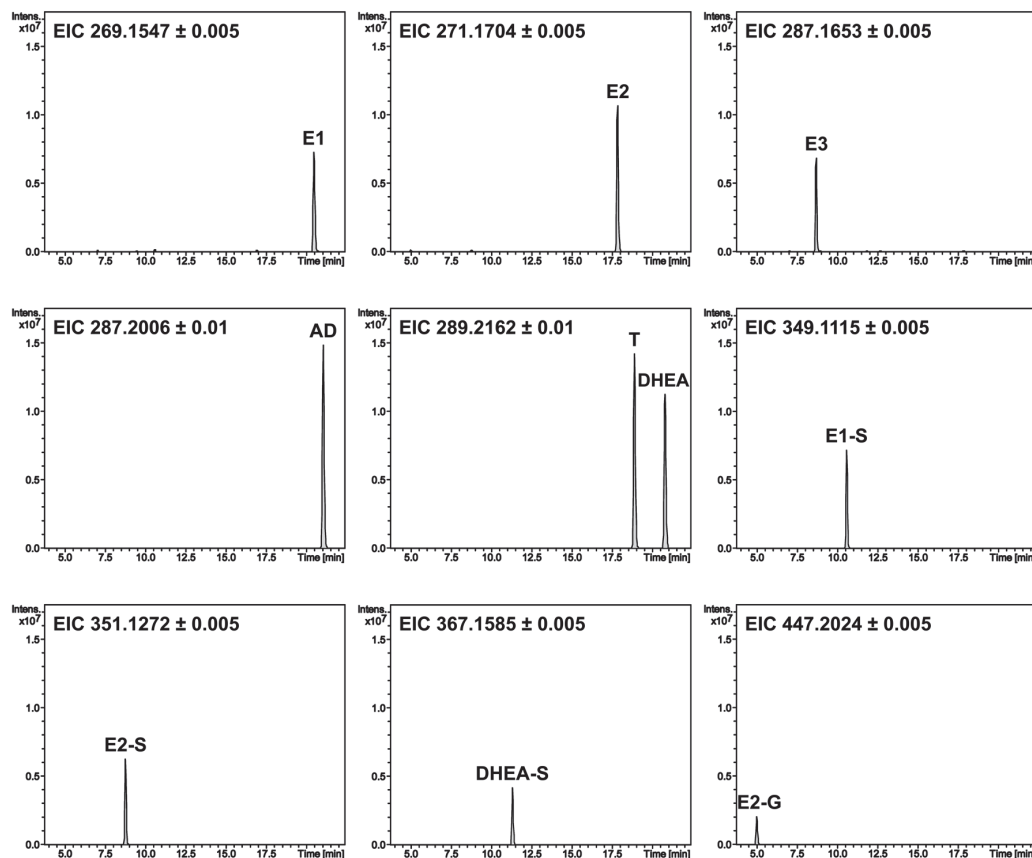


Fig. 2. Extracted ion chromatograms (EICs) of a high-concentration (600 times LLOQ) quality control sample containing all 10 analytes.

3.2.2. Stability and extraction efficiency

All analytes demonstrated sufficient stability in cell medium when samples were subjected to five freeze–thaw-cycles followed by SPE sample clean-up, with calculated survival rates ranging from 95.7% to 100.4% compared to freshly extracted control samples. Using standard solutions we further showed that SPE conditions had no impact on the stability of the conjugated steroids. All analytes were stable in cell free medium at incubation conditions (37 °C, 95% humidity, 5% CO₂) for 48 h and in culture medium when stored at –80 °C for at least two weeks (data not shown). Furthermore, stability of the compounds in the autosampler at 8 °C was also confirmed by repeated analysis of a sample containing all 10 standards in acetonitrile/ammonium acetate buffer (10 mM, pH=5.0) 25:75 (v/v) for up to 54 days.

The mean overall recovery rates, determined by comparison of the absolute peak areas of the analytes in buffer control samples without SPE versus analytes spiked in cell medium followed by SPE, were at least above 76.8% (see Table 3). SPE accuracy was assessed by calculating the analyte/internal standard peak area ratios. As recovery of the non-deuterated analytes and the deuterated internal standards were nearly identical, accuracy was excellent, ranging from 96.9% to 102.0% for all 10 steroids.

3.3. Comparison to previous methods

Up to date, published LC–MS methods are often limited by the number of analytes [10–14] or have to use multiple analytical procedures for quantification of conjugated and unconjugated

Table 3
Assay performance characteristics.

Compound	Intra-day precision (% RSD)	Accuracy (%)	SPE-recovery (% area)	SPE-accuracy (% ratio)	Stability (%)
AD	1.84	99.7	89.7	98.7	98.1
DHEA	1.53	101.2	95.5	100.7	98.1
DHEA-S	2.62	101.1	86.7	96.9	96.5
E1	0.95	100.3	82.6	98.9	98.9
E1-S	1.54	99.7	80.8	102.0	99.7
E2	2.48	99.7	76.8	98.7	95.7
E2-G	2.73	99.4	87.6	97.1	99.5
E2-S	1.82	99.7	87.1	98.3	97.8
E3	2.80	98.8	79.9	97.2	100.4
T	2.21	98.9	92.9	98.2	98.5

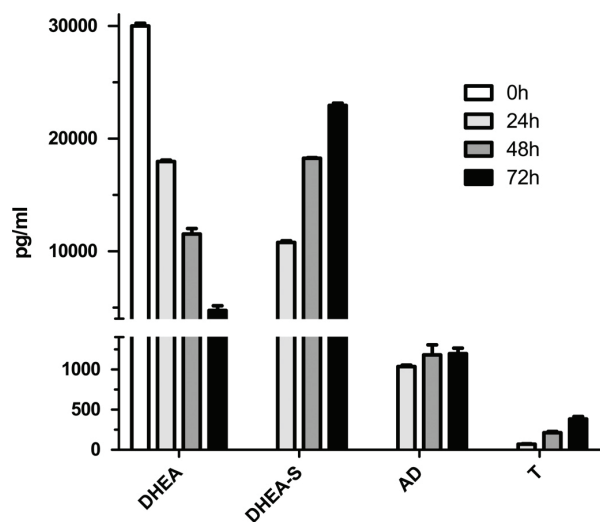


Fig. 3. Time dependent formation of metabolites by MCF-7 cells after incubation with 100 nM DHEA. Data represent means \pm SD of three independent biological replicates.

compounds [17,18]. The presented method allows the simultaneous quantification of the 10 major conjugated and unconjugated steroids of the estrogen metabolic pathway. The use of 10 deuterated internal standards in combination with the high mass accuracy of the MS ensures very high selectivity. The LC runtime of 30.5 min is comparable with other established assays [18,21]; however, throughput capability is higher than in methods using time-consuming derivatization procedures [22]. The sensitivity of our method for conjugated steroids is comparable to published assays or even higher [21], but it is less sensitive for unconjugated steroids. This is due to the fact that these more sensitive methods rely on pre-column derivatization of the analytes in order to increase ionization efficiency [15]. However, derivatization causes hydrolysis of conjugated metabolites, so that only total hormone concentrations can be quantified. Furthermore, any non-quantitative hydrolysis of

conjugates by β -glucuronidase and arylsulfatase would also lead to an underestimation of the true values [16].

3.4. Formation of estrogen metabolites in MCF-7 cells

Since MCF-7 cells are the most studied human breast cancer cell line [23] and have been extensively used for estrogen metabolism studies [24], we decided to show the functionality of this assay by treating these cells with hormone precursors (either DHEA or E1) and monitoring the formation of their metabolites over a time course of 72 h. As expected, a significant decrease in the precursor concentration concomitant with an increase of metabolites could be observed. When cells were incubated with 100 nM DHEA, we detected only three metabolites, namely DHEA-S, AD and T (Fig. 3), due to very little aromatase expression in MCF-7 cells [25]. In contrast, after incubation with 100 nM E1 as substrate, we were able to quantify the formation of E2, E3 and the conjugated estrogen metabolites E1-S, E2-G and E2-S (Fig. 4).

4. Conclusion

In conclusion, this precise and sensitive LC–HRMS assay allows the simultaneous quantification of 10 unconjugated hormone precursors, androgens, estrogens and their respective conjugated metabolites without prior derivatization. The validated calibration ranges were sufficient to selectively monitor hormone levels in a human breast cancer cell model. This novel assay is therefore a useful tool for in vitro studies of steroid metabolomics.

Conflict of interest

All authors declare no potential conflicts of interest concerning this article.

This research did not receive any specific grant from funding agencies in the public, commercial, or not-for-profit sectors.

References

- [1] J. Ferlay, I. Soerjomataram, R. Dikshit, S. Eser, C. Mathers, M. Rebelo, D. Parkin, D. Forman, F. Bray, Cancer incidence and mortality worldwide: sources, methods and major patterns in GLOBOCAN 2012, *Int. J. Cancer* 136 (2014) E359–E386.

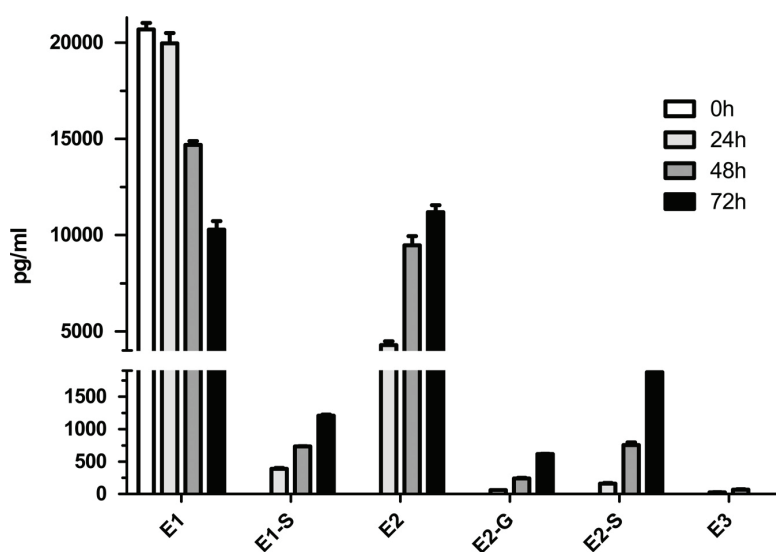


Fig. 4. Time dependent formation of metabolites by MCF-7 cells after incubation with 100 nM E1. Data represent means \pm SD of three independent biological replicates.

- [2] E. Folkert, M. Dowsett, Sex hormones and breast cancer risk and prognosis, *Breast* 22 (2013) S38–S43.
- [3] J. Limer, V. Speirs, Phyto-oestrogens and breast cancer chemoprevention, *Breast Cancer Res.* 6 (2004) 119–127.
- [4] T. Rižner, Estrogen biosynthesis, phase I and phase II metabolism and action in endometrial cancer, *Mol. Cell. Endocrinol.* 381 (2013) 124–139.
- [5] M. Krekels, W. Wouters, R. De Coster, R. Van Ginckel, A. Leonaers, P. Janssen, Aromatase in the human choriocarcinoma JEG-3: inhibition by R76 713 in cultured cells and in tumors grown in nude mice, *J. Steroid Biochem. Mol. Biol.* 38 (1991) 415–422.
- [6] T. Rižner, The important roles of steroid sulfatase and sulfotransferases in gynecological diseases, *Front. Pharmacol.* 7 (30) (2016) 1–16.
- [7] A. Purohit, L. Woo, B. Potter, Steroid sulfatase: a pivotal player in estrogen synthesis and metabolism, *Mol. Cell. Endocrinol.* 340 (2011) 154–160.
- [8] J. Mueller, L. Gilligan, J. Idkowiak, W. Arlt, P. Foster, The regulation of steroid action by sulfation and desulfation, *Endocr. Rev.* 36 (2015) 526–563.
- [9] X. Zhang, S. Tworoger, A. Eliassen, S. Hankinson, Postmenopausal plasma sex hormone levels and breast cancer risk over 20 years of follow-up, *Breast Cancer Res. Treat.* 137 (2013) 883–892.
- [10] M. Rauh, T. Koal, Standardized LC–MS/MS steroid hormone quantification, *CLB* 44 (2011) 542.
- [11] T. Guo, J. Gu, O. Soldin, R. Singh, S. Soldin, Rapid measurement of estrogens and their metabolites in human serum by liquid chromatography–tandem mass spectrometry without derivatization, *CLB* 41 (2008) 736–741.
- [12] D. Harwood, D. Handelsman, Development and validation of a sensitive liquid chromatography–tandem mass spectrometry assay to simultaneously measure androgens and estrogens in serum without derivatization, *Clin. Chim. Acta* 409 (2009) 78–84.
- [13] J. Hosogi, H. Tanaka, K. Fujita, T. Kuwabara, S. Ikegawa, N. Kobayashi, N. Mano, J. Goto, LC–MS/MS coupled with immunoaffinity extraction for determination of estrone, 17 β -estradiol and estrone 3-sulfate in human plasma, *J. Chromatogr. B* 878 (2010) 222–227.
- [14] K. Wooding, J. Hankin, C. Johnson, J. Chosich, S. Baek, A. Bradford, R. Murphy, N. Santoro, Measurement of estradiol, estrone, and testosterone in postmenopausal human serum by isotope dilution liquid chromatography tandem mass spectrometry without derivatization, *Steroids* 96 (2015) 89–94.
- [15] Y. Lin, C. Chen, G. Wang, Analysis of steroid estrogens in water using liquid chromatography/tandem mass spectrometry with chemical derivatizations, *Rapid Commun. Mass Spectrom.* 21 (2007) 1973–1983.
- [16] Q. Wang, L. Bottalico, C. Mesaros, I. Blair, Analysis of estrogens and androgens in postmenopausal serum and plasma by liquid chromatography–mass spectrometry, *Steroids* 99 (2015) 76–83.
- [17] T. Penning, S. Lee, Y. Jin, A. Gutierrez, I. Blair, Liquid chromatography–mass spectrometry (LC–MS) of steroid hormone metabolites and its applications, *J. Steroid Biochem. Mol. Biol.* 121 (2010) 546–555.
- [18] Y. Zhao, J. Boyd, M. Sawyer, X. Li, Liquid chromatography tandem mass spectrometry determination of free and conjugated estrogens in breast cancer patients before and after exemestane treatment, *Anal. Chim. Acta* 806 (2014) 172–179.
- [19] Validation of Analytical Procedures: Text and Methodology Q2(R1), International Conference on Harmonisation of Technical Requirements for Registration of Pharmaceuticals for Human Use (ICH), 1994, http://www.ich.org/fileadmin/Public.Web.Site/ICH_Products/Guidelines/Quality/Q2_R1/Step4/Q2_R1_Guideline.pdf (accessed 29.10.16).
- [20] H. Gu, G. Liu, J. Wang, A. Aubry, M. Arnold, Selecting the correct weighting factors for linear and quadratic calibration curves with least-squares regression algorithm in bioanalytical LC–MS/MS assays and impacts of using incorrect weighting factors on curve stability, data quality, and assay performance, *Anal. Chem.* 86 (2014) 8959–8966.
- [21] F. Qin, Y. Zhao, M. Sawyer, X. Li, Hydrophilic interaction liquid chromatography–tandem mass spectrometry determination of estrogen conjugates in human urine, *Anal. Chem.* 80 (2008) 3404–3411.
- [22] Q. Wang, K. Rangiah, C. Mesaros, N. Snyder, A. Vachani, H. Song, I. Blair, Ultrasensitive quantification of serum estrogens in postmenopausal women and older men by liquid chromatography–tandem mass spectrometry, *Steroids* 96 (2015) 140–152.
- [23] A. Lee, S. Oesterreich, N. Davidson, MCF-7 cells-changing the course of breast cancer research and care for 45 years, *J. Natl. Cancer Inst.* 107 (2015) djv073.
- [24] D. Xu, S. Lin, Mimicking postmenopausal steroid metabolism in breast cancer cell culture: differences in response to DHEA or other steroids as hormone sources, *J. Steroid Biochem. Mol. Biol.* 161 (2016) 92–100.
- [25] D. Zhou, J. Wang, E. Chen, J. Murai, P. Siiteri, S. Chen, Aromatase gene is amplified in MCF-7 human breast cancer cells, *J. Steroid Biochem. Mol. Biol.* 46 (1993) 147–153.

CHAPTER IV

THE IMPACTS OF GENISTEIN AND DAIDZEIN ON ESTROGEN CONJUGATIONS IN HUMAN BREAST CANCER CELLS: A TARGETED METABOLOMICS APPROACH

Authors:

Stefan Poschner, Alexandra Maier-Salamon, Martin Zehl, Judith Wackerlig,
Daniel Dobusch, Bettina Pachmann, Konstantin L. Sterlini and Walter Jäger

Published in:

Frontiers in Pharmacology **2017**, 8, 699

doi: 10.3389/fphar.2017.00699



The Impacts of Genistein and Daidzein on Estrogen Conjugations in Human Breast Cancer Cells: A Targeted Metabolomics Approach

Stefan Poschner¹, Alexandra Maier-Salamon¹, Martin Zehl², Judith Wackerlig³, Daniel Dobusch³, Bettina Pachmann¹, Konstantin L. Sterlini¹ and Walter Jäger^{1,4*}

¹ Division of Clinical Pharmacy and Diagnostics, Department of Pharmaceutical Chemistry, University of Vienna, Vienna, Austria, ² Department of Analytical Chemistry, Faculty of Chemistry, University of Vienna, Vienna, Austria, ³ Division of Drug Design and Medicinal Chemistry, Department of Pharmaceutical Chemistry, University of Vienna, Vienna, Austria, ⁴ Vienna Metabolomics Center (VIME), University of Vienna, Vienna, Austria

OPEN ACCESS

Edited by:

Maria Angela Sortino,
Università degli Studi di Catania, Italy

Reviewed by:

Ilpo Huhtaniemi,
Imperial College London,
United Kingdom
Taisen Iguchi,
National Institute for Basic Biology,
Japan

*Correspondence:

Walter Jäger
walter.jaeger@univie.ac.at

Specialty section:

This article was submitted to
Experimental Pharmacology and Drug
Discovery,
a section of the journal
Frontiers in Pharmacology

Received: 27 June 2017

Accepted: 19 September 2017

Published: 05 October 2017

Citation:

Poschner S, Maier-Salamon A, Zehl M, Wackerlig J, Dobusch D, Pachmann B, Sterlini KL and Jäger W (2017) The Impacts of Genistein and Daidzein on Estrogen Conjugations in Human Breast Cancer Cells: A Targeted Metabolomics Approach. *Front. Pharmacol.* 8:699. doi: 10.3389/fphar.2017.00699

The beneficial effect of dietary soy food intake, especially for women diagnosed with breast cancer, is controversial, as *in vitro* data has shown that the soy isoflavones genistein and daidzein may even stimulate the proliferation of estrogen-receptor alpha positive (ER α +) breast cancer cells at low concentrations. As genistein and daidzein are known to inhibit key enzymes in the steroid metabolism pathway, and thus may influence levels of active estrogens, we investigated the impacts of genistein and daidzein on the formation of estrogen metabolites, namely 17 β -estradiol (E2), 17 β -estradiol-3-(β -D-glucuronide) (E2-G), 17 β -estradiol-3-sulfate (E2-S) and estrone-3-sulfate (E1-S) in estrogen-dependent ER α + MCF-7 cells. We found that both isoflavones were potent inhibitors of E1 and E2 sulfation (85–95% inhibition at 10 μ M), but impeded E2 glucuronidation to a lesser extent (55–60% inhibition at 10 μ M). The stronger inhibition of E1 and E2 sulfation compared with E2 glucuronidation was more evident for genistein, as indicated by significantly lower inhibition constants for genistein [K_i s: E2-S (0.32 μ M) < E1-S (0.76 μ M) < E2-G (6.01 μ M)] when compared with those for daidzein [K_i s: E2-S (0.48 μ M) < E1-S (1.64 μ M) < E2-G (7.31 μ M)]. Concomitant with the suppression of E1 and E2 conjugation, we observed a minor but statistically significant increase in E2 concentration of approximately 20%. As the content of genistein and daidzein in soy food is relatively low, an increased risk of breast cancer development and progression in women may only be observed following consumption of high-dose isoflavone supplements. Further long-term human studies monitoring free estrogens and their conjugates are therefore highly warranted to evaluate the potential side effects of high-dose genistein and daidzein, especially in patients diagnosed with ER α + breast cancer.

Keywords: soy, genistein, daidzein, breast cancer, estrogens, metabolomics

Abbreviations: CYP, cytochrome P450 enzyme; DMEM, Dulbecco's modified Eagle's medium; DMSO, dimethyl sulfoxide; DPBS, Dulbecco's phosphate-buffered saline; E1, estrone; E1-S, estrone-3-sulfate; E2, 17 β -estradiol; E2-G, 17 β -estradiol-3-(β -D-glucuronide); E2-S, 17 β -estradiol-3-sulfate; E3, estriol (16 α -OH-17 β -estradiol); EIC, extracted ion chromatogram; ER α , estrogen receptor alpha; ER β , estrogen receptor beta; ESI, electrospray ionization; 17 β -HSD, 17 β -hydroxysteroid dehydrogenase; K_i , inhibition constant; K_m , Michaelis constant; LC-HRMS, liquid chromatography-high resolution mass spectrometry; LLOQ, lower limit of quantification; SD, standard deviation; SPE, solid phase extraction; SULT, sulfotransferase; UGT, UDP-glucuronosyl transferase; V_{max} , maximum reaction velocity.

INTRODUCTION

Breast cancer is the most prevalent cancer in women and the second leading cause of cancer-related deaths among females worldwide (Ferlay et al., 2015). Chemoprevention in combination with anticancer treatment is therefore crucial to reduce rates of morbidity and mortality. Evidence from epidemiological and experimental studies indicates that several natural products may act as chemopreventive agents and inhibit mammary carcinogenesis (Pan et al., 2015). Among these products is soy, which contains variable amounts of genistein and daidzein as the major isoflavones (approximately 47 and 44%, respectively) and minor amounts of glycitein (approximately 9% of the total isoflavones in soybeans). The genistein and daidzein content is therefore also predominant in soy-derived foods and dietary supplements (Wiseman et al., 2002; Clarke et al., 2008).

Epidemiological studies have indicated that soy intake post-diagnosis not only improves prognosis but is also associated with statistically significant reductions in breast cancer recurrence (Kang et al., 2010; Chi et al., 2013). However, based on the weak estrogen-like effects of the isoflavones genistein and daidzein, some researchers and clinicians are concerned that a high soy intake may increase the cancer risk. Indeed, *in vitro* studies have shown that both genistein and daidzein stimulate the proliferation of MCF-7 human estrogen-receptor alpha positive (ER α +) breast cancer cells at low concentrations, but inhibit tumor growth at higher doses. In ER alpha negative (ER α -) cells (MDA-MB-231), this biphasic effect is not observed; both phytoestrogens exhibit an anti-proliferative effect only. This indicates that the proliferative effect of genistein and daidzein, as observed at low doses, is ER α -mediated, while ER β , which is expressed at low levels in both MCF-7 and MDA-MB-231 cells, seems to oppose ER α actions and exhibits anti-migratory and anti-invasive properties (Vladusic et al., 2000; Al-Bader et al., 2011; Wang et al., 2012; Uifălean et al., 2016).

Besides an ER α -mediated interaction, low concentrations of both isoflavones can also induce cell proliferation via G protein coupled estrogen receptor 1 (GPER1) by stimulating cAMP production, intracellular Ca²⁺ mobilization and cSrc activation. Subsequently, the transactivation of the epidermal growth factor receptor (EGFR) is triggered, leading to an activation of downstream signaling pathways such as PI3K/Akt and MAPK/ERK (Uifălean et al., 2016).

In addition to ER α interaction and activation of signaling pathways, the stimulatory effect of genistein and daidzein on ER α + breast cancer cells might also be linked to increased steroid hormone levels, which drive cellular proliferation and thus are an important factor for carcinogenesis (Folkerd and Dowsett, 2013). Mechanism for altered steroid levels between ER α + and ER α - breast cancer cells include differences in estrogen metabolism. Indeed, incubation of human ER α + MCF-7 breast cancer cells with E1 for 24 h resulted in a more than sevenfold higher formation of estrogen sulfates compared to ER α - MDA-MB-231 cells, as cellular SULT expression is significantly higher in MCF-7 cells (Pasqualini, 2009). However, estrogen conjugates do not promote ER-mediated activity but represent a local reservoir of native E1 and E2 after hydrolysis by sulfatases

(Samavat and Kurzer, 2015). Interestingly, a previous human trial demonstrated that participants who consumed a high-soy diet for 13 months showed a non-significant increase of urinary E2 levels of 18% (Maskarinec et al., 2012), suggesting a possible role of E2 in the observed increased cellular growth of ER α + breast tumors by genistein and daidzein.

This prompted us to hypothesize that genistein and daidzein might dose-dependently alter steroid hormone levels by inhibiting the conjugation of estrogens and their precursors. Our hypothesis was supported by *in vitro* studies showing that soy isoflavonoids are able to inhibit various enzymes involved in the metabolism of estrogens, including cytochrome P450 3A4 (CYP3A4), 17 β -HSD, SULTs, and UGTs (Mesía-Vela and Kauffman, 2003; Mohamed and Frye, 2011; Ronis, 2016; Cassetta et al., 2017).

Whether soy components influences the estrogen metabolism is not yet known. Therefore, the aim of the present study was to investigate the impacts of genistein and daidzein on estrogen metabolism in human ER α + MCF-7 breast cancer cells. For this purpose, a newly established specific and sensitive analytical LC-HRMS assay was conducted to simultaneously quantify the main steroids of the estrogenic pathway namely E1, E2, estriol (16 α -OH-17 β -estradiol, E3), E1-S, E2-G and E2-S (Rižner, 2013; Mueller et al., 2015). The outcomes of metabolism were subsequently correlated with cell growth in order to better understand the effects of soy isoflavones in ER α + breast cancer.

MATERIALS AND METHODS

Materials

16 α -hydroxy-17 β -estradiol (E3), E2, 17 β -estradiol-3-(β -D-glucuronide) sodium salt (E2-G) and E1, as well as acetic acid, acetonitrile, ammonium acetate, DMSO, genistein and daidzein, were purchased from Sigma-Aldrich Chemical Co. (Munich, Germany). 17 β -estradiol-3-sulfate sodium salt (E2-S) and estrone-3-sulfate sodium salt (E1-S) were obtained from Steraloids, Inc. (Newport, RI, United States). 16 α -hydroxy-17 β -estradiol-2,4,17-d₃ (E3-d₃), 17 β -estradiol-2,4,16,16-d₄ (E2-d₄), 17 β -estradiol-16,16,17-d₃-3-(β -D-glucuronide) sodium salt (E2-G-d₃), 17 β -estradiol-2,4,16,16-d₄-3-sulfate sodium salt (E2-S-d₄), estrone-2,4,16,16-d₄ (E1-d₄) and estrone-2,4,16,16-d₄-3-sulfate sodium salt (E1-S-d₄) were purchased from C/D/N Isotopes, Inc. (Pointe-Claire, QC, Canada). Purified water was obtained using an arium® pro ultrapure water system (Sartorius AG, Göttingen, Germany).

Cell Proliferation Studies

MCF-7 breast cancer cells were purchased from the American Type Culture Collection (ATCC; Rockville, MD, United States). All experiments were performed during the exponential growth phase of the cell line. MCF-7 cells were routinely cultivated at 37°C (95% humidity and 5% CO₂) in phenol red-free Dulbecco's Modified Eagle Medium F-12 (DMEM/F-12; Invitrogen, Karlsruhe, Germany), fortified with 1% PenStrep®-solution and 10% fetal bovine serum (Invitrogen). For experimental

conditions, cells were seeded at a density of 1.0×10^6 cells per well and allowed to attach for 24 h. Prior to the application of genistein and daidzein, cells were washed twice with DPBS (Invitrogen), and DMEM/F-12, containing 10% HyClone® heat-inactivated charcoal-stripped fetal bovine serum (THP Medical Products, Vienna, Austria), was subsequently added to exclude external hormones. To evaluate the potential influence of genistein and daidzein on MCF-7 cell proliferation, cells were incubated for 48 h with E1 (100 nM) as an estrogen precursor in the presence of 1, 5, and 10 μ M genistein or daidzein, respectively. Genistein, daidzein and E1 were dissolved in DMSO prior to their addition to the cell medium to give a final DMSO concentration of 0.05%. Prior to cell counting with a Coulter® Z1 cell counter (Beckman Coulter GmbH, Krefeld, Germany), supernatant medium was removed and cells were detached using 400 μ l TrypLe® solution (Invitrogen). The effect of E1 (10, 25, 50, 75, and 100 nM) on the growth of MCF-7 cells was also determined using the same protocol as for genistein and daidzein. All experiments were performed in triplicate and the data are reported as means \pm SD of all values.

Inhibition Studies

MCF-7 breast cancer cells were cultivated in the presence of HyClone® heat-inactivated charcoal-stripped fetal bovine serum as described above, and then treated with increasing concentrations of E1 (10, 25, 50, 75, and 100 nM) in the presence of 1, 5, and 10 μ M genistein or daidzein, respectively. After 24 and 48 h, 2000 μ l media aliquots were mixed with 20 μ l deuterated internal standard solution and pre-cleaned by SPE on Oasis HLB 1 cc SPE cartridges (30 mg; Waters Corporation, Milford, MA, United States), as described previously (Poschner et al., 2017). Briefly, reconditioning of the cartridges was achieved using 2×1.0 ml acetonitrile and 3×1.0 ml ammonium acetate buffer (10 mM, pH = 5.0). Subsequently, samples were loaded onto the SPE cartridges and washed with 1×1.0 ml ammonium acetate buffer (10 mM, pH = 5.0) and 2×1.0 ml acetonitrile/ammonium acetate buffer (10 mM, pH 5.0) 10:90 (v/v). Analytes were then eluted using 2×650 μ l acetonitrile/ammonium acetate buffer (10 mM, pH = 5.0) 95:5 (v/v), evaporated to dryness, and reconstituted in 270 μ l acetonitrile/ammonium acetate buffer (10 mM, pH = 5.0) 25:75 (v/v). After media collection, cells were washed five times with 2.0 ml DPBS, detached using 200 μ l TrypLe® solution (37°C, 15 min), mixed with 800 μ l DPBS and transferred into plastic vials. Aliquots of these suspensions (100 μ l each) were used to determine the exact number of cells per sample well. For this, the aliquots were diluted 100-fold and counted using a Coulter® Z1 cell counter. To additionally quantify cytosolic steroid levels, the remaining cell suspensions (900 μ l each) were gently centrifuged (1000 rpm, 8 min) and the supernatants were discarded. The cell pellets were subsequently resuspended in 100 μ l aqueous ammonium acetate buffer (10 mM, pH = 5.0) and lysed by five freeze-thaw-cycles in liquid nitrogen (3 min each), followed by thawing at ambient temperature. Ammonium acetate buffer (1000 μ l) was then added and the suspensions were centrifuged (14000 rpm, 5 min), and the clear supernatants

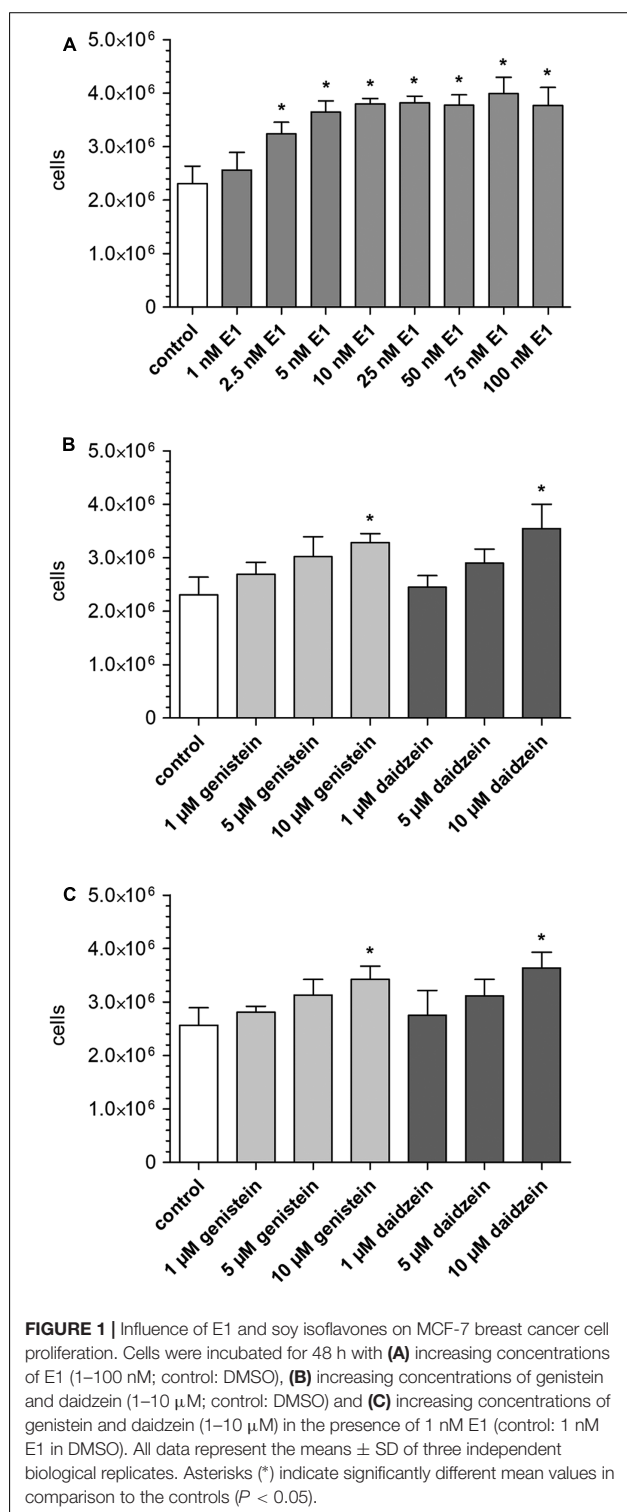
were concentrated using the SPE protocol described above. All processed samples were then stored at -80°C until further LC-HRMS analysis. Four biologically independent experiments were performed, and reported values represent the overall means \pm SD of all determinations.

LC-HRMS Assay

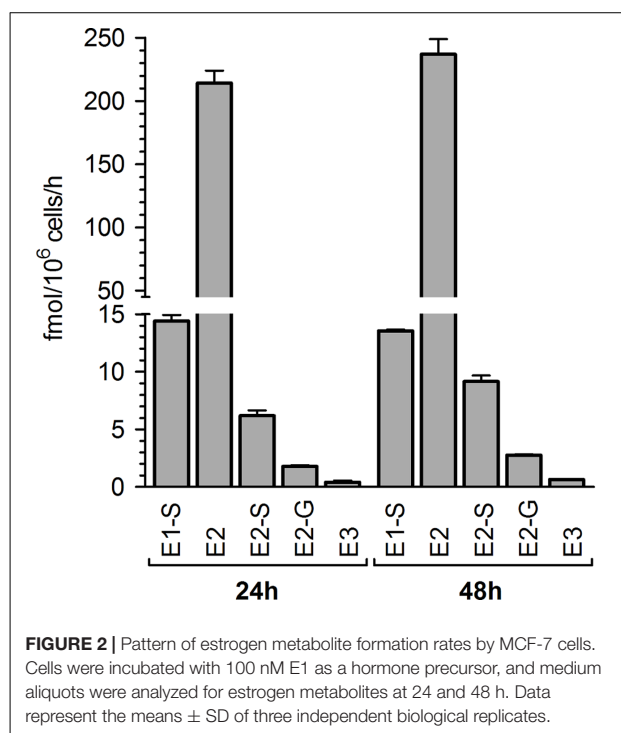
E1, E1-S, E2, E2-S, E2-G, and E3 were quantified using an LC-HRMS assay, validated according to the ICH Q2(R1) guidelines as described previously (Poschner et al., 2017). LC was performed using an UltiMate 3000 RSLC-series system (Dionex; Thermo Fisher Scientific, Inc., Germering, Germany) coupled to a maXis HD ESI-Qq-TOF mass spectrometer (Bruker Corporation, Bremen, Germany). Solvent A was aqueous ammonium acetate buffer (10 mM, pH = 5.0) and solvent B was acetonitrile. A Phenomenex Luna® 3 μ m C18(2) 100 Å LC column (250 mm \times 4.6 mm I.D.; Phenomenex, Inc., Torrance, CA, United States), preceded by a Hypersil® BDS-C18 guard column (5 μ m, 10 mm \times 4.6 mm I.D.; Thermo Fisher Scientific, Inc.) and maintained constantly at 43°C, was used for steroid separation at a flow rate of 1 ml/min. The injection volume was 100 μ l for each sample. The gradient used was as follows: 25% solvent B at 0 min, 56.3% solvent B at 19 min, a washing step at 90% solvent B from 19.5 to 24.0 min and column re-equilibration with 25% solvent B from 24.5 to 30.5 min. The ESI ion source settings were as follows: Capillary voltage, -4.5 kV; nebulizer, 1.0 bar N₂; dry gas flow rate, 8.0 l/min N₂; and dry temperature, 200°C. The ion transfer parameters were set to 400 Vpp funnel RF and 300 Vpp multipole RF, the quadrupole ion energy was 8.0 eV and the collision cell parameters were as follows: Collision energy, 10.0 eV; collision RF, 1100 Vpp; transfer time, 38 μ s; and pre-pulse storage, 18 μ s. Full-scan mass spectra were recorded in the range of m/z 150–500. Control samples consisting of unspiked cell culture medium showed no detectable background traces of the analyzed hormones. To ensure accurate quantification results, quality control samples, containing each analyte at a concentration of 6-fold or 600-fold of the respective lower limits of quantification (LLOQs), were analyzed in triplicate with each LC batch. The LLOQs were determined as follows: E1, 19.0 pg/ml; E1-S, 4.0 pg/ml; E2, 140.9 pg/ml; E2-S, 3.4 pg/ml; E2-G, 12.0 pg/ml; E3, 28.4 pg/ml cell medium.

Data Analysis

Liquid chromatography-high resolution mass spectrometry data were analyzed using Compass DataAnalysis 4.2 and QuantAnalysis 2.2 software (Bruker Corporation). EICs were created for each analyte and internal standard pair, from which the respective peak areas were determined to calculate the analyte/internal standard ratios for quantification. Kinetic analysis of estrogen metabolite formation in the presence and absence of genistein or daidzein using E1 as an estrogen precursor (10–100 nM for 48 h) was performed. All data best fitted to the Michaelis–Menten model: $V = V_{\max} \times [S] / (K_m + [S])$, where V is the rate of the reaction, V_{\max} is the maximum reaction velocity, K_m is the Michaelis constant and $[S]$ is the substrate concentration. Kinetic parameters were calculated



using GraphPad Prism 6.0 software (GraphPad Software Inc., La Jolla, CA, United States). Inhibition modes were determined from Lineweaver–Burk plots, and corresponding K_i were calculated



by plotting the slopes of the primary Lineweaver–Burk plots against the respective inhibitor concentrations using GraphPad Prism 6.0. The same software package was used for statistical analyses. All values were expressed as means \pm SD and the Student's *t*-test and ANOVA with Tukey's post-test were used to compare differences between control samples and treatment groups. The statistical significance level was set to $P < 0.05$.

RESULTS

Influence of Estrone and Soy Isoflavones on MCF-7 Cell Proliferation

To assess the influence of E1 on MCF-7 cancer cell growth, cells were incubated with increasing concentrations of E1 for 48 h, detached by application of TrypLe[®] solution and counted using a Coulter[®] Z1 cell counter. Compared with control samples (containing DMSO only), the number of viable MCF-7 cells was significantly increased in the presence of E1 ($2.31 \pm 0.33 \times 10^6$ vs. $3.99 \pm 0.31 \times 10^6$ cells) (Figure 1A), confirming the hormone-dependency of the MCF-7 cell line. The observed proliferative effect of E1 on the breast cancer cells was concentration-dependent with a mean maximum cell growth increase of 73% at 75 nM E1. Additionally, we evaluated the effect of E1 in combination with the soy isoflavones genistein or daidzein on MCF-7 cell growth. For this purpose, cells were co-incubated with 0, 1, 2.5, and 100 nM E1 as a hormone precursor in the presence of increasing concentrations of genistein or daidzein (1–10 μ M). These concentrations were chosen as they represent

plasma levels measured after the administration of isoflavone supplements. As shown in **Figure 1B**, the presence of both isoflavones in the absence of E1 had a significant effect on cell proliferation (+42% for genistein and +54% for daidzein). Co-incubation with the isoflavones and 1 nM E1 led to similar results with a mean cell number increase of +34% for genistein and +42% for daidzein (**Figure 1C**). When the E1 concentration was further increased to 2.5 nM, we observed only a slightly higher cell growth (+16 and +15%, respectively) compared to the incubation with E1 alone. In the presence of 100 nM E1, genistein and daidzein did not show any further increase of cellular growth because of the already high cell number stimulated by E1.

Formation of Estrogen Metabolites by MCF-7 Cells

In preliminary experiments, MCF-7 breast cancer cells were treated with 100 nM E1 as a hormone precursor and cell media aliquots were analyzed for E1 and its metabolites after 24 and 48 h. By using a highly specific and sensitive LC-HRMS assay, five biotransformation products could be quantified besides the precursor E1 in the cellular medium (**Figure 2**). As metabolite formation showed a linear trend with time up to 48 h, incubations in all further experiments were finalized after this time-span as it ensured the most precise quantification of the biotransformation products.

E2 represented the main metabolite in the cellular supernatant, with a mean formation rate of 233.1 ± 6.9 fmol/10⁶ cells/h after 48 h (**Figure 2** and **Table 1**). It was further sulfated and glucuronidated to E2-S and E2-G, with a markedly favoritism for the sulfated product (9.15 ± 1.21 vs. 2.76 ± 0.37 fmol/10⁶ cells/h). In addition to the conjugation reactions, E2 was also hydroxylated to E3, though this was a minor metabolite in MCF-7 cells with a formation rate of only 0.65 ± 0.05 fmol/10⁶ cells/h. Alongside the two E2 conjugates, we also observed the sulfation of the precursor E1 to E1-S (13.5 ± 2.1 fmol/10⁶ cells/h). Concomitant with the formation of these five metabolites, the E1 concentration in the medium decreased by 29% from 100 nM to 71.0 ± 0.9 nM after 48 h. The total molar proportion of all five metabolites was 28.9% indicating that these five biotransformation products represent almost 100% of all

metabolites formed from the precursor E1 by the MCF-7 cells (un-metabolized E1 + total detected metabolites: 99.9%). Interestingly, intracellular metabolite concentrations in all samples were below the respective detection limits (data not shown).

Kinetic profiles for the formation of estrogen metabolites by MCF-7 cells were then evaluated over an E1 concentration range of 10–100 nM for 48 h. 17 β -HSD-mediated formation of the main metabolite E2 best fitted to the Michaelis–Menten model, with a mean V_{\max} value of 464.5 ± 39.2 fmol/10⁶ cells/h and a mean K_m value of 95.4 ± 14.0 nM (**Table 2**). E2-S and E2-G formation also exhibited Michaelis–Menten kinetics with similar K_m values (95.9 ± 5.4 and 92.7 ± 9.0 nM, respectively), though the V_{\max} value for sulfation was 3.3-fold higher than that for glucuronidation (18.3 ± 0.7 vs. 5.52 ± 0.37 fmol/10⁶ cells/h), confirming the preference for E2 sulfation by MCF-7 cells. Kinetic parameters calculated for the sulfation of the precursor E1 ($V_{\max} = 26.8 \pm 2.3$ fmol/10⁶ cells/h, $K_m = 88.3 \pm 11.3$ nM) were comparable to those for E2 sulfation, probably because both are substrates of the same enzyme isoforms SULT1A1 and SULT1E1 (Harris et al., 2004). Evaluation of the kinetic profile for E3 formation was not possible, as only the highest E1 concentration (100 nM) but not the lower ones, resulted in E3 concentrations above the LLOQ of the presented assay.

Inhibition of Estrogen Conjugations by Genistein

To assess the possible inhibitory effect of genistein on estrogen metabolism, MCF-7 cells were first treated with E1 (100 nM) for 48 h in the presence and absence of increasing genistein concentrations (1, 5, and 10 μ M). As shown in **Table 1**, a marked inhibition of E1 and E2 conjugation by this isoflavone was observed (Supplementary Figure S1A). Even in the presence of 1 μ M genistein, the formation rates of E1-S, E2-S and E2-G decreased by approximately 25–35% compared to control. At 10 μ M genistein, the inhibition was more obvious, and more pronounced for sulfation than for glucuronidation. The formation rates of E1-S and E2-S were reduced by approximately 90–95%, respectively, compared with the control (E1-S, 1.27 ± 0.22 vs. 13.5 ± 2.1 fmol/10⁶ cells/h; E2-S, 0.54 ± 0.05 vs.

TABLE 1 | Estrogen metabolism by MCF-7 cells in the presence of genistein and daidzein.

Inhibitor	E2 (fmol/10 ⁶ cells/h)	E1-S (fmol/10 ⁶ cells/h)	E2-S (fmol/10 ⁶ cells/h)	E2-G (fmol/10 ⁶ cells/h)
Control	233.1 \pm 6.9	13.5 \pm 2.1	9.15 \pm 1.21	2.76 \pm 0.37
1 μ M genistein	242.1 \pm 16.7	10.2 \pm 1.8	5.90 \pm 0.76*	2.12 \pm 0.34*
5 μ M genistein	264.0 \pm 8.8*	2.26 \pm 0.27*	1.12 \pm 0.37*	1.41 \pm 0.33*
10 μ M genistein	277.2 \pm 18.2*	1.27 \pm 0.22*	0.54 \pm 0.05*	1.06 \pm 0.10*
1 μ M daidzein	244.2 \pm 9.0	8.15 \pm 1.26*	5.91 \pm 1.27*	2.39 \pm 0.27
5 μ M daidzein	260.7 \pm 19.2*	3.11 \pm 0.34*	1.27 \pm 0.34*	1.94 \pm 0.30*
10 μ M daidzein	275.4 \pm 5.9*	2.00 \pm 0.30*	0.69 \pm 0.16*	1.26 \pm 0.15*

Cells were incubated with increasing concentrations of the soy isoflavones genistein and daidzein and 100 nM E1 as hormone precursor for 48 h. All data represent the means \pm SD of four independent biological replicates. Values in bold and marked with an asterisk (*) are significantly different in comparison to the control values ($P < 0.05$).

TABLE 2 | Kinetic parameters of estrogen metabolism by MCF-7 cells in the presence of genistein and daidzein.

Inhibitor	E2		E1-S		E2-S		E2-G	
	V_{\max} (fmol/10 ⁶ cells/h)	K_m (nM)	V_{\max} (fmol/10 ⁶ cells/h)	K_m (nM)	V_{\max} (fmol/10 ⁶ cells/h)	K_m (nM)	V_{\max} (fmol/10 ⁶ cells/h)	K_m (nM)
Control	464.5 ± 39.2	95.4 ± 14.0	26.8 ± 2.3	88.3 ± 11.3	18.3 ± 0.7	95.9 ± 5.4	5.52 ± 0.37	92.7 ± 9.0
1 μM genistein	463.3 ± 39.7	87.1 ± 13.4	19.1 ± 2.0*	84.1 ± 12.9	13.5 ± 0.6*	98.2 ± 4.5	4.13 ± 0.34*	91.3 ± 10.9
5 μM genistein	520.7 ± 32.9	95.2 ± 10.5	4.28 ± 0.42*	91.6 ± 12.9	2.19 ± 0.07*	96.8 ± 4.5	2.84 ± 0.20*	106.4 ± 10.3
10 μM genistein	543.9 ± 31.6*	93.8 ± 9.51	2.58 ± 0.25*	93.9 ± 13.3	1.04 ± 0.07*	97.8 ± 9.8	2.16 ± 0.06*	106.3 ± 9.1
1 μM daidzein	488.2 ± 36.4	96.4 ± 12.4	17.1 ± 1.4*	102.6 ± 11.5	11.9 ± 0.9*	101.2 ± 10.8	4.83 ± 0.27*	98.0 ± 7.8
5 μM daidzein	508.7 ± 22.7	95.6 ± 7.39	6.43 ± 0.28*	104.4 ± 14.3	2.64 ± 0.22*	102.8 ± 11.9	3.99 ± 0.18*	100.4 ± 6.6
10 μM daidzein	543.5 ± 32.9*	96.8 ± 10.1	4.20 ± 0.47*	105.7 ± 16.5	1.35 ± 0.11*	98.6 ± 11.9	2.63 ± 0.32*	105.6 ± 18.3

Cells were incubated with increasing concentrations of the soy isoflavones genistein and daidzein and 10 to 100 nM E1 as hormone precursor for 48 h. All data represent the means ± SD of four independent biological replicates. Values in bold and marked with an asterisk (*) are significantly different in comparison to the control values ($P < 0.05$).

9.15 ± 1.21 fmol/10⁶ cells/h), whereas E2-G formation was only reduced by approximately 60% (1.06 ± 0.10 vs. 2.76 ± 0.37 fmol/10⁶ cells/h). Genistein also showed a pronounced inhibition on E3 formation (data not shown); based on its low concentration in the cellular medium, the corresponding K_i could not be calculated.

In order to determine the kinetic parameters for the observed inhibition processes, cells were treated with 10–100 nM E1 as hormone precursor and increasing concentrations of genistein (1–10 μM). As shown in **Figure 3**, the presence of genistein did not alter the kinetic profiles for E1 or E2 conjugations; the data still best-fitted to the Michaelis–Menten kinetic model. However, the mean V_{\max} values for the formation of the conjugates were significantly decreased by increasing genistein concentrations, while the corresponding K_m values were almost unaffected (**Table 2**). In order to gain further insight into the inhibition process, we determined the mode of inhibition by genistein on E1 and E2 metabolism and calculated the corresponding K_i by plotting the slopes of the primary Lineweaver–Burk plots against the respective inhibitor concentrations (**Figure 3**). As reported in **Table 3**, non-competitive inhibition by genistein was confirmed for all E1 and E2 conjugates, as initially indicated by the altered V_{\max} values and the almost unchanged K_m values (**Table 2**). The more pronounced inhibition of E1 and E2 sulfation over E2 glucuronidation by genistein (**Figure 3**) was also reflected by significantly lower K_i values for sulfation (E2-S, 0.32 μM and E1-S, 0.76 μM vs. E2-G, 6.01 μM), indicating decreased rates of sulfate formation even at very low genistein concentrations.

Inhibition of Estrogen Conjugations by Daidzein

Analogous to the cell experiments conducted with genistein, we first investigated the possible inhibition of E1 and E2 metabolism by daidzein. Again, the formation rates of E1-S, E2-S and E2-G were significantly decreased by approximately 15–40% compared to control, even at 1 μM daidzein (**Table 1** and Supplementary Figure S1B). The increase in daidzein concentration to 10 μM led to more pronounced suppression of E1 and E2 sulfation by approximately 85 and 90% compared to control (E1-S, 2.00 ± 0.30 vs. 13.5 ± 2.1 fmol/10⁶ cells/h; E2-S, 0.69 ± 0.16 vs. 9.15 ± 1.21 fmol/10⁶ cells/h), while E2 glucuronidation was only reduced by approximately 55% (1.26 ± 0.15 vs. 2.76 ± 0.37 fmol/10⁶ cells/h). Like genistein, also daidzein showed a pronounced inhibition of the very minor metabolite E3 (data not shown). However, based on its low concentration in the cellular medium, we were not able to calculate the kinetics for its inhibition.

Figure 4 and **Table 2** show the Michaelis–Menten parameters for the formation of E1-S, E2-S, and E2-G by MCF-7 cells in the presence of increasing daidzein concentrations (1–10 μM). The V_{\max} and K_m values were comparable to those calculated for the inhibition by genistein. The observed decrease in V_{\max} values and unaltered K_m values, together with the corresponding Lineweaver–Burk plots, again indicated that a non-competitive mechanism was the most likely mode of inhibition by daidzein. As shown in **Table 3**, the K_i values were also significantly

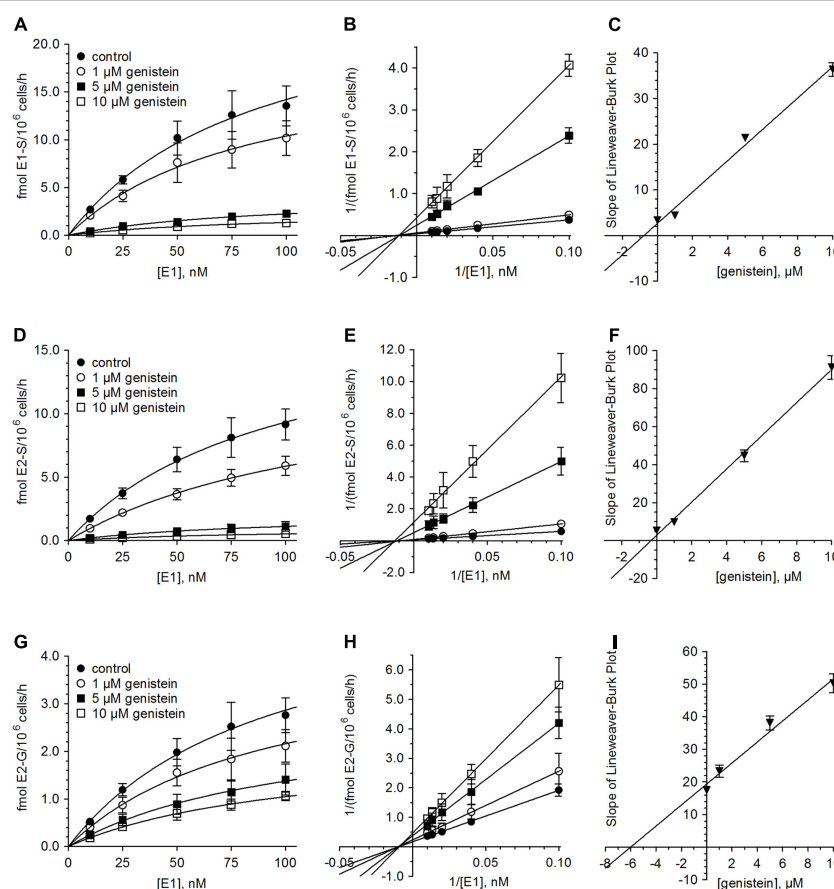


FIGURE 3 | Inhibition of estrogen conjugation by genistein. The kinetics of (A–C) E1 sulfation, (D–F) E2 sulfation and (G–I) E2 glucuronidation were calculated following incubation of MCF-7 cells with 10 to 100 nM E1 for 48 h in the presence (1–10 μM) and absence of genistein. Data is displayed in Michaelis–Menten, Lineweaver–Burk and K_i value plots. All data represent the means \pm SD of four independent biological replicates.

lower for sulfation compared with glucuronidation [E2-S (0.48 μM) < E1-S (1.64 μM) < E2-G (7.31 μM)].

Effect of Genistein and Daidzein on E2 Formation

Concomitant with the observed suppression of SULT- and UGT-mediated conjugation of E1 and E2, we observed a minor but statistically significant increase in E2 formation (Figure 5). When MCF-7 cells were exposed to 100 nM E1 in the presence of 1 μM isoflavone, E2 levels were elevated by approximately 4–5% (242.1 \pm 16.7 fmol/10⁶ cells/h for genistein and 244.2 \pm 9.0 fmol/10⁶ cells/h for daidzein) compared to control (233.1 \pm 6.9 fmol/10⁶ cells/h). Inhibition of E1 and E2 conjugation with 10 μM genistein or daidzein further increased E2 formation by ~20% compared to control (277.2 \pm 18.2 fmol/10⁶ cells/h for genistein and 275.4 \pm 5.9 fmol/10⁶ cells/h for daidzein) (Table 1).

In parallel, V_{max} values increased from 464.5 \pm 39.2 fmol/10⁶ cells/h to 543.9 \pm 31.6 or 543.5 \pm 32.9 fmol/10⁶ cells/h, when cells were treated with 10 μM genistein or daidzein, respectively.

TABLE 3 | Inhibition constants (K_i) and modes of inhibition.

Isoflavone	Metabolic activity	K_i (μM)	Mode of inhibition
Genistein	E1 sulfation	0.76	Non-competitive
	E2 sulfation	0.32	Non-competitive
	E2 glucuronidation	6.01	Non-competitive
Daidzein	E1 sulfation	1.64	Non-competitive
	E2 sulfation	0.48	Non-competitive
	E2 glucuronidation	7.31	Non-competitive

K_i values were obtained by plotting the slopes of the respective Lineweaver–Burk plots against isoflavone concentration. All data represent the means \pm SD of four independent biological replicates.

As already shown for E1 and E2 conjugates, K_m values were not affected by either isoflavone.

DISCUSSION

To the best of our knowledge, the present study was the first to investigate the concentration-dependent impacts of the

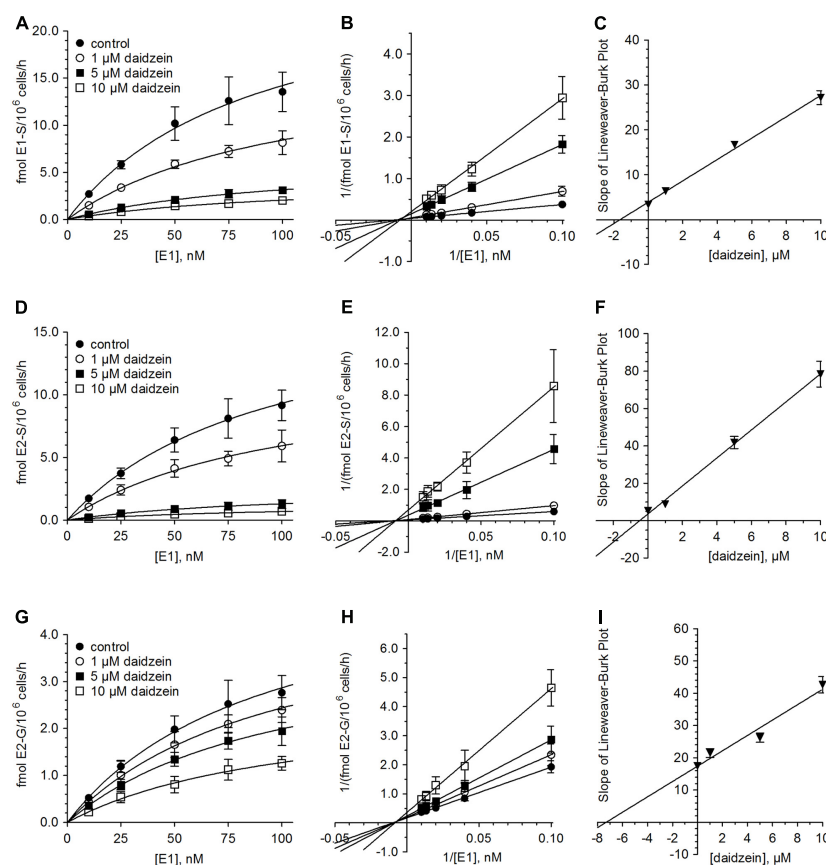


FIGURE 4 | Inhibition of estrogen conjugation by daidzein. The kinetics of (A–C) E1 sulfation, (D–F) E2 sulfation and (G–I) E2 glucuronidation were calculated following incubation of MCF-7 cells with 10 to 100 nM E1 for 48 h in the presence (1–10 μ M) and absence of daidzein. Data is displayed in Michaelis–Menten, Lineweaver–Burk and K_i value plots. All data represent the means \pm SD of four independent biological replicates.

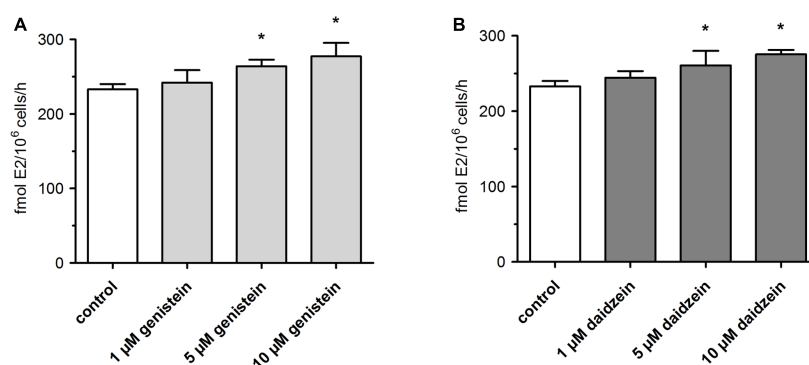
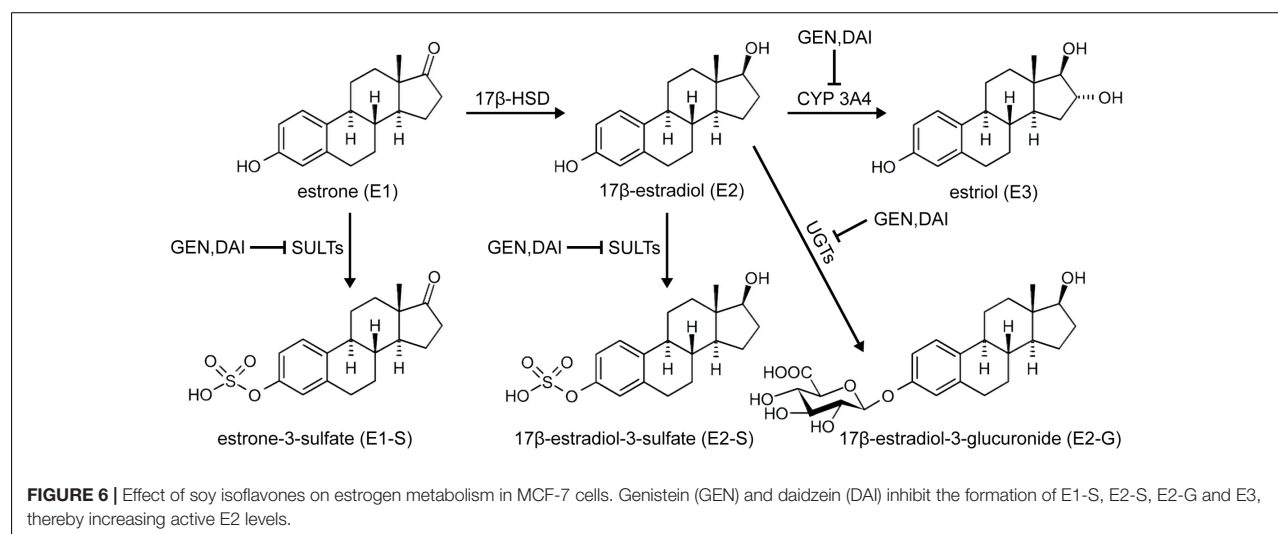


FIGURE 5 | Formation of active E2 by MCF-7 breast cancer cells. Cells were incubated with 100 nM E1 in the presence of (A) genistein or (B) daidzein. All data represent the means \pm SD of four independent biological replicates. Asterisks (*) indicate significantly different mean values in comparison to the controls ($P < 0.05$).

soy isoflavones genistein and daidzein on the formation of estrogen conjugates in human ER α + breast cancer cells (MCF-7). When cells were exposed solely to the hormone precursor E1, proliferation increased up to 1.6-fold. A stimulatory effect on cell

proliferation was also observed when cells were incubated with genistein or daidzein (1–10 μ M) in the absence or in the presence of low E1 concentrations (1 and 2.5 nM). Our findings are in line with previous studies that have also reported a stimulatory effect



of these isoflavone concentrations on MCF-7 cell growth (Chen et al., 2015; Wei et al., 2015). Our data also correlate with the *in vitro* study by Kuiper et al. (1998), which shows that genistein presents a 20- to 30-fold higher binding affinity for ER β than for ER α while daidzein has only a fivefold increased affinity for ER β , explaining the observed slightly increased proliferative effect of daidzein on ER α + MCF-7 cell growth (Figure 1).

After an incubation-period of 48 h, we were able to observe the formation of five metabolites, namely E1-S, E2, E2-S, E2-G and E3. Based on Michaelis–Menten parameters, the predominant metabolite was E2 (V_{\max} , 464.5 ± 39.2 fmol/ 10^6 cells/h), while the conjugates E1-S, E2-S and E2-G exhibited significantly lower V_{\max} values. Estimations of K_m values for E1-S, E2, E2-S and E2-G gave comparable results, indicating similar affinities to 17β-HSD, SULTs and UGTs. The CYP3A4-mediated hydroxylation of E2 to E3, however, represented only a very minor metabolic pathway by MCF-7 cells, as the formation of E3 could not be quantified at E1 concentrations of <100 nM.

Sulfation is therefore the main conjugation pathway of estrogens in MCF-7 cells as it accounted for 8.64% of total metabolites rate compared to only 1.05% for glucuronidation. The CYP3A4-mediated formation of E3 is negligible with a proportion of only 0.25% of the total E1 metabolism. These data are in line with previous *in vitro* investigations, which revealed a more than sevenfold higher formation of estrogen sulfates in human ER α + MCF-7 breast cancer cells than ER α –MDA-MB-231 cells after incubation with E1 for 24 h, based on significantly higher SULT expression (Pasqualini, 2009). Higher SULT expression in ER α + breast tumors compared to ER α –breast cancer tissues was also found in human primary tumor tissue samples (Adams et al., 1979).

When the cells were incubated with E1 in the presence of soy isoflavones (up to 10 μ M), estrogen conjugations were markedly decreased. Genistein inhibited E1-S and E2-S formation by 90 and 95% compared to control, while E2 glucuronidation was less affected and only decreased by 60%. Interestingly, daidzein, which differs from genistein only by the absence of a

hydroxyl group in position 5, showed slightly weaker inhibitory effects (E1-S, 85%; E2-S, 90%; E2-G, 55%). These findings are in accordance with previous data, which also reported a stronger inhibition of E1 and E2 sulfation by genistein than by daidzein, potentially due to a higher potency of this isoflavone against SULT1A1 (Mesía-Vela and Kauffman, 2003). Kinetic analysis in combination with corresponding Lineweaver–Burk plots showed that both isoflavones non-competitively inhibited estrogen conjugations by MCF-7 cells, with very low K_i values for E1 sulfation (genistein, 0.76 μ M; daidzein, 1.64 μ M). E2 sulfation was affected to an even greater extent by either isoflavone (genistein, 0.32 μ M; daidzein, 0.48 μ M). By contrast, the calculated K_i values for E2 glucuronidation were markedly higher (genistein, 6.01 μ M; daidzein, 7.31 μ M), confirming the stronger impact of isoflavone treatment on sulfation compared with glucuronidation. Non-competitive inhibition of E1 and E2 metabolite formation by both isoflavones is of clinical importance, as it suggests that the extent of inhibition depends only on the inhibitor concentration (indicated by marked decreases in V_{\max}) and not on the binding of E1 and E2 to the respective enzymes (indicated by largely unaltered K_m values).

Whether dietary soy intake or high-dose isoflavone supplements may cause or exacerbate breast cancer in post-menopausal women remains controversial. Although soy food and its isoflavones have been widely investigated in the past few decades as cancer chemopreventives, conflicting data regarding their efficacy and safety have been reported. Population-based studies (Nechuta et al., 2012; Zhang et al., 2017) have indicated beneficial effects of dietary soy food consumption for women diagnosed with ER α – breast cancer, such as reduced risk of mortality and improved treatment outcomes; however, these effects have not been observed in patients expressing ER α . Clinical trials have also raised concerns that isoflavone intake may drive cancer cell proliferation (Shike et al., 2014) and significantly increase the Ki-67 labeling index in premenopausal women (Khan et al., 2012). Therefore, understanding of

the metabolic interplay between genistein, daidzein and the concentration of active E2, which is associated with breast cancer risk and progression (Folkerd and Dowsett, 2013), is crucial for risk assessments.

Concomitant with the observed inhibition of E1 and E2 conjugation, genistein and daidzein caused a minor, but statistically significant increase of approximately 20% in the active E2 levels (Figure 5). Based on increased E2 formation in the presence of genistein and daidzein, inhibition of 17 β -HSD can be excluded. Our data are in contrast to a very recent study showing an inhibition of this enzyme by genistein (Cassetta et al., 2017). This discrepancy might be explained by the fact that the authors used purified recombinant 17 β -HSD from the filamentous fungus *Cochliobolus lunatus* and not a human enzyme which might differ in activity. Both isoflavones, however, significantly inhibited the activity of cellular SULTs responsible for the formation of E1-S thereby increasing the E1 pool and consequently leading to a higher E2-formation by 17 β -HSD. Furthermore, genistein and daidzein also demonstrated a pronounced inhibition of E2-S, E2-G and E3 formation thereby contributing to the observed increased E2 level (Figure 6).

The observed increase in E2 in our *in vitro* model was also found in a previous human trial which examined the effect of soy foods on urinary estrogens in premenopausal women (Maskarinec et al., 2012). Participants who consumed a high-soy diet for 13 months showed a non-significant increase of urinary E2 levels of 18%. These findings were confirmed by a meta-analysis (Hooper et al., 2009), in which the authors also reported a small, non-significant increase in total estradiol concentrations of 14% in post-menopausal women following soy isoflavone consumption. Although both studies observed a minor, non-significant increase in urinary E2 levels, soy food consumption should be considered safe, as even the daily intake of two dietary servings of soy powder (25 g each) for up to 30 days lead to mean total plasma levels (parent compound, glucuronides and sulfates) of only 11.6 ng/ml (0.042 μ M) for genistein and 6.7 ng/ml (0.026 μ M) for daidzein (Shike et al., 2014). These concentrations are far below our calculated K_i values (0.3–1.6 μ M for E1 and E2 sulfates, and 6.0–7.3 μ M for E2 glucuronide) therefore suggesting no significant effect of dietary soy intake on estrogen metabolism.

On the other hand, daily high-dose supplementation with genistein (600 mg) and daidzein (300 mg) for 84 days has been found to increase the trough plasma levels up to a concentration of 15 μ g/ml (55 μ M) total isoflavones (Pop et al., 2008). Taking into account that the majority of isoflavones are extensively metabolized *in vivo* (up to 98%), the remaining free genistein and daidzein plasma concentrations would reach approximately

1 μ M, which is still high enough to inhibit E1 and E2 sulfation, while leaving E2 glucuronidation unaffected. Whether genistein or daidzein glucuronides and sulfates also exhibit an inhibitory activity toward E1 and E2 conjugation is not known yet. However, any additive inhibitory effects would further increase the plasma concentration of free E2 following isoflavone supplementation.

CONCLUSION

The present work identified a non-competitive inhibition of E1 and E2 conjugation by low micromolar concentrations of soy isoflavones in the human breast cancer cell line MCF-7, which leads to a minor but statistically significant increase in unconjugated E2 of approximately 20%. As the content of genistein and daidzein in soy food is relatively low, an increased risk of breast cancer development and progression in women might only be observed after the continuous consumption of high-dose isoflavone supplements. Further long-term human studies monitoring free estrogens and their conjugates are therefore highly warranted to evaluate the efficacy and safety of high-dose genistein and daidzein supplementation, especially in patients diagnosed with ER α + breast cancer.

AUTHOR CONTRIBUTIONS

SP performed all the cell culture experiments, the LC-HRMS analysis and the data analysis, and contributed to the manuscript. AM-S analyzed the data and contributed to the manuscript. MZ, JW, and DD performed the LC-HRMS analysis. BP and KS cultivated the MCF-7 cells and performed inhibition experiments; and WJ planned the experiments, analyzed the data and wrote the final version of the manuscript.

ACKNOWLEDGMENTS

This research was supported by a grant from the Austrian Science Fund (FWF) [I 3417-B31] awarded to WJ.

SUPPLEMENTARY MATERIAL

The Supplementary Material for this article can be found online at: <https://www.frontiersin.org/articles/10.3389/fphar.2017.00699/full#supplementary-material>

REFERENCES

- Adams, J. B., Pownim, T., Chandra, D. P., Archibald, L., and Foo, M. S. (1979). A correlation between estrogen sulfotransferase levels and estrogen receptor status in human primary breast carcinoma. *Cancer Res.* 39, 5124–5126.
- Al-Bader, M., Ford, C., Al-Ayadhy, B., and Francis, I. (2011). Analysis of estrogen receptor isoforms and variants in breast cancer cell lines. *Exp. Ther. Med.* 2, 537–544. doi: 10.3892/etm.2011.226
- Cassetta, A., Stojan, J., Krastanova, I., Kristan, K., Brunskole Šveglj, M., Lamba, D., et al. (2017). Structural basis for inhibition of 17 β -hydroxysteroid dehydrogenases by phytoestrogens: the case of fungal 17 β -HSDcl. *J. Steroid Biochem. Mol. Biol.* 171, 80–93. doi: 10.1016/j.jsbmb.2017.02.020
- Chen, J., Duan, Y., Zhang, X., Ye, Y., Ge, B., and Chen, J. (2015). Genistein induces apoptosis by the inactivation of the IGF-1R/p-Akt signaling pathway in MCF-7 human breast cancer cells. *Food Funct.* 6, 995–1000. doi: 10.1039/c4fo01141d

- Chi, F., Wu, R., Zeng, Y. C., Xing, R., Liu, Y., and Xu, Z. G. (2013). Post-diagnosis soy food intake and breast cancer survival: a meta-analysis of cohort studies. *Asian Pac. J. Cancer Prev.* 14, 2407–2412.
- Clarke, D. B., Bailey, V., and Lloyd, A. S. (2008). Determination of phytoestrogens in dietary supplements by LC-MS/MS. *Food Addit. Contam. Part A Chem. Anal. Control Expo. Risk Assess.* 25, 534–547. doi: 10.1080/02652030701658340
- Ferlay, J., Soerjomataram, I., Dikshit, R., Eser, S., Mathers, C., Rebelo, M., et al. (2015). Cancer incidence and mortality worldwide: sources, methods and major patterns in GLOBOCAN 2012. *Int. J. Cancer.* 136, E359–E386. doi: 10.1002/ijc.29210
- Folkerd, E., and Dowsett, M. (2013). Sex hormones and breast cancer risk and prognosis. *Breast* 22(Suppl. 2), 38–43. doi: 10.1016/j.breast.2013.07.007
- Harris, R. M., Wood, D. M., Bottomley, L., Blagg, S., Owen, K., Hughes, P. J., et al. (2004). Phytoestrogens are potent inhibitors of estrogen sulfation: implications for breast cancer risk and treatment. *J. Clin. Endocrinol. Metab.* 89, 1779–1787.
- Hooper, L., Ryder, J. J., Kurzer, M. S., Lampe, J. W., Messina, M. J., Phipps, W. R., et al. (2009). Effects of soy protein and isoflavones on circulating hormone concentrations in pre- and post-menopausal women: a systematic review and meta-analysis. *Hum. Reprod. Update* 15, 423–440. doi: 10.1093/humupd/dmp010
- Kang, X., Zhang, Q., Wang, S., Huang, X., and Jin, S. (2010). Effect of soy isoflavones on breast cancer recurrence and death for patients receiving adjuvant endocrine therapy. *CMAJ* 182, 1857–1862. doi: 10.1503/cmaj.091298
- Khan, S. A., Chatterton, R. T., Michel, N., Bryk, M., Lee, O., Ivancic, D., et al. (2012). Soy isoflavone supplementation for breast cancer risk reduction: a randomized phase II trial. *Cancer Prev. Res.* 5, 309–319. doi: 10.1158/1940-6207.CAPR-11-0251
- Kuiper, G. G., Lemmen, J. G., Carlsson, B., Corton, J. C., Safe, S. H., van der Saag, P. T., et al. (1998). Interaction of estrogenic chemicals and phytoestrogens with estrogen receptor beta. *Endocrinology* 139, 4252–4263.
- Maskarinec, G., Morimoto, Y., Heak, S., Isaki, M., Steinbrecher, A., Custer, L., et al. (2012). Urinary estrogen metabolites in two soy trials with premenopausal women. *Eur. J. Clin. Nutr.* 66, 1044–1049. doi: 10.1038/ejcn.2012.71
- Mesia-Vela, S., and Kauffman, F. C. (2003). Inhibition of rat liver sulfotransferases SULT1A1 and SULT2A1 and glucuronosyltransferase by dietary flavonoids. *Xenobiotica* 33, 1211–1220.
- Mohamed, M. E., and Frye, R. F. (2011). Effects of herbal supplements on drug glucuronidation. Review of clinical, animal, and in vitro studies. *Planta Med.* 77, 311–321. doi: 10.1055/s-0030-1250457
- Mueller, J. W., Gilligan, L. C., Idkowiak, J., Arlt, W., and Foster, P. A. (2015). The regulation of steroid action by sulfation and desulfation. *Endocr. Rev.* 36, 526–563. doi: 10.1210/er.2015-1036
- Nechuta, S. J., Caan, B. J., Chen, W. Y., Lu, W., Chen, Z., Kwan, M. L., et al. (2012). Soy food intake after diagnosis of breast cancer and survival: an in-depth analysis of combined evidence from cohort studies of US and Chinese women. *Am. J. Clin. Nutr.* 96, 123–132. doi: 10.3945/ajcn.112.035972
- Pan, M. H., Chiou, Y. S., Chen, L. H., and Ho, C. T. (2015). Breast cancer chemoprevention by dietary natural phenolic compounds: specific epigenetic related molecular targets. *Mol. Nutr. Food Res.* 59, 21–35. doi: 10.1002/mnfr.201400515
- Pasqualini, J. R. (2009). Estrogen sulfotransferases in breast and endometrial cancers. *Ann. N. Y. Acad. Sci.* 1155, 88–98. doi: 10.1111/j.1749-6632.2009.04113.x
- Pop, E. A., Fischer, L. M., Coan, A. D., Gitzinger, M., Nakamura, J., and Zeisel, S. H. (2008). Effects of a high daily dose of soy isoflavones on DNA damage, apoptosis and estrogenic outcomes in healthy, postmenopausal women – a phase I clinical trial. *Menopause* 15, 684–692. doi: 10.1097/gme.0b013e318167b8f2
- Poschner, S., Zehl, M., Maier-Salamon, A., and Jäger, W. (2017). Simultaneous quantification of estrogens, their precursors and conjugated metabolites in human breast cancer cells by LC-HRMS without derivatization. *J. Pharm. Biomed. Anal.* 138, 344–350. doi: 10.1016/j.jpba.2017.02.033
- Rižner, T. L. (2013). Estrogen biosynthesis, phase I and phase II metabolism, and action in endometrial cancer. *Mol. Cell. Endocrinol.* 381, 124–139. doi: 10.1016/j.mce.2013.07.026
- Ronis, M. J. (2016). Effects of soy containing diet and isoflavones on cytochrome P450 enzyme expression and activity. *Drug Metab. Rev.* 48, 331–341. doi: 10.1080/03602532.2016.1206562
- Samavat, H., and Kurzer, M. S. (2015). Estrogen metabolism and breast cancer. *Cancer Lett.* 356, 231–243. doi: 10.1016/j.canlet.2014.04.018
- Shike, M., Doane, A. S., Russo, L., Cabal, R., Reis-Filho, J. S., Gerald, W., et al. (2014). The effects of soy supplementation on gene expression in breast cancer: a randomized placebo-controlled study. *J. Natl. Cancer Inst.* 106:dju189. doi: 10.1093/jnci/dju189
- Uifălean, A., Schneider, S., Gierok, P., Ionescu, C., Iuga, C. A., and Lalk, M. (2016). The impact of soy isoflavones on MCF-7 and MDA-MB-231 breast cancer cells using a global metabolomic approach. *Int. J. Mol. Sci.* 17:E1443. doi: 10.3390/ijms17091443
- Vladusic, E., Hornby, A., Guerra-Vladusic, F., Lakins, J., and Lupu, R. (2000). Expression and regulation of estrogen receptor beta in human breast tumors and cell lines. *Oncol. Rep.* 7, 157–224. doi: 10.3892/or.7.1.157
- Wang, D., Huang, P., Zhu, B., Sun, L., Huang, Q., and Wang, J. (2012). Induction of estrogen receptor (β -36 expression by bone morphogenetic protein 2 in breast cancer cell lines. *Mol. Med. Rep.* 6, 591–596. doi: 10.3892/mmr.2012.945
- Wei, Y. K., Gamra, I., Davenport, A., Lester, R., Zhao, L., and Wei, Y. (2015). Genistein induces cytochrome P450 1B1 gene expression and cell proliferation in human breast cancer MCF-7 cells. *J. Environ. Pathol. Toxicol. Oncol.* 34, 153–159.
- Wiseman, H., Casey, K., Clarke, D. B., Barnes, K. A., and Bowey, E. (2002). Isoflavone aglycon and glucoside content of high- and low-soy U.K. foods used in nutritional studies. *J. Agric. Food Chem.* 50, 1404–1410.
- Zhang, F. F., Haslam, D. E., Terry, M. B., Knight, J. A., Andrulis, I. L., Daly, M. B., et al. (2017). Dietary isoflavone intake and all-cause mortality in breast cancer survivors: the breast cancer family registry. *Cancer* 123, 2070–2079. doi: 10.1002/cncr.30615

Conflict of Interest Statement: The authors declare that the research was conducted in the absence of any commercial or financial relationships that could be construed as a potential conflict of interest.

Copyright © 2017 Poschner, Maier-Salamon, Zehl, Wackerlig, Dobusch, Pachmann, Sterlini and Jäger. This is an open-access article distributed under the terms of the Creative Commons Attribution License (CC BY). The use, distribution or reproduction in other forums is permitted, provided the original author(s) or licensor are credited and that the original publication in this journal is cited, in accordance with accepted academic practice. No use, distribution or reproduction is permitted which does not comply with these terms.

CHAPTER V

RESVERATROL INHIBITS KEY STEPS OF STEROID METABOLISM IN A HUMAN ESTROGEN-RECEPTOR POSITIVE BREAST CANCER MODEL: IMPACT ON CELLULAR PROLIFERATION

Authors:

Stefan Poschner, Alexandra Maier-Salamon, Martin Zehl, Judith Wackerlig,
Daniel Dobusch, Anastasia Meshcheryakova, Diana Mechtcheriakova,
Theresia Thalhammer, Bettina Pachmann and Walter Jäger

Published in:

Frontiers in Pharmacology **2018**, 9, 742

doi: 10.3389/fphar.2018.00742



Resveratrol Inhibits Key Steps of Steroid Metabolism in a Human Estrogen-Receptor Positive Breast Cancer Model: Impact on Cellular Proliferation

Stefan Poschner¹, Alexandra Maier-Salamon¹, Martin Zehl², Judith Wackerlig³, Daniel Dobusch³, Anastasia Meshcheryakova⁴, Diana Mechtcheriakova⁴, Theresia Thalhammer⁴, Bettina Pachmann¹ and Walter Jäger^{1,5*}

¹ Division of Clinical Pharmacy and Diagnostics, Department of Pharmaceutical Chemistry, University of Vienna, Vienna, Austria, ² Department of Analytical Chemistry, Faculty of Chemistry, University of Vienna, Vienna, Austria, ³ Division of Drug Design and Medicinal Chemistry, Department of Pharmaceutical Chemistry, University of Vienna, Vienna, Austria, ⁴ Department of Pathophysiology and Allergy Research, Center for Pathophysiology, Infectiology and Immunology, Medical University of Vienna, Vienna, Austria, ⁵ Vienna Metabolomics Center, University of Vienna, Vienna, Austria

OPEN ACCESS

Edited by:

Dagmar Meyer zu Heringdorf,
Goethe-Universität Frankfurt am Main,
Germany

Reviewed by:

Marc Poirat,
Institut National de la Santé et de la
Recherche Médicale (INSERM),
France
Dan Cacsire Castillo-Tong,
Medizinische Universität Wien, Austria

*Correspondence:

Walter Jäger
walter.jaeger@univie.ac.at

Specialty section:

This article was submitted to
Experimental Pharmacology
and Drug Discovery,
a section of the journal
Frontiers in Pharmacology

Received: 26 March 2018

Accepted: 19 June 2018

Published: 10 July 2018

Citation:

Poschner S, Maier-Salamon A, Zehl M, Wackerlig J, Dobusch D, Meshcheryakova A, Mechtcheriakova D, Thalhammer T, Pachmann B and Jäger W (2018) Resveratrol Inhibits Key Steps of Steroid Metabolism in a Human Estrogen-Receptor Positive Breast Cancer Model: Impact on Cellular Proliferation. *Front. Pharmacol.* 9:742. doi: 10.3389/fphar.2018.00742

The role of resveratrol (RES) in preventing breast cancer is controversial, as low concentrations may stimulate the proliferation of estrogen-receptor alpha positive (ERα+) breast cancer cells. As metabolism is the key factor in altering cellular estrogens, thereby influencing breast tumor growth, we investigated the effects of RES on the formation of estrogen metabolites, namely 4-androstene-3,17-dione (AD), dehydroepiandrosterone (DHEA), dehydroepiandrosterone-3-O-sulfate (DHEA-S), estrone (E1), estrone-3-sulfate (E1-S), 17β-estradiol (E2), 17β-estradiol-3-O-(β-D-glucuronide) (E2-G), 17β-estradiol-3-O-sulfate (E2-S), 16α-hydroxy-17β-estradiol (estriol, E3), and testosterone (T) in ERα– MDA-MB-231 and ERα+ MCF-7 cells. Incubation of both of the cell lines with the hormone precursors DHEA and E1 revealed that sulfation and glucuronidation were preferred metabolic pathways for DHEA, E1 and E2 in MCF-7 cells, compared with in MDA-MB-231 cells, as the V_{max} values were significantly higher (DHEA-S: 2873.0 ± 327.4 fmol/10⁶ cells/h, E1-S: 30.4 ± 2.5 fmol/10⁶ cells/h, E2-S: 24.7 ± 4.9 fmol/10⁶ cells/h, E2-G: 7.29 ± 1.36 fmol/10⁶ cells/h). RES therefore significantly inhibited DHEA-S, E1-S, E2-S and E2-G formation in MCF-7, but not in MDA-MB-231 cells (K_i s: E2-S, 0.73 ± 0.07 μM < E1-S, 0.94 ± 0.03 μM < E2-G, 7.92 ± 0.24 μM < DHEA-S, 13.2 ± 0.2 μM). Suppression of these metabolites subsequently revealed twofold higher levels of active E2, concomitant with an almost twofold increase in MCF-7 cell proliferation, which was the most pronounced upon the addition of 5 μM RES. As the content of RES in food is relatively low, an increased risk of breast cancer progression in women is likely to only be observed following the continuous consumption of high-dose RES supplements. Further long-term human studies simultaneously monitoring free estrogens and their conjugates are therefore highly warranted to evaluate the efficacy and safety of RES supplementation, particularly in patients diagnosed with ERα+ breast cancer.

Keywords: resveratrol, breast cancer, MDA-MB-231, MCF-7, steroids, metabolomics

INTRODUCTION

Breast cancer is a major cause of death in women worldwide (Ferlay et al., 2015). Chemoprevention is therefore crucial to reduce morbidity and mortality. Several epidemiological and experimental studies have indicated that certain natural phenolic compounds may inhibit mammary carcinogenesis, and may therefore act as chemopreventive agents (Pan et al., 2015). One of such compound is *trans*-resveratrol (3,5,4'-trihydroxy-*trans*-stilbene), a naturally occurring polyphenol found in red wine and foods, including peanuts, blueberries and cranberries, as well as the skin of grapes (Aiyer et al., 2012). The anti-proliferative properties of RES have been demonstrated *in vitro* against hormone-dependent and hormone-independent breast cancer cells through the induction of apoptosis via the down-regulation of p53, NF- κ B and Bcl-2, the inhibition of ribonucleotide reductase and DNA polymerases, and the suppression of the RhoA/Lats1/YAP signaling axis (Saluzzo et al., 2016; Kim et al., 2017). RES is also a radical scavenger and an inhibitor of cyclooxygenases (COX-1 and COX-2), which partly explains why this compound may reduce the occurrence of breast cancer (Murias et al., 2005). In addition, animal experiments identified significantly reduced tumor growth in human breast cancer xenografts subsequent to RES treatment, therefore supporting the use of this polyphenol as a chemotherapeutic agent (Garvin et al., 2006). Furthermore, a human case-control study using data from 369 cases and 602 controls reported a significant inverse association for the relationship between dietary RES intake and the risk of developing breast cancer (Levi et al., 2005).

However, based on the estrogen-like effects of RES due to its structural similarity with 17 β -estradiol (E2) (Yildiz, 2005), some researchers and clinicians are concerned that the intake of RES may negatively affect hormone-dependent malignancies. Indeed, RES stimulates the proliferation of estrogen-receptor alpha positive (ER α +) breast cancer cells at low concentrations, but inhibits tumor growth at high doses. In ER alpha negative (ER α -) cells, this biphasic effect has not been observed; RES only exhibits anti-proliferative effects (Basly et al., 2000).

In addition to interactions with ERs, the stimulatory effects of RES on ER α + breast cancer cells may also be linked to increased steroid hormone levels, which induce cellular proliferation and

thus are an important factor for carcinogenesis (Folkert and Dowsett, 2013). Indeed, RES treatment of mice (4 mg/kg i.p. for 7 days) resulted in an approximately twofold increase in E2 levels (El-Sayed and Bayan, 2015). Also a previous clinical study of post-menopausal women who were administered 1 g RES once a day for 12 weeks demonstrated a non-significant increase in serum E2 concentrations by 22.4% (Chow et al., 2014). Another study in healthy female volunteers (Chow et al., 2010) reported RES-associated menstrual changes as an adverse event in 4.8% of the subjects after oral consumption (1 g once a day for 4 weeks); again indicating altered steroid hormone levels.

We therefore hypothesized that RES may increase the level of active E2 in a dose-dependent manner, either by increasing the concentration of estrogen precursor steroids, or via inhibition of the biotransformation of E2 to conjugated metabolites, which do not promote ER-mediated activity (Samavat and Kurzer, 2015). Our hypothesis was supported by several previous *in vitro* and *in vivo* studies, which showed that RES inhibits various enzymes involved in the metabolism of estrogens, including 3 β -hydroxysteroid dehydrogenase (3 β -HSD), cytochrome P450 3A4 (CYP3A4), sulfotransferases (SULTs) and UDP-glucuronosyltransferases (UGTs) (Chan and Delucchi, 2000; Mesia-Vela and Kauffman, 2003; Furimsky et al., 2008; Chow et al., 2010; Mohamed and Frye, 2011; Li et al., 2014).

Therefore, the aim of the present study was to investigate the impact of RES on steroid metabolism in human ER α - MDA-MB-231 and ER α + MCF-7 breast cancer cells. For this purpose, a specific and sensitive LC-HRMS assay was conducted to simultaneously quantify the 10 main steroids of the estrogenic metabolic pathway (Poschner et al., 2017). Differences in metabolism should be correlated with cell proliferation, which may explain the observed tumor-promoting effect of RES in ER α + breast cancer.

MATERIALS AND METHODS

Materials

4-Androstene-3,17-dione, 16 α -hydroxy-17 β -estradiol, 17 β -estradiol, 17 β -estradiol-3-O-(β -D-glucuronide) sodium salt, dehydroepiandrosterone, dehydroepiandrosterone-2,2,3,4,4,6-d₆, dehydroepiandrosterone-3-O-sulfate, dehydroepiandrosterone-3-O-sulfate-2,2,3,4,4,6-d₆-sodium salt, estrone and testosterone, as well as acetic acid, acetonitrile, ammonium acetate, dimethylsulfoxide, and *trans*-resveratrol, were obtained from Merck KGaA (Darmstadt, Germany). 17 β -estradiol-3-O-sulfate sodium salt and estrone-3-O-sulfate sodium salt were purchased from Steraloids, Inc. (Newport, RI, United States). 4-Androstene-3,17-dione-2,2,4,6,6,16,16-d₇ (AD-d₇), 16 α -hydroxy-17 β -estradiol-2,4,17-d₃ (E3-d₃), 17 β -estradiol-2,4,16,16-d₄ (E2-d₄), 17 β -estradiol-16,16,17-d₃-3-O-(β -D-glucuronide) sodium salt (E2-G-d₃), 17 β -estradiol-2,4,16,16-d₄-3-O-sulfate sodium salt (E2-S-d₄), estrone-2,4,16,16-d₄ (E1-d₄), estrone-2,4,16,16-d₄-3-O-sulfate sodium salt (E1-S-d₄), and testosterone-2,2,4,6,6-d₅ (T-d₅) were obtained from C/D/N Isotopes, Inc. (Pointe-Claire, QC, Canada). *Trans*-resveratrol-3-O-(β -D-glucuronide) sodium salt,

Abbreviations: 3 β -HSD, 3 β -hydroxysteroiddehydrogenase; 17 β -HSD, 17 β -hydroxysteroiddehydrogenase; AD, 4-androstene-3,17-dione; AhR, aryl hydrocarbon receptor; cDNA, complementary deoxyribonucleic acid; CYP, cytochrome P450; DHEA, dehydroepiandrosterone; DHEA-S, dehydroepiandrosterone-3-O-sulfate; DMEM, Dulbecco's modified Eagle's medium; DMSO, dimethylsulfoxide; DPBS, Dulbecco's phosphate-buffered saline; E1, estrone; E1-S, estrone-3-O-sulfate; E2, 17 β -estradiol; E2-G, 17 β -estradiol-3-O-(β -D-glucuronide); E2-S, 17 β -estradiol-3-O-sulfate; E3, estriol (16 α -OH-17 β -estradiol); EIC, extracted ion chromatogram; ER α , estrogen-receptor alpha; ESI, electro-spray ionization; HKGs, housekeeping genes; K_i, inhibition constant; K_m, Michaelis constant; LC-HRMS, liquid chromatography-high resolution mass spectrometry; LLOQ, lower limit of quantification; mRNA, messenger ribonucleic acid; PCR, polymerase chain reaction; PXR, pregnane X receptor; RES, *trans*-resveratrol; RES-3G, *trans*-resveratrol-3-O-(β -D-glucuronide); RES-3S, *trans*-resveratrol-3-O-sulfate; RES-4G, *trans*-resveratrol-4'-O-(β -D-glucuronide); RES-4S, *trans*-resveratrol-4'-O-sulfate; RES-DS, *trans*-resveratrol-3-O-4'-O-disulfate; SD, standard deviation; SPE, solid phase extraction; SULT, sulfotransferase; T, testosterone; UGT, UDP-glucuronosyl transferase; V_{max}, maximum reaction velocity.

trans-resveratrol-3-*O*-sulfate sodium salt, *trans*-resveratrol-4'-*O*-(β -D-glucuronide) sodium salt, *trans*-resveratrol-4'-*O*-sulfate sodium salt, and *trans*-resveratrol-3-*O*-4'-*O*-disulfate disodium salt were purchased from Santa Cruz Biotechnology, Inc. (Dallas, TX, United States). Purified water was obtained using an arium pro ultrapure water system (Sartorius AG, Göttingen, Germany).

Cell Proliferation Studies

MDA-MB-231 and MCF-7 breast cancer cells were purchased from the American Type Culture Collection (ATCC; Manassas, VA, United States) and routinely cultivated at 37°C (95% humidity and 5% CO₂) in phenolred-free Dulbecco's modified Eagle medium F-12 (DMEM/F-12), fortified with 1% PenStrep[®]-solution and 10% fetal bovine serum (Invitrogen; Thermo Fisher Scientific, Inc., Waltham, MA, United States). All experiments were performed during the exponential growth phase of both cell lines. For the experiments, cells were seeded in 6-well-plates at a density of 1.0×10^6 cells per well and allowed to attach for 24 h. Prior to incubation with RES or hormone precursors (DHEA and E1), the cells were washed twice with Dulbecco's phosphate-buffered saline (DPBS; Invitrogen), and DMEM/F-12, containing 10% HyClone[®] heat-inactivated charcoal-stripped fetal bovine serum (GE Healthcare Life Sciences, Logan, UT, United States), was subsequently added to exclude the interference of external hormones.

To elucidate the influence of RES, DHEA and E1 on MDA-MB-231 and MCF-7 cell proliferation, cells were incubated for 48 h with RES (0–100 μ M), DHEA (0–100 nM), and E1 (0–100 nM), respectively. RES, DHEA, and E1 were dissolved in sterile-filtered DMSO prior to their addition to the cell medium to give a final DMSO concentration of 0.1%. Prior to cell counting with a Casy[®] TT Cell Counter (OLS OMNI Life Science, Bremen, Germany), the supernatant medium was removed and cells were detached using 400 μ l TrypLe[®] solution (Invitrogen). All experiments were performed in triplicate, and the data were reported as the means \pm standard deviation of all values.

Metabolism of RES in MDA-MB-231 and MCF-7 Cells

MDA-MB-231 and MCF-7 cells were cultivated as described above and incubated with increasing concentrations of RES (0–100 μ M). After 48 h, the cellular media (100 μ l) were mixed with 200 μ l ice-cold (–20°C) methanol and subsequently centrifuged (14000 rpm, 5 min). The clear supernatants were then diluted 1:1 with aqueous ammonium acetate buffer (5 mM, pH = 7.4), and 80 μ l of the samples were injected onto the HPLC column. RES and its five glucuronidated and sulfated biotransformation products were quantified by HPLC, as described previously (Riha et al., 2014), using a Dionex UltiMate 3000 system (Sunnyvale, CA, United States) equipped with an L-7250 injector, an L-7100 pump, an L-7300 column oven (set at 15°C), a D-7000 interface and an L-7400 UV detector (Thermo Fisher Scientific, Inc.) set at a wavelength of 307 nm. Calibration of the chromatogram was accomplished using the external standard method. Linear calibration curves were produced by spiking drug-free DMEM/F-12 medium with standard solutions of RES, RES-3G, RES-3S,

RES-4G, RES-4S, and RES-DS to give a concentration range from 0.001 to 10.0 μ g/ml (mean correlation coefficients: >0.999). For this method, the lower limits of quantification (LLOQs) for RES, RES glucuronides and RES sulfates were 2.5, 10.1, and 4.0 ng/ml, respectively. The coefficients of accuracy and precision for these compounds were <11%.

Inhibition of Steroid Metabolism by RES

Both cell lines were cultivated in the presence of HyClone[®] heat-inactivated charcoal-stripped fetal bovine serum as described above and then treated with increasing concentrations of DHEA or E1 (0–100 nM), respectively, in the absence and presence of RES (0–100 μ M). After 48 h (preliminary experiments showed the linearity of metabolite formation for this time-span), 2000 μ l media aliquots were mixed with 20 μ l deuterated internal standard solution and pre-cleaned using SPE on Oasis HLB 1 cc SPE cartridges (30 mg; Waters Corporation, Milford, MA, United States), as described previously (Poschner et al., 2017). Briefly, cartridges were preconditioned with 2×1.0 ml acetonitrile and 3×1.0 ml ammonium acetate buffer (10 mM, pH = 5.0), and the samples were loaded onto the columns. After washing with 1×1.0 ml ammonium acetate buffer (10 mM, pH = 5.0) and 2×1.0 ml acetonitrile/ammonium acetate buffer (10 mM, pH 5.0) 10:90 (v/v), the analytes were eluted using 2×650 μ l acetonitrile/ammonium acetate buffer (10 mM, pH = 5.0) 95:5 (v/v) and evaporated until dry. Subsequently, samples were reconstituted in 270 μ l acetonitrile/ammonium acetate buffer (10 mM, pH = 5.0) 25:75 (v/v) and stored at –80°C until further LC–HRMS analysis.

After media collection, cell monolayers were washed five times with 2.0 ml DPBS, detached using 400 μ l TrypLe[®] solution (37°C, 5 min), mixed with 600 μ l DPBS and transferred into sample vials. Aliquots of these suspensions (100 μ l each) were diluted and counted using the Casy[®] TT Cell Counter to determine the exact number of cells per sample well. The remaining cell suspensions (900 μ l each) were gently centrifuged (1000 rpm, 8 min), and the supernatants were discarded. The cell pellets were subsequently resuspended in 100 μ l aqueous ammonium acetate buffer (10 mM, pH = 5.0) and lysed by five freeze-thaw-cycles in liquid nitrogen (3 min each), followed by thawing at ambient temperature. Ammonium acetate buffer (1000 μ l) was added, and the suspensions were centrifuged (14000 rpm, 5 min). Subsequently, the supernatants were concentrated using the same SPE protocol as described above. All processed samples were then stored at –80°C until further LC–HRMS analysis. For each condition, three biologically independent experiments were performed; the reported values represent the overall means \pm SD of all values.

Steroid Hormone Quantification Using LC–HRMS

The 10 predominant metabolites of the estrogenic metabolic pathway (AD, DHEA, DHEA-S, E1, E1-S, E2, E2-S, E2-G, E3, and T) were then quantified using a selective and sensitive LC–HRMS assay, which was validated according to the ICH Q2(R1) guidelines, as described previously (Poschner et al.,

2017). LC was performed with an UltiMate 3000 RSLC-series system coupled to a maXis HD ESI-Qq-TOF mass spectrometer (Bruker Corporation, Bremen, Germany). A Phenomenex Luna® 3 µm C18(2) 100 Å LC column (250 mm × 4.6 mm I.D.; Phenomenex, Inc., Torrance, CA, United States), preceded by a Hypersil® BDS-C18 guard column (5 µm, 10 mm × 4.6 mm I.D.; Thermo Fisher Scientific, Inc.) was used for the separation of the analytes at a flow rate of 1.0 ml/min and a temperature of 43°C. The injection volume was set to 100 µl for each sample; aqueous ammonium acetate buffer (10 mM, pH = 5.0) was used as solvent A, and acetonitrile as solvent B. The gradient was as follows: 25% solvent B at 0 min, 56.3% solvent B at 19 min, a washing step at 90% solvent B from 19.5 to 24.0 min, and column re-equilibration with 25% solvent B from 24.5 to 30.5 min. The ESI ion source settings were as follows: capillary voltage: −4.5 kV; dry gas flow rate: 8.0 l/min N₂; nebulizer: 1.0 bar N₂; and dry temperature: 200°C. The ion transfer parameters were set to 400 V_{pp} funnel RF and 300 V_{pp} multipole RF, the quadrupole ion energy was 8.0 eV, and the collision cell parameters were as follows: collision RF, 1100 V_{pp}; collision energy, 10.0 eV; transfer time, 38 µs; and pre-pulse storage, 18 µs. In the range of *m/z* 150–500, full-scan mass spectra were recorded. Quality control samples, containing each analyte at a concentration of 6-, 60-, or 600-fold of the respective LLOQs, were analyzed in triplicate with each LC batch to ensure accurate quantification results (Supplementary Figure S1). The LLOQs for all 10 analytes, defined as the concentrations where the signal to noise ratio (S/N) is ≥9, were determined as follows: AD: 74.9 pg/ml; DHEA: 1904.0 pg/ml; DHEA-S: 8.0 pg/ml; E1: 19.0 pg/ml; E1-S: 4.0 pg/ml; E2: 140.9 pg/ml; E2-G: 12.0 pg/ml; E2-S: 3.4 pg/ml; E3: 28.4 pg/ml; and T: 54.1 pg/ml.

Real-Time PCR Analysis

MCF-7 breast cancer cells were seeded in 6-well plates at a density of 1.0×10^6 cells per well and allowed to attach overnight. Next day, cells were treated in kinetics (2, 4, 24, and 48 h, respectively) with 10 µM RES or with DMSO for the control samples (0 h time-point). Expression profiling of genes of interest was performed as detailed previously (Mechtcheriakova et al., 2007; Meshcheryakova et al., 2016). Upon treatment, total RNA was isolated using peqGOLD TriFAST™ reagent (VWR, Vienna, Austria) according to the manufacturer's protocol. 1 µg RNA was used for cDNA generation using the High Capacity cDNA Reverse Transcription Kit (Thermo Fisher Scientific, Inc.) according to the instructions of the manufacturer. Real-time PCR analysis was performed in the 96-well plate format on a QuantStudio 12K Flex Real-Time PCR System (Thermo Fisher Scientific, Inc.). *SULT1A1* and *SULT2A1* were detected using the corresponding TaqMan Assays (Thermo Fisher Scientific, Inc.). *UBC*, *GAPDH*, and *ACTB* were used as HKGs for normalization, based on the selection for the most stable expression during the treatment conditions among four pre-tested HKGs (*ACTB*, *UBC*, *GAPDH*, and *HPRT*). HKGs primers were self-designed using the Primer Express 3.0 software (Thermo Fisher Scientific, Inc.) and validated using the Human Total RNA Master Panel (TaKaRa Bio, Inc., Saint-Germain-en-Laye, France), as described before (Mechtcheriakova et al., 2007, 2011); Primers: *UBC* forward: ATTTGGGTCGCAGTTCTTG;

UBC reverse: TGCCTTGACATTCTCGATGGT; *GAPDH* forward: CGGGTCAACGGATTGGTC; *GAPDH* reverse: TGGCAACAATATCCACTTTACCAG; *ACTB* forward: AGGCACCAGGGCGTGAT; *ACTB* reverse: TGTAGAAGGTGTGGTGCCAGATT. For relative quantification, data were analyzed by applying the $\Delta\Delta CT$ method. Expression levels of target genes were normalized to the average of the HKGs and shown relative to unstimulated cells (0 h time-point). Gene(s) with Ct > 36 are classified herein as *not expressed*; gene(s) with Ct > 30 are classified as *low expressing gene(s)*. Using the GENEVESTIGATOR and the Affymetrix Human Genome U133 Plus 2.0 Array web based analysis platforms (Hruz et al., 2008), *SULT1E1* was found to be not expressed in MCF-7 cells and was therefore not assessed by real-time PCR.

Data Analysis and Statistics

Compass DataAnalysis 4.2 and QuantAnalysis 2.2 software (Bruker Corporation) were used to analyze the acquired LC–HRMS data. For each analyte and internal standard pair, EICs were created, from which the respective peak areas were determined and the analyte/internal standard ratios were calculated for quantification.

Kinetic analyses of RES metabolism and steroid metabolism in the presence and absence of RES in both cell lines were performed using GraphPad Prism 6.0 software (GraphPad Software, Inc., La Jolla, CA, United States). Kinetic parameters for the formation of RES metabolites were best fitted to the substrate inhibition model: $V = V_{\max}/(1 + K_m/[S] + [S]/K_i)$, or the sigmoidal Hill model: $V = V_{\max} \times [S]^n/([S]_{50}^n + [S]^n)$, whereas kinetics regarding steroid hormone metabolism were better estimated using the Michaelis–Menten model: $V = V_{\max} \times [S]/(K_m + [S])$, where *V* is the rate of the reaction, *V*_{max} is the maximum reaction velocity, *K*_m is the Michaelis constant, [*S*] is the initial substrate concentration, *K*_i is the inhibition constant, *n* is the Hill slope and *S*₅₀ the concentration of substrate that produces a half-maximal enzyme velocity. The modes of inhibition were subsequently determined from Lineweaver–Burk plots, and the corresponding *K*_i values were calculated from Dixon plots using GraphPad Prism 6.0.

The same software package was also used for all statistical analyses. All values were expressed as the means ± SD of three independent biological replicates and one-way ANOVA combined with Tukey's post-test were used to compare differences between control samples and treatment groups. The statistical significance threshold was defined as *P* < 0.05 for all calculations.

RESULTS

Effects of RES on the Proliferation of MDA-MB-231 and MCF-7 Cells

To evaluate the effects of RES on breast cancer cell growth, ERα− MDA-MB-231 and ERα+ MCF-7 cells were exposed to increasing concentrations of RES (0–100 µM) in the absence of DHEA and E1. As shown in **Figure 1A**, RES inhibited the

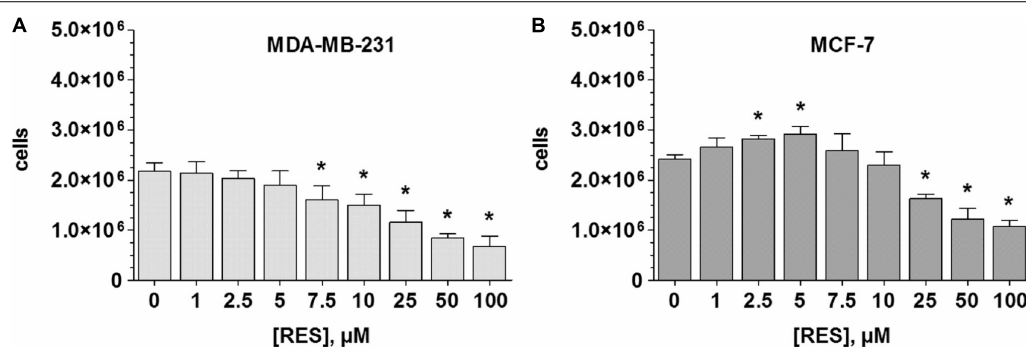


FIGURE 1 | Influence of RES on MDA-MB-231 and MCF-7 cell proliferation. **(A)** MDA-MB-231 or **(B)** MCF-7 cells were incubated for 48 h with increasing concentrations of RES (0–100 μM) in steroid-deprived conditions. All data represent the means \pm SD of three independent biological replicates. * $P < 0.05$ vs. untreated control samples.

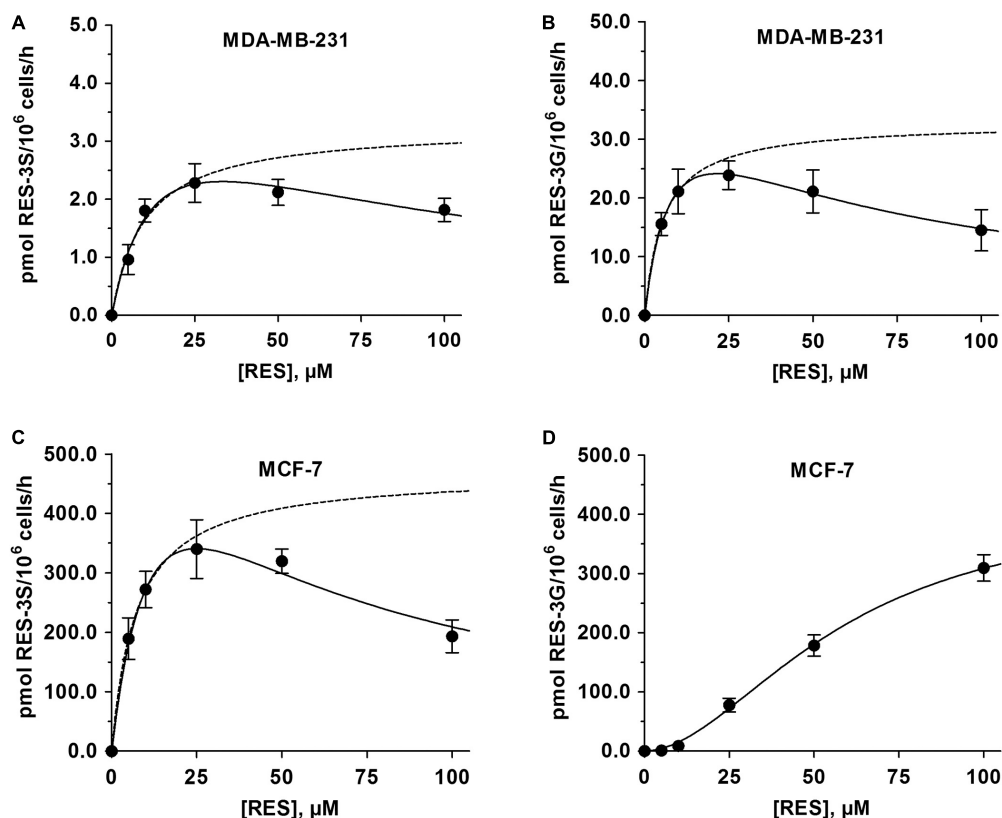


FIGURE 2 | Kinetic profiles for the formation of 3-O-conjugated RES-metabolites by MDA-MB-231 and MCF-7 cells. The formation of **(A)** RES-3S and **(B)** RES-3G by MDA-MB-231 cells was determined following incubation with 0–100 μM RES for 48 h, and modeled using the substrate inhibition model. The formation of **(C)** RES-3S and **(D)** RES-3G by MCF-7 cells were evaluated with the same protocol. While the formation of RES-3S correlated with the substrate inhibition model, the formation of RES-3G was best described by the sigmoidal Hill model. Dashed lines represent the kinetic profiles without substrate inhibition. All data represent the means \pm SD of three independent biological replicates.

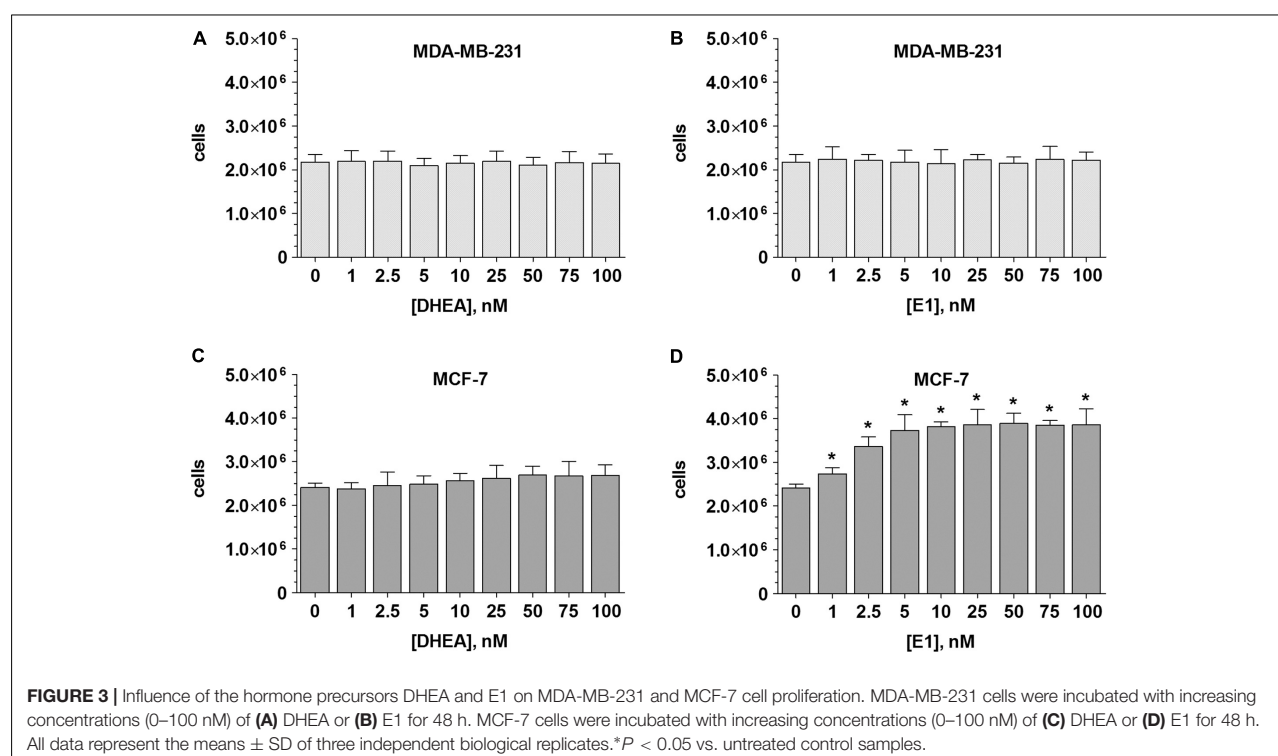
cell growth of MDA-MB-231 cells in a concentration-dependent manner. Even after the addition of 2.5 μM RES, the number of viable cells decreased non-significantly from $2.17 \pm 0.18 \times 10^6$ to $2.03 \pm 0.16 \times 10^6$ cells, but 100 μM RES resulted in a significant

reduction by $68.6 \pm 4.7\%$. Contrary to the MDA-MB-231 cells, RES demonstrated a biphasic effect in MCF-7 cells, as concentrations below 10 μM stimulated cellular growth with a maximal effect by $21.2 \pm 3.3\%$ to $2.92 \pm 0.16 \times 10^6$ cells at

TABLE 1 | Kinetic parameters of RES metabolism by MDA-MB-231 and MCF-7 cells.

Cell line	Metabolite	Model	Parameters				
			K_m (μM)	V_{\max} (pmol/ 10^6 cells/h)	Slope (n)	R^2	K_i (μM)
MDA-MB-231	RES-3S	Michaelis-Menten	9.83 ± 3.18	3.25 ± 0.44	n.a.	0.9395	n.a.
		Substrate inhibition	14.4 ± 5.6	4.31 ± 0.97	n.a.	0.9873	76.3 ± 35.2
	RES-3G	Michaelis-Menten	5.55 ± 3.43	32.8 ± 8.6	n.a.	0.9522	n.a.
		Substrate inhibition	8.61 ± 0.85	43.4 ± 2.2	n.a.	0.9992	54.0 ± 5.3
MCF-7	RES-3S	Michaelis-Menten	7.30 ± 0.44	468.4 ± 9.9	n.a.	0.9991	n.a.
		Substrate inhibition	8.19 ± 0.56	501.4 ± 17.1	n.a.	0.9889	39.4 ± 14.3
	RES-3G	Hill	58.5 ± 6.2	422.9 ± 38.9	1.86 ± 0.18	0.9988	n.a.

Kinetic parameters were calculated using GraphPad Prism 6.0 software following the incubation of the cells with increasing concentrations of RES (0–100 μM) for 48 h. All data represent the means \pm SD of three independent biological replicates. n.a., not applicable.



5 μM RES (Figure 1B). A further increase of RES concentration (> 10 μM), however, led to a significant inhibition of cell growth ($1.08 \pm 0.11 \times 10^6$ cells at 100 μM RES). Interestingly, the inhibitory effect of RES was more evident in MDA-MB-231 compared with MCF-7 cells, as indicated by lower IC_{50} values (15.1 ± 4.9 vs. 37.4 ± 14.5 μM).

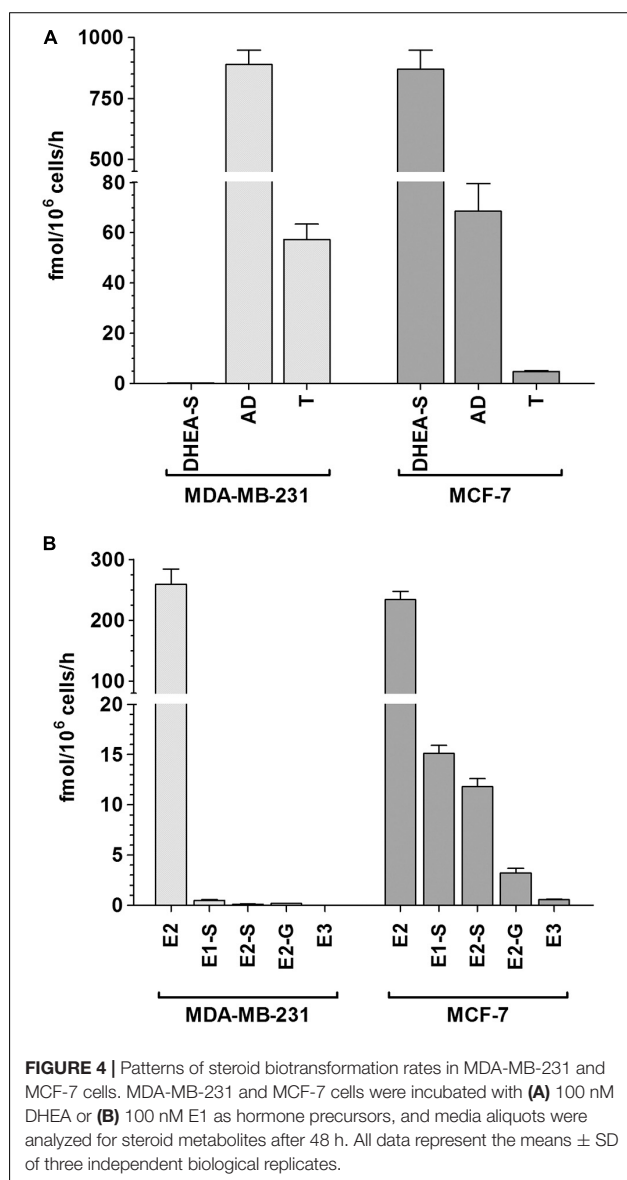
RES Metabolism by MDA-MB-231 and MCF-7 Cells

In order to investigate whether the observed differences in the proliferation of MDA-MB-231 and MCF-7 cells by RES were due to alterations in RES metabolism, both cell lines were screened for the formation of the five major human conjugated RES metabolites. In addition to native RES, only RES-3G and RES-3S

could be quantified in both cell lines, as the levels of RES-4G, RES-4S, or RES-DS formation were below the detection limit.

In MDA-MB-231 cells, the maximum metabolite formation was observed following incubation with 25 μM RES, with a notable preference for glucuronidation (23.9 ± 2.4 pmol RES-3G/ 10^6 cells/h) compared with sulfation (2.28 ± 0.33 pmol RES-3S/ 10^6 cells/h) (Figures 2A,B). At higher RES concentrations, the formation of both RES conjugates decreased, best fitting to the substrate inhibition model, with K_i values of 54.0 ± 5.3 μM for RES-3G and 76.3 ± 35.2 μM for RES-3S.

Compared with MDA-MB-231 cells, the formation of RES-3S in MCF-7 cells was increased by 150-fold, with a mean maximum formation rate of 340.1 ± 49.4 pmol RES-3S/ 10^6 cells/h (Figure 2C). As observed in MDA-MB-231 cells, treatment with RES up to 100 μM led to a pronounced reduction in RES-3S by



43.2%, again indicating substrate inhibition (K_i : $39.4 \pm 14.3 \mu\text{M}$). Glucuronidation of RES in MCF-7 cells was also higher (10-fold increase), demonstrating a sigmoidal Hill kinetic pattern, with a maximum formation rate of $309.4 \pm 22.2 \text{ pmol RES-3G}/10^6 \text{ cells/h}$ at $100 \mu\text{M RES}$ (Figure 2D). Individual kinetic parameters for RES-S and RES-G in both cell lines are presented in Table 1.

Effects of DHEA and E1 on the Proliferation of MDA-MB-231 and MCF-7 Cells

ER α - MDA-MB-231 and ER α + MCF-7 breast cancer cells were cultured in a hormone-deprived environment for 48 h. In these conditions, the number of MDA-MB-231 cells doubled from 1.0×10^6 to $2.17 \pm 0.18 \times 10^6$. A comparable increase in cell

proliferation was also observed in the MCF-7 cell line (final cell count: $2.41 \pm 0.94 \times 10^6$ cells). Incubation of ER α - MDA-MB-231 cells with either DHEA or E1 (0–100 nM) did not further increase cell growth (Figures 3A,B). In ER α + MCF-7 cells, the presence of DHEA only led to a minor, non-significant increase in cell numbers, to $2.69 \pm 0.24 \times 10^6$ cells at 100 nM (Figure 3C). Incubation with E1, however, significantly stimulated the proliferation of MCF-7 cells by 59.8%, to $3.85 \pm 0.36 \times 10^6$ cells at 100 nM (Figure 3D), confirming the hormone-dependency of this cell line.

DHEA and E1 Metabolism by MDA-MB-231 and MCF-7 Cells

To assess differences in the metabolism of steroids by MDA-MB-231 and MCF-7 cells, both cell lines were incubated in the presence and absence of DHEA (100 nM) as a hormone precursor, and the formation of the nine major biotransformation products, namely DHEA-S, AD, T, E1, E1-S, E2, E2-S, E2-G and E3, was investigated by using a specific and sensitive LC-HRMS assay. The control samples (containing DMSO only) were performed for both cell lines to evaluate a possible endogenous steroid formation; however, neither in MCF-7 nor in MDA-MB-231 cells any endogenous steroid metabolites could be detected. Upon addition of 100 nM DHEA, the three metabolites DHEA-S, AD, and T could be quantified besides native DHEA in the supernatants of both cell lines; all other metabolites were below the LLOQ (Figure 4A).

In MDA-MB-231 cells, we observed that the 3 β -HSD-mediated formation of AD was evidently favored (mean formation rate: $888.9 \pm 60.1 \text{ fmol}/10^6 \text{ cells/h}$). AD was further metabolized via 17 β -HSD to T, however, to a significantly lower extent ($57.1 \pm 6.2 \text{ fmol}/10^6 \text{ cells/h}$). The sulfation of DHEA was negligible, as the formation rate of DHEA-S was only $0.14 \pm 0.02 \text{ fmol}/10^6 \text{ cells/h}$. Concomitant with the formation of these metabolites, DHEA concentration in the medium decreased by 26.8% from 100 to $73.2 \pm 2.5 \text{ nM}$ after 48 h. The total molar proportion of AD, T, and DHEA-S was 26.2%, indicating that these three biotransformation products represent almost 100% of all metabolites formed from the precursor DHEA in MDA-MB-231 cells (unmetabolized DHEA + total detected metabolites: 99.4%).

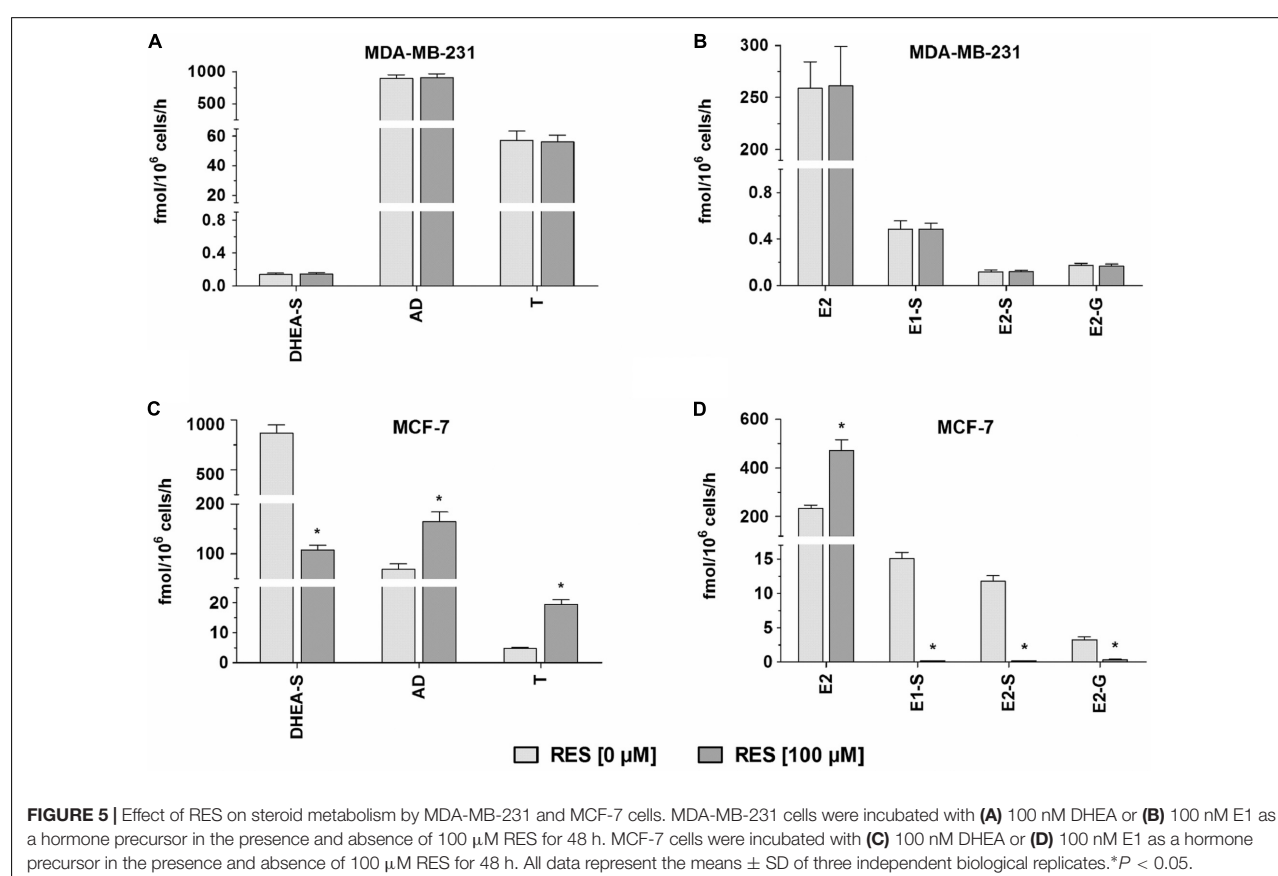
In MCF-7 cells, the formation rates of DHEA-S, AD, and T notably differed from MDA-MB-231 cells. DHEA-S was now the primary metabolite (mean formation rate: $870.0 \pm 79.1 \text{ fmol}/10^6 \text{ cells/h}$), whereas the formation of AD and T was less pronounced (68.5 ± 11.1 and $4.78 \pm 0.38 \text{ fmol}/10^6 \text{ cells/h}$, respectively). Concomitantly, the remaining DHEA concentration decreased by 54.9% from 100.0 to $45.1 \pm 1.8 \text{ nM}$, which once again reflected the total molar proportion of these three metabolites (54.7%).

To further evaluate the formation rates of estrogens and their respective conjugates, MDA-MB-231 and MCF-7 cells were also incubated in the presence and absence of 100 nM E1 as a hormone precursor (Figure 4B). Again, control samples (containing DMSO only) revealed no endogenous formation of estrogen metabolites in both cell lines. E2 was identified as the predominant metabolite with comparable formation rates

TABLE 2 | Kinetic parameters of steroid metabolism by MDA-MB-231 and MCF-7 cells.

Hormone precursor	Metabolite	MDA-MB-231		MCF-7	
		K_m (nM)	V_{max} (fmol/10 ⁶ cells/h)	K_m (nM)	V_{max} (fmol/10 ⁶ cells/h)
DHEA	DHEA-S	55.4 ± 20.5	0.22 ± 0.04	229.2 ± 52.2*	2873.0 ± 327.4*
	AD	126.1 ± 36.6	1994.0 ± 364.5	114.6 ± 3.6	147.4 ± 8.1*
	T	56.3 ± 21.4	91.2 ± 15.9	107.5 ± 6.3*	9.96 ± 1.42*
E1	E2	174.0 ± 94.1	703.0 ± 164.5	168.6 ± 8.7	628.6 ± 62.0
	E1-S	119.5 ± 68.1	1.08 ± 0.38	101.9 ± 22.9	30.4 ± 2.5*
	E2-S	38.0 ± 13.6	0.16 ± 0.02	113.8 ± 35.5*	24.7 ± 4.9*
	E2-G	87.9 ± 32.2	0.33 ± 0.07	123.5 ± 8.4	7.29 ± 1.36*

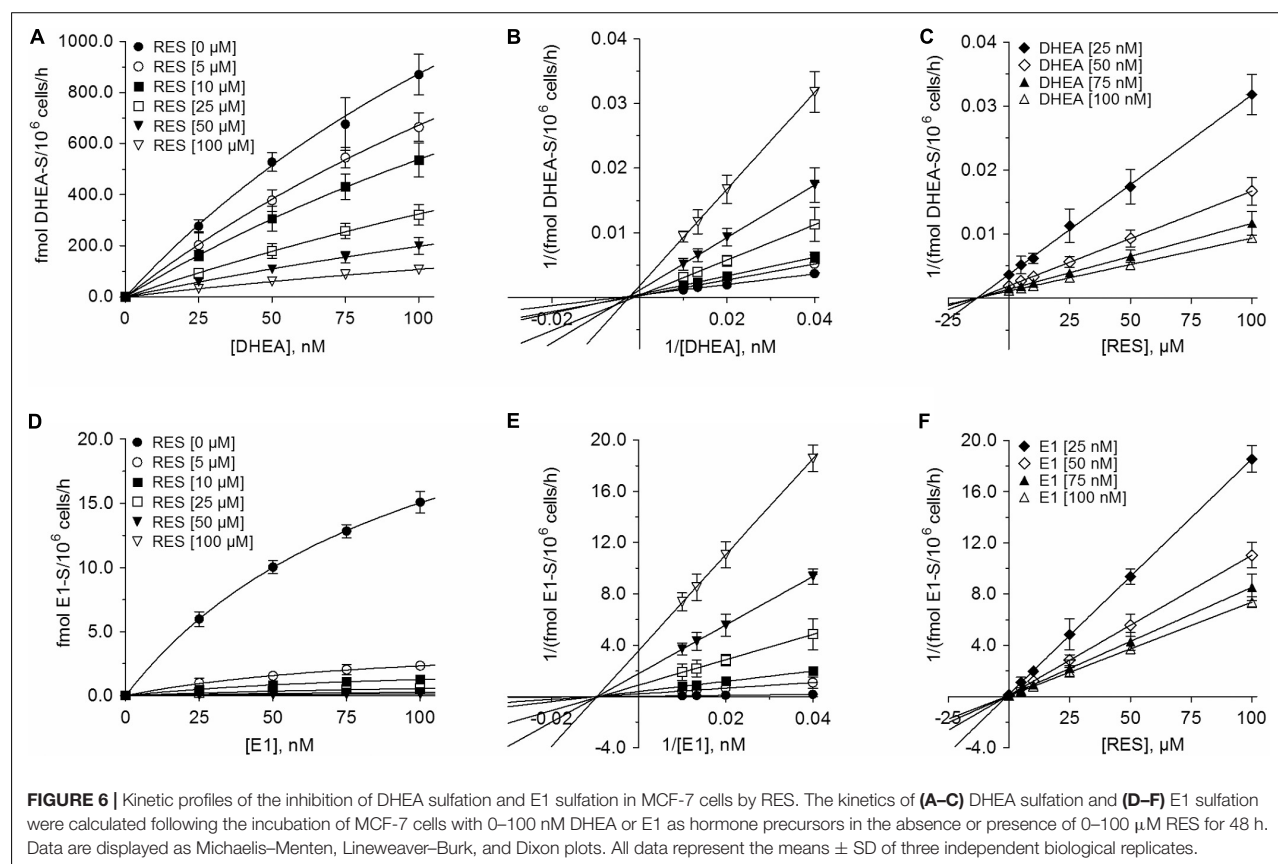
Kinetic parameters were calculated using GraphPad Prism 6.0 software following the incubation of the cells for 48 h with increasing concentrations of DHEA or E1 (25–100 nM). All data represent the means ± SD of three independent biological replicates. Values in bold and marked with an asterisk (*) are significantly different compared with MDA-MB-231 cells ($P < 0.05$).



in MDA-MB-231 and MCF-7 cells (258.9 ± 25.1 fmol/10⁶ cells/h vs. 233.9 ± 13.4 fmol/10⁶ cells/h). The hydroxylation of E2 to E3 was a minor pathway in MCF-7 cells (0.57 ± 0.06 fmol/10⁶ cells/h), and was below the LLOQ in MDA-MB-231 cells. However, the formation rates of steroid conjugates differed markedly between both cell lines. While the formation of E1-S, E2-S and E2-G were negligible in MDA-MB-231 cells (E1-S: 0.49 ± 0.07 > E2-G: 0.18 ± 0.02 > E2-S: 0.12 ± 0.02 fmol/10⁶ cells/h), the total conjugation of E1 and E2 was up to 40-fold higher in MCF-7 cells (E1-S:

15.1 ± 0.8 > E2-S: 11.8 ± 0.8 > E2-G: 3.23 ± 0.45 fmol/10⁶ cells/h). In both cell lines, the total molar proportions of all detected metabolites amounted to 12.0% and 12.8%, with a concomitant decrease of native E1 by 12.3% and 12.9%, respectively.

The kinetic profiles for the formation of DHEA and E1 metabolites by MDA-MB-231 and MCF-7 cells were then evaluated over a DHEA and E1 concentration range of 0–100 nM for 48 h. The formation kinetics of DHEA-S, AD, T, E1-S, E2, E2-S, and E2-G best fitted to a hyperbolic Michaelis–Menten



model, with the highest V_{\max} values for AD in MDA-MB-231 cells (1994.0 ± 364.5 fmol/ 10^6 cells/h) and for DHEA-S in MCF-7-cells (2873.0 ± 327.4 fmol/ 10^6 cells/h). K_m values in both cell lines were within a similar range for AD, E2, E1-S and E2-G, but were significantly lower for DHEA-S, T and E2-S in MDA-MB-231 cells, compared with in MCF-7 cells (Table 2). The kinetic parameters for the formation of E3 could not be calculated, as only the highest concentration of E1 (100 nM) resulted in concentrations of E3 above the LLOQ for this assay.

Inhibition of Conjugated DHEA and E1 Metabolites by RES

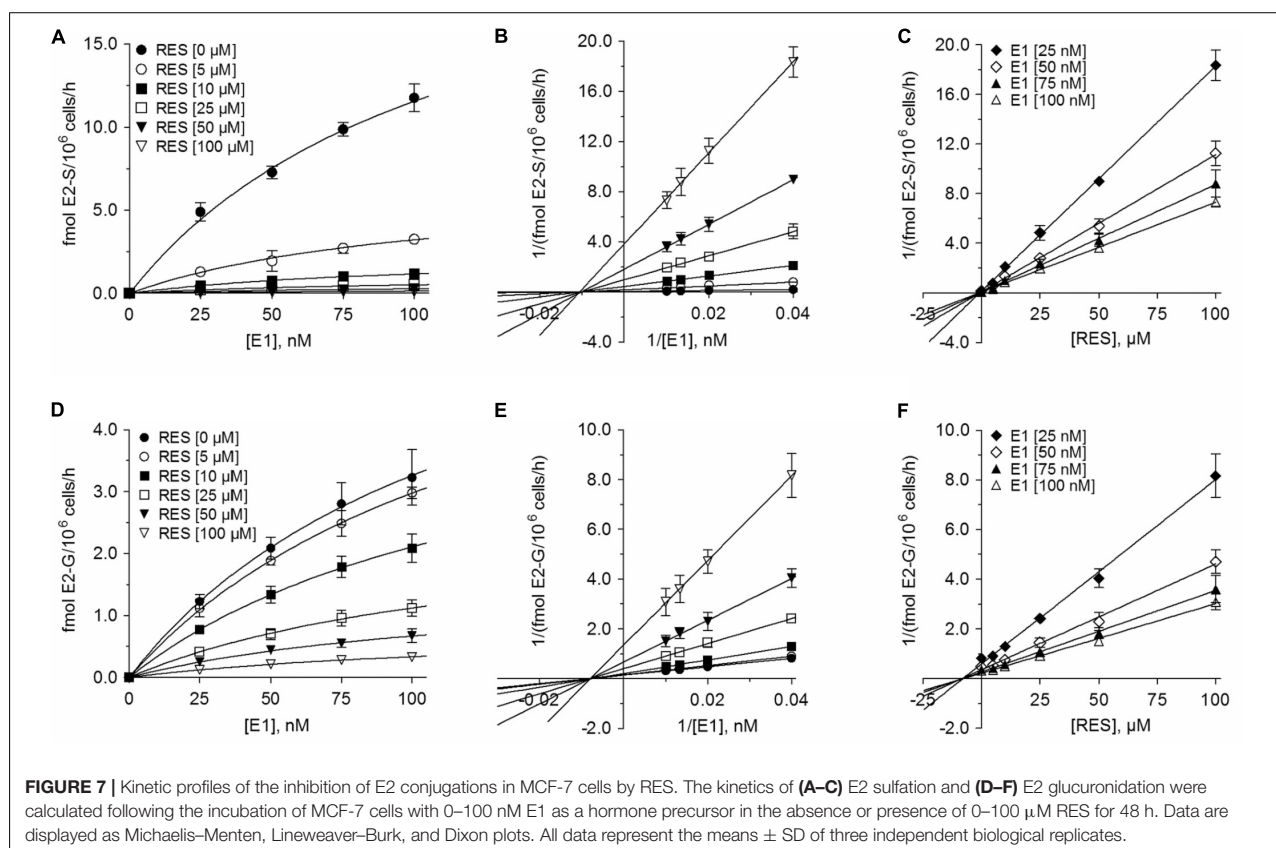
To determine whether there was a possible inhibitory effect of RES on steroid metabolism, MDA-MB-231 and MCF-7 cells were treated with 100 nM DHEA or E1 for 48 h, in the presence or absence of 100 μM RES. As shown in Figures 5A,B, RES did not affect the formation of DHEA-S, E1-S, E2-S, and E2-G in MDA-MB-231 cells. Conversely, a marked effect of RES on the conjugation of DHEA, E1, and E2 was observed in MCF-7 cells (Figures 5C,D). The mean formation of DHEA-S, E1-S, E2-S, and E2-G was almost quantitatively reduced by 87.7%, 99.1%, 98.8%, and 89.7%, respectively.

The inhibition of all four metabolites best fitted to the Michaelis–Menten kinetic model (Figures 6, 7). The V_{\max}

values for the formation of the conjugates were significantly decreased with increasing concentrations of RES, while the corresponding K_m values were virtually unaffected (Table 3). This indicated non-competitive inhibition by RES for all conjugates, which was further confirmed by Lineweaver–Burk and Dixon plots. The more pronounced inhibition of E1 and E2 sulfation compared with DHEA sulfation and E2 glucuronidation by RES was also associated with significantly lower K_i values (E2-S: 0.73 ± 0.07 μM < E1-S: 0.94 ± 0.03 μM < E2-G: 7.92 ± 0.24 μM < DHEA-S: 13.2 ± 0.2 μM), indicating decreased rates of E1-S and E2-S formation even at low RES concentrations.

Effect of RES on Unconjugated DHEA and E1 Metabolites

In addition to the quantification of steroid conjugates, we also assessed the effects of RES treatment on the formation of unconjugated AD, T, and E2. Again, RES exerted no significant influence in MDA-MB-231 cells (Figures 5A,B); however, in MCF-7 cells, RES markedly increased the levels of these three metabolites (Figures 5C,D). 100 μM RES treatment led to a significant increase in AD concentrations by 141.0% (from 68.5 ± 11.1 to 165.1 ± 18.7 fmol/ 10^6 cells/h), whereas T levels increased by 305.9% (from 4.78 ± 0.38 to 19.4 ± 1.6 fmol/ 10^6 cells/h); unconjugated E2 concentrations also increased



by 101.6% (from 233.9 ± 13.4 to 471.5 ± 43.6 fmol/ 10^6 cells/h). The kinetic profiles for AD, T, and E2 in MCF-7 cells were then evaluated over a concentration range of 0–100 nM DHEA and E1, respectively. As observed for the inhibition of DHEA, E1, and E2 conjugates, the K_m values were not affected by RES treatment, whereas the V_{max} values increased in a concentration-dependent manner (Figure 8 and Table 3), thereby confirming a stimulatory effect of RES on the formation of AD, T, and E2.

Down-Regulation of SULT1A1 and SULT2A1 mRNA Expression in MCF-7 Cells by RES

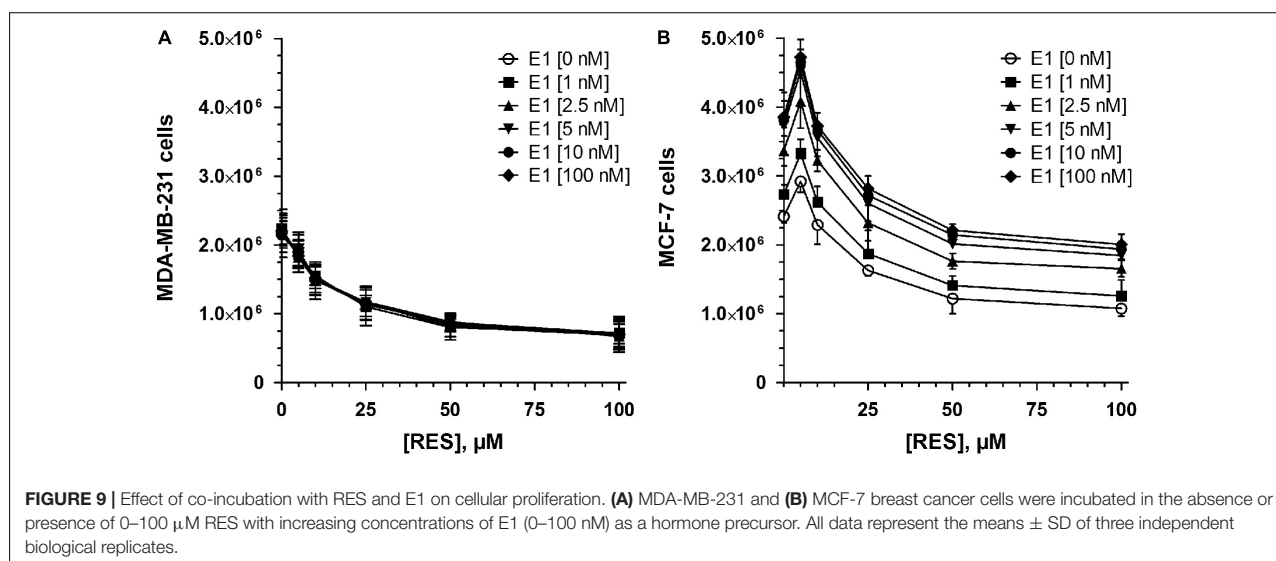
Next, we raised the question whether RES regulates *SULT1A1* and *SULT2A1* on the transcriptional level during the time of treatment. Therefore, MCF-7 cells were treated with 10 μ M RES for 2, 4, 24, and 48 h. We found that RES did not affect the transcription of *SULT1A1* for up to 4 h of treatment (Supplementary Figure S2). However, a moderate, but non-significant down-regulation on the mRNA level was observed after 24 and 48 h (23.6 ± 13.0 and $30.4 \pm 11.0\%$, respectively). Expression levels of *SULT2A1* were low at time 0 h ($Ct > 30$) and again marginally down-regulated after 24 and 48 h (data not shown).

Effect of RES in the Presence of E1 on the Proliferation of MDA-MB-231 and MCF-7 Cells

The simultaneous incubation of MDA-MB-231 cells with RES and E1 up to 100 μ M had no observable effect on cell proliferation (Figure 9A); however, in MCF-7 cells we observed a pronounced induction of cellular proliferation after co-incubation for 48 h (Figure 9B). Interestingly, the induction of cell growth was most pronounced at 5 μ M RES, resulting in a twofold increase in cell counts after co-incubation with 100 nM E1, compared with the control samples in the absence of E1. The stimulatory effects of 100 nM E1 were also observed at higher RES concentrations up to 100 μ M, thereby almost counteracting the observed anti-proliferative effects of RES in a hormone-deprived setting.

DISCUSSION

The role of RES in preventing breast cancer is controversial, as some studies have proposed it may increase its risk. Our data revealed that higher RES concentrations (up to 100 μ M) significantly inhibited proliferation in both ER α – and ER α + breast cancer cell lines, with IC_{50} values of 15.1 ± 4.9 μ M for MDA-MB-231 cells and 37.4 ± 14.5 μ M for MCF-7 cells. These data are in accordance with *in vivo* data from animal experiments



(Garvin et al., 2006), which also reported a reduction of cancer xenograft growth in mice treated with 25 mg/kg RES per day for 3 weeks. The approximately 2.5-fold higher IC₅₀ value of RES against MCF-7 cells may be partially explained by altered RES metabolism, as the formation of RES-3G and RES-3S was increased by up to 150-fold compared with MDA-MB-231 cells. Our data are supported by the findings of Murias et al. (2008), who also reported a distinct correlation between RES metabolism efficacy and cytotoxicity in various breast cancer cell lines.

However, at concentrations below 10 μM RES, the growth of ERα+ MCF-7 cells, but not ERα– MDA-MB-231 cells, was increased, with a maximal stimulatory effect of 21.2% at 5 μM RES compared with untreated controls. A similar effect was also reported by a recent *in vivo* study (Andreani et al., 2017), which reported an induction of ERα+ breast cancer growth at low RES concentrations in Δ16HER2 mice receiving 4 μg RES daily for 15 weeks.

These conflicting results with regards to RES may be attributed to altered estrogen levels in breast tissue, as breast cancer growth and progression are closely associated with female steroid hormones. As metabolism is the key factor for the alteration of cellular estrogens, we investigated, for the first time, the effects of RES on the metabolism of steroids within ERα– MDA-MB-231, and ERα+ MCF-7 human breast cancer cells. In the absence of RES, DHEA, and E1 induced no effect on the proliferation of ERα– MDA-MB-231 cells after 48 h. Conversely, in ERα+ MCF-7 cells, DHEA produced a slight increase and E1 a significant increase in cell proliferation, which once again indicated the hormone-dependency of this breast cancer cell line. Additionally, we screened for the formation of DHEA and E1 metabolites in both cell lines. After incubation with DHEA, three metabolites, namely DHEA-S, AD and T, were quantified in the supernatant media of both cell lines. Interestingly, the sulfation of DHEA was identified as the dominant pathway in MCF-7 cells (V_{\max} : 2873.0 ± 527.4 fmol/10⁶ cells/h), while in MDA-MB-231 cells, the formation levels of AD and T were approximately 10-fold

higher compared with in MCF-7 cells; the formation of DHEA-S only amounted to a V_{\max} value of 0.22 ± 0.04 fmol/10⁶ cells/h.

Subsequently, we also incubated both cell lines with E1 as a hormone precursor. LC–HRMS analyses revealed that E2 was the predominant metabolite, with V_{\max} values of 703.0 ± 164.5 fmol/10⁶ cells/h and 628.6 ± 62.0 fmol/10⁶ cells/h for MDA-MB-231 and MCF-7 cells, respectively. While the formation of all other metabolites was almost negligible in MDA-MB-231 cells (V_{\max} values < 1.1 fmol/10⁶ cells/h), E1-S, E2-S, E2-G, and E3 formation levels amounted to 11.6% of all biotransformation products in MCF-7 cells. CYP3A4-mediated hydroxylation of E2 to E3, however, was suggested to involve a minor metabolic pathway undertaken by MCF-7 cells, as the formation of E3 could not be quantified at E1 concentrations of < 100 nM. Sulfation was evidently the preferred pathway for E1 and E2 metabolism in MCF-7 cells, as the V_{\max} values were significantly higher (E1-S: 30.4 ± 2.5 fmol/10⁶ cells/h and E2-S: 24.7 ± 4.9 fmol/10⁶ cells/h) compared with those for E2 glucuronidation (7.29 ± 1.36 fmol/10⁶ cells/h). These data were supported by previous *in vitro* investigations, which also revealed, based on significantly higher SULT expression, that the formation levels of E1-S and E2-S in ERα+ MCF-7 cells were more than sevenfold higher than in ERα– MDA-MB-231 cells after incubation with E1 for 24 h (Pasqualini, 2009). This may also occur in breast cancer patients, as higher SULT expression levels were also reported in ERα+ breast tumors compared with in ERα– breast cancer tissues (Adams et al., 1979).

In the ERα– MDA-MB-231 cells, RES did not significantly affect the formation of DHEA and E1 metabolites; however, in the ERα+ MCF-7 cells, RES significantly inhibited the formation of DHEA-S, consequently increasing the pool of unconjugated DHEA and leading to increased AD and T levels. Contrary to breast tumor tissue, MCF-7 cells express low levels of aromatase (Zhou et al., 1993), explaining why AD and T were

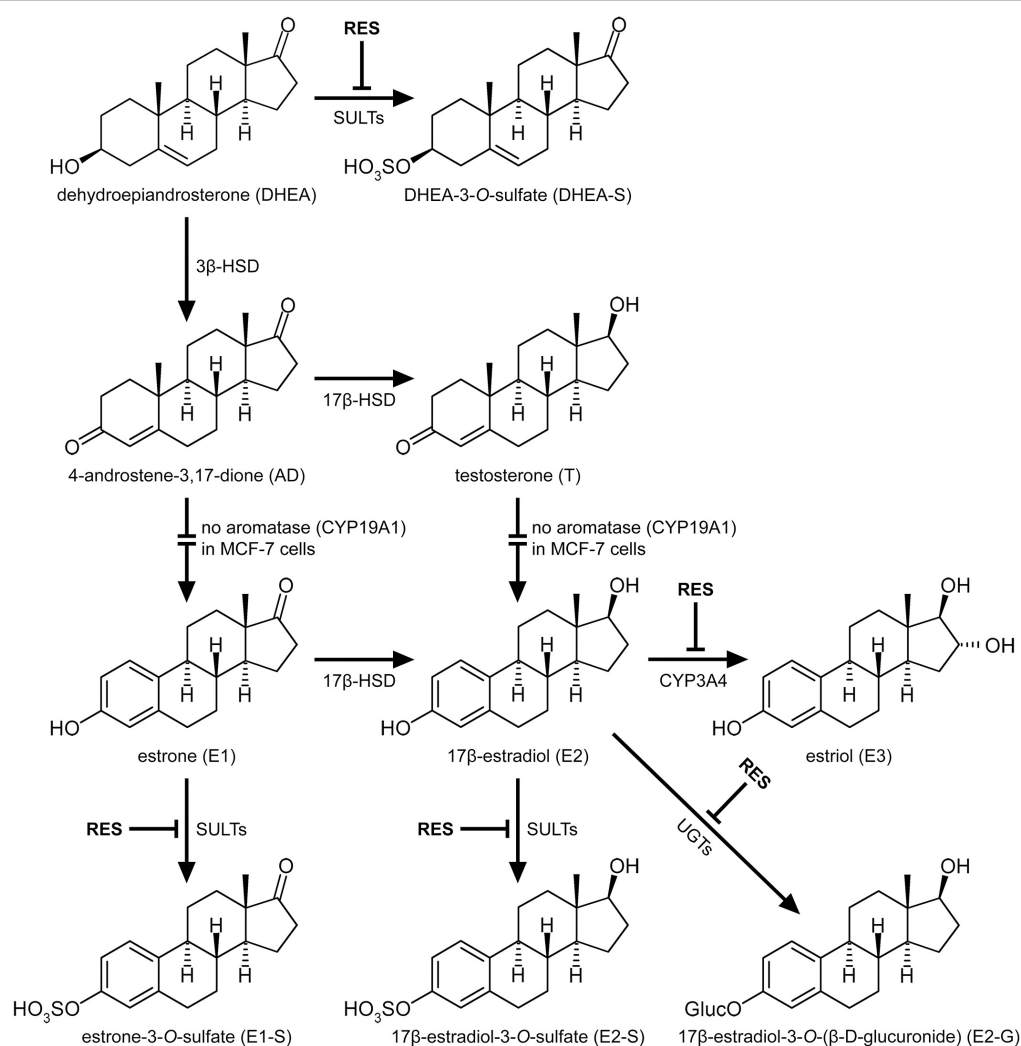


FIGURE 10 | Interaction of RES with the metabolism of steroid hormones in MCF-7 breast cancer cells. RES inhibited the formation of the conjugated metabolites DHEA-S, E1-S, E2-S and E2-G, as well as the formation of E3, in a dose-dependent manner, thereby increasing the levels of AD, T, and active E2.

not metabolized to E1 and E2, respectively. The presence of aromatase in females may thus further increase both levels (Figure 10).

We therefore incubated MCF-7 cells with E1 as a hormone precursor in the presence of RES. As shown in Figure 5, RES significantly inhibited the formation of E1-S, E2-S and E2-G, thereby resulting in an approximate twofold increase in active E2 levels (Figure 10). Our data are in line with previous animal studies, which also observed that RES increased free E2 levels via the inhibition of E2 hydroxylation, glucuronidation, or sulfation in mice (Oskarsson et al., 2014) and rats (Banu et al., 2016). A non-significant increase in E2 serum concentrations (22.4%) was also reported in post-menopausal women receiving 1 g RES once a day for 12 weeks; however, as dansylchloride-derivatization was used for steroid quantification, the authors could not

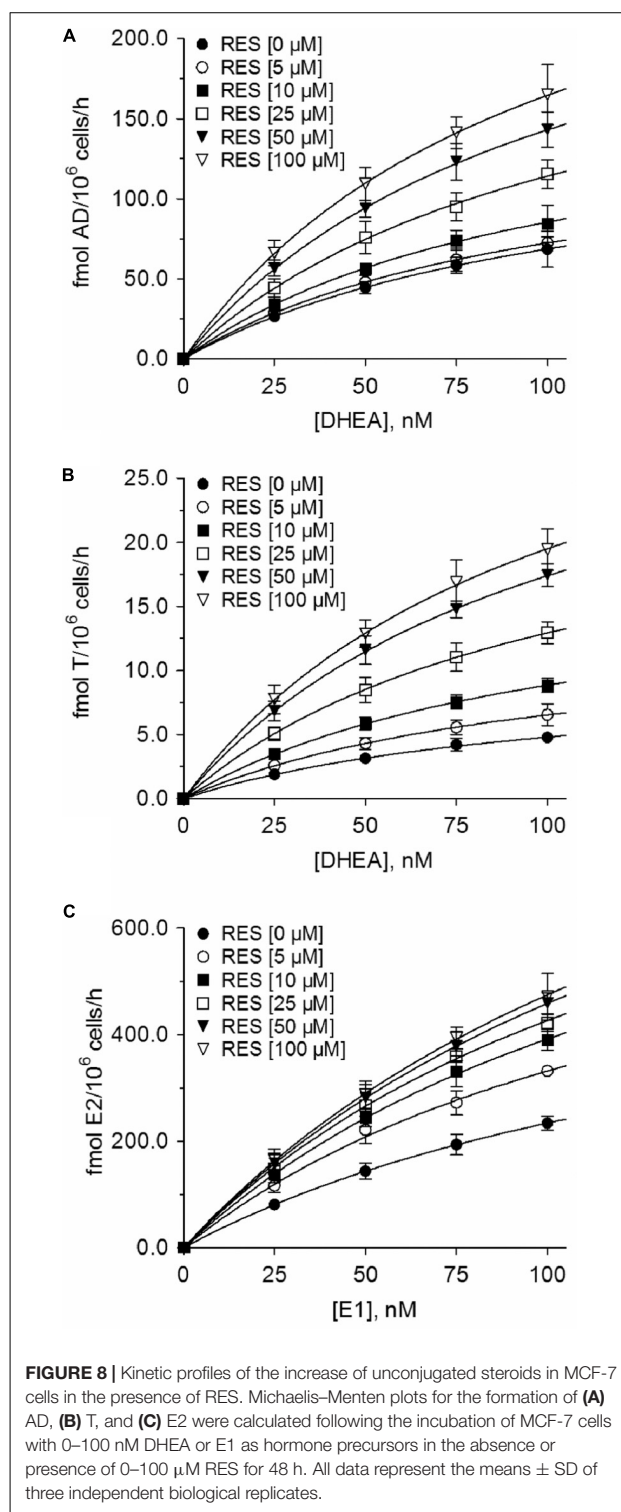
distinguish between free E2 and its conjugates (Chow et al., 2014).

This increase in unconjugated E2 may cause the observed induction of cell proliferation in ERα+ MCF-7 cells, particularly at RES concentrations < 10 μM. Similar findings have been reported by Chen et al. (2015), who also revealed that at physiological concentrations of E2, low doses of RES may stimulate the proliferation of ERα+ breast cancer cells. Therefore, increased E2 levels may be observed in hormone-dependent breast cancer patients following the intake of high-dose dietary supplements containing RES, as K_i values for the formation of E1-S and E2-S in MCF-7 breast cancer cells were 0.94 ± 0.03 and 0.73 ± 0.07 μM, respectively. The pronounced inhibition of estrogen sulfation by RES may also occur in other organs, as demonstrated by Furimsky et al. (2008) in S9 fractions from human liver (K_i : 1.1 μM) and jejunum (K_i : 0.6 μM).

TABLE 3 | Kinetic parameters of steroid metabolism by MCF-7 cells in the absence and presence of RES.

Metabolite	K_m (nM)						V_{max} (fmol/ 10^6 cells/h)					
	0 μ M RES	5 μ M RES	10 μ M RES	25 μ M RES	50 μ M RES	100 μ M RES	0 μ M RES	5 μ M RES	10 μ M RES	25 μ M RES	50 μ M RES	100 μ M RES
DHEA-S	329.2 \pm 52.2	311.7 \pm 71.9	323.7 \pm 53.7	404.1 \pm 93.1	402.8 \pm 34.7	385.0 \pm 46.6	2873.0 \pm 57.4	2766.2 \pm 53.9	2280.1 \pm 81.4*	1797.6 \pm 48.9*	993.5 \pm 74.8*	522.5 \pm 54.8*
E1-S	101.9 \pm 12.9	94.0 \pm 12.0	100.5 \pm 8.6	120.5 \pm 15.5	108.9 \pm 4.1	105.4 \pm 9.0	30.4 \pm 0.5	4.51 \pm 0.33*	2.54 \pm 0.21*	1.23 \pm 0.11*	0.57 \pm 0.02*	0.28 \pm 0.01*
E2-S	103.8 \pm 15.5	105.6 \pm 15.9	99.3 \pm 12.8	94.9 \pm 14.7	100.6 \pm 11.2	99.7 \pm 6.0	24.7 \pm 4.9	6.64 \pm 0.58*	2.34 \pm 0.19*	1.01 \pm 0.10*	0.56 \pm 0.01*	0.27 \pm 0.01*
E2-G	123.5 \pm 8.4	135.0 \pm 5.9	136.0 \pm 6.0	131.5 \pm 8.0	126.2 \pm 13.2	131.6 \pm 3.9	7.29 \pm 0.36	7.00 \pm 0.20	4.98 \pm 0.14*	2.60 \pm 0.12*	1.51 \pm 0.11*	0.77 \pm 0.02*
AD	114.6 \pm 9.6	103.5 \pm 10.4	101.9 \pm 7.9	111.8 \pm 10.7	106.3 \pm 4.2	99.6 \pm 8.2	147.4 \pm 13.1	148.5 \pm 9.4	172.6 \pm 7.7*	242.0 \pm 14.4*	295.3 \pm 9.4*	328.8 \pm 12.9*
T	107.5 \pm 6.3	107.1 \pm 5.9	107.5 \pm 3.8	106.4 \pm 2.4	106.0 \pm 4.0	103.3 \pm 4.8	9.95 \pm 0.42	13.5 \pm 0.5*	18.4 \pm 0.7*	26.7 \pm 0.4*	35.9 \pm 0.8*	39.7 \pm 1.1*
E2	168.6 \pm 11.7	146.0 \pm 15.6	155.4 \pm 9.7	152.9 \pm 13.6	171.8 \pm 14.3	174.3 \pm 12.0	628.6 \pm 72.0	816.4 \pm 76.6*	1001.4 \pm 43.0*	1079.8 \pm 71.4*	1247.3 \pm 56.2*	1302.2 \pm 64.6*

Kinetic parameters were calculated using GraphPad Prism 6.0 software following the incubation of the cells with increasing concentrations of RES (0–100 μ M) and DHEA or E1 (25 to 100 nM) as hormone precursors for 48 h. All data represent the means \pm SD of three independent biological replicates. Values in bold and marked with an asterisk (*) are significantly different in comparison to the control values ($P < 0.05$).



In breast tumor tissue, steroid sulfation is catalyzed by SULT1E1, SULT1A1, and SULT2A1 (Mueller et al., 2015). Contrary to tumor tissue, MCF-7 cells do not express SULT1E1;

steroid sulfation by this enzyme can be therefore excluded (Falany et al., 2002; Hruz et al., 2008). As the sulfation of E1, E2, and DHEA was strongly inhibited by RES in MCF-7 cells even upon addition of low concentrations, we also investigated a possible regulation of *SULT1A1* and *SULT2A1* mRNA expression after incubating MCF-7 cells with 10 μ M RES. RES at this concentration showed an almost complete inhibition of E1 and E2 sulfation ($91.6 \pm 1.1\%$ and $90.0 \pm 1.0\%$, respectively, see **Figures 6D, 7A**), but had no effect on the cellular proliferation (**Figure 1B**) even after 48 h. Possible candidates for RES mediating a down-regulation of estrogen sulfating enzymes are the AhR and the pregnane X receptor (PXR) (Casper et al., 1999; Kodama and Negishi, 2013; Moscovitz et al., 2018). Both receptors are known to regulate mRNA expression of estrogen-metabolizing enzymes including SULTs. Because RES is known to work as an antagonist for AhR and PXR and is capable of down-regulating both nuclear receptors and SULTs, RES might inhibit estrogen sulfation via these pathways.

We found only an insignificant down-regulation of *SULT1A1* mRNA by $30.4 \pm 11.0\%$ after longer-term application of 10 μ M RES, suggesting that transcriptional regulation by these receptors might not contribute significantly to the observed reduction in the formation of steroid sulfates in the MCF-7 cells. These data might also implicate that breast cancer cell lines are different from the benign MCF-10A breast epithelial cells, where down-regulation of the AhR by RES significantly affect estrogen-metabolizing enzymes and cause a down-regulation of *SULT1E1*, particularly as *SULT1E1* is not expressed in MCF-7 cells (Licznarska et al., 2017). Further *in vitro* studies are therefore needed to elucidate the differences in the down-regulation of steroid metabolizing enzymes between benign and malignant human breast cell lines.

Our data also showed that autophagy might not be induced in MCF-7 cells by 10 μ M RES since cell proliferation was not affected. However, at higher RES concentrations, formation of autophagosomes might become important and was indeed observed by Scarlatti et al. (2008) in MCF-7 cells incubated with 64 μ M RES for 48 h.

Based on our data, RES inhibits steroid sulfation in MCF-7 cells mainly via direct binding to SULT enzymes, thereby reducing their activities. This is supported by the Lineweaver-Burk plots in our study that clearly show non-competitive inhibition of E1, E2, and DHEA sulfation by 5–100 μ M RES (**Figures 6B,E, 7B**); both RES and the steroid substrates bind to the SULT enzymes at any given time forming an enzyme-substrate-inhibitor complex. Our observation is confirmed by the *in vitro* study of Ung and Nagar (2009), demonstrating RES-induced *SULT1A1* and *SULT1E1* inhibition in stably transfected MCF-7 cells.

Whether RES may accumulate to levels in human breast tissue necessary to inhibit DHEA, E1, and E2 metabolism remains unknown. Our recent study demonstrated that following oral application to rats (10 mg/kg), RES distributes to a variety of organs, including the liver, spleen, kidney, heart, lung and brain, strongly indicating the potential uptake of RES also into breast tissue (Böhmendorfer et al., 2017). Due to its low oral bioavailability, blood and tissue concentrations of RES

following the dietary intake of red wine, peanuts or berries to inhibit estrogen metabolism may be markedly lower than our calculated K_i values, suggesting no significant effect on E2 levels. However, the daily high-dose administration of RES (0.5–5.0 g/day) for up to 29 days to 40 healthy subjects resulted in peak plasma concentrations of up to 4.24 μ M (Brown et al., 2010). Additionally, the levels of RES-3S and RES-3G were approximately 10- and 6-fold higher, respectively. Whether RES glucuronides and sulfates also exhibit inhibitory effects toward DHEA, E1, and E2 conjugation remains to be investigated. Any inhibitory effects may further increase the plasma concentration of free E2 following high-dose RES supplementation, thereby inducing the progression of ER α + breast cancer.

CONCLUSION

The present study demonstrated the non-competitive inhibition of the steroid metabolomics pathway in ER α + MCF-7 but not in ER α – MDA-MB-231 breast cancer cells by low micromolar concentrations of RES, which led to a significant, twofold increase of free E2, capable of stimulating the proliferation of ER α + breast cancer cells. As the content of RES in food is relatively low, an increased risk of breast cancer progression may only be observed after the continuous consumption of high-dose RES supplements. Further long-term human studies simultaneously monitoring free estrogens and their conjugates are therefore highly warranted to evaluate the efficacy and safety of RES supplementation, particularly in patients diagnosed with ER α + breast cancer.

AUTHOR CONTRIBUTIONS

SP performed all cell culture experiments, the LC–HRMS analysis and the data analysis, and contributed to the manuscript. AM-S analyzed the data and contributed to the manuscript. MZ, JW, and DD performed the LC–HRMS analyses. AM and DM performed the real-time PCR analyses and contributed to the manuscript together with TT. BP cultivated the breast cancer cell lines and performed the inhibition experiments. WJ supervised the experiments, analyzed the data, and wrote the final version of the manuscript.

FUNDING

This research was supported by grants from the Austrian Science Fund (FWF) awarded to WJ (Grant No. I 3417-B31) and to DM (Grant No. P23228-B19).

SUPPLEMENTARY MATERIAL

The Supplementary Material for this article can be found online at: <https://www.frontiersin.org/articles/10.3389/fphar.2018.00742/full#supplementary-material>

REFERENCES

- Adams, J. B., Pewnim, T., Chandra, D. P., Archibald, L., and Foo, M. S. (1979). A correlation between estrogen sulfotransferase levels and estrogen receptor status in human primary breast carcinoma. *Cancer Res.* 39, 5124–5126.
- Aiyer, H. S., Warri, A. M., Woode, D. R., Hilakivi-Clarke, L., and Clarke, R. (2012). Influence of berry polyphenols on receptor signaling and cell-death pathways: implications for breast cancer prevention. *J. Agric. Food Chem.* 60, 5693–5708. doi: 10.1021/jf204084f
- Andreani, C., Bartolacci, C., Wijnant, K., Crinelli, R., Bianchi, M., Magnani, M., et al. (2017). Resveratrol fuels HER2 and ER α -positive breast cancer behaving as proteasome inhibitor. *Aging* 9, 508–523. doi: 10.18632/aging.101175
- Banu, S. K., Stanley, J. A., Sivakumar, K. K., Arosh, J. A., and Burghardt, R. C. (2016). Resveratrol protects the ovary against chromium-toxicity by enhancing endogenous antioxidant enzymes and inhibiting metabolic clearance of estradiol. *Toxicol. Appl. Pharmacol.* 303, 65–78. doi: 10.1016/j.taap.2016.04.016
- Basly, J. P., Marre-Fournier, F., Le Bail, J. C., Habrioux, G., and Chulia, A. J. (2000). Estrogenic/antiestrogenic and scavenging properties of (E)- and (Z)-resveratrol. *Life Sci.* 66, 769–777. doi: 10.1016/S0024-3205(99)00650-5
- Böhmdorfer, M., Szakmary, A., Schiestl, R. H., Vaquero, J., Riha, J., Brenner, S., et al. (2017). Involvement of UDP-glucuronosyltransferases and sulfotransferases in the excretion and tissue distribution of resveratrol in mice. *Nutrients* 9:E1347. doi: 10.3390/nu9121347
- Brown, V. A., Patel, K. R., Viskaduraki, M., Crowell, J. A., Perloff, M., Booth, T. D., et al. (2010). Repeat dose study of the cancer chemopreventive agent resveratrol in healthy volunteers: safety, pharmacokinetics, and effect on the insulin-like growth factor axis. *Cancer Res.* 70, 9003–9011. doi: 10.1158/0008-5472.CAN-10-2364
- Casper, R. F., Quesne, M., Rogers, I. M., Shirota, T., Jolivet, A., Milgrom, E., et al. (1999). Resveratrol has antagonist activity on the aryl hydrocarbon receptor: implications for prevention of dioxin toxicity. *Mol. Pharmacol.* 56, 784–790.
- Chan, W. K., and Delucchi, A. B. (2000). Resveratrol, a red wine constituent, is a mechanism-based inactivator of cytochrome P450 3A4. *Life Sci.* 67, 3103–3112. doi: 10.1016/S0024-3205(00)00888-2
- Chen, F. P., Chien, M. H., and Chern, I. Y. (2015). Impact of lower concentrations of phytoestrogens on the effects of estradiol in breast cancer cells. *Climacteric* 18, 574–581. doi: 10.3109/13697137.2014.1001357
- Chow, H. H., Garland, L. L., Heckman-Stoddard, B. M., Hsu, C. H., Butler, V. D., Cordova, C. A., et al. (2014). A pilot clinical study of resveratrol in postmenopausal women with high body mass index: effects on systemic sex steroid hormones. *J. Transl. Med.* 12:223. doi: 10.1186/s12967-014-0223-0
- Chow, H. H., Garland, L. L., Hsu, C. H., Vining, D. R., Chew, W. M., Miller, J. A., et al. (2010). Resveratrol modulates drug- and carcinogen-metabolizing enzymes in a healthy volunteer study. *Cancer Prev. Res.* 3, 1168–1175. doi: 10.1158/1940-6207.CAPR-09-0155
- El-Sayed, N. S., and Bayan, Y. (2015). Possible role of resveratrol targeting estradiol and neprilysin pathways in lipopolysaccharide model of Alzheimer disease. *Adv. Exp. Med. Biol.* 822, 107–118. doi: 10.1007/978-3-319-08927-0_12
- Falany, J. L., Macrina, N., and Falany, C. N. (2002). Regulation of MCF-7 breast cancer cell growth by beta-estradiol sulfation. *Breast Cancer Res. Treat.* 74, 167–176. doi: 10.1023/A:1016147004188
- Ferlay, J., Soerjomataram, I., Dikshit, R., Eser, S., Mathers, C., Rebelo, M., et al. (2015). Cancer incidence and mortality worldwide: sources, methods and major patterns in GLOBOCAN 2012. *Int. J. Cancer.* 136, E359–E386. doi: 10.1002/ijc.29210
- Folkerd, E., and Dowsett, M. (2013). Sex hormones and breast cancer risk and prognosis. *Breast* 22(Suppl. 2), 38–43. doi: 10.1016/j.breast.2013.07.007
- Furimsky, A. M., Green, C. E., Sharp, L. E., Catz, P., Adjei, A. A., Parman, T., et al. (2008). Effect of resveratrol on 17 β -estradiol sulfation by human hepatic and jejunal S9 and recombinant sulfotransferase 1E1. *Drug Metab. Dispos.* 36, 129–136. doi: 10.1124/dmd.107.016725
- Garvin, S., Ollinger, K., and Dabrosin, C. (2006). Resveratrol induces apoptosis and inhibits angiogenesis in human breast cancer xenografts in vivo. *Cancer Lett.* 231, 113–122. doi: 10.1016/j.canlet.2005.01.031
- Hruz, T., Laule, O., Szabo, G., Wessendorp, F., Bleuler, S., Oertle, L., et al. (2008). Genevestigator v3: a reference expression database for the meta-analysis of transcriptomes. *Adv. Bioinformatics* 2008:420747. doi: 10.1155/2008/420747
- Kim, Y. N., Choe, S. R., Cho, K. H., Cho, D. Y., Kang, J., Park, C. G., et al. (2017). Resveratrol suppresses breast cancer cell invasion by inactivating a RhoA/YAP signaling axis. *Exp. Mol. Med.* 49:e296. doi: 10.1038/emmm.2016.151
- Kodama, S., and Negishi, M. (2013). Sulfotransferase genes: regulation by nuclear receptors in response to xeno/endo-biotics. *Drug Metab. Rev.* 45, 441–449. doi: 10.3109/03602532.2013.835630
- Levi, F., Pasche, C., Lucchini, F., Ghidoni, R., Ferraroni, M., and La Vecchia, C. (2005). Resveratrol and breast cancer risk. *Eur. J. Cancer Prev.* 14, 139–142. doi: 10.1097/00008469-200504000-00009
- Li, L., Chen, X., Zhu, Q., Chen, D., Guo, J., Yao, W., et al. (2014). Disrupting androgen production of Leydig cells by resveratrol via direct inhibition of human and rat 3 β -hydroxysteroid dehydrogenase. *Toxicol. Lett.* 226, 14–19. doi: 10.1016/j.toxlet.2014.01.022
- Licznarska, B., Szafer, H., Wierchowski, M., Sobierajska, H., and Baer-Dubowska, W. (2017). Resveratrol and its methoxy derivatives modulate the expression of estrogen metabolism enzymes in breast epithelial cells by AhR down-regulation. *Mol. Cell. Biochem.* 425, 169–179. doi: 10.1007/s11010-016-2871-2
- Mechtcheriakova, D., Sobanov, Y., Holtappels, G., Bajna, E., Svoboda, M., Jaritz, M., et al. (2011). Activation-induced cytidine deaminase (AID)-associated multigene signature to assess impact of AID in etiology of diseases with inflammatory component. *PLoS One* 6:e25611. doi: 10.1371/journal.pone.0025611
- Mechtcheriakova, D., Wlachs, A., Sobanov, J., Kopp, T., Reuschel, R., Bornancin, F., et al. (2007). Sphingosine 1-phosphate phosphatase 2 is induced during inflammatory responses. *Cell. Signal.* 19, 748–760. doi: 10.1016/j.cellsig.2006.09.004
- Meshcheryakova, A., Svoboda, M., Tahir, A., Kofeler, H. C., Triebel, A., Mungenast, F., et al. (2016). Exploring the role of sphingolipid machinery during the epithelial to mesenchymal transition program using an integrative approach. *Oncotarget* 7, 22295–22323. doi: 10.18632/oncotarget.7947
- Mesía-Vela, S., and Kauffman, F. C. (2003). Inhibition of rat liver sulfotransferases SULT1A1 and SULT2A1 and glucuronosyltransferase by dietary flavonoids. *Xenobiotica* 33, 1211–1220. doi: 10.1080/00498250310001615762
- Mohamed, M. E., and Frye, R. F. (2011). Effects of herbal supplements on drug glucuronidation. Review of clinical, animal, and in vitro studies. *Planta Med.* 77, 311–321. doi: 10.1055/s-0030-1250457
- Moscovitz, J. E., Kalgutkar, A. S., Nulick, K., Johnson, N., Lin, Z., Goosen, T. C., et al. (2018). Establishing transcriptional signatures to differentiate PXR-, CAR-, and AhR-mediated regulation of drug metabolism and transport genes in cryopreserved human hepatocytes. *J. Pharmacol. Exp. Ther.* 365, 262–271. doi: 10.1124/jpet.117.247296
- Mueller, J. W., Gilligan, L. C., Idkowiak, J., Arlt, W., and Foster, P. A. (2015). The regulation of steroid action by sulfation and desulfation. *Endocr. Rev.* 36, 526–563. doi: 10.1210/er.2015-1036
- Murias, M., Jäger, W., Handler, N., Erker, T., Horvath, Z., Szekeres, T., et al. (2005). Antioxidant, prooxidant and cytotoxic activity of hydroxylated resveratrol analogues: structure-activity relationship. *Biochem. Pharmacol.* 69, 903–912. doi: 10.1016/j.bcp.2004.12.001
- Murias, M., Miksits, M., Aust, S., Spatzenegger, M., Thalhammer, T., Szekeres, T., et al. (2008). Metabolism of resveratrol in breast cancer cell lines: impact of sulfotransferase 1A1 expression on cell growth inhibition. *Cancer Lett.* 261, 172–182. doi: 10.1016/j.canlet.2007.11.008
- Oskarsson, A., Spatafora, C., Tringali, C., and Andersson, Å. O. (2014). Inhibition of CYP17A1 activity by resveratrol, piceatannol, and synthetic resveratrol analogs. *Prostate* 74, 839–851. doi: 10.1002/pros.22801
- Pan, M. H., Chiou, Y. S., Chen, L. H., and Ho, C. T. (2015). Breast cancer chemoprevention by dietary natural phenolic compounds: specific epigenetic related molecular targets. *Mol. Nutr. Food Res.* 59, 21–35. doi: 10.1002/mnfr.201400515
- Pasqualini, J. R. (2009). Estrogen sulfotransferases in breast and endometrial cancers. *Ann. N. Y. Acad. Sci.* 1155, 88–98. doi: 10.1111/j.1749-6632.2009.04113.x
- Poschner, S., Zehl, M., Maier-Salamon, A., and Jäger, W. (2017). Simultaneous quantification of estrogens, their precursors and conjugated metabolites in human breast cancer cells by LC-HRMS without derivatization. *J. Pharm. Biomed. Anal.* 138, 344–350. doi: 10.1016/j.jpba.2017.02.033

- Riha, J., Brenner, S., Böhmendorfer, M., Giessrigl, B., Pignitter, M., Schueller, K., et al. (2014). Resveratrol and its major sulfated conjugates are substrates of organic anion transporting polypeptides (OATPs): impact on growth of ZR-75-1 breast cancer cells. *Mol. Nutr. Food Res.* 58, 1830–1842. doi: 10.1002/mnfr.201400095
- Saluzzo, J., Hallman, K. M., Aleck, K., Dwyer, B., Quigley, M., Mladenovik, V., et al. (2016). The regulation of tumor suppressor protein, p53, and estrogen receptor (ER α) by resveratrol in breast cancer cells. *Genes Cancer* 7, 414–425. doi: 10.18632/genesandcancer.125
- Samavat, H., and Kurzer, M. S. (2015). Estrogen metabolism and breast cancer. *Cancer Lett.* 356, 231–243. doi: 10.1016/j.canlet.2014.04.018
- Scarlatti, F., Maffei, R., Beau, I., Codogno, P., and Ghidoni, R. (2008). Role of non-canonical Beclin 1-independent autophagy in cell death induced by resveratrol in human breast cancer cells. *Cell Death Differ.* 15, 1318–1329. doi: 10.1038/cdd.2008.51
- Ung, D., and Nagar, S. (2009). Trans-resveratrol-mediated inhibition of beta-oestradiol conjugation in MCF-7 cells stably expressing human sulfotransferases SULT1A1 or SULT1E1, and human liver microsomes. *Xenobiotica* 39, 72–79. doi: 10.1080/00498250802604082
- Yildiz, F. (2005). *Phytoestrogens in Functional Foods*. Boca Raton, FL: CRC Press. doi: 10.1201/9781420027594
- Zhou, D., Wang, J., Chen, E., Murai, J., Siiteri, P., and Chen, S. (1993). Aromatase gene is amplified in MCF-7 human breast cancer cells. *J. Steroid Biochem. Mol. Biol.* 46, 147–153. doi: 10.1016/0960-0760(93)90289-9

Conflict of Interest Statement: The authors declare that the research was conducted in the absence of any commercial or financial relationships that could be construed as a potential conflict of interest.

Copyright © 2018 Poschner, Maier-Salamon, Zehl, Wackerlig, Dobusch, Meshcheryakova, Mechtcheriakova, Thalhammer, Pachmann and Jäger. This is an open-access article distributed under the terms of the Creative Commons Attribution License (CC BY). The use, distribution or reproduction in other forums is permitted, provided the original author(s) and the copyright owner(s) are credited and that the original publication in this journal is cited, in accordance with accepted academic practice. No use, distribution or reproduction is permitted which does not comply with these terms.

CHAPTER VI

ACTAEA RACEMOSA L. EXTRACT INHIBITS STEROID SULFATION IN HUMAN BREAST CANCER CELLS: EFFECTS ON ANDROGEN FORMATION

Authors:

Stefan Poschner, Judith Wackerlig, Daniel Dobusch, Bettina Pachmann,
Santosa J. Banh, Theresia Thalhammer and Walter Jäger

Under revision in:

Phytomedicine 2020

***Actaea racemosa* L. extract inhibits steroid sulfation in human breast cancer cells: Effects on androgen formation**

1 Stefan Poschner^a, Judith Wackerlig^a, Daniel Dobusch^a, Bettina Pachmann^a, Santosa
2 J. Banh^a, Theresia Thalhammer^b, Walter Jäger^{a,c,*}

3 ^aDepartment of Pharmaceutical Chemistry, University of Vienna, 1090 Vienna,
4 Austria.

5 ^bDepartment of Pathophysiology and Allergy Research, Center for Pathophysiology,
6 Infectiology and Immunology, Medical University of Vienna, 1090 Vienna,
7 Austria.

8 ^cVienna Metabolomics Center (VIME), University of Vienna, 1090 Vienna, Austria.

9 *Abbreviations:* 3 β -HSD, 3 β -hydroxysteroiddehydrogenase; 17 β -HSD, 17 β -
10 hydroxysteroiddehydrogenase; AD, 4-androstene-3,17-dione; BCE, black cohosh
11 extract (*Actaea racemosa* L. extract); DHEA, dehydroepiandrosterone; DHEA-S,
12 dehydroepiandrosterone-3-*O*-sulfate; DMEM/F-12, Dulbecco's Modified Eagle
13 Medium F-12; DMSO, dimethylsulfoxide; DPBS, Dulbecco's phosphate buffered
14 saline; DTT, dithiothreitol; ER α , estrogen receptor alpha; E1, estrone; E1-S, estrone-
15 3-*O*-sulfate; E2, 17 β -estradiol; E2-G, 17 β -estradiol-3-*O*-(β -D-glucuronide); E2-S,
16 17 β -estradiol-3-*O*-sulfate; E3, 16 α -hydroxy-17 β -estradiol; HRMS, high resolution
17 mass spectrometry; PAPS, adenosine-3'-phosphate-5'-phosphosulfate; SULT,
18 sulfotransferase; T, testosterone.

19 *Corresponding author: Department of Pharmaceutical Chemistry, University of
20 Vienna, Althanstrasse 14, 1090 Vienna, Austria. Tel: +431427755576; *E-mail*
21 address: walter.jaeger@univie.ac.at

22

23 **ABSTRACT**

24 *Background:* *Actaea racemosa* L., also known as black cohosh, is a popular herb
25 commonly used for the treatment of menopausal symptoms. Because of its purported
26 estrogenic activity, black cohosh root extract (BCE) may trigger breast cancer
27 growth.

28 *Study design/methods:* The potential effects of standardized BCE and its main
29 constituent actein on cellular proliferation and steroid hormone metabolism were
30 investigated in estrogen receptor alpha positive (ER α +) MCF-7 and -negative (ER α -)
31 MDA-MB-231 human breast cancer cells. Cellular proliferation was determined
32 following incubation of both cell lines with the steroid hormone precursors
33 dehydroepiandrosterone (DHEA) and estrone (E1) for 48 h, in the presence and
34 absence of BCE or actein. Using a validated liquid chromatography-high resolution
35 mass spectrometry assay, cell culture supernatants were simultaneously analyzed for
36 the ten main steroids of the estrogen pathway.

37 *Results:* Inhibition of MCF-7 and MDA-MB-231 cell proliferation (up to 36.9%) was
38 observed following treatment with BCE (0-25 μ g/ml) or actein (0-50 μ M).
39 Incubation of MCF-7, but not of MDA-MB-231 cells, with DHEA and BCE caused a
40 20.9% reduction in DHEA-3-O-sulfate (DHEA-S) formation, leading to a
41 concomitant increase in the androgens 4-androstene-3,17-dione (AD) and
42 testosterone (T). Actein was shown to exert an even stronger inhibitory effect on
43 DHEA-S formation in MCF-7 cells (up to 89.6%) and consequently resulted in 12- to
44 15-fold higher androgen levels compared with BCE. The formation of 17 β -estradiol
45 (E2) and its glucuronidated and sulfated metabolites was not affected by BCE or
46 actein after incubation with the estrogen precursor estrone (E1) in either cell line.

47 *Conclusions:* The results of the present study suggest that actein and BCE do not
48 promote breast cancer cell proliferation or influence estrogen levels. However,
49 androgen formation was strongly stimulated by BCE and actein, which may
50 contribute to their ameliorating effects on menopausal symptoms in women. Future
51 studies monitoring the levels of AD and T upon BCE supplementation of patients are
52 warranted to verify an association between BCE and endogenous androgen
53 metabolism.

54

55 ***Keywords:*** *Actaea racemosa L., actein, breast cancer, steroid hormones,*
56 *metabolism, SULT2A1.*

57

58 **1. Introduction**

59 Endocrine therapy with antiestrogens has become a promising strategy for the
60 treatment of estrogen receptor alpha positive (ER α +) breast cancer (Chiba *et al.*,
61 2017). Although endocrine therapy is highly effective (Takei *et al.*, 2008), patients
62 often suffer from considerable side effects, including hot flashes, sleep problems,
63 mood swings and depressive symptoms, ultimately resulting in a poor quality of life
64 (Merchant and Stebbing, 2015). A treatment option for these adverse symptoms is
65 hormone replacement therapy (HRT) with estrogens and/or progestins (Garrido
66 Oyarzún and Castelo-Branco, 2017). However, HRT may promote the proliferation
67 of breast cancer cells, and is therefore contraindicated for patients with breast cancer
68 (Beral, 2003; Hickey *et al.*, 2005). Thus, many patients take plant-derived
69 alternatives to ameliorate the neurovegetative and psychic symptoms of endocrine
70 therapy.

71 *Actaea racemosa* L. (former *Cimicifuga racemosa* L.) is one such plant; more
72 commonly known as black cohosh, a commercially available North American herb
73 that is globally used as a natural remedy for alleviating climacteric symptoms
74 (McKenna *et al.*, 2001). Black cohosh root and rhizome extract (BCE) contains
75 several triterpene glycoside saponines responsible for its *in vivo* activity against
76 menopausal disorders, of which actein is the major constituent (Avula *et al.*, 2009).
77 However, due to its purported estrogenic activity, there is controversy surrounding
78 the safety of BCE use in patients with breast cancer. A number of studies have
79 reported that BCE triggers breast cancer growth (Liu *et al.*, 2001), while others have
80 documented an inhibitory effect on breast cancer cell proliferation (Einbond *et al.*,
81 2004; Crone *et al.*, 2019), possibly via the down-regulation of ER α gene and protein
82 expression, as was shown in MCF-7 and T-47D cells (Park *et al.*, 2012; Szymd *et al.*,
83 2018; Crone *et al.*, 2019). Controversy also exists around the effect of BCE on the
84 reproductive organs, as demonstrated in animal studies. While various researchers
85 have demonstrated an increased uterine weight in BCE-treated rodents (Eagon *et al.*,
86 1997; Liu *et al.*, 2001), indicating that BCE exhibits ER α -mediated activities,
87 Freudenstein *et al.* (2002) reported no changes in the uterine weight of rats following
88 BCE administration.

89 However, two large retrospective human studies comprising data from >45,000
90 women demonstrated no significant correlation between breast cancer development
91 and BCE administration (Obi *et al.*, 2009; Brasky *et al.*, 2010). Additionally, three
92 uncontrolled trials investigating the impact of BCE on mammographic density also
93 did not reveal any promoting effects on breast tissue fibrosis (Raus *et al.*, 2006;
94 Hirschberg *et al.*, 2007; Lundström *et al.*, 2011). Another human study examining
95 the risk of breast cancer recurrence (Henneicke-von Zepelin *et al.*, 2007) reported a

96 25% decrease following treatment with BCE. However, it remains unclear whether
97 this decrease was associated with BCE or biased by the study design, as 35.8% of
98 patients in the BCE group were simultaneously using the anticancer drug tamoxifen,
99 compared with only 24.0% in the control group. In human ER α + MCF-7 and ER α -
100 MDA-MB-231 breast cancer cells, a synergistic effect has been reported between
101 BCE and the antiestrogen tamoxifen, indicating that BCE influences steroid hormone
102 metabolism in breast cancer (Bodinet and Freudenstein, 2002; Einbond *et al.*, 2006;
103 Al-Akoum *et al.*, 2007).

104 The proliferation of breast cells is strongly influenced by the levels of steroid
105 hormones, especially 17 β -estradiol (E2) (Folkerd and Dowsett, 2013). These levels
106 are regulated by several metabolic enzymes that transform inactive steroid precursors
107 into active hormones or inactivate estrogens via conjugation to their respective
108 sulfated or glucuronidated metabolites. The effects of BCE on steroid metabolism
109 may therefore explain the possible stimulatory or inhibitory effects on breast cancer
110 growth. Indeed; BCE was shown to increase the expression of genes coding for
111 metabolic enzymes, such as members of the cytochrome-P450 (CYP) and aldo-keto-
112 reductase (AKR) families (Gaube *et al.*, 2007). Therefore, we investigated for the
113 first time the potential effect of standardized BCE and actein on steroid metabolism
114 in human ER α + MCF-7 and ER α - MDA-MB-231 breast cancer cells, using a
115 validated liquid chromatography-high resolution mass spectrometry (LC-HRMS)
116 assay. The results of the present study may improve our understanding of the
117 molecular effects of BCE on breast cancer cells, and help to assess the safety of BCE
118 supplements for patients with breast cancer.

119 2. Materials and methods

120 2.1. Chemicals and reagents

121 Adenosine-3'-phosphate-5'-phosphosulfate lithium salt hydrate (PAPS), acetic
 122 acid, acetonitrile, actein of USP reference standard quality
 123 ([[(1S,1'R,2S,3'R,4R,4'R,5R,5'R,6'R,10'S,12'S,13'S,16'R, 18'S,21'R)-2-hydroxy-
 124 1,4',6',12',17',17'-hexamethyl-18'-[(2S,3R,4S,5R)-3,4,5-trihydroxyoxan-2-
 125 yl]oxyspiro[3,6-dioxabicyclo[3.1.0]hexane-4,8'-9-
 126 oxahexacyclo[11.9.0.01,21.04,12.05,10.016,21] docosane]-3'-yl] acetate;
 127 supplementary **Fig. S1**), ammonium acetate, 4-Androstene-3,17-dione (AD),
 128 dehydroepiandrosterone (DHEA), dehydroepiandrosterone-2,2,3,4,4,6-d₆ (DHEA-
 129 d₆), dehydroepiandrosterone-3-O-sulfate sodium salt (DHEA-S),
 130 dehydroepiandrosterone-3-O-sulfate-2,2,3,4,4,6-d₆ sodium salt (DHEA-S-d₆),
 131 dimethylsulfoxide (DMSO), dithiothreitol (DTT), E2, 17 β -estradiol-3-O-(β -D-
 132 glucuronide) sodium salt (E2-G), estriol (16 α -hydroxy-17 β -estradiol; E3), estrone
 133 (E1), formic acid, powdered BCE (USP reference standard) and testosterone (T)
 134 were obtained from Merck KGaA (Darmstadt, Germany). Estrone-3-O-sulfate
 135 sodium salt (E1-S) and 17 β -estradiol-3-O-sulfate sodium salt (E2-S) were purchased
 136 from Steraloids Inc. (Newport, RI, USA); sulfotransferase 2A1 (SULT2A1) was
 137 procured from tebu-bio GmbH (Offenbach, Germany); 4-Androstene-3,17-dione-
 138 2,2,4,6,6,16,16-d₇ (AD-d₇), 16 α -hydroxy-17 β -estradiol-2,4,17-d₃ (E3-d₃), 17 β -
 139 estradiol-2,4,16,16-d₄ (E2-d₄), 17 β -estradiol-16,16,17-d₃-3-O-(β -D-glucuronide)
 140 sodium salt (E2-G-d₃), 17 β -estradiol-2,4,16,16-d₄-3-O-sulfate sodium salt (E2-S-d₄),
 141 estrone-2,4,16,16-d₄ (E1-d₄), estrone-2,4,16,16-d₄-3-O-sulfate sodium salt (E1-S-d₄)
 142 and testosterone-2,2,4,6,6-d₅ (T-d₅) were purchased from C/D/N-Isotopes Inc.

143 (Pointe-Claire, Quebec, Canada). Purified water was produced using an arium[®] pro
144 ultrapure water system (Sartorius AG, Göttingen, Germany). All standard
145 compounds were separately dissolved in DMSO and stored at -80°C until further use.
146 All deuterated standards were diluted with DMSO to their final concentration, and
147 mixed to obtain a final internal standard master mix composition, which was also
148 stored at -80°C.

149 2.2. *Quantification of actein in BCE*

150 The actein content of the standardized powdered BCE (USP certified) was
151 determined using a LaChrom L-7000 high-performance liquid chromatography
152 system (Merck Hitachi, Darmstadt, Germany), equipped with an ELSD 90
153 evaporative light scattering detector (VWR International, LLC, Radnor, PA, USA)
154 for quantification, according to the respective monography of the United States
155 Pharmacopeia 42 (USP 42, 2019). Separation was carried out using a Phenomenex
156 Luna[®] 5 µm C18(2) LC column (250 x 4.6 mm I.D.; Phenomenex, Inc., Torrance,
157 CA, USA), preceded by a Hypersil[®] BDS-C18 guard column (5 µm, 10 x 4.6 mm
158 I.D.; Thermo Fisher Scientific, Inc., Waltham, MA, USA) at 35°C. Solvent A was
159 0.1% formic acid in water, solvent B was acetonitrile, and the flow rate was set to 1.6
160 ml/min. Gradient elution was performed using the following settings: 0 min, 20% B;
161 8 min, 20% B; 15 min, 32% B; 55 min, 64% B; 65 min, 95% B; 70 min, 95% B; and
162 85 min, 20% B. All samples were dissolved in methanol, sonicated for 1 min, passed
163 through a 0.22 µm filter and 20 µl of the brownish solution were injected onto the
164 column. Actein was then quantified using external linear calibration curves obtained
165 by dissolving purified actein in methanol, resulting in a concentration range of 12.5-
166 250 µg/ml (average correlation coefficient 0.9999).

167 2.3. Cell culture and proliferation studies

168 MCF-7 (ER α +) and MDA-MB-231 (ER α -) human breast cancer cells were
169 purchased from the American Type Culture Collection (ATCC, Manassas, VA,
170 USA). Dulbecco's Modified Eagle Medium F-12 (DMEM), Dulbecco's phosphate
171 buffered saline (DPBS), fetal bovine serum (FBS.), PenStrep[®]- and TrypLE[®]-
172 solution were purchased from Invitrogen (Thermo Fisher Scientific, Inc.). HyClone[®]
173 heat-inactivated charcoal-stripped FBS (U.S. origin) was obtained from GE
174 Healthcare Life Sciences (Logan, UT, USA). Both cell lines were routinely cultured
175 at 37°C (95% humidity, 5% CO₂) in phenol red-free DMEM containing 1%
176 PenStrep[®]-solution and 10% FBS. All experiments were performed with cells in the
177 exponential growth phase.

178 For experimentation, the cells were seeded into 6-well-plates at a density of
179 1.0x10⁶ cells/well. After attachment overnight, the monolayers were washed twice
180 with DPBS and treated with 2.5 ml DMEM containing 1% PenStrep[®]-solution and
181 10% heat-inactivated charcoal-dextran-treated FBS, in order to prevent any influence
182 from external hormone sources. DHEA or E1 (dissolved in DMSO; final
183 concentration, 0.1%) were then added in triplicate as hormone precursors (0-100
184 nM), in the presence or absence of either BCE (0-25 µg/ml) or purified actein (0-50
185 µM).

186 Following a 48-h incubation period, the supernatants were discarded and the cell
187 monolayers detached with 400 µl TrypLE[®]-solution; the number of viable cells was
188 counted using a Casy[®] TT cell counter (OLS OMNI Life Science, Bremen,
189 Germany) and reported as the means \pm standard deviation (SD) of three independent
190 experiments.

191 Actein stability was investigated by spiking the cell culture media with 1, 5 or 10
 192 μM actein in DMSO (final concentration, 0.1%) and incubation at 37°C for 0, 8, 24
 193 and 48 h. Subsequently, the proteins were precipitated and 100 μl clear supernatant
 194 was analyzed using the same LC protocol as described above for actein. Data are
 195 reported as the means \pm SD of three independent experiments.

196 2.4. Steroid biotransformation studies

197 To investigate the effects of BCE and actein on steroid metabolism in ER α - and
 198 ER α + breast cancer cells, MCF-7 and MDA-MB-231 cells were cultured as
 199 described in section 0. in the presence or absence of BCE (0-25 $\mu\text{g/ml}$) or purified
 200 actein (0-10 μM), in addition to the hormone precursors DHEA or E1 (0-100 nM).
 201 All incubations were conducted for 48 h, as the linearity of metabolite formation was
 202 previously confirmed for this time period (Poschner *et al.*, 2018). Following
 203 incubation, cell supernatants (2000 μl aliquots) were mixed with the deuterated
 204 internal standard master-mix (20 μl) and concentrated using Oasis HLB 1 cc SPE
 205 cartridges (30 mg; Waters Corporation, Milford, MA, USA) for solid phase
 206 extraction, as previously described (Poschner *et al.*, 2017). The number of viable
 207 cells was assessed at the end of each incubation by washing the remaining cells with
 208 DPBS, harvesting by trypsinization (400 μl ; 37°C, 5 min) and counting as
 209 aforementioned.

210 2.5. Steroid quantification using LC-HRMS

211 Quantification of the 10 predominant estrogens, their precursors and conjugated
 212 metabolites (namely AD, DHEA, DHEA-S, E1, E1-S, E2, E2-S, E2-G, E3 and T)
 213 was achieved by applying a sensitive and validated LC-HRMS assay [ICH Q2(R1)
 214 guidelines] as described previously (Poschner *et al.*, 2017). To ensure reliable

quantification results, three independent sets of quality control samples [(containing each analyte at 6-, 60- and 600-fold the respective lower limits of quantification (LLOQs)] were quantified with each batch in triplicate. The LLOQs (signal to noise ratio ≥ 9) for the investigated compounds were as follows: AD, 74.9 pg/ml; DHEA, 1904.0 pg/ml; DHEA-S, 8.0 pg/ml; E1, 19.0 pg/ml; E1-S, 4.0 pg/ml; E2, 140.9 pg/ml; E2-G, 12.0 pg/ml; E2-S, 3.4 pg/ml; E3, 28.4 pg/ml and T, 54.1 pg/ml.

2.6. *SULT2A1* enzyme inhibition assay

As the formation of DHEA-S, but not of E1-S or E2-S, was inhibited by BCE and actein administration, their effects on SULT2A1, the primary enzyme responsible for the sulfation of DHEA, were investigated. Recombinant human SULT2A1 (2.4 $\mu\text{g/ml}$) was incubated at 37°C in $\text{KH}_2\text{PO}_4/\text{K}_2\text{HPO}_4$ buffer (50 mM, pH = 6.5) in the presence of DTT (1 mM), EDTA (0.1 mM) and PAPS (50 μM) with increasing concentrations of DHEA as the substrate (0-100 nM), and BCE (0-25 $\mu\text{g/ml}$) or actein (0-25 μM) as the inhibitors. Buffer-only samples were used as controls, and all reactions were performed in triplicate. Before initiation of the reaction, the enzyme was pre-incubated with DTT/PAPS and BCE or actein for 5 min at 37°C. After the addition of DHEA, the vials were incubated for a further 15 min, and the reactions were then terminated using ice-cold methanol (-20°C), followed by centrifugation (14,000 x g, 5 min). The clear supernatants were subsequently analyzed for DHEA-S using the same LC-HRMS assay as described above.

2.7. *Kinetic analyses and statistics*

The kinetic parameters for the biotransformation of steroids in the presence or absence of BCE or actein were calculated for both cell lines using the GraphPad Prism 6.0 software package (GraphPad Software Inc., La Jolla, CA, USA). All

kinetics best fitted the Michaelis-Menten model $V = V_{\max} \times [S] / (K_m + [S])$, where V is the rate of the reaction, V_{\max} is the maximum reaction velocity, $[S]$ is the initial substrate concentration and K_m is the Michaelis constant. After fitting the kinetic model, the mode of inhibition was determined from a Lineweaver-Burk plot, and the corresponding inhibition constant (K_i value) was calculated from a Dixon plot using the same software package. The same kinetic analyses were also performed for the SULT2A1 inhibition assay.

All data were statistically analyzed using GraphPad Prism 6.0, and - if not otherwise stated, reported as the means \pm SD of three independent experiments. One-way ANOVA followed by Tukey's post-test was then applied to compare the differences between the controls and treatment samples, with a statistical significance threshold of $P < 0.05$.

3. Results

3.1. Effects of BCE and actein on ER α + and ER α - breast cancer cell proliferation

To investigate the influence of BCE on the proliferation of human breast cancer cells, MCF-7 (ER α +) and MDA-MB-231 (ER α -) cells were treated with increasing concentrations of BCE (0-25 μ g/ml) in the absence of any steroid precursor. As shown in **Fig. 1A**, a minor, yet statistically significant inhibition of cell proliferation was observed in MDA-MB-231 ($19.6 \pm 2.2\%$) and MCF-7 cells ($25.5 \pm 9.9\%$) as a result of BCE administration.

In the presence of 100 nM E1 (**Fig. 1B**), the proliferation of MCF-7 cells was increased by $67.7 \pm 3.0\%$ compared with that in the absence of E1; MDA-MB-231 samples were almost unaffected by E1 ($-1.8 \pm 5.6\%$), consequently confirming the hormone-dependency of MCF-7 cells in contrast to MDA-MB-231 cells. Upon

subsequent treatment with BCE (up to 25 $\mu\text{g/ml}$), a dose-dependent inhibition of cancer cell proliferation was again observed; however, the inhibitory effect was less pronounced, with maximum inhibition rates of 15.5 ± 1.8 and $20.9 \pm 2.0\%$ in MDA-MB-231 and MCF-7 cells, respectively. The addition of 100 nM DHEA revealed no significant differences in the proliferation of either cell line, compared with the hormone-free controls (data not shown).

Subsequently, the same experimental setup was repeated with purified actein, which has been reported as the most potent constituent of BCE to inhibit breast cancer cell proliferation (Einbond *et al.*, 2004). Prior to incubation, the concentration of actein in the investigated USP-certified BCE was quantified, and determined to be 0.51%. We also demonstrated that actein (1, 5 and 10 μM) was stable in DMEM/F-12 cell culture medium for up to 48 h at 37°C (in the absence of cells), as no changes in actein concentration were detected at the sampling time-points (0, 8, 24 and 48 h).

Incubation of MCF-7 and MDA-MB-231 cells with increasing concentrations of actein (0-50 μM) for 48 h [in the presence or absence of E1 or DHEA (100 nM)] revealed stronger inhibition of breast cancer proliferation compared with BCE in all experimental conditions. In the absence of steroids (**Fig. 1C**), actein inhibited the proliferation of MCF-7 and MDA-MB-231 cells by 34.3 ± 2.4 and $30.1 \pm 6.8\%$, respectively. As a steroid precursor, the addition of E1 to the cell culture medium once again stimulated the proliferation of MCF-7 cells in the absence of actein; however, the inhibitory potency of actein remained unchanged in both cell lines. The reduction in proliferation rates was comparable to the hormone-deprived setting, with a reduction of $36.9 \pm 4.5\%$ in MCF-7 and $27.9 \pm 8.0\%$ in MDA-MB-231 cells (**Fig. 1D**). Again, the addition of DHEA did not alter the inhibitory effect of actein compared with the hormone-deprived controls (data not shown).

3.2. Impact of BCE on steroid metabolism in ER α + and ER α - breast cancer cells

In addition to the proliferation studies, we further investigated the effect of BCE on the metabolism of estrogens in MCF-7 and MDA-MB-231 cells (**Fig. 2A**). After 48 h, MCF-7 cells were shown to extensively metabolize E1 (100 nM) to E2 (275.8 ± 2.5 fmol/ 10^6 cells/h) in the presence of BCE (25 μ g/ml), followed by the sulfated or glucuronidated metabolites E1-S (16.2 ± 0.3 fmol/ 10^6 cells/h), E2-S (11.8 ± 0.3 fmol/ 10^6 cells/h) and E2-G (3.36 ± 0.64 fmol/ 10^6 cells/h). E3 was only a very modest biotransformation product (0.59 ± 0.04 fmol/ 10^6 cells/h). Similarly, MDA-MB-231 cells predominantly formed E2 (250.8 ± 8.5 fmol/ 10^6 cells/h), but in contrast to MCF-7 cells, formed E1-S (0.48 ± 0.02 fmol/ 10^6 cells/h), E2-S (0.10 ± 0.01 fmol/ 10^6 cells/h) and E2-G (0.20 ± 0.02 fmol/ 10^6 cells/h) to a much lower extent. The presence of E3 in the supernatant was below the detection limit in all MDA-MB-231 samples (**Fig. 2B**). The total molar proportions of these detected biotransformation products amounted to 99.5 and 97.1% of all metabolites in MCF-7 and MDA-MB-231 cells, respectively, concluding that no other major metabolic pathways were active in these cell lines upon incubation with E1. Interestingly, there were no observable differences in the formation rates of estrogenic steroids between the controls (DMSO) and BCE-treated cells, indicating that BCE does not influence estrogen metabolism.

In order to investigate a possible influence on the biotransformation of androgens, both cell lines were subsequently incubated with DHEA (100 nM) and BCE (25 μ g/ml) (**Fig. 2C and 2D**). MCF-7 cells exhibited high sulfation capacity (DHEA-S: 663.0 ± 18.3 fmol/ 10^6 cells/h), while the 3 β -hydroxysteroiddehydrogenase (3 β HSD)- and 17 β -hydroxysteroiddehydrogenase (17 β -HSD)-mediated conversions to AD and T were significantly less pronounced

(AD: 117.2 ± 11.0 fmol/ 10^6 cells/h; T: 9.08 ± 0.44 fmol/ 10^6 cells/h). By contrast, the formation of DHEA-S in MDA-MB-231 cells was almost negligible (0.83 ± 0.15 fmol/ 10^6 cells/h), while the formation of AD (860.9 ± 47.8 fmol/ 10^6 cells/h) and T (59.5 ± 1.5 fmol/ 10^6 cells/h) was several fold higher, compared with that in MCF-7 cells. These three quantified metabolites also amounted to almost all of the biotransformation products in both cell lines (MCF-7: 99.8%; MDA-MB-231: 97.9%).

Compared with the untreated controls, BCE (25 μ g/ml) inhibited DHEA sulfation by 20.9% in MCF-7 cells, with a concomitant increase in AD and T of 52.0 and 58.1%, respectively, indicating a strong effect of BCE on DHEA metabolism. By contrast, no differences were observed in the formation rates of androgens between the control- (DMSO) and BCE-treated MDA-MB-231 cells. Detailed values determined over a concentration range of 0-25 μ g/ml BCE are presented in **Table 1**.

3.3. Impact of actein on steroid metabolism in MCF-7 breast cancer cells

As no significant changes were observed in the metabolomics profile of MDA-MB-231 cells following treatment with BCE, all further experiments investigating the impact of purified actein on steroids metabolism were performed using MCF-7 cells only. Cells were incubated in the presence of E1 (0-100 nM) with increasing concentrations of actein (0-10 μ M) for 48 h; however, as already observed for BCE (see section 3.2.), purified actein did not affect the levels of E2, E1-S, E2-S, E2-G or E3 in MCF-7 cells (data not shown).

By contrast, when the cells were exposed to DHEA (100 nM) as a precursor steroid, the presence of actein (0-10 μ M) strongly inhibited DHEA sulfation from its precursor state. Even the lowest concentration of actein (0.5 μ M) reduced the

formation of DHEA-S by 45.2% (from 827.4 ± 75.5 to 453.8 ± 52.2 fmol/ 10^6 cells/h), whereas 10 μ M actein caused almost complete inhibition of this biotransformation step (a 94.6% reduction), resulting in a formation rate of only 44.9 ± 6.1 fmol/ 10^6 cells/h (**Fig. 3**). Subsequent kinetic analyses over a concentration range of 0-100 nM DHEA revealed that the inhibition of DHEA sulfation best fitted to the Michaelis-Menten model. As the K_m values were largely unaffected, and all V_{max} values decreased in a dose-dependent manner with increasing concentrations of actein (**Table 2**), a non-competitive inhibition mode was assumed, and further confirmed by the Lineweaver-Burk plot. The inhibition constant was calculated from the Dixon plot and determined to be $K_i = 0.58 \pm 0.02$ μ M.

Incubation of MCF-7 cells with 100 nM DHEA and 0.5 μ M actein also induced AD formation by 101.2% (from 66.5 ± 4.0 to 133.8 ± 15.7 fmol/ 10^6 cells/h) and T formation by 50.2% (from 4.60 ± 0.44 to 6.91 ± 1.08 fmol/ 10^6 cells/h). Strikingly, an increase in actein concentration (up to 10 μ M) increased the levels of AD and T by 727.1 (550.0 ± 22.6 fmol/ 10^6 cells/h) and 651.5% (34.6 ± 1.0 fmol/ 10^6 cells/h), respectively (**Fig. 4**). Michaelis-Menten kinetics were again determined as the best-fitting model for the formation of AD and T over a concentration range of 0-100 nM DHEA, with concentration-dependent increases in V_{max} values, while the K_m values remained largely unaffected (**Table 2**).

3.4. Inhibition of SULT2A1 by BCE and actein

As the sulfotransferase SULT2A1 is the only enzyme expressed in MCF-7 cells to catalyze the conversion of DHEA to DHEA-S (Falany *et al.*, 1989; Mueller *et al.*, 2015; Licznarska *et al.*, 2017), we hypothesized that actein, and therefore also BCE, may inhibit the activity of this isoenzyme. To study this approach, recombinant

human SULT2A1 was incubated with increasing concentrations of BCE (0-25 $\mu\text{g/ml}$) or actein (0-25 μM) in the presence of 25 nM DHEA (**Fig. 5**). After 15 min at 37°C, BCE reduced the formation of DHEA-S by up to 26.5% (from 8.1 ± 1.2 to 6.0 ± 0.9 pmol/min/mg protein). Purified actein inhibited the sulfation of DHEA to an even greater extent: While the lowest actein concentrations tested (1.0 and 2.5 μM) reduced the formation of DHEA-S by 9.2 and 14.7%, respectively, an increase in actein to 25 μM led to a further inhibition of SULT2A1, with a maximum reduction rate of 64.3% (from 8.1 ± 0.9 to 2.9 ± 0.1 pmol/min/mg protein). Subsequently, the K_i values for these reactions were determined over a concentration range up to 100 nM DHEA, and calculated from the corresponding Dixon plots (**Fig. 5B** and **5D**) as 67.7 ± 1.5 $\mu\text{g/ml}$ for BCE and 14.0 ± 0.2 μM for actein. Furthermore, Lineweaver-Burk plots clearly indicated a non-competitive inhibition mode, where each inhibitor and DHEA form an enzyme-substrate-inhibitor complex at any given time. The inhibition of SULT1A1 (catalyzing the sulfation of E1 and E2) by BCE (25 $\mu\text{g/ml}$) or actein (10 μM) can be excluded, as E1-S and E2-S levels were not affected in the cell experiments.

4. Discussion

BCE is an herbal supplement often used for the treatment of menopausal disorders. As antiestrogenic therapies, such as tamoxifen, cause adverse side-effects such as hot flashes and sweating, thus BCE is often taken by breast cancer patients to relieve these complaints. However, the use of BCE by breast cancer patients is controversial, as a number of studies have proposed that it may promote tumor progression. Our investigation of BCE in human breast cancer cell lines revealed a moderate, concentration-dependent inhibition of cancer cell proliferation from BCE

385 (0-25 µg/ml), with maximum reduction rates of roughly 26 and 20% in ER α + MCF-7
386 and ER α - MDA-MB-231 cells, respectively. Purified actein, the major active
387 triterpene glycoside component of BCE, exerted an even more pronounced growth
388 inhibition in both cells lines (34 and 30%, respectively), also indicating estrogen-
389 independent effects on cellular proliferation. These findings are in line with previous
390 data, also reporting BCE induced inhibition of MCF-7, MDA-MB-453 and T-47D
391 breast cancer cell proliferation (Einbond *et al.*, 2004; Crone *et al.*, 2019),.

392 Next, we investigated whether BCE or actein might affect the biotransformation
393 of estrogens to their respective unconjugated and conjugated metabolites in MCF-7
394 and MDA-MB-231 cells. After incubating both cell lines with BCE and actein in the
395 presence of E1, no change in the formation of E2, E3, E1-S, E2-S or E2-G was
396 revealed, compared with the untreated controls. Interestingly, formation of the main
397 metabolite E2 did not differ between MCF-7 and MDA-MB-231 cells, supporting
398 ER α -independent biotransformation. The five quantified biotransformation products
399 accounted for 97.6 and 99.2% of all metabolites formed upon E1 treatment in both
400 cell lines, suggesting that BCE does not affect estrogen metabolism in these breast
401 cancer cells. These *in vitro* findings are in line with data from a double-blind,
402 placebo-controlled study by Wuttke *et al.* (2006), who also reported no change in the
403 total serum E2 levels of 62 postmenopausal women receiving a daily dose of 5 mg
404 BCE for 12 weeks. Similarly, Reed *et al.* (2008) determined the total E2
405 concentrations in serum samples of 133 postmenopausal women after 12 months of
406 treatment with BCE, which also revealed no significant changes in E2 levels.
407 However, the concentrations of other steroid hormones and metabolites were not
408 investigated in these studies.

Therefore in the present study, we also assessed the formation of DHEA-S and the androgens AD and T in MDA-MB-231 and MCF-7 cells; this was conducted in the presence and absence of BCE and actein, following incubation with the androgen precursor DHEA. While BCE and actein did not significantly alter the metabolic profile of MDA-MB-231 cells, DHEA sulfation was significantly inhibited in MCF-7 cells by up to 20.9%, with a concomitant increase in the unconjugated androgens AD (+52.0%) and T (+58.1%) (**Fig. 6**). This effect was even more pronounced when purified actein was used as inhibitor, resulting in almost complete inhibition of DHEA-S formation (up to 94.6%), with a corresponding sub-micromolar K_i value of $0.58 \pm 0.02 \mu\text{M}$. Concurrently, AD and T levels were strongly increased by 722 and 652%, respectively. As aromatase (CYP19A1) is not expressed in either cell line (Zhou *et al.*, 1993), further conversion of AD and T to the estrogens E1 and E2, respectively, could not be observed. In contrast, aromatase is expressed in adipocytes adjacent to ER α + breast tumors *in vivo*, so that patients diagnosed with hormone-dependent breast cancer may exhibit an increased androgen-to-estrogen conversion rate following treatment with BCE. However, this is highly unlikely, as data from two large studies including over 10,000 and 35,000 women, respectively, did not confirm any estrogenic effects of BCE supplements *in vivo*. Indeed; both studies even reported a protective effect of BCE against invasive breast cancer (Obi *et al.*, 2009; Brasky *et al.*, 2010).

The increased levels of unconjugated AD and T observed in the present study may explain - at least partly - the effect of BCE (6.5 mg/day for 12 weeks) on hot flashes in 122 menopausal women suffering from moderate to severe menopausal disorders (Frei-Kleiner *et al.* (2005), as elevated T levels have been proven to alleviate vasomotor symptoms such as hot flashes (Øverlie *et al.*, 2002). Continuous

434 treatment of 300 pre- and postmenopausal women with a subcutaneous T implant
435 (75-160 mg total dosage, based on patients' weight) over three months resulted in the
436 effective and dose-dependent relief of hot flashes and sweating (Glaser *et al.*, 2011).
437 Moreover, Bai *et al.*, 2007 documented that the intake of BCE (5 mg daily, over 12
438 weeks) by 244 menopausal Chinese women (age, 40-60) reduced climacteric
439 symptoms such as hot flashes comparative to oral supplementation with the synthetic
440 steroid hormone tibolone (2.5 mg/day).

441 To elucidate the mechanism responsible for the BCE- and actein-associated
442 increased AD and T formation, inhibition of SULT2A1, the sulfotransferase
443 responsible for the sulfation of DHEA in MCF-7 cells (Falany *et al.*, 1989; Mueller
444 *et al.*, 2015; Licznarska *et al.*, 2017), was further investigated. Indeed, the presence
445 of BCE resulted in a moderate, concentration-dependent inhibition of DHEA
446 sulfation of up to 30.6%, while actein exerted more pronounced inhibition of up to
447 61.6% (**Fig. 5**). The low overall triterpene glycoside content in BCE (approximately
448 2.5%) may explain this discrepancy between BCE and purified actein.

449 After daily peroral dietary intake of BCE, actein and other BCE triterpene
450 glycosides should accumulate in human breast tissue in concentrations high enough
451 to inhibit DHEA sulfation. *In vitro* investigations by Disch *et al.* (2017) showed that
452 actein, the main constituent of BCE, easily permeates through Caco-2 monolayers,
453 suggesting high bioavailability *in vivo*. Indeed; the same authors demonstrated that
454 actein was absorbed in the duodenum, jejunum, ileum and colon of rats, which is in
455 line with earlier animal studies also describing high systemic levels following oral
456 administration in rats (Einbond *et al.*, 2009; Gai *et al.*, 2012) and Beagle dogs (Wang
457 *et al.*, 2012). To verify the interaction between BC extract and endogenous androgen
458 metabolism, future *in vivo* studies in females, monitoring the levels of actein as well

as conjugated and unconjugated steroids (DHEA-S, DHEA, AD and T) following BC extract supplementation, are therefore highly warranted.

5. Conclusions

The results of the present study demonstrate that BCE and actein inhibit the proliferation of ER α + MCF-7 and ER α - MDA-MB-231 human breast cancer cells. While BCE and actein do not alter the formation of estrogens in either cell line upon incubation with the hormone precursor E1, treatment of MCF-7 cells with BCE and actein inhibited the formation of DHEA-S via SULT2A1 at sub-micromolar concentrations, thereby increasing the levels of the androgens AD and T by up to 7-fold. This increase in androgen levels might contribute to the improvement of menopausal symptoms.

Conflict of interest

All authors declare no potential conflicts of interest concerning this article.

Funding

This research was supported by a grant from the Austrian Science Fund (FWF) awarded to WJ (grant no. I 3417-B31).

Author contributions

Conceptualization, S.P. and W.J.; most of the experiments, S.P.; LC-HRMS analyses, J.W. and D.D.; MCF-7 and MDA-MB-231 breast cancer cell culture, B.P. and S.J.B.; kinetic calculations, S.P.; writing – original draft preparation, S.P., T.T. and W.J.; writing – review and editing, S.P., T.T. and W.J.; visualization, S.P.; supervision, T.T. and W.J. All authors have read and agree to the published version of the manuscript.

482 **References**

- 483 Al-Akoum, M., Dodin, S., Akoum, A., 2007. Synergistic cytotoxic effects of
484 tamoxifen and black cohosh on MCF-7 and MDA-MB-231 human breast cancer
485 cells: an in vitro study. *Can. J. Physiol. Pharmacol.* 85, 1153-1159. doi:
486 10.1139/Y07-111.
- 487 Avula, B., Wang, Y.H., Smillie, T.J., Khan, I.A., 2009. Quantitative determination of
488 triterpenoids and formononetin in rhizomes of black cohosh (*Actaea racemosa*) and
489 dietary supplements by using UPLC-UV/ELS detection and identification by UPLC-
490 MS. *Planta Med.* 75, 381-386. doi: 10.1055/s-0028-1088384.
- 491 Bai, W., Henneicke-von Zepelin, H.H., Wang, S., Zheng, S., Liu, J., Zhang, Z.,
492 Geng, L., Hu, L., Jiao, C., Liske, E., 2007. Efficacy and tolerability of a medicinal
493 product containing an isopropanolic black cohosh extract in Chinese women with
494 menopausal symptoms: a randomized, double blind, parallel-controlled study versus
495 tibolone. *Maturitas* 58, 31-41. doi: 10.1016/j.maturitas.2007.04.009.
- 496 Beral, V., 2003. Million Women Study Collaborators, Breast cancer and hormone-
497 replacement therapy in the Million Women Study. *Lancet* 362, 419-427. doi:
498 10.1016/S0140-6736(03)14065-2.
- 499 Bodinet, C., Freudenstein, J., 2002. Influence of *Cimicifuga racemosa* on the
500 proliferation of estrogen receptor-positive human breast cancer cells. *Breast Cancer*
501 *Res. Treat.* 76, 1-10. doi: 10.1023/a:1020241509382.
- 502 Brasky, T.M., Lampe, J.W., Potter, J.D., Patterson, R.E., White, E., 2010. Specialty
503 supplements and breast cancer risk in the VITamins And Lifestyle (VITAL) Cohort.
504 *Cancer Epidemiol. Biomarkers Prev.* 19, 1696-1708. doi: 10.1158/1055-9965.EPI-
505 10-0318.
- 506 Chiba, A., Hoskin, T.L., Heins, C.N., Hunt, K.K., Habermann, E.B., Boughey, J.C.,
507 2017. Trends in Neoadjuvant Endocrine Therapy Use and Impact on Rates of Breast
508 conservation in Hormone Receptor-Positive Breast Cancer: A National Cancer Data
509 Base Study. *Ann. Surg. Oncol.* 24, 418-424. doi: 10.1245/s10434-016-5585-5.
- 510 Crone, M., Hallman, K., Lloyd, V., Szmyd, M., Badamo, B., Morse, M., Dinda, S.,
511 2019. The antiestrogenic effects of black cohosh on BRCA1 and steroid receptors in
512 breast cancer cells. *Breast Cancer (Dove Med Press)* 11, 99-110. doi:
513 10.2147/BCTT.S181730.
- 514 Disch, L., Forsch, K., Siewert, B., Drewe, J., Fricker, G., 2017. In Vitro and In Situ
515 Characterization of Triterpene Glycosides From *Cimicifuga racemosa* Extract. *J.*
516 *Pharm. Sci.* 106, 3642-3650. doi: 10.1016/j.xphs.2017.07.023.
- 517 Eagon, C.L., Elm, M.S., Teepe, A.G., Eagon, P.K., 1997. Medicinal botanicals:
518 Estrogenicity in rat uterus and liver. *Proceeding of the American Association for*
519 *Cancer Research* 38, 293.
- 520 Einbond, L.S., Shimizu, M., Xiao, D., Nuntanakorn, P., Lim, J.T., Suzui, M., Seter,
521 C., Pertel, T., Kennelly, E.J., Kronenberg, F., Weinstein, I.B., 2004. Growth
522 inhibitory activity of extracts and purified components of black cohosh on human
523 breast cancer cells. *Breast Cancer Res. Treat.* 83, 221-231. doi:
524 10.1023/B:BREA.0000014043.56230.a3.

- Einbond, L.S., Shimizu, M., Nuntanakorn, P., Seter, C., Cheng, R., Jiang, B., Kronenberg, F., Kennelly, E.J., Weinstein, I.B., 2006. Actein and a fraction of black cohosh potentiate antiproliferative effects of chemotherapy agents on human breast cancer cells. *Planta Med.* 72, 1200-1206. doi: 10.1055/s-2006-947225.
- Einbond, L.S., Soffritti, M., Esposti, D.D., Park, T., Cruz, E., Su, T., Wu, H.A., Wang, X., Zhang, Y.J., Ham, J., Goldberg, I.J., Kronenberg, F., *et al.*, 2009. Actein activates stress- and statin-associated responses and is bioavailable in Sprague-Dawley rats. *Fundam. Clin. Pharmacol.* 23, 311-321. doi: 10.1111/j.1472-8206.2009.00673.x.
- Falany, C.N., Vazquez, M.E., Kalb, J.M., 1989. Purification and characterization of human liver dehydroepiandrosterone sulphotransferase. *Biochem. J.* 260, 641-646. doi: 10.1042/bj2600641.
- Folkerd, E., Dowsett, M., 2013. Sex hormones and breast cancer risk and prognosis. *Breast* 22 (Suppl. 2), 38-43. doi: 10.1016/j.breast.2013.07.007.
- Frei-Kleiner, S., Schaffner, W., Rahlfs, V.W., Bodmer, C., Birkhauser, M., 2005. *Cimicifuga racemosa* dried ethanolic extract in menopausal disorders: a double-blind placebo-controlled clinical trial. *Maturitas* 51, 397-404. doi: 10.1016/j.maturitas.2004.10.003.
- Freudenstein, J., Dasenbrock, C., Nisslein, T., 2002. Lack of promotion of estrogen-dependent mammary gland tumors in vivo by an isopropanolic *Cimicifuga racemosa* extract. *Cancer Res.* 62, 3448-3452.
- Gai, Y.Y., Liu, W.H., Sha, C.J., Wang, Y.L., Sun, Y.T., Li, X.J., Fawcett, P.J., Gu, J.K., 2012. Pharmacokinetics and bioavailability of cimicifugosides after oral administration of *Cimicifuga foetida* L. extract to rats. *J. Ethnopharmacol.* 143, 249-255. doi: 10.1016/j.jep.2012.06.031.
- Garrido Oyarzún, M.F., Castelo-Branco, C., 2017. Use of hormone therapy for menopausal symptoms and quality of life in breast cancer survivors. Safe and ethical? *Gynecol. Endocrinol.* 33, 10-15. doi: 10.1080/09513590.2016.1247798.
- Gaube, F., Wolfl, S., Pusch, L., Kroll, T.C., Hamburger, M., 2007. Gene expression profiling reveals effects of *Cimicifuga racemosa* (L.) NUTT. (black cohosh) on the estrogen receptor positive human breast cancer cell line MCF-7. *BMC Pharmacol.* 7, 11. doi: 10.1186/1471-2210-7-11.
- Glaser, R., York, A.E., Dimitrakakis, C., 2011. Beneficial effects of testosterone therapy in women measured by the validated Menopause Rating Scale (MRS). *Maturitas* 68, 355-361. doi: 10.1016/j.maturitas.2010.12.001.
- Henneicke-von Zepelin, H.H., Meden, H., Kostev, K., Schröder-Bernhardi, D., Stammwitz, U., Becher, H., 2007. Isopropanolic black cohosh extract and recurrence-free survival after breast cancer. *Int. J. Clin. Pharmacol. Ther.* 45, 143-154. doi: 10.5414/cpp45143.
- Hickey, M., Saunders, C.M., Stuckey, B.G., 2005. Management of menopausal symptoms in patients with breast cancer: an evidence-based approach. *Lancet Oncol.* 6, 687-695. doi: 10.1016/S1470-2045(05)70316-8.
- Hirschberg, A.L., Edlund, M., Svane, G., Azavedo, E., Skoog, L., von Schoultz, B., 2007. An isopropanolic extract of black cohosh does not increase mammographic

- 569 breast density or breast cell proliferation in postmenopausal women. *Menopause* 14,
570 89-96. doi: 10.1097/01.gme.0000230346.20992.34.
- 571 Licznarska, B., Szafer, H., Wierchowski, M., Sobierajska, H., Baer-Dubowska,
572 W., 2017. Resveratrol and its methoxy derivatives modulate the expression of
573 estrogen metabolism enzymes in breast epithelial cells by AhR down-regulation.
574 *Mol. Cell. Biochem.* 425, 169-179. doi: 10.1007/s11010-016-2871-2.
- 575 Liu, Z.P., Yu, B., Huo, J.S., Lu, C.Q., Chen, J.S., 2001. Estrogenic Effects of
576 *Cimicifuga racemosa* (Black Cohosh) in Mice and on Estrogen Receptors in MCF-7
577 Cells. *J. Med. Food* 4, 171-178. doi: 10.1089/109662001753165756.
- 578 Lundström, E., Hirschberg, A.L., Söderqvist, G., 2011. Digitized assessment of
579 mammographic breast density--effects of continuous combined hormone therapy,
580 tibolone and black cohosh compared to placebo. *Maturitas* 70, 361-364. doi:
581 10.1016/j.maturitas.2011.08.009.
- 582 McKenna, D.J., Jones, K., Humphrey, S., Hughes, K., 2001. Black cohosh: efficacy,
583 safety, and use in clinical and preclinical applications. *Altern. Ther. Health Med.* 7,
584 93-100.
- 585 Merchant, S., Stebbing, J., 2015. Black cohosh, hot flushes, and breast cancer.
586 *Lancet Oncol.* 16, 137-138. doi: 10.1016/S1470-2045(15)70041-0.
- 587 Mueller, J.W., Gilligan, L.C., Idkowiak, J., Arlt, W., Foster, P.A., 2015. The
588 regulation of steroid action by sulfation and desulfation. *Endocr. Rev.* 36, 526-563.
589 doi: 10.1210/er.2015-1036.
- 590 Obi, N., Chang-Claude, J., Berger, J., Braendle, W., Slanger, T., Schmidt, M.,
591 Steindorf, K., Ahrens, W., Flesch-Janys, D., 2009. The use of herbal preparations to
592 alleviate climacteric disorders and risk of postmenopausal breast cancer in a German
593 case-control study. *Cancer Epidemiol. Biomarkers Prev.* 18, 2207-2213. doi:
594 10.1158/1055-9965.EPI-09-0298.
- 595 Øverlie, I., Moen, M.H., Holte, A., Finset, A., 2002. Androgens and estrogens in
596 relation to hot flushes during the menopausal transition. *Maturitas* 41, 69-77.
597 doi:10.1016/s0378-5122(01)00256-0.
- 598 Park, J., Shim, M., Rhyu, M.R., Lee, Y., 2012. Estrogen receptor mediated effects of
599 *Cimicifuga* extracts on human breast cancer cells. *Pharmazie* 67, 947-950.
- 600 Poschner, S., Zehl, M., Maier-Salamon, A., Jäger, W., 2017. Simultaneous
601 quantification of estrogens, their precursors and conjugated metabolites in human
602 breast cancer cells by LC-HRMS without derivatization. *J. Pharm. Biomed. Anal.*
603 138, 344-350. doi: 10.1016/j.jpba.2017.02.033.
- 604 Poschner, S., Maier-Salamon, A., Zehl, M., Wackerlig, J., Dobusch, D.,
605 Meshcheryakova, A., Mechtcheriakova, D., Thalhammer, T., Pachmann, B., Jäger,
606 W., 2018. Resveratrol Inhibits Key Steps of Steroid Metabolism in a Human
607 Estrogen-Receptor Positive Breast Cancer Model: Impact on Cellular Proliferation.
608 *Front. Pharmacol.* 9, 742. doi: 10.3389/fphar.2018.00742.
- 609 Raus, K., Brucker, C., Gorkow, C., Wuttke, W., 2006. First-time proof of
610 endometrial safety of the special black cohosh extract (*Actaea* or *Cimicifuga*
611 *racemosa* extract) CR BNO 1055. *Menopause* 13, 678-691. doi:
612 10.1097/01.gme.0000196813.34247.e2.

- 613 Reed, S.D., Newton, K.M., LaCroix, A.Z., Grothaus, L.C., Grieco, V.S., Ehrlich, K.,
614 2008. Vaginal, endometrial, and reproductive hormone findings: randomized,
615 placebo-controlled trial of black cohosh, multibotanical herbs, and dietary soy for
616 vasomotor symptoms: the Herbal Alternatives for Menopause (HALT) Study.
617 Menopause 15, 51-58.
- 618 Szmyd, M., Lloyd, V., Hallman, K., Aleck, K., Mladenovik, V., McKee, C., Morse,
619 M., Bedgood, T., Dinda, S., 2018. The effects of black cohosh on the regulation of
620 estrogen receptor (ER α) and progesterone receptor (PR) in breast cancer cells. Breast
621 Cancer (Dove Med Press) 10, 1-11. doi: 10.2147/BCTT.S144865.
- 622 Takei, H., Suemasu, K., Inoue, K., Saito, T., Okubo, K., Koh, J., Sato, K., Tsuda, H.,
623 Kurosumi, M., Tabei, T., Saitama Breast Cancer Clinical Study Group, 2008.
624 Multicenter phase II trial of neoadjuvant exemestane for postmenopausal patients
625 with hormone receptor-positive, operable breast cancer: Saitama Breast Cancer
626 Clinical Study Group (SBCCSG-03). Breast Cancer Res. Treat. 107, 87-94.
627 doi:10.1007/s10549-007-9529-4.
- 628 United States Pharmacopeial Convention Inc., 2019. USP 42 - NF 37 The United
629 States Pharmacopeia and National Formulary 2019. Deutscher Apotheker Verlag,
630 Stuttgart, Germany. ISBN-13: 978-3769273304.
- 631 Wang, Y., Sha, C., Liu, W., Gai, Y., Zhang, H., Qu, H., Wang, W., 2012.
632 Simultaneous determination of cimicifugoside H-2, cimicifugoside H-1, 23-epi-26-
633 deoxyactein, cimigenol xyloside and 25-O-acetylcimigenoside in beagle dog plasma
634 by LC-MS/MS. J. Pharm. Biomed. Anal. 62, 87-95. doi: 10.1016/j.jpba.2011.11.029.
- 635 Wuttke, W., Gorkow, C., Seidlová-Wuttke, D., 2006. Effects of black cohosh
636 (*Cimicifuga racemosa*) on bone turnover, vaginal mucosa, and various blood
637 parameters in postmenopausal women: a double-blind, placebo-controlled, and
638 conjugated estrogens-controlled study. Menopause 13, 185-196. doi:
639 10.1097/01.gme.0000174470.44822.57.
- 640 Zhou, D., Wang, J., Chen, E., Murai, J., Siiteri, P., Chen, S., 1993. Aromatase gene is
641 amplified in MCF-7 human breast cancer cells. J. Steroid Biochem. Mol. Biol. 46,
642 147-153. doi: 10.1016/0960-0760(93)90289-9.
- 643

644 **Figure legends**

645 **Fig. 1. Impact of black cohosh extract (BCE) and actein on ER α + and ER α -**
646 **breast cancer cell proliferation.** MCF-7 (ER α +) and MDA-MB-231 (ER α -) breast
647 cancer cells were treated for 48 h with increasing concentrations of BCE (0-25
648 μ g/ml) in the **(A)** absence and **(B)** presence of estrone (E1, 100 nM) as a hormone
649 precursor. Furthermore, cells were treated with increasing concentrations of actein
650 (0-50 μ M) in the **(C)** absence and **(D)** presence of E1 (100 nM) for 48 h. All data
651 represent the means \pm SD of three independent experiments. *P<0.05 vs. untreated
652 control samples.

653 **Fig. 2. Patterns of steroid biotransformation rates in MCF-7 and MDA-MB-231**
654 **cells in the presence and absence of black cohosh extract (BCE).** **(A)** MCF-7 and
655 **(B)** MDA-MB-231 cells were incubated with 100 nM estrone (E1) for 48 h in the
656 absence and presence of 25 μ g/ml BCE. **(C)** MCF-7 and **(D)** MDA-MB-231 cells
657 were incubated with 100 nM dehydroepiandrosterone (DHEA) for 48 h in the
658 presence and absence of 25 μ g/ml BCE. All data represent the means \pm SD of three
659 independent experiments. *P<0.05. E1-S, estrone-3-*O*-sulfate; E2, 17 β -estradiol; E2-
660 S, 17 β -estradiol-3-*O*-sulfate; E2-G, 17 β -estradiol-3-*O*-(β -D-glucuronide); E3, estriol;
661 DHEA-S, DHEA-3-*O*-sulfate.

662 **Fig. 3. Inhibition of dehydroepiandrosterone (DHEA) sulfation in MCF-7 cells**
663 **following actein administration.** **(A)** MCF-7 cells were incubated with 100 nM
664 DHEA as a hormone precursor, in the absence or presence of 0-10 μ M actein for 48
665 h, and the formation of dehydroepiandrosterone-3-*O*-sulfate (DHEA-S) was
666 determined. Subsequently, the kinetics of DHEA sulfation were calculated following
667 incubation with DHEA (0-100 nM) and actein (0-10 μ M) for 48 h. Data are

presented as **(B)** Lineweaver-Burk and **(C)** Dixon plots. All data represent the means \pm SD of three independent experiments. *P<0.05 vs. untreated control samples.

Fig. 4. Increased androgen levels in MCF-7 cells in the presence of actein. MCF-7 cells were incubated with 100 nM dehydroepiandrosterone (DHEA) as a hormone precursor, in the absence or presence of 0-10 μ M actein for 48 h, and the formation rates of **(A)** 4-androstene-3,17-dione (AD) and **(B)** testosterone (T) were subsequently determined. Formation kinetics for **(C)** AD and **(D)** T were calculated after incubating the cells with DHEA (0-100 nM) and actein (0-10 μ M), and are reported as Lineweaver-Burk plots. All data represent the means \pm SD of three independent experiments. *P<0.05 vs. untreated control samples.

Fig. 5. Inhibition of recombinant human sulfotransferase 2A1 (SULT2A1) by black cohosh extract (BCE) and actein. Recombinant SULT2A1 (2.4 μ g/ml) was incubated at 37°C with increasing concentrations of dehydroepiandrosterone (DHEA) as a substrate (0-100 nM) and **(A-B)** BCE (0-25 μ g/ml) or **(C-D)** actein (0-25 μ M) as inhibitors for 15 min. Data are shown as concentration-dependent inhibition curves and the corresponding Dixon plots. All data represent the means \pm SD of three independent experiments.

Fig. 6. Interaction between black cohosh extract (BCE) and the metabolism of steroid hormones in MCF-7 breast cancer cells. BCE inhibits the formation of dehydroepiandrosterone-3-O-sulfate (DHEA-S) via sulfotransferase 2A1 (SULT2A1) in a dose-dependent manner, thereby increasing the concentrations of the unconjugated androgens 4-androstene-3,17-dione (AD) and testosterone (T). DHEA, dehydroepiandrosterone; E1, estrone; E1-S, estrone-3-O-sulfate; E2, 17 β -estradiol; E2-S, 17 β -estradiol-3-O-sulfate; E2-G, 17 β -estradiol-3-O-(β -D-glucuronide); E3, estriol.

Table 1: Formation rates of dehydroepiandrosterone (DHEA) metabolites by MCF-7 and MDA-MB-231 cells in the presence and absence of black cohosh extract (BCE).

BCE	MCF-7 (fmol/10 ⁶ cells/h)		MDA-MB-231 (fmol/10 ⁶ cells/h)			
	DHEA-S	AD	T	DHEA-S	AD	T
0 µg/ml	837.7 ± 71.9	77.1 ± 5.1	5.75 ± 0.19	0.86 ± 0.12	841.9 ± 88.0	60.8 ± 5.7
1 µg/ml	836.1 ± 36.8	88.8 ± 7.7	5.66 ± 0.24	0.67 ± 0.11	915.0 ± 41.0	61.7 ± 2.2
5 µg/ml	762.7 ± 25.5	100.4 ± 7.4*	7.32 ± 0.38*	0.64 ± 0.11	908.5 ± 96.0	63.6 ± 10.2
10 µg/ml	695.8 ± 24.2*	108.8 ± 5.8*	8.40 ± 0.41*	0.62 ± 0.15	891.3 ± 21.8	61.9 ± 4.7
25 µg/ml	663.0 ± 18.3*	117.2 ± 11.0*	9.08 ± 0.44*	0.83 ± 0.09	862.0 ± 47.9	60.8 ± 5.6

Formation rates were determined by LC-HRMS following cellular incubation with DHEA (100 nM) as a hormone precursor, and increasing concentrations of BCE (0-25 µg/ml) for 48 h. All data represent the means ± SD of three independent experiments. Values in bold and marked with an asterisk (*) are significantly different in comparison to the control values (P<0.05). DHEA-S, DHEA-3-O-sulfate; AD, 4-androstene-3,17-dione; T, testosterone.

Table 2: Kinetic parameters of dehydroepiandrosterone (DHEA) metabolism by MCF-7 cells in the presence and absence of

actein.

Actein	K _m (nM)		V _{max} (fmol/10 ⁶ cells/h)			
	DHEA-S	AD	T	DHEA-S	AD	T
0 μ M	240.3 \pm 13.3	120.1 \pm 18.5	105.9 \pm 12.2	2808.3 \pm 117.6	144.6 \pm 13.8	9.6 \pm 0.7
0.5 μ M	249.2 \pm 8.0	113.1 \pm 27.2	100.6 \pm 15.8	1586.8 \pm 39.0*	278.6 \pm 40.7*	14.1 \pm 1.3*
1.0 μ M	241.2 \pm 49.4	112.6 \pm 12.0	103.2 \pm 17.5	1030.0 \pm 159.5*	342.3 \pm 22.1*	22.4 \pm 2.2*
2.5 μ M	245.0 \pm 13.7	119.9 \pm 32.5	103.5 \pm 7.6	535.1 \pm 22.6*	411.4 \pm 72.2*	34.3. \pm 1.5*
5.0 μ M	250.9 \pm 19.0	110.2 \pm 29.2	102.4 \pm 6.1	301.2 \pm 17.4*	629.8 \pm 100.5*	44.3. \pm 1.5*
10.0 μ M	248.5 \pm 35.4	110.9 \pm 22.5	105.1 \pm 5.9	157.6 \pm 17.1*	1175.9 \pm 143.8*	71.2 \pm 2.4*

Kinetic parameters were calculated using GraphPad Prism 6.0 software following the incubation of MCF-7 cells with DHEA (0-100

nM) as a hormone precursor, and increasing concentrations of actein (0-10 μ M) for 48 h. All data represent the means \pm SD of three

independent experiments. Values in bold and marked with an asterisk (*) are significantly different in comparison to the control values

(P<0.05). DHEA-S, DHEA-3-O-sulfate; AD, 4-androstene-3,17-dione; T, testosterone.

Fig. 1.

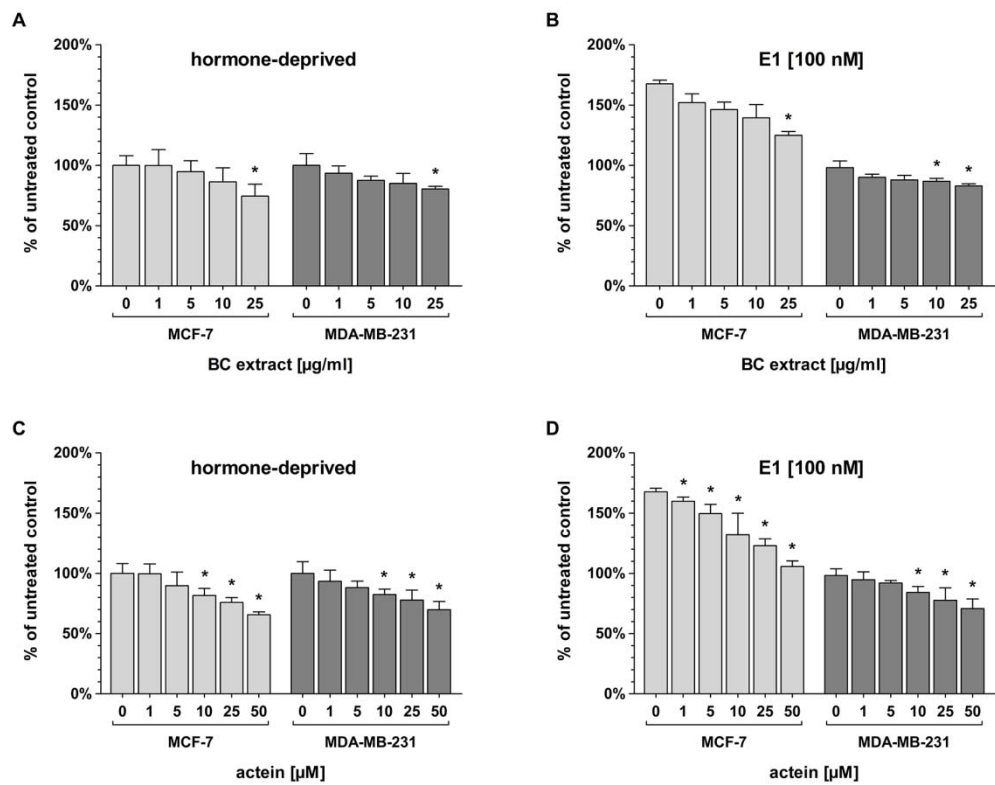


Fig. 2.

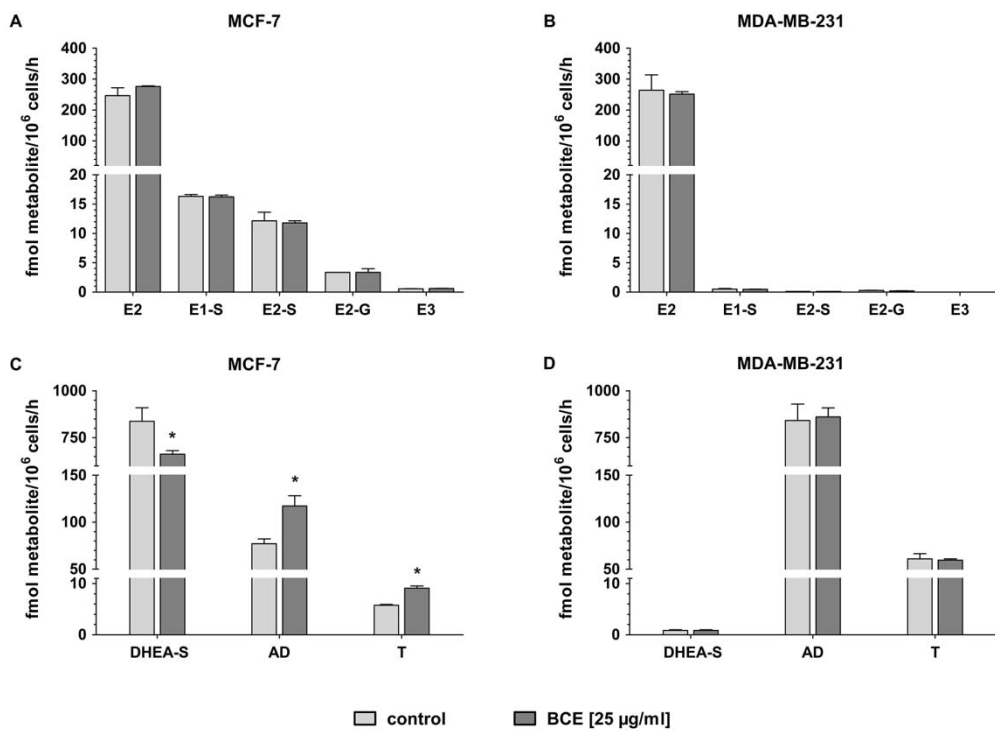


Fig. 3.

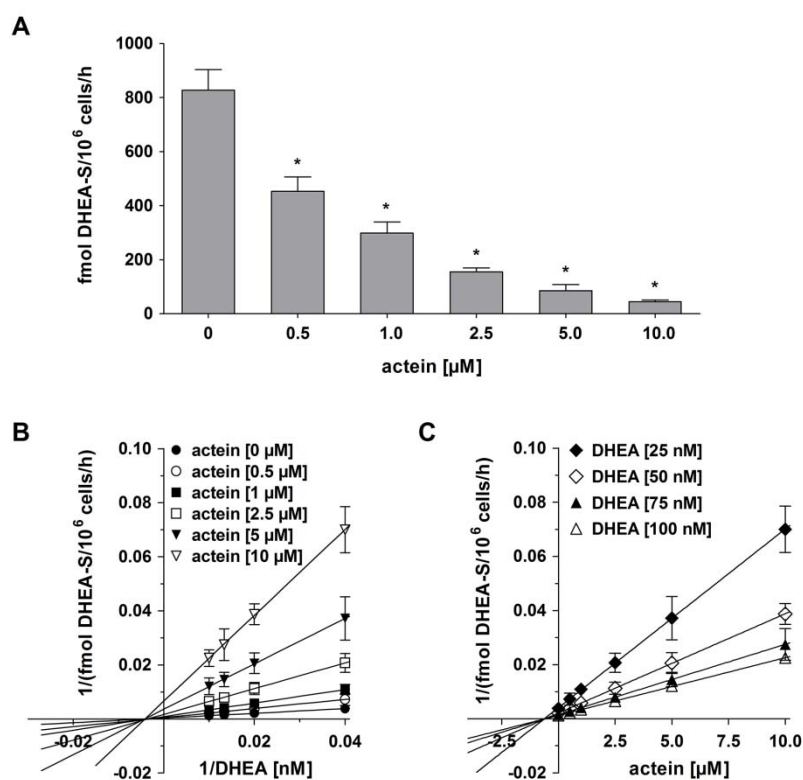


Fig. 4.

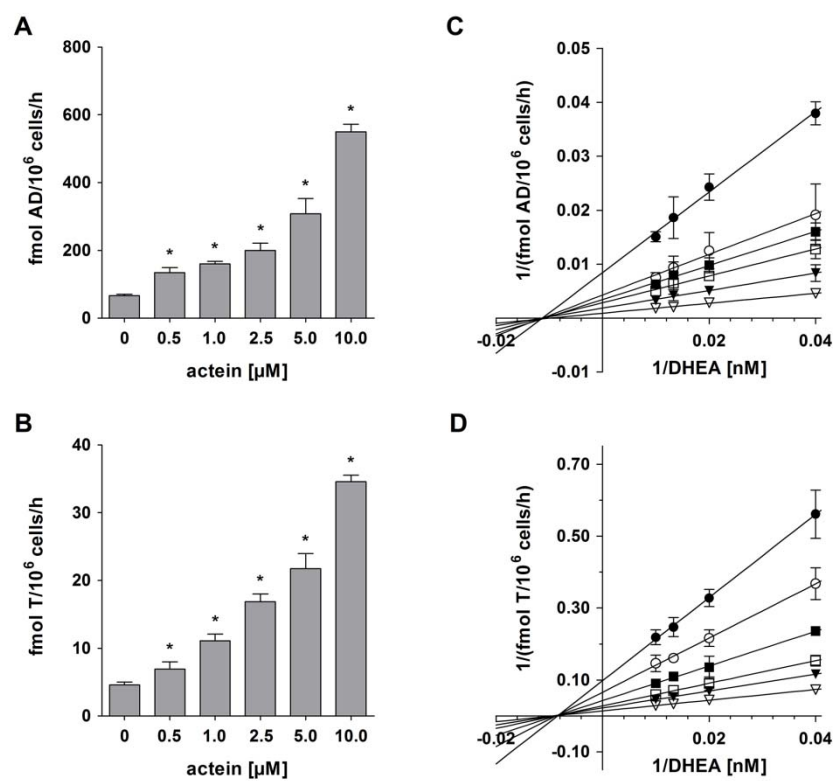


Fig. 5.

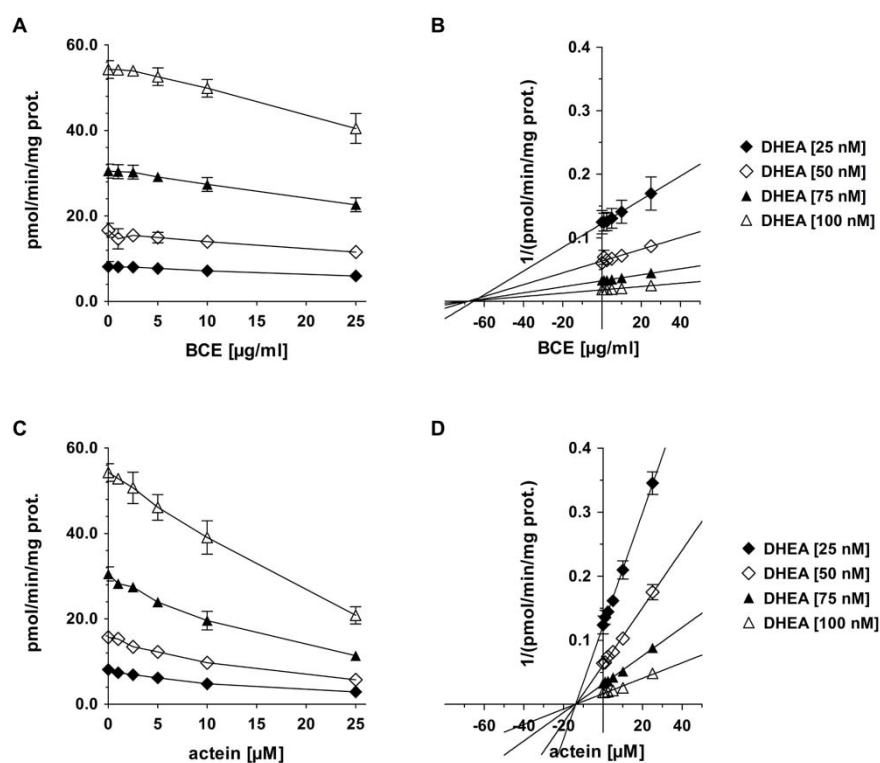
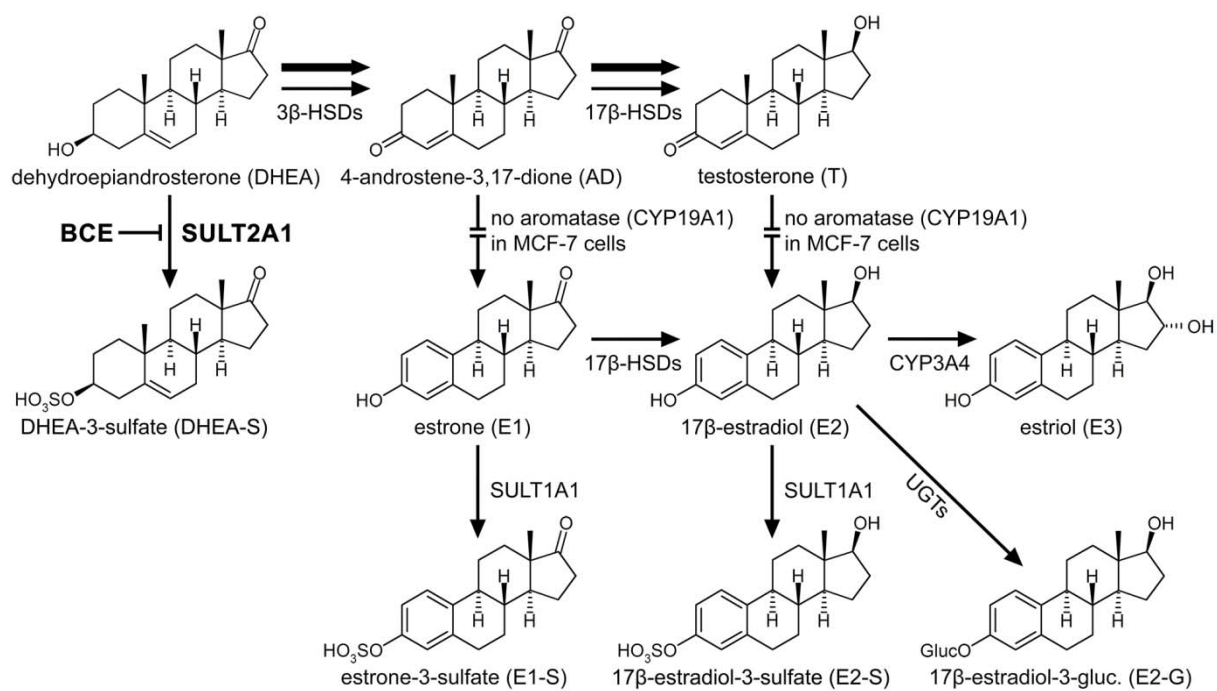


Fig. 6.



CHAPTER VII

METABOLISM OF ESTROGENS: TURNOVER DIFFERS BETWEEN PLATINUM-SENSITIVE AND -RESISTANT HIGH-GRADE SEROUS OVARIAN CANCER CELLS

Authors:

Stefan Poschner, Judith Wackerlig, Dan C. Castillo-Tong, Andrea Wolf,
Isabel van der Decken, Tea L. Rižner, Renata Pavlič, Anastasia Meshcheryakova,
Diana Mechtcheriakova, Monika Fritzer-Szekeres, Theresia Thalhammer and
Walter Jäger



Published in:

Cancers (Basel) **2020**, *12*, pii: E279

doi: 10.3390/cancers12020279

Article

Metabolism of Estrogens: Turnover Differs between Platinum-Sensitive and -Resistant High-Grade Serous Ovarian Cancer Cells

Stefan Poschner ¹, Judith Wackerlig ², Dan Cacsire Castillo-Tong ³, Andrea Wolf ³, Isabel von der Decken ³, Tea Lanišnik Rižner ⁴, Renata Pavlič ⁴ , Anastasia Meshcheryakova ⁵, Diana Mechtcheriakova ⁵ , Monika Fritzer-Szekeres ⁶, Theresia Thalhammer ⁵ and Walter Jäger ^{1,7,*}

- ¹ Division of Clinical Pharmacy and Diagnostics, Department of Pharmaceutical Chemistry, University of Vienna, 1090 Vienna, Austria; stefan.poschner@univie.ac.at
- ² Division of Drug Design and Medicinal Chemistry, Department of Pharmaceutical Chemistry, University of Vienna, 1090 Vienna, Austria; judith.wackerlig@univie.ac.at
- ³ Translational Gynecology Group, Department of Obstetrics and Gynecology, Comprehensive Cancer Center, Medical University of Vienna, 1090 Vienna, Austria; dan.cacsire-castillo@meduniwien.ac.at (D.C.C.-T.); andrea.wolf@meduniwien.ac.at (A.W.); isabel.vonderdecken@meduniwien.ac.at (I.v.d.D.)
- ⁴ Institute of Biochemistry, Faculty of Medicine, University of Ljubljana, 1000 Ljubljana, Slovenia; tea.lanisnik-rizner@mf.uni-lj.si (T.L.R.); renata.pavlic@mf.uni-lj.si (R.P.)
- ⁵ Department of Pathophysiology and Allergy Research, Center for Pathophysiology, Infectiology and Immunology, Medical University of Vienna, 1090 Vienna, Austria; anastasia.meshcheryakova@meduniwien.ac.at (A.M.); diana.mechtcheriakova@meduniwien.ac.at (D.M.); theresia.thalhammer@meduniwien.ac.at (T.T.)
- ⁶ Department of Medical and Chemical Laboratory Diagnostics, Medical University of Vienna, 1090 Vienna, Austria; monika.fritzer-szekeres@meduniwien.ac.at
- ⁷ Vienna Metabolomics Center (VIME), University of Vienna, 1090 Vienna, Austria
- * Correspondence: walter.jaeger@univie.ac.at; Tel.: (+43)-1-4277-55576

Received: 9 December 2019; Accepted: 21 January 2020; Published: 23 January 2020



Abstract: High-grade serous ovarian cancer (HGSOC) is currently treated with cytoreductive surgery and platinum-based chemotherapy. The majority of patients show a primary response; however, many rapidly develop drug resistance. Antiestrogens have been studied as low toxic treatment options for HGSOC, with higher response rates in platinum-sensitive cases. Mechanisms for this difference in response remain unknown. Therefore, the present study investigated the impact of platinum resistance on steroid metabolism in six established HGSOC cell lines sensitive and resistant against carboplatin using a high-resolution mass spectrometry assay to simultaneously quantify the ten main steroids of the estrogenic metabolic pathway. An up to 60-fold higher formation of steroid hormones and their sulfated or glucuronidated metabolites was observed in carboplatin-sensitive cells, which was reversible by treatment with interleukin-6 (IL-6). Conversely, treatment of carboplatin-resistant cells expressing high levels of endogenous IL-6 with the monoclonal anti-IL-6R antibody tocilizumab changed their status to “platinum-sensitive”, exhibiting a decreased IC₅₀ value for carboplatin, decreased growth, and significantly higher estrogen metabolism. Analysis of these metabolic differences could help to detect platinum resistance in HGSOC patients earlier, thereby allowing more efficient interventions.

Keywords: high-grade serous ovarian cancer; steroid hormones; metabolomics; LC-HRMS; carboplatin resistance; interleukin-6

1. Introduction

Epithelial ovarian cancer (EOC), the most lethal type of gynecological cancer, is the fourth leading cause of cancer-associated mortality among women in the USA and Europe [1,2]. Although the total incidence in 2018 was relatively low with 300,000 new cases worldwide, its fatality rate is high, as the number of deaths was almost 200,000 in the same year [3]. The most frequent form of EOC, accounting for almost 75% of all cases, is high-grade serous ovarian cancer (HGSOC), an aggressive subtype that shows only a 30% to 40% five-year survival rate for all patients [4–6].

Cytoreductive debulking surgery and platinum-based chemotherapy is the standard for HGSOC treatment [7,8]. However, although most patients demonstrate a good primary response, the majority (80% to 90%) relapses and develops drug resistance within one year [9]. Novel therapeutic approaches with targeted therapeutics, including poly(ADP-ribose)-polymerase 1 (PARP) and vascular endothelial growth factor (VEGF) inhibitors can increase cytotoxic activity and apoptosis in platinum-resistant HGSOC when given in combination with cisplatin or carboplatin [10]. However, not all HGSOC patients are sensitive to PARP and VEGF inhibitors [11]. Moreover, the majority of patients are likely to develop drug resistance against these targeted therapies [12]. Therefore, women diagnosed with recurrent platinum-resistant HGSOC have a poor survival rate, often fewer than 12 months [13]. Improving the therapeutic outcome by preventing drug resistance as long as possible requires the use of alternative treatment strategies. Preclinical studies have shown that estrogens can promote the proliferation of ovarian cancer cells lines and fuel tumor growth in mouse xenograft models [14], which is partly blocked by antiestrogens. Therefore, the use of endocrine disrupting agents in HGSOC could be promising [15]. Indeed, treatment of women with recurrent HGSOC using the antiestrogen tamoxifen or the aromatase inhibitor letrozole resulted in response rates between 10% and 15% and disease stabilization rates of 30% to 40% [16].

Clinical studies have demonstrated that the overall response rate of an endocrine therapy is significantly higher in platinum-sensitive cases as compared with platinum-resistant HGSOC patients (55% vs. 40%) [17], independent of the estrogen receptor alpha (ER α) status of the tumor [18]. Mechanisms for these different response rates of antiestrogens against platinum-sensitive and -resistant HGSOC cells remain unknown. In vitro data reported by Ren et al. [19] indicate altered cellular steroid metabolism, as estrone (E1) is differentially metabolized in normal human ovarian surface epithelium as compared with epithelial ovarian cancer cells SKOV-3 and PEO-1, with higher sulfation rates of E1 and 17 β -estradiol (E2) in the noncancerous ovarian surface epithelium cells. Recent studies have also demonstrated that HGSOC cells should be able to inactivate estrogens, as sulfotransferase 1E1 (SULT1E1), a key enzyme responsible for the sulfation of E1, E2, and dehydroepiandrosterone (DHEA), was detected in tumor sections from 137 HGSOC patients by immunohistochemical staining. Notably, multivariate Cox regression analysis revealed that SULT1E1 abundance is a significant predictor for overall survival, as sulfated metabolites exhibit no or only minimal estrogenic activity [20].

How estrogens are metabolized in HGSOC cells and whether platinum resistance affects the formation rates of biotransformation products, particularly that of the most potent estrogen E2, remains unknown. Therefore, the present study simultaneously quantified for the first time the metabolism of the ten major steroids of the estrogenic pathway in HGSOC cell lines sensitive and resistant against carboplatin. Using a validated liquid chromatography high-resolution mass spectrometry (LC-HRMS) assay [21], we were able to selectively determine the levels of precursor steroids, active estrogens, and sulfated or glucuronidated conjugates, which should then be correlated with the platinum sensitivity of the respective cell lines. Furthermore, we screened all six cell lines for endogenous interleukin-6 (IL-6) formation, as IL-6 treatment of A2780 ovarian cancer cells was shown to induce platinum resistance [22]. IL-6 was also described as a marker for platinum resistance in 32 EOC patients [23,24], and elevated levels of IL-6 in the serum and ascites of ovarian cancer patients at the time of diagnosis correlated with a poor initial response to chemotherapy and poor prognosis [25]. Such comprehensive analysis holds promise for a better understanding of drug-resistance mechanisms in HGSOC, which could allow earlier and more efficient interventions for this lethal cancer subtype.

2. Results

2.1. Characterization of the Investigated HGSOC Cell Lines

As criteria for HGSOC, all six investigated cell lines produce high levels of p53 and PAX8 and carry a mutation in *TP53*. The 13914_1 cell line has an additional mutation in *BRCA1*, the OVSAHO cells in *BRCA2*, and the Kuramochi cells in *BRCA2* and *KRAS*. *EGFR/ERBB2* was strongly expressed in all cell lines. A moderate/high expression of *ESR1* and *AR* was only seen in 13699 cells and in Kuramochi cells, whereas a moderate expression of *ESRRG* was found in 13363 and Kuramochi cells. Expression of *ESR2* and *PGR* was low in all six investigated cell lines. All relevant mutations and gene expressions are given in detail in Tables S1 and S2. To classify all cell lines as “platinum-sensitive” or “platinum-resistant”, their respective IC_{50} values against carboplatin were determined over a concentration range of 0–50 μ M for 72 h. As shown in Figure 1, 13363 and 13699 cells were highly sensitive to carboplatin with IC_{50} values of 2.8 ± 0.4 and 3.4 ± 0.3 μ M, respectively. 13914_1, 15233, Kuramochi, and OVSAHO cells demonstrated three to five times higher IC_{50} values (11.8 ± 2.6 , 14.9 ± 2.8 , 12.0 ± 1.9 , and 9.4 ± 2.0 μ M, respectively), and therefore were classified as “platinum-resistant”.

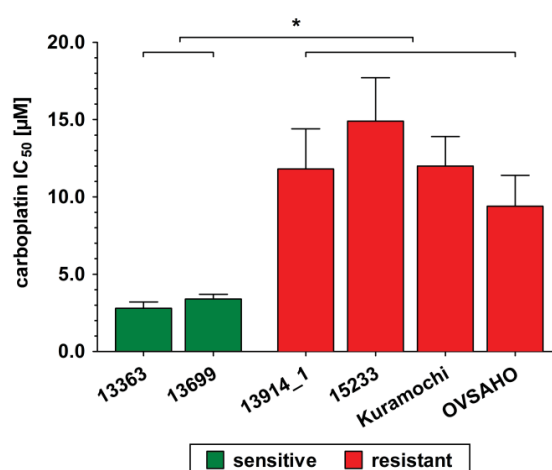


Figure 1. Sensitivity of all investigated high-grade serous ovarian cancer (HGSOC) cell lines in response to carboplatin. Cells were incubated in the presence of increasing carboplatin concentrations (0 to 50 μ M) for 72 h and the remaining viable cells were determined using a CASY® TT cell counter. Green color indicates sensitivity and red color indicates resistance against carboplatin to the respective cell line. All data are presented as the means \pm SD of three independent experiments. * $p < 0.05$.

2.2. DHEA Metabolism by Platinum-Sensitive and -Resistant HGSOC Cells

To investigate the biotransformation of steroids in relation to platinum resistance, all six cell lines were incubated with DHEA (500 nM) and the formation of the nine major human metabolites, namely dehydroepiandrosterone-3-sulfate (DHEA-S); 4-androstene-3,17-dione (AD); testosterone (T); E1, E2, estriol (E3; 16α -hydroxy- 17β -estradiol); estrone-3-sulfate (E1-S); 17β -estradiol-3-sulfate (E2-S); and 17β -estradiol-3-O-(β -D-glucuronide) (E2-G) was quantified using a previously validated LC-HRMS assay [21]. Control samples containing dimethylsulfoxide (DMSO) only were also performed to ensure that there was no endogenous steroid formation. After adding 500 nM DHEA, the three biotransformation products DHEA-S, AD, and T could be quantified in addition to parent DHEA in the cellular supernatants (Figure 2). Other biotransformation products could not be detected, indicating no aromatase (CYP19A1) activity. Indeed, *CYP19A1* expression was near the lower limit of detection (LLOQ) in all six cell lines (Section 4.3).

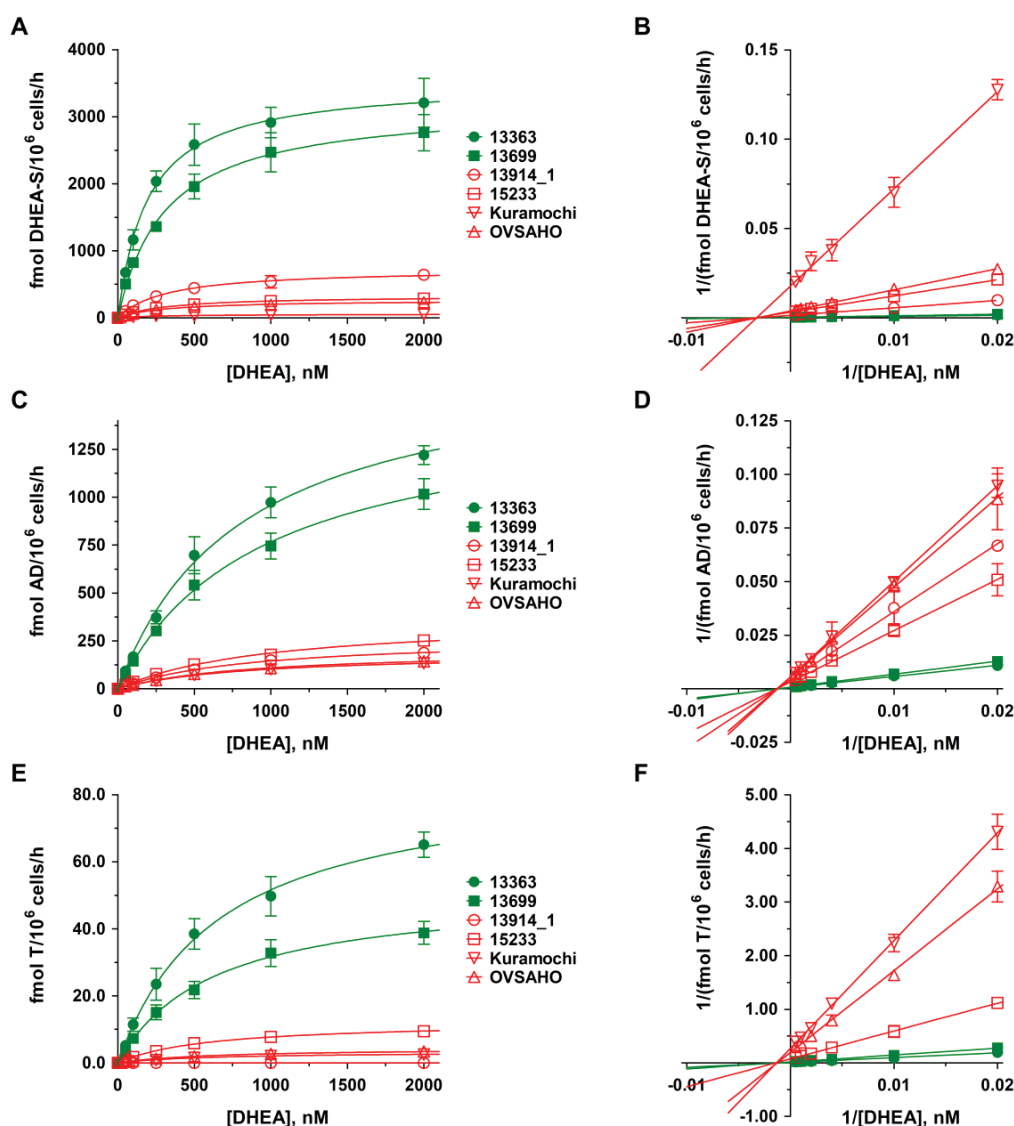


Figure 2. Kinetic profiles of dehydroepiandrosterone (DHEA) metabolite formation in platinum-sensitive and -resistant HGSOc cells. The kinetics of (A–B) DHEA sulfation, (C–D) AD formation, and (E–F) T formation were calculated following the incubation of all HGSOc cell lines with 0 to 2000 nM DHEA as a hormone precursor for 48 h. Data are displayed as Michaelis–Menten and Lineweaver–Burk plots and represent the means \pm SD of three independent experiments. Green curves indicate sensitivity and red curves indicate resistance against carboplatin to the investigated HGSOc cell lines. Differences were statistically significant between these two groups ($p < 0.05$).

As the levels of metabolites are strongly dependent on incubation time, the number of viable cells and the used steroid precursor concentrations, we decided to show the formation rates (in fmol/10⁶ cells/h) and not absolute concentrations to better allow a comparison between the two carboplatin-sensitive and four carboplatin-resistant HGSOc cell lines. In the platinum-sensitive cell lines 13363 and 13699, sulfation of DHEA to inactive DHEA-S was clearly the favored metabolic pathway, with formation rates of 2583.1 ± 306.9 and 1958.5 ± 184.2 fmol/10⁶ cells/h, respectively. In addition, approximately 20% of DHEA was oxidized to AD via 3 β -hydroxysteroid-dehydrogenase (3 β -HSD) activity (13363: 697.2 ± 96.5 ; 13699: 541.9 ± 77.3 fmol/10⁶ cells/h), which was then further converted to

T by the action of 17β -hydroxysteroid-dehydrogenase (17β -HSD); however, to a significantly lower extent of only approximately 5% (13363: 38.5 ± 4.5 and 13699: 21.8 ± 2.6 fmol/ 10^6 cells/h).

In the platinum-resistant cell lines 13914_1, 15233, Kuramochi, and OVSAHO, the formation rates of DHEA-S, AD, and T were notably lower (maximum 20%) as compared with the platinum-sensitive cells. The formation of DHEA-S was significantly less pronounced (13914_1: 444.2 ± 31.5 , 15233: 199.5 ± 9.9 , Kuramochi: 32.1 ± 5.3 , and OVSAHO: 165.5 ± 15.5 fmol/ 10^6 cells/h) and in the same range as the formation of AD (13914_1: 100.2 ± 11.6 , 15233: 127.9 ± 13.5 , Kuramochi: $72.8.1 \pm 5.6$, and OVSAHO: 76.6 ± 1.4 fmol/ 10^6 cells/h). Formation of T was negligible in 15233 cells (7.7 ± 0.4 fmol/ 10^6 cells/h), Kuramochi cells (2.1 ± 0.2 fmol/ 10^6 cells/h), and OVSAHO cells (2.6 ± 0.2 fmol/ 10^6 cells/h), and undetectable in the 13914_1 cell line.

2.3. E1 Metabolism by Platinum-Sensitive and -Resistant HGSOE Cells

To determine estrogen biotransformation, all six cell lines were also incubated with 500 nM E1 as a precursor steroid. Control samples (DMSO) again demonstrated no endogenous estrogen metabolites.

As presented in Figure 3, E2 was the predominant steroid in all HGSOE cell lines, with higher formation rates (3545.6 ± 162.7 and 3374.1 ± 200.2 fmol/ 10^6 cells/h) in the platinum-sensitive 13363 and 13699 cells. In the four platinum-resistant cell lines, formation rates were markedly lower (13914_1: 2506.9 ± 149.3 , 15233: 2180.8 ± 143.5 , Kuramochi: 2030.0 ± 13.3 , and OVSAHO: 1997.1 ± 126.5 fmol/ 10^6 cells/h). Both E1 and E2 were further conjugated to inactive E1-S and E2-S, and to a minor extent to E2-G, while the CYP3A4-mediated hydroxylation of E2 to E3 could not be quantified in any of the cell lines, due to marginal expression levels of this enzyme (Section 4.3). Again, the formation rates differed markedly between platinum-sensitive and -resistant HGSOE cells. While conjugation of E1 to E1-S amounted to 1381.4 ± 97.2 and 1199.3 ± 53.4 fmol/ 10^6 cells/h in the 13363 and 13699 cells, respectively, the E1-S formation rates were up to eight-fold lower in the resistant cell lines (13914_1: 179.4 ± 12.0 , 15233: 263.6 ± 16.4 , Kuramochi: 286.7 ± 46.9 , and OVSAHO: 250.3 ± 19.0 fmol/ 10^6 cells/h). Additionally, the formation of E2-S was up to 18-fold higher in the platinum-sensitive HGSOE cells (13363: 108.2 ± 8.7 and 13699: 212.3 ± 21.7 fmol/ 10^6 cells/h) as compared with the platinum-resistant HGSOE cells (13914_1: 11.7 ± 1.5 , 15233: 20.3 ± 1.4 , Kuramochi: 22.8 ± 2.2 , and OVSAHO: 38.9 ± 1.9 fmol/ 10^6 cells/h). Glucuronidation of E2 to E2-G was only a minor pathway in all investigated cell lines, and was again up to 11-fold lower in platinum-resistant cells (13914_1: 1.7 ± 0.1 , 15233: 1.3 ± 0.1 , Kuramochi: 1.8 ± 0.2 , and OVSAHO: 1.9 ± 0.2 fmol/ 10^6 cells/h) as compared with the platinum-sensitive cells (13363: 14.2 ± 0.7 and 13699: 11.9 ± 1.2 fmol/ 10^6 cells/h).

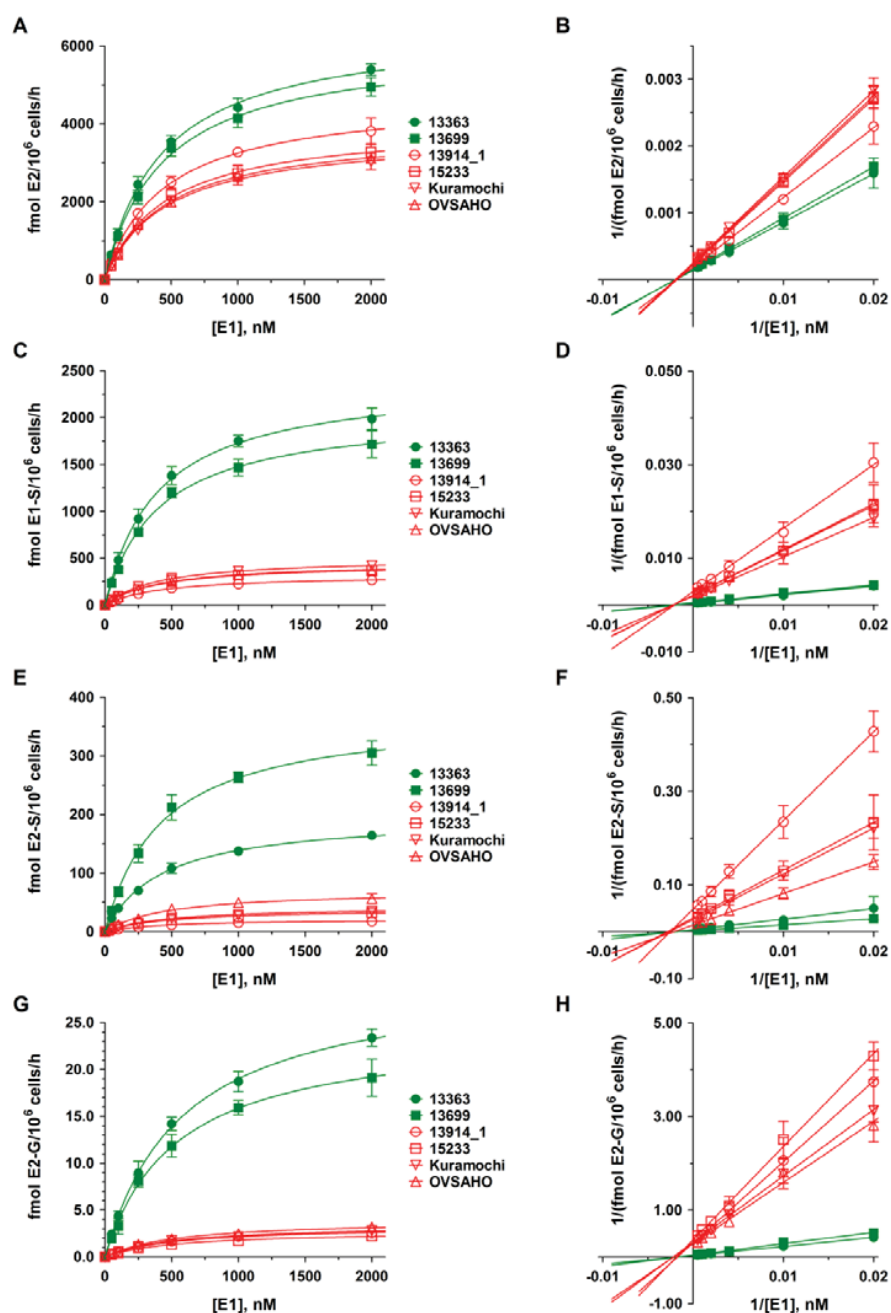


Figure 3. Kinetic profiles of E1 metabolite formation in platinum-sensitive and -resistant HGSOc cells. The kinetics of (A–B) E2 formation, (C–D) E1 sulfation, (E–F) E2 sulfation, and (G–H) E2 glucuronidation were calculated following the incubation of all HGSOc cell lines with 0 to 2000 nM E1 as a hormone precursor for 48 h. Data are displayed as Michaelis–Menten and Lineweaver–Burk plots and represent the means \pm SD of three independent experiments. Green curves indicate sensitivity and red curves indicate resistance against carboplatin to the investigated HGSOc cell lines. Differences were statistically significant between these two groups ($p < 0.05$).

2.4. Kinetics of DHEA and E1 Metabolism in HGSOc Cells

Kinetic profiles for DHEA and E1 metabolites in all HGSOc cell lines were subsequently evaluated over a DHEA and E1 concentration range of 0 to 2000 nM for 48 h. As demonstrated in Figures 2 and 3, the formation kinetics of all seven quantified metabolites (DHEA-S, AD, T, E2, E1-S, E2-S, and E2-G)

best fitted to a hyperbolic Michaelis–Menten model (R^2 : 0.9943 to 0.9997). Notably, Michaelis constants (K_m values) for each metabolite were within a similar range in all six tested cell lines, indicating that the affinities of the same enzymes involved in the biotransformation of DHEA and E1 are comparable between carboplatin-sensitive and -resistant HGSOC cells. The maximum reaction velocities (V_{max} values), however, were significantly higher in platinum-sensitive as compared with platinum-resistant cell lines, supporting lower enzymatic activity in the latter ones. All kinetic parameters are presented in detail in Tables 1 and 2.

Table 1. Kinetic parameters of DHEA metabolism by the investigated HGSOC cells. K_m and V_{max} values were calculated using GraphPad Prism 6.0 software following the incubation of the cell lines with increasing concentrations of DHEA (0 to 2000 nM) as a hormone precursor for 48 h. All data are presented as the means \pm SD of three independent experiments. Values in bold and marked with an asterisk (*) are significantly different as compared with both carboplatin-sensitive cell lines 13363 and 13699 ($p < 0.05$). n.c., not calculable.

Cell Line	K_m [nM]			V_{max} [fmol/10 ⁶ Cells/h]		
	DHEA-S	AD	T	DHEA-S	AD	T
Carboplatin-sensitive						
13363	193.9 \pm 9.3	812.7 \pm 79.7	657.7 \pm 52.4	3523.7 \pm 47.8	1736.6 \pm 75.9	85.6 \pm 2.8
13699	308.7 \pm 19.2	929.4 \pm 68.8	623.5 \pm 50.2	3192.4 \pm 64.7	1478.8 \pm 51.1	51.4 \pm 1.7
Carboplatin-resistant						
13914_1	318.7 \pm 18.6	854.1 \pm 39.9	n.c.	729.0 \pm 13.9 *	269.8 \pm 5.7 *	0.0 *
15233	314.1 \pm 11.1	980.4 \pm 88.6	592.0 \pm 33.0	328.5 \pm 3.8 *	369.7 \pm 15.9 *	12.3 \pm 0.3 *
Kuramochi	318.5 \pm 36.2	841.7 \pm 43.4	621.5 \pm 45.4	56.9 \pm 2.1 *	189.0 \pm 4.4 *	3.4 \pm 0.1 *
OVSCHO	310.8 \pm 20.7	871.4 \pm 36.7	631.4 \pm 30.8	264.8 \pm 5.7 *	204.9 \pm 3.9 *	4.4 \pm 0.1 *

Table 2. Kinetic parameters of E1 metabolism by the investigated HGSOC cells. K_m and V_{max} values were calculated using GraphPad Prism 6.0 software following the incubation of the cell lines with increasing concentrations of E1 (0–2000 nM) as a hormone precursor for 48 h. All data are presented as the means \pm SD of three independent experiments. Values in bold and marked with an asterisk (*) are significantly different as compared with both carboplatin-sensitive cell lines 13363 and 13699 ($p < 0.05$).

Cell line	K_m [nM]			
	E2	E1-S	E2-S	E2-G
Carboplatin-sensitive				
13363	430.4 \pm 22.9	390.5 \pm 18.4	426.8 \pm 22.1	580.1 \pm 20.0
13699	434.8 \pm 27.9	399.3 \pm 25.5	422.5 \pm 29.8	532.9 \pm 34.3
Carboplatin-resistant				
13914_1	440.8 \pm 13.2	398.0 \pm 9.1	418.0 \pm 16.8	535.3 \pm 39.6
15233	451.4 \pm 22.8	407.3 \pm 29.0	458.8 \pm 38.7	537.0 \pm 44.3
Kuramochi	454.0 \pm 23.4	402.8 \pm 14.1	452.0 \pm 23.7	521.2 \pm 52.6
OVSCHO	450.0 \pm 19.8	403.3 \pm 18.3	464.6 \pm 54.5	534.4 \pm 48.5
Cell line	V_{max} (fmol/10 ⁶ Cells/h)			
	E2	E1-S	E2-S	E2-G
Carboplatin-sensitive				
13363	6492.9 \pm 124.7	2404.8 \pm 39.7	198.3 \pm 3.7	30.0 \pm 0.4
13699	6028.7 \pm 140.4	2067.9 \pm 46.6	373.7 \pm 9.5	24.3 \pm 0.6
Carboplatin-resistant				
13914_1	4687.8 \pm 51.2 *	318.9 \pm 2.6 *	21.5 \pm 0.3 *	3.3 \pm 0.1 *
15233	4017.7 \pm 74.5 *	455.7 \pm 11.5 *	38.8 \pm 1.2 *	2.8 \pm 0.1 *
Kuramochi	3750.0 \pm 71.0 *	508.4 \pm 6.3 *	42.7 \pm 0.8 *	3.5 \pm 0.1 *
OVSCHO	3833.8 \pm 61.9 *	443.9 \pm 7.1 *	70.8 \pm 3.1 *	3.9 \pm 0.1 *

2.5. Proliferation of Platinum-Sensitive and -Resistant HGSOC Cell Lines

Subsequently, the proliferation rates of the six HGSOC cell lines were evaluated starting from 1.00×10^6 viable cells/well in the absence of any steroid hormone over a time span of 48 h. While the platinum-sensitive cell lines 13363 and 13699 demonstrated a moderate increase in cell numbers to 1.42 ± 0.25 and $1.24 \pm 0.23 \times 10^6$ viable cells/well, respectively, all platinum-resistant cell lines revealed significantly higher proliferation (13914_1: 1.61 ± 0.39 , 15233: 2.07 ± 0.13 , Kuramochi: 2.07 ± 0.10 , and OVSAHO: $2.00 \pm 0.03 \times 10^6$ viable cells/well). Addition of DHEA or E1 (0 to 2000 nM) for 48 h did not further stimulate cellular proliferation, indicating that the growth of the investigated cells is independent of stimulation by these steroid precursors (Figure S1).

2.6. Effect of IL-6 on Proliferation, Metabolism, and Carboplatin Resistance of Platinum-Sensitive HGSOC Cells

Formation of IL-6 was increased up to 600-fold in the platinum-resistant 13914_1 cell line ($302.6 \text{ pg}/10^6 \text{ cells/h}$), whereas all other cell lines demonstrated comparably low rates between 0.12 and $2.75 \text{ pg}/10^6 \text{ cells/h}$. These findings are also in line with the gene expression data which revealed high IL-6 expression only in the 13914_1 cell line (Table S2).

Platinum-sensitive 13699 cells, which exhibit low endogenous IL-6 production and express moderate/high levels of *ESR1* and *AR*, but low levels of *ESR2* and *PGR* (Table S2), were, then, used to investigate whether stimulation of the cells with IL-6 could increase cell proliferation and concomitantly affect estrogen metabolism. As shown in Figure 4A,B, carboplatin-sensitive 13699 cells were treated with IL-6 (10 ng/mL) for 72 h. Afterwards, increasing concentrations of the hormone precursors DHEA or E1 (0 to 2000 nM) were added. IL-6 was further present in the medium and the cellular proliferation was determined after 48 h. Compared with the IL-6 untreated controls, the presence of IL-6 significantly increased cellular growth by 36.3% from 1.24 ± 0.23 to $1.69 \pm 0.14 \times 10^6$ cells/well. Consistently with the previous experiments (Section 2.5), addition of DHEA or E1 (50 to 2000 nM) to the cells had no further impact on cellular growth.

In contrast to the increased cellular proliferation upon IL-6 treatment, metabolism of DHEA (2000 nM) by 13699 cells to DHEA-S, AD and T was strongly decreased (Figure 4C). While the formation of DHEA-S and AD was reduced by 52.8% and 61.0% (from 2761.2 ± 272.5 to $1302.9 \pm 219.1 \text{ fmol}/10^6 \text{ cells/h}$ and 1016.6 ± 80.3 to $369.7 \pm 26.5 \text{ fmol}/10^6 \text{ cells/h}$, respectively), the concentration of T was even decreased by 87.1% (from 38.8 ± 3.4 to $5.0 \pm 0.3 \text{ fmol}/10^6 \text{ cells/h}$). Decreased metabolite formation was also observed upon addition of E1 (2000 nM) in the presence of IL-6. The concentration of unconjugated E2 decreased by 49.9% from 4948.6 ± 232.7 to $2479.5 \pm 179.4 \text{ fmol}/10^6 \text{ cells/h}$, whereas the decrease of E1-S, E2-S, and E2-G levels was much more pronounced, resulting in a reduction by 68.4%, 76.2%, and 92.2%, respectively (E1-S: 1714.8 ± 143.7 to $541.7 \pm 29.9 \text{ fmol}/10^6 \text{ cells/h}$, E2-S: 305.0 ± 20.7 to $72.7 \pm 6.7 \text{ fmol}/10^6 \text{ cells/h}$, and E2-G: 19.1 ± 2.0 to $1.5 \pm 0.5 \text{ fmol}/10^6 \text{ cells/h}$) (Figure 4D).

Concomitant with these changes in the metabolic activity of 13699 cells, platinum resistance was increased more than three-fold, shifting the IC_{50} against carboplatin from 3.4 ± 0.3 to $11.2 \pm 2.4 \text{ }\mu\text{M}$ (Figure S2A), indicating that the proinflammatory cytokine IL-6 can convert this cell line from “platinum-sensitive” to “platinum-resistant”.

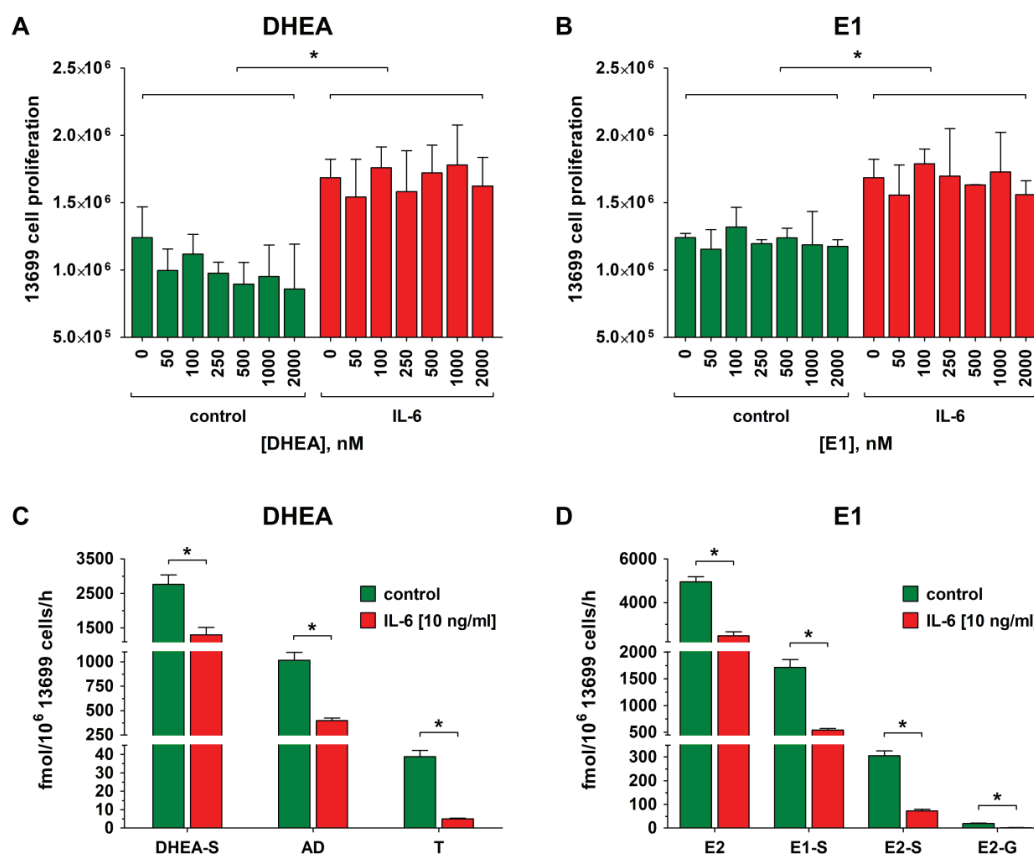


Figure 4. Effect of IL-6 treatment on proliferation and steroid metabolism of 13699 cells. Platinum-sensitive 13699 cells, demonstrating a low endogenous IL-6 formation ($2.75 \text{ pg}/10^6 \text{ cells/h}$), were incubated with IL-6 (10 ng/mL) for 72 h, followed by incubation with IL-6 in the presence of increasing concentrations (0 to 2000 nM) of (A) DHEA and (B) E1 for 48 h and the viable cells were counted on a CASY® TT cell counter. Subsequently, the cellular supernatants of the samples containing 2000 nM of the steroid precursor (C) DHEA or (D) E1 were analyzed for steroid metabolites using liquid chromatography high-resolution mass spectrometry (LC-HRMS). Green indicates sensitivity for carboplatin and red represents carboplatin resistance. All data are presented as the means \pm SD of three independent experiments. * $p < 0.05$.

2.7. Effect of Tocilizumab (TCZ) Treatment on Proliferation, Metabolism, and Carboplatin Resistance of Platinum-Resistant HGSOC Cells

To verify that the observed reduced steroid metabolism and increased platinum resistance are indeed related to the action of IL-6, 13914_1 cells (the cell line with the highest endogenous IL-6 formation) were treated with the monoclonal anti-IL-6R antibody TCZ ($250 \text{ }\mu\text{g/mL}$) for 72 h before addition of DHEA or E1 (0 to 2000 nM) in the further presence of TCZ for 48 h. As shown in Figure 5A,B, TCZ reduced the proliferation of 13914_1 cells by 25.6% from 1.61 ± 0.39 to $1.20 \pm 0.20 \times 10^6$ cells/well as compared with the TCZ-untreated controls, while co-incubation with increasing concentrations of DHEA or E1 and TCZ again did not further affect cellular proliferation.

Concomitant with the reduced proliferation of the TCZ-treated 13914_1 cells, the overall metabolic activity significantly increased when DHEA (2000 nM) was added. Formation of DHEA-S and AD increased by 33.0% and 61.0% (DHEA-S: 641.0 ± 47.1 to $852.6 \pm 103.7 \text{ fmol}/10^6 \text{ cells/h}$ and AD: 134.5 ± 80.9 to $216.5 \pm 38.7 \text{ fmol}/10^6 \text{ cells/h}$). Even T, the formation of which was below the LLOQ in the absence of TCZ, could be now quantified with a formation rate of $2.1 \pm 0.5 \text{ fmol}/10^6 \text{ cells/h}$ (Figure 5C). Also addition of the estrogen precursor E1 (2000 nM) demonstrated a significant increase of

E2 by 113.5% (4365.6 ± 718.7 to 9319.8 ± 1703.9 fmol/ 10^6 cells/h), which was concomitant with strongly elevated levels of glucuronidated and sulfated metabolites; E2-G increased by 282.0% from 2.2 ± 0.3 to 8.6 ± 0.8 fmol/ 10^6 cells/h, whereas E1-S and E2-S were induced by 279.0% and 290.3%, respectively, (221.8 ± 24.2 to 840.4 ± 95.6 fmol/ 10^6 cells/h and 17.3 ± 3.0 to 67.7 ± 15.4 fmol/ 10^6 cells/h) (Figure 5D).

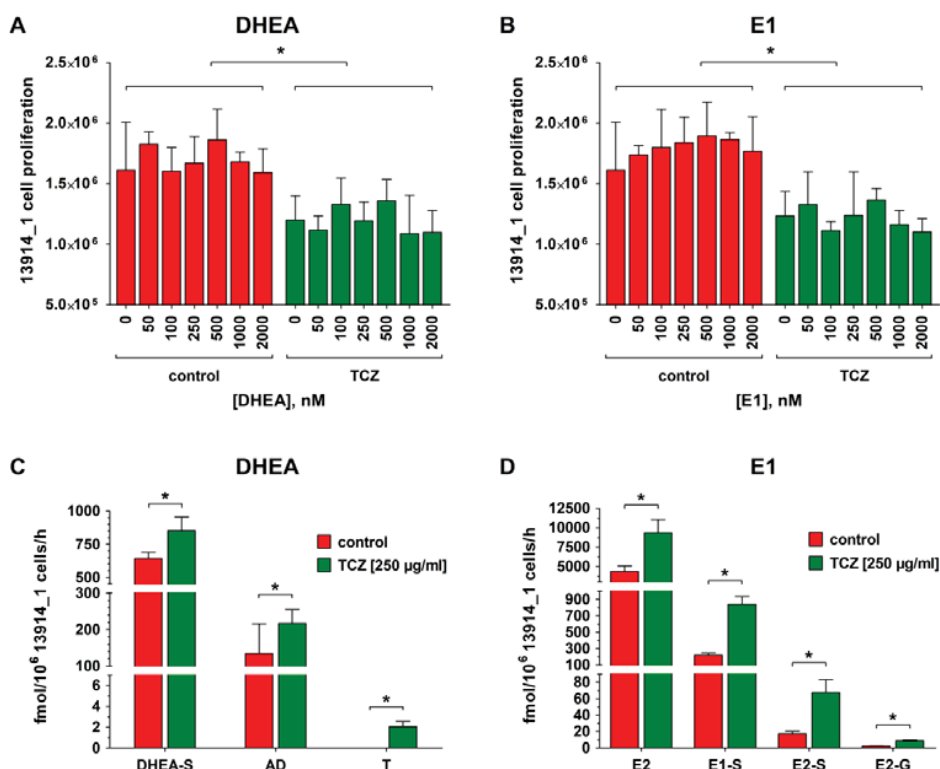


Figure 5. Effect of tocilizumab (TCZ) treatment on the proliferation and steroid metabolism of 13914_1 cell line. Platinum-resistant 13914_1 cells, demonstrating a high endogenous IL-6 formation (302.6 pg/ 10^6 cells/h), were incubated with TCZ (250 μ g/mL) for 72 h, followed by incubation with TCZ in the presence of increasing concentrations (0 to 2000 nM) of (A) DHEA and (B) E1 for 48 h and the viable cells were counted on a CASY[®] TT cell counter. Subsequently, the cellular supernatants of the samples containing 2000 nM of the steroid precursor (C) DHEA or (D) E1 were analyzed for steroid metabolites using LC-HRMS. Green indicates sensitivity for carboplatin and red represents carboplatin resistance. All data are presented as the means \pm SD of three independent experiments. * $p < 0.05$.

The TCZ treatment (250 μ g/mL) strongly affected also the resistance of 13914_1 cells against carboplatin. While untreated cells demonstrated an IC_{50} value of 11.2 ± 2.4 μ M against carboplatin, treatment with the anti-IL-6R antibody decreased this value significantly to 3.4 ± 0.3 μ M, therefore, re-establishing the sensitivity for platinum-based chemotherapy in this cell line (Figure S2B).

3. Discussion

There is evidence that estrogens play a pivotal role in the progression of ovarian cancer, and that the expression levels of key enzymes vary between benign and cancerous tissues [19]. As differences in the steroid metabolism between platinum-sensitive and -resistant HGSOC cells have not been investigated yet, the present study screened the formation of DHEA and E1 biotransformation products in four recently established and two commercially available HGSOC cell lines as in vitro models for HGSOC.

First, the respective IC_{50} values against carboplatin were determined. Two cell lines were sensitive, whereas the other four cell lines exhibited up to 5.3-fold higher IC_{50} values against carboplatin, and

therefore were considered carboplatin-resistant. Notably, 13363 cells, established from a patient prior to chemotherapy, demonstrated sensitivity for carboplatin treatment; while the corresponding 15233 cell line (harvested during chemotherapy) was resistant against carboplatin. These findings are in line with previous data [26,27]. Differences were only found for the OVSAHO cell line, which was considered carboplatin-resistant in the present study but described as cisplatin-sensitive by Haley et al. [27], which is most likely based on different experimental settings, as the MTT assay used by the authors for cell viability measurements is known to generate artifacts causing altered IC₅₀ values [28,29].

Following incubation with DHEA, three metabolites, namely DHEA-S, AD, and T, could be quantified in the cellular supernatants. Formation rates of these metabolites were 5- to 60-fold higher in platinum-sensitive cells as compared with the platinum-resistant ones. This is particularly interesting, as the platinum-sensitive 13363 cells were harvested before treatment and the platinum-resistant 15233 cells were harvested during the second cycle of standard platinum-based chemotherapy, thereby, suggesting that the progression of the disease correlates with decreased metabolic activity.

A similar pattern was seen when the cells were incubated with E1. Again, the formation of all metabolites, namely E2, E1-S, E2-S, and E2-G, was significantly higher (up to 1.7-, 7.8-, 17-, and 11-fold, respectively) in carboplatin-sensitive cell lines, with E2, the most potent estrogen, as the main biotransformation product, followed by the sulfated metabolites E1-S and E2-S. E2-G concentrations in the media were low, indicating that sulfation and not glucuronidation is the preferred metabolic pathway in HGSOE cells, which has also been observed in breast cancer [30]. In all six cell lines, hydroxylation of E2 to E3 could not be observed based on low CYP3A4 levels. Conversion of AD to E1 and T to E2 was also not seen in all six cell lines, suggesting no or only very low levels of aromatase (CYP19A1). This is in agreement with the present gene expression analyses and the expression studies by Imai et al. [31], which also detected no aromatase in ovarian cancer cell culture and ovarian carcinoma tissue samples. However, in contrast to the cancer cells, aromatase immunoreactivity was observed in stromal cells adjacent to the tumor [32,33]. Aromatase inhibitors such as letrozole can, therefore, act not on tumor cells directly, but rather indirectly by preventing E2 formation in adjacent cells, thereby, reducing tumor progression and can be a treatment option to increase the progression-free survival of platinum-resistant HGSOE patients via targeting the tumor microenvironment [34].

All four carboplatin-resistant cell lines revealed up to 67% higher proliferation rates as compared with the carboplatin-sensitive cells, independent of the presence of DHEA or E1. Notably, the proliferation rates of the two cell lines derived from the same patient (13363 and 15233 cells) were significantly different (Figure S1). This difference between sensitive and resistant cells was also observed by Xu et al. [35], who reported a higher migration and invasion of platinum-resistant ovarian cancer cells as compared with platinum-sensitive ones, explaining, at least partly, why patients diagnosed with platinum-resistant HGSOE often face faster tumor progression and worse prognosis of the disease.

Recent data showed that autocrine production of the cytokine IL-6 confers cisplatin resistance in ovarian cancer cells [36]. Extracellular IL-6 binds to the cell surface receptor glycoprotein 130 (gp130), thereby activating signaling pathways that promote inflammation, immune reaction, and tumor progression. Elevated serum IL-6 levels in ovarian cancer patients, therefore, correlate with poor prognosis [37]. Most important, elevated IL-6 levels have also been shown to decrease the expression of various estrogen-metabolizing phase I and II enzymes, including members of the cytochrome P450 family (CYPs) and uridine 5'-diphospho-glucuronosyltransferases (UGTs) [38–40]. Among other mechanisms, these interactions of IL-6 with E1 and DHEA metabolism is related to the suppression of the nuclear pregnane X receptor (PXR) by IL-6 via JAK/STAT3 signaling, which subsequently leads to a downregulation of genes responsible for estrogen metabolism and transport [41–43]. Therefore, it can be hypothesized that increased IL-6 activity in carboplatin-resistant HGSOE cells can contribute to the observed decreased biotransformation of estrogen precursors, increased proliferation rates, and therefore induce platinum resistance.

To verify this hypothesis, carboplatin-sensitive 13699 cells were treated with recombinant IL-6 for 72 h and, afterwards, their sensitivity for carboplatin, their proliferation rates, and the metabolic

activity were again determined. As expected, the presence of IL-6 in the culture medium switched their sensitivity status to “resistant”, with a three-fold higher IC_{50} value, which was concomitant with an increased cellular proliferation and decreased DHEA and E1 metabolism (Figure 6). Consequently, IL-6 can act as a resistance marker for some but not all HGSOC cases. Conversely, treatment of the carboplatin-resistant cell line 13914_1, which expresses high endogenous IL-6 levels, with the IL-6R specific monoclonal antibody TCZ changed the cell status to “sensitive”, demonstrating a decreased IC_{50} value for carboplatin, decreased cellular growth, and significantly higher DHEA and E1 metabolism. These findings are in line with previous data, which have also shown that treatment of EOC cells with TCZ inhibited cellular proliferation, whereas a combination of TCZ with carboplatin further synergistically reduced cell growth [44]. These effects were also observed in paclitaxel-resistant SKOV-3 and CAOV-3 ovarian cancer cells, where the anti-IL-6 antibody siltuximab increased paclitaxel sensitivity, leading to lower cell viability and decreased IC_{50} values [45].

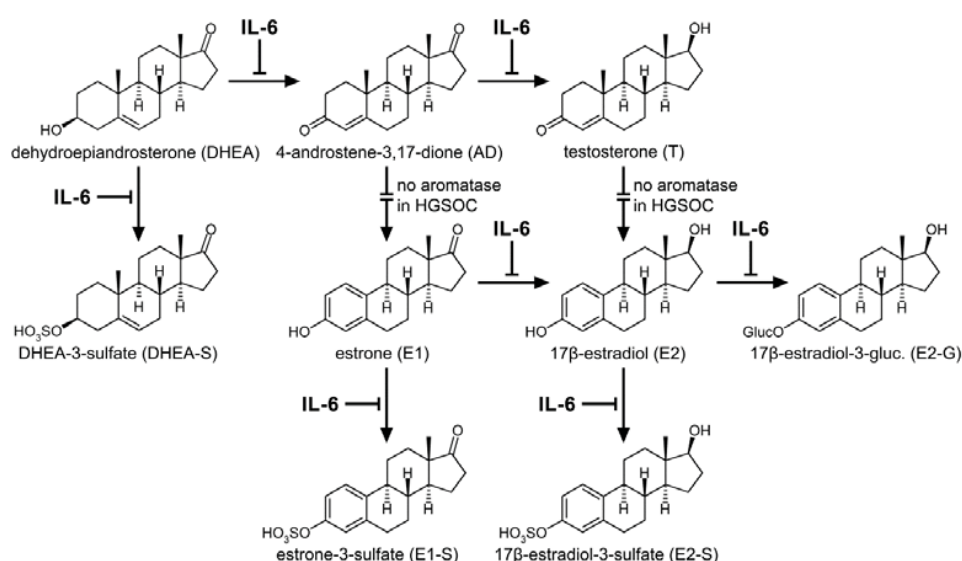


Figure 6. Interaction of IL-6 with the estrogen synthesis and metabolism in HGSOC. IL-6 influences several key steps in the formation of estrogen precursors, active estrogens, and their respective conjugates leading to decreased levels of steroid metabolites. By contrast, treatment with the anti-IL-6 antibody TCZ can antagonize this effect, thereby, stimulating the biotransformation of estrogens. Intersected arrows indicate no expression of aromatase (*CYP19A1*) in HGSOC cells.

Although TCZ stimulated the conjugation, and therefore the inactivation of estrogens in carboplatin-resistant 13914_1 cells, the formation of E2 via 17β-HSDs was strongly increased and resulted in higher unconjugated E2 concentrations as compared with untreated cells. This elevation of active estrogens upon anti-IL-6R treatment can contribute to disease progression and explain, at least partly, the lack of efficacy of antibody monotherapy in HGSOC [46]. Therapeutic combination of TCZ with standard chemotherapy (carboplatin as a single drug or in combination with paclitaxel [47]) could be a promising treatment strategy to re-establish platinum sensitivity in HGSOC patients. As only patients with high endogenous plasma levels of IL-6 and IL-6R expression could benefit from this therapy, platinum-resistant HGSOC cases have to be screened for IL-6 levels before treatment with a recombinant monoclonal anti-IL-6R antibody.

The altered expression of the genes *ESR1* and *AR* encoding ERα and AR, whose abundances are inhomogeneous in the investigated HGSOC model cell lines, also influence the action of estrogens and, consequently, proliferation of platinum-resistant HGSOC cells. Whereas 13699 and Kuramochi cells express moderate/high levels of *ESR1* and *AR*, but poor levels of *ESR2* and *PGR*, the other investigated cell lines have low or undetectable levels of all steroid hormone receptors (Table S2). Despite these

differences in receptor status, incubation of all six HGSOC cell lines with DHEA and E1 did not increase cellular proliferation, thereby, defining these cell lines as hormone independent.

The lack of additional proliferation in the presence of hormone precursors is most likely a consequence of the fact that all cell lines already reached their respective maximum proliferation capacity from the stimulatory effect of numerous other factors. Mutations in *TP53* will fuel tumor cell growth by preventing cell cycle arrest and apoptosis [43], and the moderate/high expression levels of *EGFR* and *ERBB2* in all six cell lines (Table S2) could also contribute to an uncontrolled cellular growth [44].

Our data showed that estrogen metabolism did not correlate with *ESR1*, *ESR2*, and *ESRRG* expression. This is supported by a previous paper by Andersen et al. [48], showing that approximately 80% of HGSOC tumor samples express *ESR1*; however, the response to an antiestrogenic therapy in patients is rather poor. This group also reported that the ER α status in HGSOC cells is not a sufficient tool to predict the response to an antiestrogenic therapy. Other proteins, e.g., IGFBP3, could also be important for the response.

All six cell lines also carry distinct mutations in *TP53* in the DNA binding domain or oligomerization domain (Table S1), leading to a truncated protein. The lack of additional proliferation in the presence of hormone precursors is most likely a consequence of the fact that all cell lines already reached their respective maximum proliferation capacity from the stimulatory effect of various cyclins (e.g., *D1*, *E1*, *A1*, and *B*) overexpressed in these cell lines. Genes such as *CDKN1A* *BAX* or *TIGAR*, controlling apoptosis and cell cycle arrest, are furthermore downregulated [26,49]. These data indicate that the loss of wild type p53 function is the major driving force of tumor cell progression [50]. Additionally, the moderate/high expression levels of *EGFR* and *ERBB2* in all six cell lines (Table S2) could also contribute to an uncontrolled cellular growth [51].

Although our data indicate that estrogen metabolism can differ between platinum-sensitive and -resistant HGSOC cells, clinical data are highly warranted to verify this observation in platinum-resistant cancer patients. We are well aware that several other mechanisms for platinum resistance are known that could be used as clinical markers, including an alteration in cellular accumulation or detoxification of platinum drugs. A decreased expression of the membrane copper transporter CTR1 or the organic cation transporter OCT2, as well as a high expression of the copper-exporting P-type ATPases, ATP7A and ATP7B, or the ATP-binding cassette multidrug transporter, MRP2, could lead to decreased intracellular levels of platinum drugs, thereby causing resistance. Furthermore, high expression levels of glutathione S-transferase, a detoxifying enzyme responsible for the formation of platinum-glutathione conjugates, would also facilitate resistance [52]. A combination of these already identified markers with differences in estrogen metabolism could allow a better prediction of platinum resistance in patients.

4. Materials and Methods

4.1. Reagents

AD, DHEA, dehydroepiandrosterone-2,2,3,4,4,6-d₆ (DHEA-d₆), DHEA-S (sodium salt), dehydroepiandrosterone-3-sulfate-2,2,3,4,4,6-d₆ (DHEA-S-d₆ sodium salt), E1, E1-S (sodium salt), E2, E2-G (sodium salt), E3, T, acetic acid, acetonitrile, ammonium acetate, carboplatin, DMSO, and human IL-6 (HumanKine[®], expressed in HEK 293 cells, suitable for cell culture) were obtained from Merck KGaA (Darmstadt, Germany). All solvents and additives were purchased with HPLC/MS grade purity. 4-Androstene-3,17-dione-2,2,4,6,6,16,16-d₇ (AD-d₇), 17 β -estradiol-2,4,16,16-d₄ (E2-d₄), 17 β -estradiol-16,17-d₃-3-O-(β -D-glucuronide) (E2-G-d₃ sodium salt), 17 β -estradiol-2,4,16,16-d₄-3-sulfate (E2-S-d₄ sodium salt), estriol-2,4,17-d₃ (E3-d₃), estrone-2,4,16,16-d₄ (E1-d₄), estrone-2,4,16,16-d₄-3-sulfate (E1-S-d₄ sodium salt), and testosterone-2,2,4,6,6-d₅ (T-d₅) were obtained from C/D/N-Isotopes Inc. (Pointe-Claire, Quebec, Canada). E2-S (sodium salt) was purchased from Steraloids Inc. (Newport, RI, USA). The anti-IL-6R antibody TCZ (RoActemra[®]) was purchased from Roche Austria GmbH (Vienna, Austria). Water for all experiments was purified using an arium[®] pro ultrapure water system (Sartorius AG, Göttingen,

Germany). If not stated otherwise, all standards were dissolved in DMSO to their final concentration and stored at -80°C until further usage. All deuterated standards were then mixed to obtain the final internal standard master mix composition. Dulbecco's modified Eagle medium F-12 (DMEM/F-12), Dulbecco's phosphate buffered saline (DPBS), fetal bovine serum (FBS), PenStrep[®], and TrypLe[®] solutions were purchased from Invitrogen; Thermo Fisher Scientific, Inc. (Waltham, MA, USA). HyClone[®] heat-inactivated charcoal/dextran treated FBS was obtained from THP Medical Products (Vienna, Austria).

4.2. Cell Lines

13363, 13699, 13914_1, and 15233 HGSOC cancer cells, characterized and authenticated via short tandem repeats (STR) profiling as described previously [26], were kindly provided by the Translational Gynecology Group at the Medical University of Vienna. The four cell lines were established from the ascites of three grade 3 HGSOC patients. The 13363 and 15233 cells were harvested from the same patient (age 33 and FIGO: IV); the first ones at the time of diagnosis and the latter ones under the treatment with carboplatin/paclitaxel. The 13699 and 13914_1 cells originated from two patients (both FIGO: IIIC), aged 53 and 66, respectively. Kuramochi (RRID:CVCL_1345) and OVSAHO (RRID:CVCL_3114) cell lines were originally established from undifferentiated ovarian adenocarcinoma [53] and serous papillary ovarian adenocarcinoma [54], respectively, and were described as the best commercial in vitro models for HGSOC [55]. Both cell lines were obtained from the JCRB Cell Bank (Osaka, Japan) which certified the authenticity of their STR profiles. The *P53* and *PAX8* gene expression confirmed that all cell lines were high grade. Cells were routinely cultivated in phenol red-free DMEM/F-12 containing 10% FBS and 1% PenStrep[®] solution at 37°C (95% humidity and 5% CO_2) and the experiments were performed during the exponential growth phases of the cells.

4.3. Gene Expression Analyses and Identification of Gene Mutations

Expression of selected genes (*CYP3A4*, *CYP19A1*, *TP53*, *PAX8*, *AR*, *ESR1*, *ESR2*, *PGR*, *IL6*, *EGFR*, *ERBB2*, and *ESRRG*) in the HGSOC cell lines 13363, 13699, 13914_1, and 15233 was analyzed by next-generation sequencing, as described previously [49]. Expression data for these selected genes in Kuramochi and OVSAHO cells were taken from the GENEVESTIGATOR platform [56]. The *TP53* mutation was determined by a modified p53 functional yeast assay and Sanger sequencing. In addition, ddPCR systems for each unique *TP53* mutation were established to determine the percentage of the *TP53* mutant cells in cell culture. The *BRCA1*, *BRCA2*, and *KRAS* mutations were determined by Sanger sequencing [49]. Data for Kuramochi and OVSAHO cells were obtained from the Cancer Cell Line Encyclopedia (CCLE) [57].

4.4. Carboplatin Resistance

To elucidate the sensitivity of all investigated cell lines to carboplatin treatment, cells were seeded in triplicate in 6-well plates at a concentration of 1.00×10^6 cells/well and allowed to attach overnight. Cells were washed with DPBS and incubated with phenol red-free DMEM/F-12 supplemented with 10% FBS and 1% PenStrep[®] solution at 37°C (95% humidity and 5% CO_2) containing 0 to 50 μM carboplatin. Carboplatin was dissolved in sterile-filtered water according to Hall et al. [58] (final concentration 0.1%) before addition to the culture media, as other solvents, such as DMSO, inactivate platinum complexes. After 72 h, the supernatant media were discarded, and the cell layers were washed with DPBS and detached using 400 μL TrypLe[®] solution. Immediately afterwards, cell suspensions were analyzed for the number of viable cells using a CASY[®] TT cell counting system (OLS OMNI Life Science, Bremen, Germany), described as an improved method for cell viability measurements at least for platinum complexes, as the MTT assay might generate artifacts leading to altered IC_{50} values [28,29].

4.5. Metabolism of Steroid Hormones by Platinum-Sensitive and -Resistant HGSOC Cells

For the metabolomic analyses, cells were cultivated and seeded in 6-well plates, as described in Section 4.4. Prior to the incubation with either DHEA or E1 (0 to 2000 nM) as hormone precursors

(dissolved in sterile-filtered DMSO, final concentration 0.05%), the cell layers were washed twice with DPBS, and phenol red-free DMEM/F-12, containing only 10% heat-inactivated charcoal-stripped fetal bovine serum and 1% PenStrep[®] solution was added to exclude any effects of hormones and growth factors from standard FBS. After 48 h, which was determined in preliminary experiments as the most suitable time point (Poschner, S.; Jäger, W. University of Vienna, Vienna, Austria. Unpublished work, 2019), the supernatant cell media were collected and stored at -80°C until further analysis. The remaining cells were detached by adding 400 μL TrypLe[®] solution and subsequently counted.

Then, 2000 μL media aliquots, mixed with 20 μL deuterated internal standard solution were put onto Oasis HLB 1 cc solid phase extraction cartridges (30 mg; Waters Corporation, Milford, MA, USA), as described previously [21]. Briefly, after preconditioning the cartridges twice with 1.0 mL acetonitrile and three times with 1.0 mL ammonium acetate buffer (10 mM and $\text{pH} = 5.0$), the samples were loaded onto the columns and washed with 1.0 mL ammonium acetate buffer (10 mM and $\text{pH} = 5.0$) and twice with 1.0 mL acetonitrile/ammonium acetate buffer (10 mM and $\text{pH} = 5.0$) 10:90 (*v/v*). Analyte elution was, then, achieved by two washes with 650 μL acetonitrile/ammonium acetate buffer (10 mM and $\text{pH} = 5.0$) 95:5 (*v/v*), and the samples were left to evaporate until dry. The dried residues were reconstituted in 270 μL acetonitrile/ammonium acetate buffer (10 mM and $\text{pH} = 5.0$, 25:75) (*v/v*) and stored until further LC-HRMS analysis at -80°C .

4.6. LC-HRMS Assay for Steroid Quantification

To quantify the ten most prevalent estrogen precursors, active estrogens and their metabolites (DHEA, DHEA-S, AD, T, E1, E2, E3, E1-S, E2-S, and E2-G) in the media samples, a previously established and validated LC-HRMS was used [21]. Chromatographic separation was achieved on an UltiMate 3000 RSLC-series system (Dionex/Thermo Fisher Scientific, Inc.) coupled to a maXis HD ESI-Qq-TOF mass spectrometer (Bruker Daltonics, Bremen, Germany), which was equipped with a Phenomenex Luna[®] 3 μm C18(2) 100 Å LC column (250 \times 4.6 mm I.D.; Phenomenex Inc., Torrance, CA, USA) and a Hypersil[®] BDS-C18 guard column (5 μm , 10 \times 4.6 mm I.D.; Thermo Fisher Scientific, Inc.). Then, 100 μL of the reconstituted media samples were injected onto the column. Chromatographic separation was performed at 43°C using a continuous gradient mixed from aqueous ammonium acetate buffer (10 mM and $\text{pH} = 5.0$) as mobile phase A and acetonitrile as mobile phase B at a flow rate of 1.0 mL/min. Mobile phase B linearly increased from 25% at 0 min to 56.3% at 19 min, further increased to 90% at 19.5 min and was kept constant until 24.0 min. The percentage of acetonitrile was, then, decreased within 0.5 min to 25% in order to equilibrate the column for 6 min before application of the next sample. The injection volume for each sample was set to 100 μL .

The ESI ion source settings were identical for both modes, except for the polarity: Capillary voltage, ± 4.5 kV; nebulizer, 1.0 bar N_2 ; dry gas flow, 8.0 L/min N_2 ; and dry temperature, 200°C . Values for the ion optics and the quadrupole and collision cell parameters were as follows: Funnel RF, 400 Vpp; multipole RF, 300 Vpp; quadrupole ion energy, 8.0 eV; collision RF, 1100 Vpp; collision energy, 10.0 eV; transfer time, 38 ms; and prepulse storage, 18 ms. Full scan mass spectra in the range of m/z 150–500 were recorded in both negative and positive ion mode. The LLOQs for all analytes (signal to noise ratio ≥ 9) were calculated to be as follows: AD, 74.9 pg/mL; DHEA, 1904.0 pg/mL; DHEA-S, 8.0 pg/mL; E1, 19.0 pg/mL; E1-S, 4.0 pg/mL; E2, 140.9 pg/mL; E2-G, 12.0 pg/mL; E2-S, 3.4 pg/mL; E3, 28.4 pg/mL; and T, 54.1 pg/mL. Quality control samples (containing each analyte at a concentration of 6-, 60- or 600-fold of the respective LLOQ) were performed with each batch.

4.7. IL-6 Determination in the Cellular Supernatants

In order to quantify the endogenous IL-6 formation, all HGSOC cell lines were cultivated in T-75 tissue culture flasks (75 cm^2 ; BD-Falcon[®], Thermo Fisher Scientific, Inc.) until confluence. Subsequently, the cell layers were washed twice with 6.0 mL DPBS, and 8.0 mL phenol red-free DMEM/F-12, containing 10% heat-inactivated charcoal-stripped FBS and 1% PenStrep[®] solution, were added to exclude any external interference with the assay. After incubation for 24 h, the supernatants were collected and

stored at -80°C until further analysis. The remaining cell layers were detached using 2.0 mL TrypLe[®] solution and counted to obtain the number of viable cells in each flask. The contents of IL-6 in the supernatant media were, then, determined using a commercial cobas[®] Elecsys IL-6 kit (Roche Diagnostics GmbH, Mannheim, Germany) according to the manufacturer's instructions.

4.8. Impact of IL-6 and TCZ on Metabolism and Progression of HGSOC Cells

To investigate the impact of the proinflammatory cytokine IL-6 on the platinum resistance and estrogen metabolism of HGSOC cells, carboplatin-sensitive 13699 HGSOC cells, which exhibited low endogenous IL-6 formation, were treated with 10 ng/mL IL-6 for 72 h in phenol red-free DMEM/F-12, supplemented with only 10% heat-inactivated charcoal-stripped fetal bovine serum and 1% PenStrep[®] solution. Then, cells were seeded in 6-well plates in the presence of IL-6 (10 ng/mL), and their sensitivity for carboplatin (0 to 50 μM) was assessed again as described in Section 4.4. Furthermore, IL-6-treated cells were also incubated in the presence of DHEA or E1 (2000 nM) for 48 h (as described in Section 4.5) and the levels of steroid metabolites in the cell supernatants were quantified using the same LC-HRMS assay as mentioned in Section 4.6. The same experimental protocol was used with 250 $\mu\text{g/mL}$ monoclonal anti-IL-6R antibody TCZ in the platinum-resistant 13914_1 cell line, which was the cell line with the highest endogenous IL-6 formation, to investigate whether TCZ can reverse the proinflammatory effects of IL-6 in HGSOC cells.

4.9. Data Analysis and Statistics

The acquired LC-HRMS data were analyzed using the Compass DataAnalysis 4.2 and QuantAnalysis 2.2 software packages (Bruker Daltonics). For all analytes and internal standards, extracted ion chromatograms were calculated and the respective peak areas were determined. The ratios of the peak areas of each analyte/internal standard pair were subsequently used for quantification. The kinetic analyses of steroid metabolism in all HGSOC cell lines were then performed using GraphPad Prism 6.0 software (GraphPad Software, Inc., La Jolla, CA, USA) and best followed the Michaelis–Menten model:

$$V = V_{\max} \times [S]/(K_m + [S]), \quad (1)$$

where V is the rate of the reaction, V_{\max} is the maximum reaction velocity, $[S]$ is the initial substrate concentration, and K_m is the Michaelis constant. The same software package was also used for all other calculations and statistical analyses. All experiments were conducted with three independent experiments; and the data were reported as the mean \pm standard deviation (SD) of all analyzed samples. One-way ANOVA combined with Tukey's post-hoc test was used to determine differences between treatment groups and controls, with a statistical significance level of $p < 0.05$.

5. Conclusions

Resistance against platinum-based drugs is a main obstacle in the therapy of HGSOC patients. Novel markers can allow earlier and more efficient interventions for this lethal cancer subtype. In the present study, we demonstrated that steroid metabolism significantly differs between carboplatin-sensitive and -resistant HGSOC cells. Further experiments also revealed that treatment of carboplatin-sensitive cells with IL-6 decreased platinum-sensitivity concomitant with a decreased metabolic activity but increased proliferation. Treatment of carboplatin-resistant cells expressing high levels of IL-6 with the anti-IL-6R antibody TCZ also changed their resistance status back to sensitive, now showing increased estrogen metabolism and decreased IC_{50} values against carboplatin. Further studies using tumor specimens from HGSOC patients are warranted to establish estrogen metabolism as a marker for platinum resistance in the clinics.

Supplementary Materials: The following are available online at <http://www.mdpi.com/2072-6694/12/2/279/s1>, Figure S1: Proliferation of HGSOC cell lines in the presence of the hormone precursors DHEA and E1, Figure S2: IC_{50} values of HGSOC cell lines in response to carboplatin in the presence and absence of IL-6 or TCZ, Table S1:

Mutations of the investigated HGSOC cell lines, and Table S2: Expression of selected genes in the investigated HGSOC cell lines.

Author Contributions: Conceptualization, S.P. and W.J.; most of the experiments, S.P.; LC-HRMS analyses, J.W.; 13363, 13699, 15233, and 13914_1 HGSOC cell culture, D.C.C.-T., A.W., and I.v.d.D.; gene sequencing analyses, D.C.C.-T., A.W. and I.v.d.D.; Kuramochi and OVSAHO cell culture, T.L.R. and R.P.; gene expression analyses in Kuramochi and OVSAHO cells, A.M. and D.M.; IL-6 ELISA assay, M.F.-S.; kinetic calculations, S.P.; writing—original draft preparation, S.P., T.L.R., R.P., T.T., and W.J.; writing—review and editing, S.P., T.T., and W.J.; visualization, S.P.; supervision, T.T. and W.J. All authors have read and agree to the published version of the manuscript.

Funding: This research was funded by a grant from the Austrian Science Fund (FWF) awarded to W.J. (grant no. I 3417-B31), a grant from the European Union Seventh Framework Programme OCTIPS (Ovarian Cancer Therapy—Innovative Models Prolong Survival, project no: 279113), a grant from the Slovenian Research Agency (J3-8212) awarded to T.L.R. and a Young Researcher grant awarded to R.P.

Acknowledgments: Open Access Funding by the Austrian Science Fund (FWF).

Conflicts of Interest: The authors declare no conflict of interest.

Abbreviations

17 β -HSD	17 β -hydroxysteroid-dehydrogenase
3 β -HSD	3 β -hydroxysteroid-dehydrogenase
AD	4-androstene-3,17-dione
CYP	cytochrome P450
DHEA	dehydroepiandrosterone
DHEA-S	dehydroepiandrosterone-3-sulfate
DMEM/F-12	Dulbecco's modified Eagle medium F-12
DPBS	Dulbecco's phosphate buffered saline
E1	estrone
E1-S	estrone-3-sulfate
E2	17 β -estradiol
E2-G	17 β -estradiol-3-O-(β -D-glucuronide)
E2-S	17 β -estradiol-3-sulfate
E3	estriol
EOC	epithelial ovarian cancer
ER α	estrogen receptor alpha
ESR1	estrogen receptor alpha gene
ESR2	estrogen receptor beta gene
ESRRG	estrogen-related receptor gamma gene
FBS	fetal bovine serum
HGSOC	high grade serous ovarian cancer
IL-6	interleukin-6
IL-6R	interleukin-6 receptor
K _m	Michaelis constant
LC-HRMS	liquid chromatography high-resolution mass spectrometry
LLOQ	lower limit of quantification
PARP	poly(ADP-ribose)-polymerase 1
PXR	pregnane X receptor
STR	short tandem repeats
SULT	sulfotransferase
T	testosterone
TCZ	tocilizumab
UGT	uridine 5'-diphospho-glucuronosyltransferase
VEGF	vascular endothelial growth factor
V _{max}	maximum reaction velocity

References

- Longuespée, R.; Boyon, C.; Desmons, A.; Vinatier, D.; Leblanc, E.; Farré, I.; Wisztorski, M.; Ly, K.; D'Anjou, F.; Day, R.; et al. Ovarian cancer molecular pathology. *Cancer Metastasis Rev.* **2012**, *31*, 713–732. [[CrossRef](#)]
- Siegel, R.L.; Miller, K.D.; Jemal, A. Cancer statistics, 2016. *CA Cancer J. Clin.* **2016**, *66*, 7–30. [[CrossRef](#)] [[PubMed](#)]
- Bray, F.; Ferlay, J.; Soerjomataram, I.; Siegel, R.L.; Torre, L.A.; Jemal, A. Global cancer statistics 2018: GLOBOCAN estimates of incidence and mortality worldwide for 36 cancers in 185 countries. *CA Cancer J. Clin.* **2018**, *68*, 394–424. [[CrossRef](#)] [[PubMed](#)]
- Makar, A.P. Hormone therapy in epithelial ovarian cancer. *Endocr.-Relat. Cancer* **2000**, *7*, 85–93. [[CrossRef](#)] [[PubMed](#)]
- Rainczuk, A.; Rao, J.R.; Gathercole, J.L.; Fairweather, N.J.; Chu, S.; Masadah, R.; Jobling, T.W.; Deb-Choudhury, S.; Dyer, J.; Stephens, A.N. Evidence for the antagonistic form of CXC-motif chemokine CXCL10 in serous epithelial ovarian tumours. *Int. J. Cancer* **2014**, *134*, 530–541. [[CrossRef](#)]
- Kroeger, P.T.; Drapkin, R. Pathogenesis and heterogeneity of ovarian cancer. *Curr. Opin. Obstet. Gynecol.* **2017**, *29*, 26–34. [[CrossRef](#)]
- Angioli, R.; Palaia, I.; Zullo, M.A.; Muzii, L.; Mancini, N.; Calcagno, M.; Panici, P.B. Diagnostic open laparoscopy in the management of advanced ovarian cancer. *Gynecol. Oncol.* **2016**, *100*, 455–461. [[CrossRef](#)]
- Vaughan, S.; Coward, J.I.; Bast, R.C., Jr.; Berchuck, A.; Berek, J.S.; Brenton, J.D.; Coukos, G.; Crum, C.C.; Drapkin, R.; Etemadmoghadam, D.; et al. Rethinking ovarian cancer: Recommendations for improving outcomes. *Nat. Rev. Cancer* **2011**, *11*, 719–725. [[CrossRef](#)]
- Bowtell, D.D.; Böhm, S.; Ahmed, A.A.; Aspúria, P.J.; Bast, R.C.; Beral, V.; Berek, J.S.; Birrer, M.J.; Blagden, S.; Bookman, M.A.; et al. Rethinking ovarian cancer II: Reducing mortality from high-grade serous ovarian cancer. *Nat. Rev. Cancer* **2015**, *15*, 668–679. [[CrossRef](#)]
- Ivy, S.P.; Liu, J.F.; Lee, J.M.; Matulonis, U.A.; Kohn, E.C. Cediranib, a pan-VEGFR inhibitor, and olaparib, a PARP inhibitor, in combination therapy for high grade serous ovarian cancer. *Expert Opin. Investig. Drugs* **2016**, *25*, 597–611. [[CrossRef](#)]
- D'Andrea, A.D. Mechanisms of PARP inhibitor sensitivity and resistance. *DNA Repair* **2018**, *71*, 172–176. [[CrossRef](#)] [[PubMed](#)]
- Bitler, B.G.; Watson, Z.L.; Wheeler, L.J.; Behbakht, K. PARP inhibitors: Clinical utility and possibilities of overcoming resistance. *Gynecol. Oncol.* **2017**, *147*, 695–704. [[CrossRef](#)] [[PubMed](#)]
- Karam, A.; Ledermann, J.A.; Kim, J.W.; Sehouli, J.; Lu, K.; Gourley, C.; Katsumata, N.; Burger, R.A.; Nam, B.H.; Bacon, M.; et al. Fifth Ovarian Cancer Consensus Conference of the Gynecologic Cancer InterGroup: First-line interventions. *Ann. Oncol.* **2017**, *28*, 711–717. [[CrossRef](#)] [[PubMed](#)]
- Mungenast, F.; Thalhammer, T. Estrogen biosynthesis and action in ovarian cancer. *Front. Endocrinol. (Lausanne)* **2014**, *5*, 192. [[CrossRef](#)] [[PubMed](#)]
- Moyle-Heyrman, G.; Schipma, M.J.; Dean, M.; Davis, D.A.; Burdette, J.E. Genome-wide transcriptional regulation of estrogen receptor targets in fallopian tube cells and the role of selective estrogen receptor modulators. *J. Ovarian Res.* **2016**, *9*, 5. [[CrossRef](#)] [[PubMed](#)]
- Stanley, B.; Hollis, R.L.; Nunes, H.; Towler, J.D.; Yan, X.; Rye, T.; Dawson, C.; Mackean, M.J.; Nussey, F.; Churchman, M.; et al. Endocrine treatment of high grade serous ovarian carcinoma; quantification of efficacy and identification of response predictors. *Gynecol. Oncol.* **2019**, *152*, 278–285. [[CrossRef](#)]
- Paleari, L.; Gandini, S.; Provinciali, N.; Puntoni, M.; Colombo, N.; DeCensi, A. Clinical benefit and risk of death with endocrine therapy in ovarian cancer: A comprehensive review and meta-analysis. *Gynecol. Oncol.* **2017**, *146*, 504–513. [[CrossRef](#)]
- Stasenka, M.; Plegue, M.; Sciallis, A.P.; McLean, K. Clinical response to antiestrogen therapy in platinum-resistant ovarian cancer patients and the role of tumor estrogen receptor expression status. *Int. J. Gynecol. Cancer* **2015**, *25*, 222–228. [[CrossRef](#)]
- Ren, X.; Wu, X.; Hillier, S.G.; Fegan, K.S.; Critchley, H.O.; Mason, J.I.; Sarvi, S.; Harlow, C.R. Local estrogen metabolism in epithelial ovarian cancer suggests novel targets for therapy. *J. Steroid Biochem. Mol. Biol.* **2015**, *150*, 54–63. [[CrossRef](#)]

20. Mungenast, F.; Aust, S.; Vergote, I.; Vanderstichele, A.; Sehouli, J.; Braicu, E.; Mahner, S.; Castillo-Tong, D.C.; Zeillinger, R.; Thalhammer, T. Clinical significance of the estrogen-modifying enzymes steroid sulfatase and estrogen sulfotransferase in epithelial ovarian cancer. *Oncol. Lett.* **2017**, *13*, 4047–4054. [\[CrossRef\]](#)
21. Poschner, S.; Zehl, M.; Maier-Salamon, A.; Jäger, W. Simultaneous quantification of estrogens, their precursors and conjugated metabolites in human breast cancer cells by LC-HRMS without derivatization. *J. Pharm. Biomed. Anal.* **2017**, *138*, 344–350. [\[CrossRef\]](#) [\[PubMed\]](#)
22. Wang, Y.; Niu, X.L.; Qu, Y.; Wu, J.; Zhu, Y.Q.; Sun, W.J.; Li, L.Z. Autocrine production of interleukin-6 confers cisplatin and paclitaxel resistance in ovarian cancer cells. *Cancer Lett.* **2010**, *295*, 110–123. [\[CrossRef\]](#) [\[PubMed\]](#)
23. Macciò, A.; Madeddu, C. Inflammation and ovarian cancer. *Cytokine* **2012**, *58*, 133–147. [\[CrossRef\]](#) [\[PubMed\]](#)
24. Bonneau, C.; Rouzier, R.; Geyl, C.; Cortez, A.; Castela, M.; Lis, R.; Daraï, E.; Touboul, C. Predictive markers of chemoresistance in advanced stages epithelial ovarian carcinoma. *Gynecol. Oncol.* **2015**, *136*, 112–120. [\[CrossRef\]](#) [\[PubMed\]](#)
25. Penson, R.T.; Kronish, K.; Duan, Z.; Feller, A.J.; Stark, P.; Cook, S.E.; Duska, L.R.; Fuller, A.F.; Goodman, A.K.; Nikrui, N.; et al. Cytokines IL-1beta, IL-2, IL-6, IL-8, MCP-1, GM-CSF and TNFalpha in patients with epithelial ovarian cancer and their relationship to treatment with paclitaxel. *Int. J. Gynecol. Cancer* **2000**, *10*, 33–41. [\[CrossRef\]](#)
26. Kreuzinger, C.; Gamperl, M.; Wolf, A.; Heinze, G.; Geroldinger, A.; Lambrechts, D.; Boeckx, B.; Smeets, D.; Horvat, R.; Aust, S.; et al. Molecular characterization of 7 new established cell lines from high grade serous ovarian cancer. *Cancer Lett.* **2015**, *362*, 218–228. [\[CrossRef\]](#)
27. Haley, J.; Tomar, S.; Pulliam, N.; Xiong, S.; Perkins, S.M.; Karpf, A.R.; Mitra, S.; Nephew, K.P.; Mitra, A.K. Functional characterization of a panel of high-grade serous ovarian cancer cell lines as representative experimental models of the disease. *Oncotarget* **2016**, *7*, 32810–32820. [\[CrossRef\]](#)
28. He, Y.; Zhu, Q.; Chen, M.; Huang, Q.; Wang, W.; Li, Q.; Huang, Y.; Di, W. The changing 50% inhibitory concentration (IC50) of cisplatin: A pilot study on the artifacts of the MTT assay and the precise measurement of density-dependent chemoresistance in ovarian cancer. *Oncotarget* **2016**, *7*, 70803–70821. [\[CrossRef\]](#)
29. Lindl, T.; Lewandowski, B.; Sheyrogg, S.; Staudte, A. Evaluation of the In Vitro Cytotoxicities of 50 Chemicals by using an Electronic Current Exclusion Method versus the Neutral Red Uptake and MTT Assays. *ATLA* **2005**, *33*, 591–601.
30. Murias, M.; Miksits, M.; Aust, S.; Spatzenegger, M.; Thalhammer, T.; Szekeres, T.; Jaeger, W. Metabolism of resveratrol in breast cancer cell lines: Impact of sulfotransferase 1A1 expression on cell growth inhibition. *Cancer Lett.* **2008**, *261*, 172–182. [\[CrossRef\]](#)
31. Imai, A.; Ohno, T.; Takahashi, K.; Furui, T.; Tamaya, T. Lack of evidence for aromatase expression in human ovarian epithelial carcinoma. *Ann. Clin. Biochem.* **1994**, *31*, 65–71. [\[CrossRef\]](#) [\[PubMed\]](#)
32. Sasano, H.; Harada, N. Intratumoral aromatase in human breast, endometrial, and ovarian malignancies. *Endocr. Rev.* **1998**, *19*, 593–607. [\[CrossRef\]](#) [\[PubMed\]](#)
33. Blanco, L.Z., Jr.; Kuhn, E.; Morrison, J.C.; Bahadirli-Talbott, A.; Smith-Sehdev, A.; Kurman, R.J. Steroid hormone synthesis by the ovarian stroma surrounding epithelial ovarian tumors: A potential mechanism in ovarian tumorigenesis. *Mod. Pathol.* **2017**, *30*, 563–576. [\[CrossRef\]](#) [\[PubMed\]](#)
34. Heinzelmann-Schwarz, V.; Knipprath Mészáros, A.; Stadlmann, S.; Jacob, F.; Schoetzau, A.; Russell, K.; Friedlander, M.; Singer, G.; Vetter, M. Letrozole may be a valuable maintenance treatment in high-grade serous ovarian cancer patients. *Gynecol. Oncol.* **2018**, *148*, 79–85. [\[CrossRef\]](#)
35. Xu, Y.; Zhang, Q.; Miao, C.; Dongol, S.; Li, Y.; Jin, C.; Dong, R.; Li, Y.; Yang, X.; Kong, B. CCNG1 (Cyclin G1) regulation by mutant-P53 via induction of Notch3 expression promotes high-grade serous ovarian cancer (HGSOC) tumorigenesis and progression. *Cancer Med.* **2019**, *8*, 351–362. [\[CrossRef\]](#)
36. Browning, L.; Patel, M.R.; Bring Horvath, E.; Tawara, K.; Jorcyk, C.L. IL-6 and ovarian cancer: Inflammatory cytokines in promotion of metastasis. *Cancer Manag. Res.* **2018**, *10*, 6685–6693. [\[CrossRef\]](#)
37. Coward, J.; Kulbe, H.; Chakravarty, P.; Leader, D.; Vassileva, V.; Leinster, D.A.; Thompson, R.; Schioppa, T.; Nemeth, J.; Vermeulen, J.; et al. Interleukin-6 as a therapeutic target in human ovarian cancer. *Clin. Cancer Res.* **2011**, *17*, 6083–6096. [\[CrossRef\]](#)
38. Strasser, S.I.; Mashford, M.L.; Desmond, P.V. Regulation of uridine diphosphate glucuronosyltransferase during the acute-phase response. *J. Gastroenterol. Hepatol.* **1998**, *13*, 88–94. [\[CrossRef\]](#)

39. Simon, F.; Garcia, J.; Guyot, L.; Guitton, J.; Vilchez, G.; Bardel, C.; Chenel, M.; Tod, M.; Payen, L. Impact of Interleukin-6 on Drug-Metabolizing Enzymes and Transporters in Intestinal Cells. *AAPS J.* **2019**, *22*, 16. [\[CrossRef\]](#)
40. Kim, S.; Östör, A.J.; Nisar, M.K. Interleukin-6 and cytochrome-P450, reason for concern? *Rheumatol. Int.* **2012**, *32*, 2601–2604. [\[CrossRef\]](#)
41. Ning, R.; Zhan, Y.; He, S.; Hu, J.; Zhu, Z.; Hu, G.; Yan, B.; Yang, J.; Liu, W. Interleukin-6 Induces DEC1, Promotes DEC1 Interaction with RXR α and Suppresses the Expression of PXR, CAR and Their Target Genes. *Front. Pharmacol.* **2017**, *8*, 866. [\[CrossRef\]](#) [\[PubMed\]](#)
42. Johnson, D.E.; O’Keefe, R.A.; Grandis, J.R. Targeting the IL-6/JAK/STAT3 signalling axis in cancer. *Nat. Rev. Clin. Oncol.* **2018**, *15*, 234–248. [\[CrossRef\]](#) [\[PubMed\]](#)
43. Abualsunun, W.A.; Sahin, C.; Cummins, C.L.; Piquette-Miller, M. Essential role of STAT-3 dependent NF- κ B activation on IL-6-mediated downregulation of hepatic transporters. *Eur. J. Pharm. Sci.* **2019**, *143*, 105151. [\[CrossRef\]](#) [\[PubMed\]](#)
44. Yousefi, H.; Momeny, M.; Ghaffari, S.H.; Parsanejad, N.; Poursheikhani, A.; Javadikooshesh, S.; Zarrinrad, G.; Esmaeili, F.; Alishahi, Z.; Sabourinejad, Z.; et al. IL-6/IL-6R pathway is a therapeutic target in chemoresistant ovarian cancer. *Tumori* **2019**, *105*, 84–91. [\[CrossRef\]](#) [\[PubMed\]](#)
45. Guo, Y.; Nemeth, J.; O’Brien, C.; Susa, M.; Liu, X.; Zhang, Z.; Choy, E.; Mankin, H.; Hornicek, F.; Duan, Z. Effects of siltuximab on the IL-6-induced signaling pathway in ovarian cancer. *Clin. Cancer Res.* **2010**, *16*, 5759–5769. [\[CrossRef\]](#)
46. Angevin, E.; Tabernero, J.; Elez, E.; Cohen, S.J.; Bahleda, R.; van Laethem, J.L.; Ottensmeier, C.; Lopez-Martin, J.A.; Clive, S.; Joly, F.; et al. A phase I/II, multiple-dose, dose-escalation study of siltuximab, an anti-interleukin-6 monoclonal antibody, in patients with advanced solid tumors. *Clin. Cancer Res.* **2014**, *20*, 2192–2204. [\[CrossRef\]](#)
47. Dijkgraaf, E.M.; Santegoets, S.J.; Reyners, A.K.; Goedemans, R.; Wouters, M.C.; Kenter, G.G.; van Erkel, A.R.; van Poelgeest, M.I.; Nijman, H.W.; van der Hoeven, J.J.; et al. A phase I trial combining carboplatin/doxorubicin with tocilizumab, an anti-IL-6R monoclonal antibody, and interferon- α 2b in patients with recurrent epithelial ovarian cancer. *Ann. Oncol.* **2015**, *26*, 2141–2149. [\[CrossRef\]](#)
48. Andersen, C.L.; Sikora, M.J.; Boisen, M.M.; Ma, T.; Christie, A.; Tseng, G.; Park, Y.; Luthra, S.; Chandran, U.; Haluska, P.; et al. Active Estrogen Receptor- α Signaling in Ovarian Cancer Models and Clinical Specimens. *Clin. Cancer Res.* **2017**, *23*, 3802–3812. [\[CrossRef\]](#)
49. Kreuzinger, C.; von der Decken, I.; Wolf, A.; Gamperl, M.; Koller, J.; Karacs, J.; Pfaffinger, S.; Bartl, T.; Reinthaller, A.; Grimm, C.; et al. Patient-derived cell line models revealed therapeutic targets and molecular mechanisms underlying disease progression of high grade serous ovarian cancer. *Cancer Lett.* **2019**, *459*, 1–12. [\[CrossRef\]](#)
50. Silwal-Pandit, L.; Langerød, A.; Børresen-Dale, A.L. TP53 Mutations in Breast and Ovarian Cancer. *Cold Spring Harb. Perspect. Med.* **2017**, *7*, a026252. [\[CrossRef\]](#)
51. Wang, Z. ErbB Receptors and Cancer. *Methods Mol. Biol.* **2017**, *1652*, 3–35. [\[CrossRef\]](#) [\[PubMed\]](#)
52. Chen, S.H.; Chang, J.Y. New Insights into Mechanisms of Cisplatin Resistance: From Tumor Cell to Microenvironment. *Int. J. Mol. Sci.* **2019**, *20*, 4136. [\[CrossRef\]](#) [\[PubMed\]](#)
53. Motoyama, T. Biological characterization including sensitivity to mitomycin C of cultured human ovarian cancers. *Nippon Sanka Fujinka Gakkai Zasshi* **1981**, *33*, 1197–1204. [\[PubMed\]](#)
54. Yanagibashi, T.; Gorai, I.; Nakazawa, T.; Miyagi, E.; Hirahara, F.; Kitamura, H.; Minaguchi, H. Complexity of expression of the intermediate filaments of six new human ovarian carcinoma cell lines: New expression of cytokeratin 20. *Br. J. Cancer* **1997**, *76*, 829–835. [\[CrossRef\]](#) [\[PubMed\]](#)
55. Domcke, S.; Sinha, R.; Levine, D.A.; Sander, C.; Schultz, N. Evaluating cell lines as tumour models by comparison of genomic profiles. *Nat. Commun.* **2013**, *4*, 2126. [\[CrossRef\]](#)
56. Hruz, T.; Laule, O.; Szabo, G.; Wessendorp, F.; Bleuler, S.; Oertle, L.; Widmayer, P.; Gruissem, W.; Zimmermann, P. Genevestigator V3: A reference expression database for the meta-analysis of transcriptomes. *Adv. Bioinform.* **2008**, *2008*, 420747. [\[CrossRef\]](#)

57. Ghandi, M.; Huang, F.W.; Jané-Valbuena, J.; Kryukov, G.V.; Lo, C.C.; McDonald, E.R.; Barretina, J.; Gelfand, E.T.; Bielski, C.M.; Li, H.; et al. Next-generation characterization of the Cancer Cell Line Encyclopedia. *Nature* **2019**, *569*, 503–508. [[CrossRef](#)]
58. Hall, M.D.; Telma, K.A.; Chang, K.E.; Lee, T.D.; Madigan, J.P.; Lloyd, J.R.; Goldlust, I.S.; Hoeschele, J.D.; Gottesman, M.M. Say no to DMSO: Dimethylsulfoxide inactivates cisplatin, carboplatin, and other platinum complexes. *Cancer Res.* **2014**, *74*, 3913–3922. [[CrossRef](#)]



© 2020 by the authors. Licensee MDPI, Basel, Switzerland. This article is an open access article distributed under the terms and conditions of the Creative Commons Attribution (CC BY) license (<http://creativecommons.org/licenses/by/4.0/>).

CHAPTER VIII

CONCLUSIONS AND OUTLOOK

In conclusion, the present thesis demonstrated for the first time an interaction of selected natural dietary supplements used for the treatment of menopausal disorders with endogenous estrogen metabolism using a newly established and validated LC-HRMS method. These findings provide a better understanding of the involved molecular mechanisms and contribute to the evaluation of efficacy and safety of herbal treatment options. However, as these investigations were only based on cellular *in vitro* models; future clinical studies in women quantifying blood and/or tissue levels of conjugated and unconjugated estrogens in the presence and absence of these dietary supplements, as well as other parameters such as body weight, age and enzyme expression patterns, should be conducted to confirm the observed interactions *in vivo*.

Furthermore, the interplay may not only apply for the compounds investigated for this thesis (soy isoflavones, resveratrol and black cohosh extract), but also for other marketed phytoestrogens, such as quercetin and its glycosylated form rutin, formononetin and biochanin A, which are mainly found in red clover, or the hops polyphenols xanthohumol and 8-prenylnaringenin. Moreover, the modulation of various estrogen metabolizing enzymes and transporters, including CYPs, SULTs, UGTs and OATPs, has been observed for other plants and a wide range of pharmaceutical drugs in numerous *in vitro* and *in vivo* studies. The induction of hepatic enzymes, such as CYP3A4, may cause an increased elimination of active estrogens, which has been reported for St. John's wort, rifampicin and several anticonvulsant drugs. By contrast, an increase in E2 may be expected upon the intake of non-steroidal antiphlogistics (NSAIDs), the most prescribed drugs worldwide, as these have been proven to inhibit SUL1A1 and consequently the inactivation of estrogens. Yet, although estrogenic steroids play a pivotal role in human physiology, detailed data from clinical trials concerning a possible interaction of dietary supplements and pharmaceuticals with the endogenous formation and metabolism of estrogens are scarce. Future studies assessing the relevance of this potential risk of side-effects are therefore highly warranted, especially in women diagnosed with ER α + breast cancer.

In addition to the altered estrogen metabolism upon treatment with natural supplements against menopausal disorders, an increase in the formation of androgens, such as T, was also observed. However, as the LC-HRMS assay performed herein covered only a few selected androgens, future research should focus on the development and application of a targeted assay for detailed androgen metabolomics, including their respective conjugated and unconjugated metabolites, to better understand the molecular mechanisms of these interactions and evaluate their clinical significance. Most importantly, a possible impact of dietary supplements on androgen metabolism may not be limited to women and gynecological diseases, but also apply for males. Botanicals increasing the levels of active androgens by interfering with metabolizing enzymes may therefore be used for the enhancement of sexual dysfunction in men or could even act as some type of “natural anabolic doping”. On the other hand, these products may also exacerbate androgen-sensitive diseases, such as hormone-dependent prostate cancer. Further clinical trials need to be conducted to assess the efficacy and safety of these herbal supplements by monitoring the plasma concentrations of active androgens and their respective metabolites upon the treatment of healthy women and men, as well as of patients diagnosed with androgen-dependent malignancies.

The present work further revealed that changes in the metabolism of steroid hormones cannot only be observed following the administration of herbal remedies, but also depend on the different disease states of breast and ovarian cancer, such as ER status or resistance against certain chemotherapeutics. These alterations in the metabolomics pattern may therefore be used as diagnostic markers to determine progression, metastasis or drug resistance, which are still major obstacles in the treatment of cancer. Moreover, steroid metabolism was strongly correlated with the IL-6-driven inflammatory status of cancer cells in the present experiments, suggesting that targeted steroid metabolomics may not only be applied for estrogen- and androgen-dependent cancers, but possibly also as markers for other disease states linked to increased inflammation, such as rheumatoid arthritis, Crohn’s disease, ulcerative colitis, psoriasis and other related

autoimmune disorders. Certainly, these hypotheses have to be further verified in clinical studies using larger data sets obtained from human patients, including plasma and/or tissue samples (including cancer specimens of various stages and grades); yet, targeted metabolomics of estrogens and/or androgens may be promising new tools for monitoring various diseases, especially hormone-dependent cancers, in the clinic.

APPENDIX

ABBREVIATIONS

3 β -HSD	3 β -hydroxysteroid dehydrogenase
17 β -HSD	17 β -hydroxysteroid dehydrogenase
ABC	ATP-binding cassette
AD	4-androstene-3,17-dione
AhR	aryl-hydrocarbon-receptor
BCE	black cohosh extract (<i>Actaea racemosa</i> L. extract)
CYP	cytochrome P450 isoenzyme
DAI	daidzein (4',7-dihydroxyisoflavone)
DHEA	dehydroepiandrosterone
DHEA-S	dehydroepiandrosterone-3-O-sulfate
DMEM/F-12	Dulbecco's Modified Eagle Medium F-12
DMSO	dimethylsulfoxide
DPBS	Dulbecco's phosphate buffered saline
DTT	dithiothreitol
E1	estrone
E1-S	estrone-3-O-sulfate
E2	17 β -estradiol
E2-G	17 β -estradiol-3-O-(β -D-glucuronide)
E2-S	17 β -estradiol-3-O-sulfate
E3	estriol (16 α -hydroxy-17 β -estradiol)
EGFR	epidermal growth factor receptor
EIC	extracted ion chromatogram
ELISA	enzyme-linked immunosorbent assay
EOC	epithelial ovarian cancer
ER α	estrogen receptor α
ER β	estrogen receptor β
ESI	electrospray ionization
FBS	fetal bovine serum
FSH	follicle-stimulating hormone
GC	gas chromatography
GEN	genistein (4',5,7-trihydroxyisoflavone)
GP1R	G protein-coupled estrogen receptor 1 (GPR30)
HGSOC	high-grade serous ovarian cancer
HPG axis	hypothalamic-pituitary-gonadal axis
HPLC	high performance liquid chromatography
HRT	hormone replacement therapy
IC ₅₀	half maximal inhibitory concentration
IL-6	interleukin-6
IL-6R	interleukin-6 receptor

K _i	inhibition constant
K _m	Michaelis constant
LC-HRMS	liquid chromatography high-resolution mass spectrometry
LH	luteinizing hormone
LLOQ	lower limit of quantification
MAPK	mitogen-activated protein kinase
mER	membrane-associated estrogen receptor
MRP	multidrug resistance protein
MS	mass spectrometry
OATP	organic-anion-transporting polypeptide
PARP	poly(ADP-ribose)-polymerase 1
PAPS	3'-phosphoadenosine-5'-phosphosulfate
PCR	polymerase chain reaction
PXR	pregnane X receptor
RES	resveratrol (<i>trans</i> -3,5,4'-trihydroxystilbene)
SD	standard deviation
SERM	selective estrogen-receptor modulator
SPE	solid phase extraction
STR	short tandem repeats
STS	steroid sulfatase
SULT	sulfotransferase
T	testosterone
TCZ	tocilizumab
UGT	uridine 5'-diphospho-glucuronosyltransferase
ULOQ	upper limit of quantification
VEGF	vascular endothelial growth factor
V _{max}	maximum reaction velocity

ZUSAMMENFASSUNG

Östrogene spielen eine zentrale Rolle in der menschlichen Physiologie; dennoch ist wenig über die Wechselwirkung von Nahrungsergänzungsmitteln oder verschiedenen Krankheitszuständen mit deren Metabolismus bekannt. Änderungen in der Stoffwechselaktivität könnten die aktiven Wirkkonzentrationen der Hormone erhöhen, und somit verschiedenste Krankheiten, insbesondere hormonsensitive Tumore, in der Entstehung und Progression beeinflussen. Das Ziel der vorliegenden Arbeit war daher, erstmals die Wechselwirkung ausgewählter Naturstoffe, welche typischerweise zur Linderung von Wechselbeschwerden eingesetzt werden, mit dem Östrogenstoffwechsel in humanen Brustkrebszelllinien (mit und ohne Östrogenrezeptorexpression) zu untersuchen. Hierfür wurde zunächst eine neue Analysemethode entwickelt, die auf Flüssigchromatographie und hochauflösender Massenspektrometrie basiert und nach internationalen Richtlinien auch validiert wurde. Die hohe Empfindlichkeit und Selektivität dieser Analytik ermöglicht, dass die zehn wichtigsten Steroide des Östrogenstoffwechsels (inklusive der Vorstufen, der aktiven Hormone und der entsprechenden Metaboliten) gleichzeitig quantifiziert werden können.

Die Behandlung der Krebszellen mit den Sojaisoflavonen Genistein und Daidzein, beziehungsweise mit Resveratrol (einem Polyphenol aus Weintrauben), zeigte bereits bei äußerst geringen Konzentrationen im (sub-)mikromolaren Bereich eine starke Hemmung der Sulfatierung und Glukuronidierung von Östrogenen, wodurch wiederum die Spiegel unkonjugierter Steroidhormone, vor allem die des hochpotenten 17 β -Östradiols, signifikant anstiegen. Diese Erhöhung führte weiters zu einer Stimulation des Zellwachstums von Östrogenrezeptor-exprimierenden Zellen, was die dringende Notwendigkeit weiterer Untersuchungen an Frauen unterstreicht; die Anwendungssicherheit von Nahrungsergänzungsmitteln bei Brustkrebspatientinnen könnte so besser evaluiert werden.

Im Gegensatz zu diesen Beobachtungen konnte keine Veränderung der Östrogenkonzentrationen festgestellt werden, wenn die gleichen Brustkrebszelllinien mit Traubensilberkerzenextrakt, einem weiteren oft verwendeten pflanzlichen Präparat gegen Wechselbeschwerden, inkubiert wurden. Der Extrakt bewirkte außerdem keinen Wachstumsanstieg, sondern sogar einer Wachstumshemmung der Krebszellen, was darauf hindeutet, dass die Anwendung von Traubensilberkerzenpräparaten bei Brustkrebspatientinnen weitgehend ungefährlich sein dürfte. Der Extrakt, beziehungsweise dessen Hauptbestandteil Actein, zeigte weiters eine ausgeprägte Hemmung der Sulfatierung von Dehydroepiandrosteron (DHEA) durch die Sulfotransferase 2A1, was zu erhöhten Spiegeln von unkonjugiertem DHEA und in weiterer Folge zu einem Anstieg der Androgene Androstendion und Testosteron führte. Dieser Androgenanstieg könnte als Erklärung für die klinisch erwiesene Wirkung von Traubensilberkerzenextrakt gegen menopausale Symptome, insbesondere Hitzewallungen, dienen.

Das letzte Kapitel der vorliegenden Dissertation zeigte weiters, dass der Metabolismus von Östrogenen auch als Resistenzmarker für Ovarialkarzinome dienen könnte. Hierfür wurden die Konzentrationen der Östrogene und deren Metaboliten in zwei Carboplatin-sensitiven und vier -resistenten Ovarialkarzinomzelllinien bestimmt. Dabei wurde eine signifikante Hemmung des Östrogenmetabolismus ausschließlich in resistenten Zellen beobachtet; ein Effekt, der durch die Behandlung mit dem monoklonalen anti-Interleukin-6-Rezeptor Antikörper Tocilizumab aufgehoben werden konnte.

Klinische Studien, die die Blut- und/oder Gewebskonzentrationen konjugierter und unkonjugierter Steroidhormone vor und während der Einnahme von Nahrungsergänzungsmitteln oder im Verlauf verschiedener Krankheitszustände überwachen, sind folglich dringend nötig, um die in dieser Arbeit *in vitro* beobachteten Zusammenhänge auch mit Patientendaten zu belegen.

LIST OF SCIENTIFIC PUBLICATIONS

Research Articles

2020

Metabolism of Estrogens: Turnover Differs Between Platinum-Sensitive and -Resistant High-Grade Serous Ovarian Cancer Cells

Poschner, S.; Wackerlig, J.; Castillo-Tong, D. C.; Wolf, A.; van der Decken, I.; Rižner, T. L.; Pavlič, R.; Meshcheryakova, A.; Mechtcheriakova, D.; Fritzer-Szekeres, M.; Thalhammer, T.; Jäger, W. *Cancers (Basel)* **2020**, 12, pii: E279. doi: 10.3390/cancers12020279.

Impact of thrombocytes, on bacterial growth and antimicrobial activity of selected antibiotics

Nussbaumer-Pröll, A. K.; Eberl, S.; Reiter, B.; Stimpfl, T.; Jäger, W.; **Poschner, S.**; Zeitlinger, M. *European Journal of Clinical Microbiology & Infectious Diseases* **2020**, 39, 593–597. doi: 10.1007/s10096-019-03762-1.

2019

Resveratrol and other dietary polyphenols are inhibitors of estrogen metabolism in human breast cancer cells

Poschner, S.; Maier-Salamon, A.; Thalhammer, T.; Jäger, W. *The Journal of Steroid Biochemistry and Molecular Biology* **2019**, 190, 11–18. doi: 10.1016/j.jsbmb.2019.03.001.

Inhibition of ABCB1 and ABCG2 at the Mouse Blood-Brain Barrier with Marketed Drugs To Improve Brain Delivery of the Model ABCB1/ABCG2 Substrate [(11)C]erlotinib

Traxl, A.; Mairinger, S.; Filip, T.; Sauberer, M.; Stanek, J.; **Poschner, S.**; Jäger, W.; Zoufal, V.; Novarino, G.; Tournier, N.; Bauer, M.; Wanek, T.; Langer, O. *Molecular Pharmaceutics* **2019**, 16, 1282–1293. doi: 10.1021/acs.molpharmaceut.8b01217.

Impact of erythrocytes on bacterial growth and antimicrobial activity of selected antibiotics

Nussbaumer-Pröll, A. K.; Knotzer, S.; Eberl, S.; Reiter, B.; Stimpfl, T.; Jäger, W.; **Poschner, S.**; Zeitlinger, M. *European Journal of Clinical Microbiology & Infectious Diseases* **2019**, 38, 485–495. doi: 10.1007/s10096-018-03452-4.

A Proof-of-Concept Study to Inhibit ABCG2- and ABCB1-Mediated Efflux Transport at the Human Blood-Brain Barrier

Bauer, M.; Karch, R.; Wulkersdorfer, B.; Philippe, C.; Nics, L.; Klebermass, E. M.; Weber, M.; **Poschner, S.**; Haslacher, H.; Jäger, W.; Tournier, N.; Wadsak, W.; Hacker, M.; Zeitlinger, M.; Langer, O. *The Journal of Nuclear Medicine* **2019**, 60, 486–491. doi: 10.2967/jnumed.118.216432.

2018

Effect of Rifampicin on the Distribution of [(11)C]Erlotinib to the Liver, a Translational PET Study in Humans and in Mice

Bauer, M.; Traxl, A.; Matsuda, A.; Karch, R.; Philippe, C.; Nics, L.; Klebermass, E. M.; Wulkersdorfer, B.; Weber, M.; **Poschner, S.**; Tournier, N.; Jäger, W.; Wadsak, W.; Hacker, M.; Wanek, T.; Zeitlinger, M.; Langer, O. *Molecular Pharmaceutics* **2018**, 15, 4589–4598. doi: 10.1021/acs.molpharmaceut.8b00588.

Resveratrol Inhibits Key Steps of Steroid Metabolism in a Human Estrogen-Receptor Positive Breast Cancer Model: Impact on Cellular Proliferation

Poschner, S.; Maier-Salamon, A.; Zehl, M.; Wackerlig, J.; Dobusch, D.; Meshcheryakova, A.; Mechtcheriakova, D.; Thalhammer, T.; Pachmann, B.; Jäger, W. *Frontiers in Pharmacology* **2018**, 9, 742. doi: 10.3389/fphar.2018.00742.

Concentrations of Cefuroxime in Brain Tissue of Neurointensive Care Patients

Hosmann, A.; Ritscher, L. C.; Burgmann, H.; Oesterreicher, Z.; Jäger, W.; **Poschner, S.**; Knosp, E.; Reinprecht, A.; Gruber, A.; Zeitlinger, M. *Antimicrobial Agents and Chemotherapy* **2018**, 62, pii: e02164–17. doi: 10.1128/AAC.02164-17.

Influence of OATPs on Hepatic Disposition of Erlotinib Measured With Positron Emission Tomography

Bauer, M.; Matsuda, A.; Wulkersdorfer, B.; Philippe, C.; Traxl, A.; Özvegy-Laczka, C.; Stanek, J.; Nics, L.; Klebermass, E. M.; **Poschner, S.**; Jäger, W.; Patik, I.; Bakos, É.; Szakács, G.; Wadsak, W.; Hacker, M.; Zeitlinger, M.; Langer, O. *Clinical Pharmacology & Therapeutics* **2018**, 104, 139–147. doi: 10.1002/cpt.888.

2017

The Impacts of Genistein and Daidzein on Estrogen Conjugations in Human Breast Cancer Cells: A Targeted Metabolomics Approach

Poschner, S.; Maier-Salamon, A.; Zehl, M.; Wackerlig, J.; Dobusch, D.; Pachmann, B.; Sterlini, K. L.; Jäger, W. *Frontiers in Pharmacology* **2017**, 8, 699. doi: 10.3389/fphar.2017.00699.

Human Bile Reduces Antimicrobial Activity of Selected Antibiotics against *Enterococcus faecalis* and *Escherichia coli* In Vitro

Wulkersdorfer, B.; Jaros, D.; Eberl, S.; **Poschner, S.**; Jäger, W.; Cosentini, E.; Zeitlinger, M.; Schwameis, R. *Antimicrobial Agents and Chemotherapy* **2017**, 61, pii: e00527–17. doi: 10.1128/AAC.00527-17.

Simultaneous quantification of estrogens, their precursors and conjugated metabolites in human breast cancer cells by LC-HRMS without derivatization

Poschner, S.; Zehl, M.; Maier-Salamon, A.; Jäger, W. *Journal of Pharmaceutical and Biomedical Analysis* **2017**, 138, 344–350. doi: 10.1016/j.jpba.2017.02.033.

Conference Contributions

2019

Black cohosh impairs steroid metabolism in human breast cancer cells: a targeted metabolomics approach

Poschner, S.; Maier-Salamon, A.; Wackerlig, J.; Dobusch, D.; Pachmann, B.; Banh, S. J.; Jäger, W. **Oral presentation** at the 17th *Austrian Proteomics and Metabolomics Research Symposium APMRS 2019, September 2019*, Salzburg, Austria.

2018

Targeted metabolomics of steroids by LC-HRMS: application to platinum-sensitive and -resistant human ovarian cancer cells

Poschner, S.; Zehl, M.; Wackerlig, J.; Dobusch, D.; Castillo-Tong, D. C.; Wolf, A.; Thalhammer, T.; Jäger, W. **Oral presentation** at the 16th *Austrian Proteomics and Metabolomics Research Symposium APMRS 2018, August 2018*, Vienna, Austria.

Resveratrol inhibits key steps of steroid metabolism in a human estrogen-receptor positive breast cancer model: impact on cellular Proliferation

Poschner, S.; Maier-Salamon, A.; Zehl, M.; Wackerlig, J.; Dobusch, D.; Pachmann, B.; Jäger, W. **Oral presentation** at the *4th Congress on Steroid Research CSR 2018*, **July 2018**, Seoul, South Korea.

Stipends & Awards

Förderungsstipendium nach dem Studienförderungsgesetz

University of Vienna, **2018**, Vienna, Austria.

Best Presentation Award

4th Congress on Steroid Research CSR 2018, **July 2018**, Seoul, South Korea.